FINAL REPORT

Secondary Impacts of *In Situ* Remediation on Groundwater Quality and Post-Treatment Management Strategies

SERDP Project ER-2129

JULY 2017

Kurt D. Pennell, Ph.D., P.E.
Natalie L. Cápiro, Ph.D.
Samuel Gaeth, M.S.
Tyler Marcet, M.S.
Tufts University

Frank E. Löffler, Ph.D.
Yi Yang, Ph.D.
University of Tennessee

SERDP
DOD ▪ EPA ▪ DOE

Page Intentionally Left Blank

Page Intentionally Left Blank

REPORT DOCUMENTATION PAGE

Form Approved
OMB No. 0704-0188

1. REPORT DATE *(DD-MM-YYYY)*	**2. REPORT TYPE**	**3. DATES COVERED** *(From - To)*
27-07-2017	SERDP Final Report	June 2011-December 2015

4. TITLE AND SUBTITLE
Secondary Impacts of In Situ Remediation on Groundwater Quality and Post-Treatment Management Strategies

5a. CONTRACT NUMBER
W912HQ-11-C-0068

5b. GRANT NUMBER

5c. PROGRAM ELEMENT NUMBER

6. AUTHOR(S)
Pennell, Kurt D., Ph.D, P.E.; Löffler, Frank E., Ph.D.; Cápiro, Natalie L., Ph.D.; Yang, Yi, Ph.D.; Marcet; Tyler F., M.S.; Gaeth, Samuel P., M.S.

5d. PROJECT NUMBER
SERDP ER-2129

5e. TASK NUMBER

5f. WORK UNIT NUMBER

7. PERFORMING ORGANIZATION NAME(S) AND ADDRESS(ES)
Tufts University, Civil and Environmental Engineering
200 College Ave.
Medford, MA 02155

8. PERFORMING ORGANIZATION REPORT NUMBER
ER-2129

9. SPONSORING / MONITORING AGENCY NAME(S) AND ADDRESS(ES)
Strategic Environmental Remediation Development Program
4800 Mark Center Drive, Suite 17D03
Alexandria, VA 22350-3605

10. SPONSOR/MONITOR'S ACRONYM(S)
SERDP

11. SPONSOR/MONITOR'S REPORT NUMBER(S) ER-2129

12. DISTRIBUTION / AVAILABILITY STATEMENT
Distribution A; unlimited public release

13. SUPPLEMENTARY NOTES

14. ABSTRACT

The goal of this project was to evaluate the impacts of two prominent *in situ* remediation technologies, thermal treatment and anaerobic bioremediation, on groundwater quality and relevant subsurface processes. Specific objectives of this research were to: 1) identify potential electron donors released following thermal treatment and assess the ability of these substrates to support microbial contaminant degradation; 2) characterize the extent of metal sulfide precipitation and impacts on aquifer permeability; and 3) quantify impacts of pH reduction on bioremediation performance and microbial community structure. Results of this work demonstrate that thermal treatment of soils resulted in electron donors and fermentable substrates (formate, acetate, propionate and butyrate) that were able to support microbial reductive dechlorination of PCE to ethene, reductions in permeability (up to 80%) due to the formation of iron (II) sulfide (FeS) precipitates can restrict or block pore throats and cause preferential flow, and dechlorination of PCE to ethene was possible at pH 5.5 in microcosms, but was not observed in sediment-free enrichment cultures. These research findings provide new information about the impacts of thermal treatment and biostimulation on groundwater quality and biogeochemistry and quality, and demonstrate the potential benefits of combined remedies.

15. SUBJECT TERMS: Chlorinated solvents, tetrachloroethene, thermal treatment, anaerobic bioremediation, combined remedies, reductive dechlorination, iron (II) sulfide, pH, *Dehalococcoides mccartyi*, reductive dehalogenase gene, electron donor, organic acid

16. SECURITY CLASSIFICATION OF:			**17. LIMITATION OF ABSTRACT**	**18. NUMBER OF PAGES**	**19a. NAME OF RESPONSIBLE PERSON**
a. REPORT	**b. ABSTRACT**	**c. THIS PAGE**			Kurt Pennell
UNCLASS	UNCLASS	UNCLASS	UNCLASS	163	**19b. TELEPHONE NUMBER** *(include area code)* 617-627-3099

Standard Form 298 (Rev. 8-98)
Prescribed by ANSI Std. Z39.18

Page Intentionally Left Blank

TABLE OF CONTENTS

LIST OF FIGURES

LIST OF TABLES

LIST OF ACRONYMS, ABBREVIATIONS AND SYMBOLS

Acronyms and Abbreviations

AFB	Air Force Base
Ag^{+}	silver ion
ASTM	American Society for Testing and Materials
bvcA	vinyl chloride reductive dehalogenese gene present in *Dhc*. Strain BAV1
BDI	Bio-Dechlor Inoculum™
Bgs	below ground surface
BLAST	basic local alignment search tool
^{o}C	degrees Celsius
Ca^{2+}	calcium ion
$CaMg(CO_3)_2$	dolomite
$CaSO_4$	calcium sulfate
CCl_4	carbon tetrachloride
C_2Cl_2	dichloroacetylene
C_4Cl_6	hexachlorobutadiene
C_6Cl_6	hexachlorobenzene
CES	Current Environmental Solutions, Inc.
$CHCl_3$	chloroform
$CHOO^{-}$	formate
CH_3COO^{-}	acetate
CH_4	methane
Cl^{-}	chloride ion
Cl_2HC_2OOH	dichloroacetic acid
cm	centimeter
Co^{2+}	cobalt ion
CO	carbon monoxide
CO_2	carbon dioxide
$COCl_2$	phosgene
COH_3COO^{-}	glycolate
$COOHCOO^{-}$	oxalate
CROW	Contained Recovery of Oily Wastes™
CT	carbon tetrachloride
Cu	copper
cis-DCE	*cis*-1,2-dichlororethene
trans-DCE	*trans*-1,2-dichloroethene
DCB	dithionite-citrate-bicarbonate
DCM	dichloromethane
Dhc	*Dehalococoides*
DI	deionized
DNA	deoxyribonucleic acid
DNAPL	dense non-aqueous phase liquid
DO	dissolved oxygen
DOD	Department of Defense
DUS	dynamic underground stripping

ED	electron donor
EGDY	East Gate Disposal Yard
EPICS	equilibrium partitioning in closed systems
EPR	enhanced passive remediation
ERH	electrical resistive heating
Fe	iron
Fe^{2+}	ferrous iron
Fe^{3+}	ferric iron
FeOOH	iron oxide mineral
FeS_2	pyrite
Fe_2O_3	hematite
FID	flame ionization detector
FX	flux meter
g	gram
GC	gas chromatograph
GWERD	Ground Water and Ecosystem Restoration Research
h	hour
H	hydrogen
H^+	hydrogen ion
H_2	hydrogen gas
H_2CO_3	carbonic acid
HFK	Helgeson-Kirkham-Flowers
HP	Hewlett-Packard
HPLC	high pressure liquid chromatograph
HPO	hydrous pyrolysis oxidation
hr	hour
IC	ion chromatograph
ISCO	*in-situ* chemical oxidation
ISCR	*in-situ* chemical reduction
ISTD	in-situ thermal desorption
kg	kilogram
LB	Luria Bertani
M	moles
mg	milligrams
mL	milliliter
mm	millimeter
mM	millimoles
Mg^{+2}	magnesium ion
Mn	manganese
MNA	monitored natural attenuation
MS	mass spectrometer
MSD	mass selective detector
nd	not determined
N_2	nitrogen gas
NAVFAC	Naval Facilities Engineering Command
$NaHCO_3$	sodium bicarbonate

Na_2CO_3	sodium carbonate
$Na_2S_2O_8$	sodium persulfate
NFESC	Naval Facilities Engineering Service Center
NIH	National Institutes of Health
NIST	National Institute of Standards and Technology
NOM	natural organic matter
OD	outside diameter
OW	a mixed, methanogenic, PCE-to-ethene-dechlorinating
PAH	polycyclic aromatic hydrocarbon
PCB	polychlorinated biphenyl
PCE	tetrachloroethene
PCR	polymerase chain reaction
PEEK	polyether ether ketone
pH	logarithm of hydrogen ion activity in solution
PNNL	Pacific Northwest National Laboratories
ppb	parts per billion
ppm	parts per million
ppmv	parts per million, volume basis
PMW	process monitoring well
PTFE	polytetrafluoroethene
PV	pore volume
RNA	ribonucleic acid
rRNA	ribosomal ribonucleic acid
Redox	reduction-oxidation
r^2	correlation coefficient
rpm	revolutions per minute
RSD	relative standard deviation
s	second
S^{2-}	sulfide ion
SER	steam enhanced remediation
SERDP	Strategic Environmental Research Development Program
SO_4^{2-}	sulfate
SPH	Six-Phase Heating™
SRS	Savannah River Site
tceA	trichloroethene reductive dehalogenese gene
TCA	1,1,1-trichloroethane
TCD	thermal conductivity detector
TCE	trichloroethene
USEPA	US Environmental Protection Agency
USACE	US Army Corps of Engineers
UZA	ultra zero grade air
vcrA	vinyl chloride reductive dehalogenese gene
VC	vinyl chloride
VOA	volatile organic analysis
VOC	volatile organic carbon
XRD	X-ray diffraction

Symbols

A	pre-exponential factor in Arrhenius equation
C	concentration
Δ	change
E_a	activation energy
I	ionic strength
k	first-order reaction rate constant
K_d	soil-water distribution coefficient
H	dimensionless Henry's Law constant
M	mass
μ	micro
Ω	ohms
P_o	saturated vapor pressure
R	ideal gas law constant
t	time
$t_{1/2}$	reaction half-life
T	temperature
V	volume

Subscripts

DCEs	dichloroethenes
g	gas
l	liquid
o	initial or saturated
s	solid or soil
sat	saturation
TCE	trichloroethene
VC	vinyl chloride
w	water

KEYWORDS

Chlorinated solvents, tetrachloroethene, thermal treatment, anaerobic bioremediation, combined remedies, reductive dechlorination, iron (II) sulfide, pH, *Dehalococcoides mccartyi*, reductive dehalogenase gene, electron donor, organic acid

ACKNOWLEDGEMENTS

Over the course of this research project, many faculty, staff, and students have contributed their time, energy and thought. This work was truly a collaborative endeavor and could not have been completed without the contributions of the following individuals: Dr. Kurt Pennell (Tufts Univ.), Dr. Natalie Cápiro (Tufts Univ.), Dr. Frank Löffler (Univ. of Tenn), Mr. Tyler Marcet (Tufts Univ.), Dr. Yi Yang (Univ. of Tenn), Mr. Samuel Gaeth (Tufts Univ.), Dr. Jed Costanza (US EPA) and Ms. Suzanne Warner (Tufts Univ,, now U.S. EPA).

Our sincere thanks is extended to the members of the SERDP Scientific Advisory Board for their knowledge, insights and suggestions that helped to focus our work and improved the quality and impact of the project. The SERDP staff has supported us in countless ways, and always responding in a professional and cheerful manner. Our very special thanks are extended to Andrea Leeson, the HGL support staff and the Noblis support staff, whose vision and technical support made this work possible.

ABSTRACT

Although substantial progress has been realized in the remediation and management of hazardous waste sites at Department of Defense (DoD) installations, many sites contain recalcitrant contaminants, such as chlorinated solvents, that often exist in complex hydrogeologic settings. As a consequence, these sites are characterized by failed or protracted remediation efforts, escalating costs with minimal progress toward remedial objectives, and an inability to achieve site closure with reasonable institutional or engineered controls. The unfortunate reality is that for these problematic sites significant amounts of the contaminant mass (> 10%) are likely to remain even after aggressive source zone treatment. As a result, the subsurface remediation paradigm has shifted from the development of stand-alone, "silver-bullet" technologies toward the integration of complementary remediation technologies that can be deployed in parallel (simultaneous) or in series (sequential) to more efficiently address difficult remediation scenarios and meet cleanup goals. However, the potential impacts of *in situ* remediation technologies on long-term groundwater quality and the interactions of source zone treatments on other remedies, such as microbial reductive dechlorination, are not well understood. For example, physical-chemical treatments may alter aquifer geochemistry and the microbial ecology, which could be either detrimental (e.g., aquifer clogging, reduced microbial diversity, undesired by-product formation) or beneficial (e.g., enhanced electron donor availability) to subsequent bioremediation and/or natural attenuation processes.

A.1. RESEARCH OBJECTIVES

The overarching goal of this project was to develop a more complete understanding of the impacts of *in situ* remediation technologies on groundwater quality and relevant subsurface processes. This information is needed to realize the full potential of combined remedies, to more effectively treat difficult hazardous waste sites, and to develop ecologically sound long-term site management strategies. The specific objectives of the project were to: (a) identify secondary impacts of two prominent *in situ* remediation technologies, *thermal treatment* and *anaerobic bioremediation,* on long-term groundwater quality; (b) establish methods to predict the extent of both positive and negative post-remediation impacts on groundwater quality; and (c) develop strategies to overcome, or take advantage, of secondary impacts (e.g., pH reduction, release of electron donor) to achieve both immediate and long-term remedial objectives.

A.2. TECHNICAL APPROACH

The research program was structured around four main tasks that were designed to elucidate the impacts of; (1) *thermal remediation* on groundwater quality and subsequent biological treatment, (2) *electron donor delivery* on metal sulfide formation and associated reductions in aquifer permeability, (3) *pH reductions* on groundwater geochemistry, microbial ecology and activity, (4) *project reporting* and data transfer (Figure A.1). The work was based upon the expertise of the investigators in the areas of thermal treatment (Pennell) and bioremediation (Löffler and Cápiro), and a strong track record of collaborative research to examine complex interactions between biological, physical, and chemical processes, all of which will impact post-remediation groundwater quality. Site specific materials used in the experimental program were selected in consultation with remediation project managers (RPMs) and SERDP/ESTCP personnel.

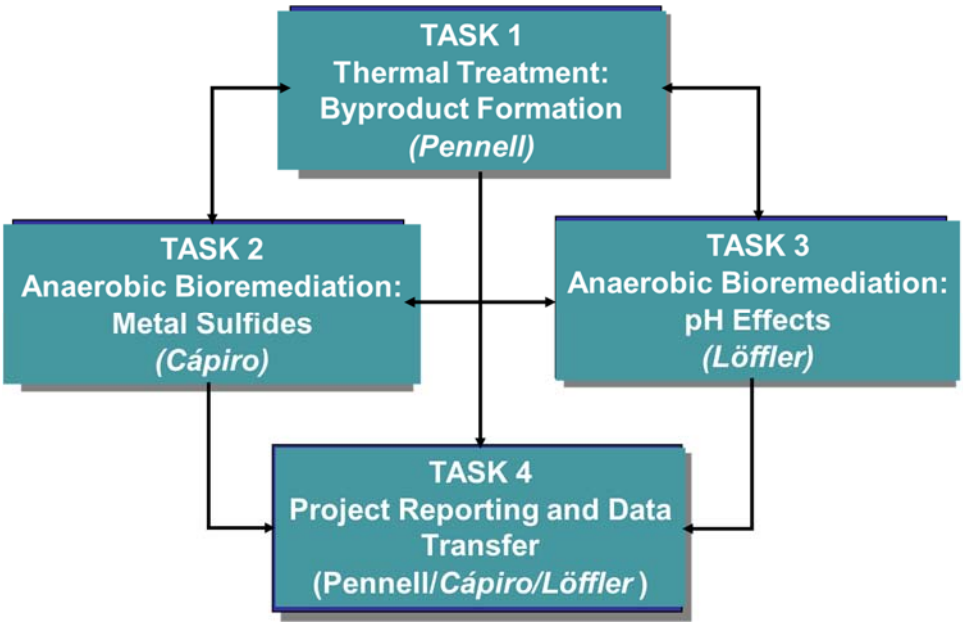

Figure A.1. Schematic flow chart illustrating the relationships between the four project tasks.

A.3. KEY FINDINGS

Task 1: Impacts of Thermal Treatment on Groundwater Geochemistry and Combined Remedies. Results from this work demonstrated that thermal treatment of soils resulted in electron donors and fermentable substrates (formate, acetate, propionate and butyrate) that were able to support microbial reductive dechlorination of PCE to ethene. Additionally, in separate column experiments, low temperature heating (35ºC) improved microbial reductive dechlorination performance, resulting in up to 3.5 times greater dechlorination of PCE to ethene compared to a typical groundwater temperature (15ºC). These observed improvements in microbial reductive dechlorination of PCE during low temperature heating of soil columns were greater than previously reported in batch enrichment culture and microcosm studies.

Task 2: *Impacts of Metal Sulfide Formation and Dissolution on Aquifer Permeability.* Substantial reductions in permeability were observed due to the formation of iron (II) sulfide (FeS) precipitates that restricted or blocked pore throats. Column studies demonstrated that FeS precipitation can cause permeability reductions of up to 80 %, and that this impact is most apparent in soils with high organic carbon content (e.g., 2.4 % w/w). In aquifer cell studies, FeS precipitation caused local reductions in permeability, which led to preferential flow. Following re-establishment of oxic conditions, iron oxide formation resulted in further reductions in permeability and changes in preferential flow paths.

Task 3: *Impacts of Remedial Strategies on pH and Microbial Reductive Dechlorination.* Dechlorination of PCE to ethene occurred at pH 5.5 in some microcosms, but was not observed in sediment-free enrichment cultures. The findings suggest that certain soils have pH buffering capacity and generate micro-environments within aggregates or near the solid-water interface where microbes may experience different pH than in the bulk liquid phase. Further, the PCE-to-

ethene dechlorinating consortium BDI failed to dechlorinate at pH 5.5, but recovered dechlorination activity following pH adjustment to pH 7. The length of low pH exposure (8 to 40 days) affected recovery of dechlorination activity; however, VC, rather than ethene was the dechlorination end product even after short-term pH 5.5 exposure, suggesting that VC-dechlorinating *Dehalococcoides mccartyi* strains are particularly susceptible to low pH inhibition.

A.4. BENEFITS

The research provides site managers, regulatory officials, consultants, and researchers with relevant new information about the impacts of thermal treatment and biostimulation on groundwater biogeochemistry and quality, and demonstrate the benefits of combined remedies. The project served to identify :(a) key secondary impacts of thermal treatment and biostimulation on groundwater quality, (b) strategies to overcome negative impacts (e.g., pH reduction) and to take advantage of positive impacts (e.g., electron donor release), and (c) guidelines for RPMs to effectively implement remedies to achieve ecologically sound and lasting solutions. A number of important conclusions and recommendations can be made from this work, including:

- Thermally-released substrates should be considered as part of a treatment train with enhanced bioremediation, particularly in low-permeability zones where substrate delivery is challenging.

- Low-temperature heating may offer a more sustainable remediation approach over traditional energy-intensive thermal treatment by enhancing microbial activity leading to more complete dechlorination to ethene.
- Local changes in soil permeability and preferential flow could contribute to slower contaminant mass transfer (e.g., dissolution and desorption), which could decrease mass flux and increase source zone longevity. Alternatively, such permeability reductions may increase local residence times, which could facilitate more complete reaction processes, including dechlorination of PCE to ethene.

- The presence of certain soils may provide protection from low pH conditions (< pH 6) potentially due to soil cation exchange capacity (CEC), and rebound from low pH exposure is possible, although complete recovery of VC to ethene reductive dechlorination may be irreversibly impacted.

- Members of the *Sulfurospirillum* genus contribute to PCE dechlorination under low pH condition.

CHAPTER 1

INTRODUCTION

1.1. PROJECT BACKGROUND AND JUSTIFICATION

Chlorinated organic solvents, such as tetrachloroethene (PCE) and trichloroethene (TCE), are common pollutants at Department of Defense (DoD) facilities and manufacturing complexes, and represent one of the most difficult remediation scenarios facing site managers. The distribution of contaminants at chlorinated solvent sites typically encompasses a highly concentrated *source zone* and a lower concentration zone that includes a *dissolved solute plume* and *sorbed-phase contaminants*. The source zone frequently contains liquid solvent (free product), commonly referred to as a non-aqueous phase liquid (NAPL) that exists as discrete ganglia entrapped within the pore space and higher-saturation "pools" residing above low permeability lenses or confining layers (Figure 1.1.1). Excluding petroleum contamination arising from underground storage tanks, there are an estimated 30,000 to 50,000 sites with groundwater contamination in the U.S. (Kavanaugh et al. 2003, NRC 2013), and approximately 80% of these sites are contaminated with organic chemicals. Of these sites, approximately 60% are suspected of containing NAPLs. As groundwater flows through the source zone, contaminants slowly dissolve into the aqueous phase, and due to the combination of low aqueous solubility and mass transfer limitations, NAPL source zones often serve as long-term sources of groundwater contamination that may persist for decades or even centuries. To achieve substantial NAPL mass removal or reduction within acceptable time frames, several *in situ* remediation technologies have been developed and implemented in the field, including chemical oxidation, thermal treatment, air sparging, bioremediation, co-solvent flushing, and surfactant flushing (Christ et al. 2005b, NRC 2004, Stroo et al. 2012, Stroo et al. 2003).

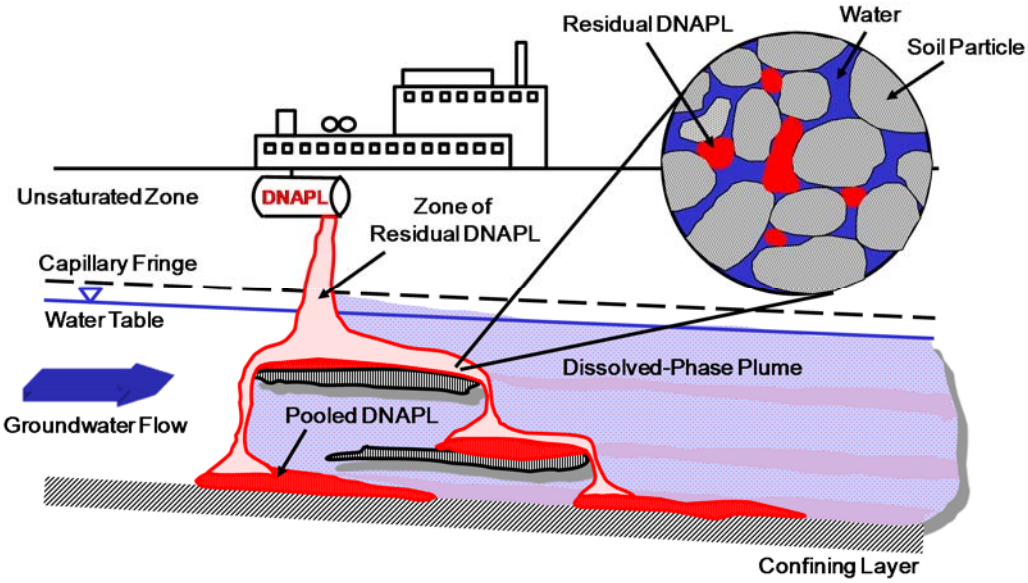

Figure 1.1.1. Schematic of a typical chlorinated solvent spill of DNAPL that is characterized by pooled and entrapped ganglia zones.

Although substantial progress has been realized in the application of these technologies, varied levels of success have been achieved in the field, especially at sites with complex hydrogeology and recalcitrant contaminants (AATDF 1997, NRC 2013). Even under ideal conditions, significant amounts of the initial contaminant mass (10-40%) are likely to persist even after aggressive source zone treatment. The remaining NAPL will continue to serve as a source for the down-gradient groundwater plume, and lasting remedial success typically requires removal or destruction of contaminant mass existing in the source zone. As a consequence, it is now widely recognized that even successful implementation of *in situ* remediation technologies is unlikely to completely remove all of the contaminant mass from most source zones. In fact, aggressive source zone treatments can increase the mobility and distribution of the residual contaminant mass in the short term, which may lead to an initial increase in aqueous phase concentrations. As a result, attention has shifted away from developing the most effective stand-alone technology, and instead, toward the development and testing of complementary *in situ* remediation technologies that can be combined, at the same time (in parallel) or sequentially (in series) to more effectively treat contaminant source zones (Figure 1.1.2) (Amos et al. 2007b, Cápiro et al. 2015, Christ et al. 2005a, Costanza et al. 2005, Fletcher et al. 2011b, Friis et al. 2006, Friis et al. 2007, Ramsburg et al. 2004). In a sequential or "treatment train" approach, an aggressive *in situ* treatment technology, such as electrical resistive heating (ERH) or surfactant flushing, is used to remove significant contaminant mass in a relatively short time-frame, while a second "polishing" technology is then applied to remove or detoxify the remaining contaminant mass. Such sequential remediation strategies have the potential to take advantage of efficient mass removal achieved by aggressive treatment technologies, while addressing limitations associated an individual technology (e.g., flow bypassing) that lead to incomplete mass removal.

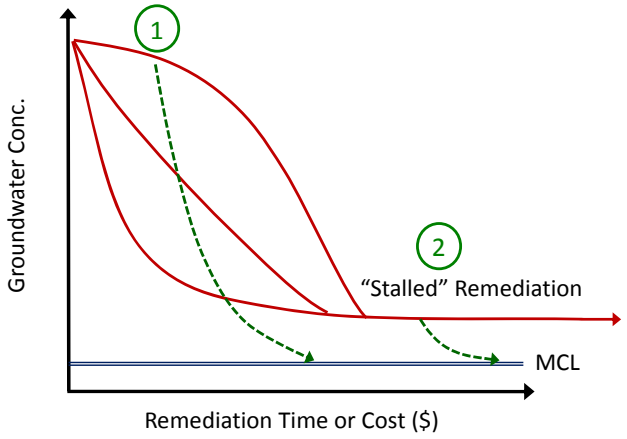

Figure 1.1.2. Conceptual diagram of reduction in contaminant levels versus time or cost, illustrating the potential use of combined remedies (1) in parallel to improve effectiveness and (2) in series to achieve remediation goals at "stalled" sites.

In addition to the need for new approaches to achieve source zone remediation, the secondary impacts of *in situ* remediation treatment technologies on groundwater quality, effectiveness of combined remedies, and long-term site management strategies are not well understood (Stroo et al. 2012, Stroo et al. 2003). Physical-chemical treatments may alter aquifer geochemical conditions and the microbial ecology, both of which can be detrimental (e.g., aquifer clogging, reduced microbial diversity) or beneficial (e.g., enhanced electron donor availability, increased chemical reactivity) to subsequent remediation and/or natural attenuation processes (Christ et al. 2005a, Stroo et al. 2003). For example, a frequently considered polishing technology is microbial reductive dechlorination, which can be coupled with thermal treatment, surfactant and/or co-solvent flushing. The propensity ERH to release electron donor has been demonstrated in prior work (Costanza et al. 2009, Friis et al. 2005), although bioaugmentation may still be required to sustain microbial reductive dechlorination activity (Friis et al. 2006). Unfortunately, current

subsurface remediation technologies do not take advantages of such synergistic effects and their stand-alone implementation may degrade groundwater quality through formation of undesirable reaction byproducts (e.g., vinyl chloride, phosgene), release of toxic metals (e.g., pH-mediated dissolution), and production of greenhouse gases (e.g., methane).

The above discussion indicates the need to understand, at a mechanistic level, the potential positive and negative impacts of *in situ* remediation technologies on groundwater quality, and more specifically, on processes that control the successful implementation of polishing remedies and long-term performance of monitored natural attenuation. Thus, the overall goal of this project was to project was to develop a more complete understanding of the impacts of in situ remediation technologies on groundwater quality and relevant hydrodynamic, geochemical and biological processes. Within this framework, we conducted a matrix of well-controlled laboratory scale studies to elucidate the secondary impacts of two prominent in situ remediation technologies, *thermal treatment* and *microbial reductive dechlorination*. To achieve the project objectives, the research activities were divided into three tasks that addressed questions associated with the release of potential electron donors (and/or precursors) following thermal treatment (Task 1), effects of metal sulfide formation on aquifer permeability and remediation (Task 2), and the implications of pH reductions on organohalide respiring bacteria growth and activity (i.e., reductive dechlorination) (Task 3). The specific background to address each of these research areas is described below.

1.2. PROJECT OBJECTIVES

The overarching goal of this project was to develop a more complete understanding of the impacts of *in situ* remediation technologies on groundwater quality and relevant hydrodynamic, geochemical and biological processes. This information is needed to realize the full potential of *in situ* remediation technologies, including combined remedies, more effectively treat difficult hazardous waste sites, and develop more effective, long-term site management strategies. The specific objectives of the project are to:

- Identify secondary impacts of two prominent *in situ* remediation technologies, *thermal treatment* and *anaerobic bioremediation,* on groundwater quality;
- Establish methods to predict the extent of both positive and negative post-remediation impacts on groundwater quality; and
- Develop strategies to overcome, or take advantage, of secondary impacts (e.g., pH reduction, release of electron donor) to achieve both immediate and long-term remedial goals.

1.3. TECHNICAL APPROACH

The research program was structured around three main tasks that were designed to elucidate the impacts of; (1) *thermal remediation* on groundwater quality and subsequent biological treatment, (2) *electron donor delivery* on metal sulfide formation and associated reductions in aquifer permeability, and (3) *pH reductions* on groundwater geochemistry, microbial ecology and activity.

1.3.1. Impacts of Thermal Treatment on Groundwater Geochemistry and Combined Remedies (Task 1)

In situ thermal treatment has been implemented at a number of sites for source zone remediation, with reported contaminant mass recoveries of greater than 90% in many cases (ESTCP 2009, USEPA 2004). Compared to other *in situ* remediation technologies discussed in this chapter, thermal treatment provides two distinct advantages; (1) no chemicals are introduced into the subsurface, and (2) the potential to efficiently treat low-permeability, heterogeneous porous media (Davis 1997). Although cost data are often difficult to obtain, *in situ* thermal treatment technologies are expensive, primarily due to infrastructure (e.g., heater wells, extraction and above-ground treatment systems) and energy costs. As a result, thermal treatment technologies are most often implemented at sites where other *in situ* remediation technologies have failed, or where low-permeability media and/or subsurface heterogeneity clearly limits the effectiveness of competing technologies, particularly those that rely on the delivery or flushing of chemical agents. Nevertheless, a steady number of source zone sites are treated each year using *in situ* thermal remediation technologies. In addition, recent advances in the use of coupled thermal technologies (Heron et al. 2005, Heron et al. 2009) and the potential for enhanced contaminant reactivity (Truex et al. 2007) suggest that thermal remediation will continue to play an important role in treatment of highly-contaminated source zones, particularly at hazardous waste sites containing low permeability media.

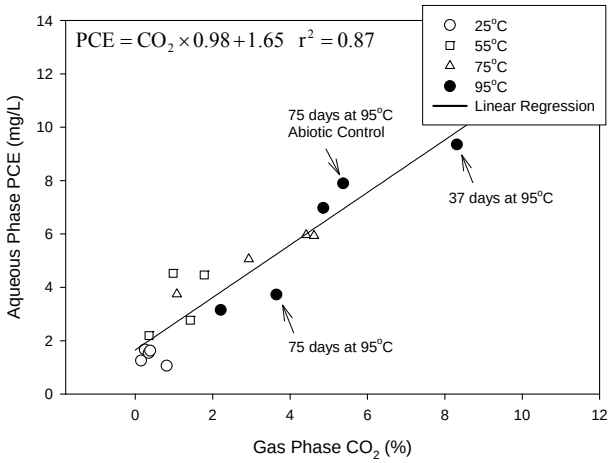

Figure 1.3.1. Correlation between aqueous phase PCE and gas phase CO_2 concentrations in ampules with Camelot soil and groundwater (Costanza and Pennell, 2007).

Despite the success of thermal technologies, the effects of subsurface heating on aquifer geochemistry and groundwater quality have received only minimal attention. Laboratory-scale studies conducted under SERDP Project ER-1419 indicate that heating contaminated soils to temperatures of up to 95 ^oC can result in the breakdown of carbonate minerals and organic matter, leading to the release of bound contaminants and the evolution of CO_2, organic acids and hydrogen (Figure 1.3.1) (Costanza et al. 2005, Costanza and Pennell 2007). However, the extent of this behavior, and the specific soil constituents that contributed to the formation of the compounds, is not known. Even with careful design, incomplete contaminant mass removal during thermal treatment remains a pressing concern, particularly at sites characterized by strongly heterogeneous and low-permeability media. We also found that even after prolonged heating (100-200 days at 95°C), a substantial fraction of the chlorinated ethene mass remained in the solid phase, requiring multiple solvent extractions to achieve complete mass recovery. This behavior was most apparent in soil collected from site undergoing ERH that contained relatively high clay and silt contents, and could lead to contaminant rebound following thermal treatment.

These results suggest that an additional treatment or "polishing" step may be necessary to achieve remedial goals at thermal treatment sites. However, the impacts soil heating on the near-

and long-term performance of microbial reductive dechlorination has received only limited attention. *In situ* heating will impact microorganisms in the vicinity of the treatment zone, resulting in an overall decline in cell numbers and changes in composition of the microbial community, as non-heat-tolerant microbes and non-spore formers are significantly reduced in numbers or eliminated (Friis et al. 2006). In work by Fletcher et al. (2011a), the PCE-dechlorinating consortia BDI and OW produced ethene when incubated at temperatures of 30 °C, but vinyl chloride (VC) accumulated when cultures were incubated at 35 or 40 °C. Cultures incubated at 40 °C for less than 49 days resumed VC dechlorination following cooling; however, incubation at 45 °C resulted in complete loss of dechlorination activity (Fletcher et al. 2011a). Furthermore, *Dehalococcoides mccartyi* (*Dhc*) 16S rRNA, bvcA, and vcrA gene abundances in these cultures showing complete dechlorination to ethene at 30 °C exceeded those measured in cultures incubated at higher temperatures, consistent with observed dechlorination activities.

However, thermal treatment also holds the potential to release organic acids and hydrogen gas (Costanza et al. 2009, Fletcher et al. 2011b, Friis et al. 2006), providing excellent conditions for microbial colonization of the open niches when temperatures decrease following periods of active heating. In the study by Fletcher et al. (2011b), H_2 was detected in autoclaved soil batch reactors following heating above 24°C (Figure II.3.1). However, the same study also demonstrated in biologically-active microcosm reactors that temperatures >35°C inhibited reductive dechlorination activity in Great Lakes, IL and Ft. Lewis, WA site materials, and that the majority of reducing equivalents released from the soil matrix during heat treatment are consumed in methanogenesis rather than reductive dechlorination (Figure 1.3.2) (Fletcher et al. 2011b). Experiments performed under SERDP Project ER-1419 suggest that aceticlastic and hydrogenotrophic methanogenic *Archaea* are highly competitive populations during the cool-down phase, and thus, excessive methane formation is a likely consequence of re-colonization following thermal treatment. This outcome is not desirable because gas formation may cause aquifer clogging, methane is a greenhouse gas, and methanogenic activity consumes electron donors, thereby limiting the activity of dechlorinating microorganisms and detoxification of residual chlorinated contaminant mass. Thus, the primary objectives of Task 1were to: (1) quantify the magnitude and rate of organic acid, hydrogen, and other compound generation and/or release as a function of soil properties and treatment temperature, (2) assess the response of relevant native and augmented microbial populations to thermally-induced release of electron donors in parallel (i.e., lower-temperature zones) and sequentially (i.e., bioaugmented following temperature reduction) operated systems, and (3) assess the benefits and limitations of low temperature heating on organohalide respiration.

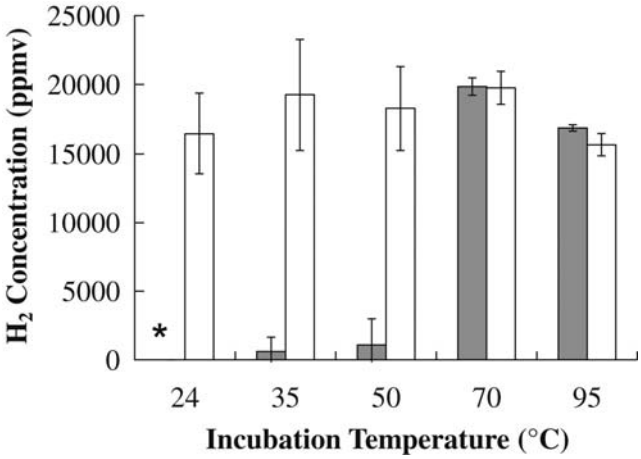

Figure 1.3.2. H_2 concentrations in live (filled bars) and autoclaved (open bars) Ft. Lewis microcosms after 28 days of incubation (Fletcher et al. 2011b).

1.3.2. Effects of Metal Sulfide Formation and Dissolution on Aquifer Permeability (Task 2)

Anaerobic bioremediation typically relies on external electron donor additions (biostimulation), often combined with inoculation with dechlorinating consortia (bioaugmentation). Oxidized metal species, such as ferric iron (Fe^{3+}) are prevalent in subsurface aquifer environments. Electron donor additions will stimulate ubiquitous metal-reducing bacteria (i.e., *Geobacter* spp.) and generate reduced metal species such as ferrous iron, Fe^{2+}. Freshwater sulfate concentrations are generally low (< 15 mg/L), but elevated levels of sulfate due to natural conditions or anthropogenic inputs are common in chlorinated solvent contaminated aquifers, and electron donor addition will stimulate sulfate-reducing bacteria (SRB) to produce sulfide. SRB reduce sulfate to hydrogen sulfide and are ubiquitous in anaerobic sediments and subsurface environments. SRB use a variety of organic compounds and hydrogen as electron donors, and many, but not all, SRB can oxidize acetate ion (CH_3COO^-) (equation II.1).

$$SO_4^{2-} + CH_3COO^- + 3H^+ \rightarrow H_2S + 2CO_2 + 2H_2O \qquad (1.3.1)$$

The hydrogen sulfide exists predominantly as HS^- at circumneutral pH and reacts with divalent dissolved metal ions, such as Fe^{2+}, to form insoluble iron(II) monosulfide (FeS) and iron(II) disulfide or pyrite (FeS_2) (equation II.2).

$$HS^- + Fe^{2+} \rightarrow FeS + H^+; \; FeS + H_2S \rightarrow FeS_2 + 2H^+ + 2e^- \qquad (1.3.2)$$

FeS has a very low solubility product and precipitates as black colloids (Ogata and Bower 1965), which bind strongly to humic and organic matter (Ford et al. 1968). Depending on the extent of sulfate and ferric iron reduction, iron(II) sulfide precipitates can block pore spaces, altering groundwater flow paths (e.g., bypassing), especially following biostimulation. Flow bypassing can potentially cause issues for contaminant dissolution and electron donor delivery, which could increase source zone longevity and corresponding remediation costs. Alternatively, increased hydraulic residence time has been shown to stimulate the growth and activity of *Dehalococcoides mccartyi* strains (Cápiro et al. 2015, Zheng et al. 2001).

While the potential for clogging is evident, especially in the presence excess soil organic matter (Daniels and Cherukuri 2005, van Beek 1984), some reports argue that hydraulic conductivity is not altered by FeS formation; however, many of these studies were performed in clean sand columns (Kristiansen 1981) and low amounts of FeS (<0.4%), which has been shown to be a cutoff for clogging to occur (Laak 1970). Additional studies clearly linked clogging with SRB activity and growth (Daniels and Cherukuri 2005, Ford et al. 1968, Mitchell and Nevo 1964, Wood and Bassett 1975).

Previous 1-D column and two-dimensional (2-D) aquifer cell experiments performed under SERDP Project ER-1293 demonstrated that biostimulation and bioaugmentation enhances rates of DNAPL dissolution and chlorinated ethene dechlorination (Amos et al. 2009a, Cápiro et al. 2015). However, aquifer cells with microbial activity turned visually black due to the formation of metal sulfides (Figure 1.3.3). These laboratory systems contained very small amounts of sulfur compounds (<0.2 mM) introduced with the medium and ferric iron present as impurities on the quartz sand. Nevertheless, formation of iron sulfides (FeS) was readily observed visually, and resulted in a 65 ± 11% reduction in the permeability of the aquifer cell (Cápiro et al. 2015). Ferric iron minerals are widely distributed in subsurface environments and many contaminated aquifers contain significant amounts of sulfate. Hence, it is highly probable that iron sulfide formation will occur at sites undergoing biostimulation, which may result in reduced aquifer permeability and flow bypassing. Since modeling efforts aimed at predicting contaminant behavior and fate use flow patterns determined prior to biostimulation, altered (i.e., reduced) groundwater flow and

bypassing due to FeS formation have the potential to markedly impact system performance, generate inconsistencies between measured data and model predictions, bias monitoring efforts, and compromise remedial success, including long-term remediation performance and groundwater quality.

FeS formation requires anoxic conditions, which will occur during biostimulation and subsequent fermentation activities; however, post-treatment redox conditions are likely to fluctuate and FeS will be exposed to oxic conditions (i.e., intrusion of aerobic groundwater) (Herczeg et al. 2004). Biotic and abiotic mechanisms contribute to FeS and FeS_2 oxidation; however, the impacts of iron sulfide dissolution on long-term aquifer permeability and groundwater geochemistry are poorly understood. To address these knowledge gaps, Task 2 was designed to investigate the impacts of FeS formation and dissolution on aquifer permeability in controlled laboratory experiments using columns and aquifer cells using a range of porous media with different permeabilities, organic carbon contents.

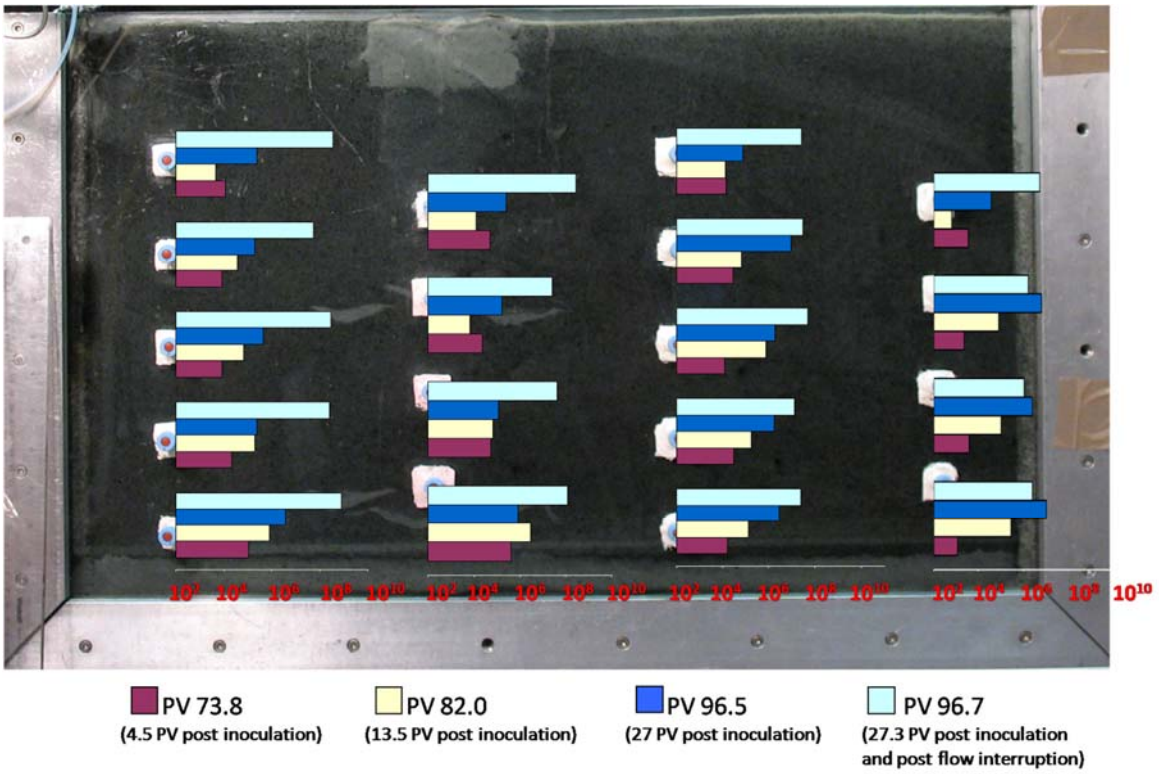

Figure 1.3.3. Background showing iron sulfide formation in 2-D aquifer cell 4.5PVs following bioaugmentation with imposed plots of spatial and temporal distribution of total *Dehalococcoides mccartyi* strains (log scale = 10^2-10^{10} gene copies per mL). Adapted from Cápiro et al. (2015).

1.3.3.. Impacts of Remedial Strategies on pH and Microbial Reductive Dechlorination (Task 3)

Groundwater pH is a major determinant of microbial activity and ecology, as well as the geochemical composition of aquifers. Generally, the solubility of many metals and metalloids increases with decreasing pH, and dissolved concentrations may exceed regulatory standards or impact desirable microbial processes (Aguilar-Hinojosa et al. 2016, Equeenuddin et al. 2013, Gadd and Griffiths 1978, Giller et al. 1998, Olaniran et al. 2013, Ruggiero et al. 2005). The activities of major microbial groups including nitrate reducers, sulfate reducers, metal reducers and methanogens are affected by pH and dissolved toxic metal species, indicating that pH changes have major impact on groundwater geochemistry. Further, the known chlorinated ethene-detoxifying bacteria are active at circumneutral pH (Table II.4.1); specifically, *Dehalococcoides mccartyi* that is solely responsible for complete transformation to ethene has been shown to have reduced dechlorination activity or no growth occurs when the pH drops below 6.5 or 6.0, respectively (Löffler et al. 2013). Based on the information reported in the literature, the known dechlorinators are neutrophils and grow under circumneutral pH conditions.

All *in situ* treatments acting on chlorinated organic compounds release the chlorine substituent as hydrochloric acid, HCl (McCarty et al. 2007). In groundwater, HCl deprotonates immediately to form inorganic chloride (Cl^-) and protons (H^+), which react with water to form the hydronium ion H_3O^+. The relative abundance of H_3O^+ to hydroxide ions (OH^-) determines the solution pH, and thus, the pH may decrease in aquifers with low buffering capacity during active microbial reductive dechlorination. Such scenarios are commonly observed in source zones where remedial actions liberate large amounts of HCl (Aziz et al. 2013). Other significant sources of acidity are fermentation processes that generate organic acids and CO_2 (Adamson et al. 2004, Cope and Hughes 2001, Ohnishi et al. 2012). Biostimulation with fermentable substrates is a common approach to establish low redox conditions and increase the flux of hydrogen, both of which are requirements for the activity of chlorinated ethene-detoxifying *Dehalococcoides mccartyi* bacteria. A variety of organic substrates, including alcohols, organic acids, emulsified vegetable oil (EVO), and complex organic materials (e.g. molasses, corn cobs, newsprint, wood chips, microbial biomass, chitin, etc.) have been supplied as sources of reducing equivalents (AFCEE 2004) and have been shown to cause acidification due to the production of organic acids (Leeson et al. 2004, Robinson et al. 2009).

To date, no microorganisms capable of growth with chlorinated ethenes at pH 5.5 or below have been described. Also, information is lacking how pH shifts (e.g., pH decreases following biostimulation) affect microbial community structure and function. Thus, the primary objectives of Task 3 were to: (1) determine the pH range of existing pure and mixed cultures capable of dechlorinating chlorinated ethenes, (2) enrich and isolate PCE dechlorinating microorganisms from low pH sites, (3) assess the effects of exposure duration to subsequent recovery by a PCE-to-ethene dechlorination consortium in laboratory biotic batch reactors, and (4) evaluate the effects of solids on pH tolerance and reductive dechlorination at pH 5.5.

Table 1.3.1. Ranges of pH values for optimal growth of dechlorinating bacteria.

Bacteria	Optimal pH range	Reference
Geobacter lovleyi strain SZ	6.5-7.5	(Sung et al. 2006)
Desulfitobacterium sp. strain Y51	6.5-7.5	(Suyama et al. 2001)
Desulfuromonas chloroethenica strain TT4B	6.5-7.4	(Sung et al. 2003)
Desulfuromonas michiganensis strain BB1	6.8-8	(Sung et al. 2003)
Sulfurospirillum multivorans	7~7.5	(Scholz-Muramatsu et al. 1995)
Dehalococcoides mccartyi	6~8	(Löffler et al. 2013)

1.4. REPORT ORGANIZATION

This report provides a comprehensive description of experimental systems, analytical methods and corresponding results obtained from the research performed during this project. The organization of chapters within this report is consistent with SERDP final technical report guidance and includes the following sections:

1. Introduction
2. Materials and Methods
3. Results and Discussion
4. Conclusions and Implications

Within the Materials and Methods and Results and Discussion sections, specific activities and research findings are organized under each of the three tasks described above.

CHAPTER 2

MATERIALS AND METHODS

2.1. IMPACTS OF THERMAL TREATMENT ON GROUNDWATER GEOCHEMISTRY AND COMBINED REMEDIES (TASK 1)

2.1.1. Identification of Byproduct Formation during Heated Ampule Experiments

2.1.1.a. Chemicals and gases

Ion chromatography (IC) standard solutions were prepared using reagent grade or higher purity sodium salts: acetate (EMD Millipore, Billerica, MA); butyrate (Alfa Aesar, Ward Hill, MA); formate; and propionate (Sigma-Aldrich Co., St. Louis, MO). Nitric acid (Certified ACS Plus, 70%) used in ampule preparation was obtained from Fisher Scientific (Fair Lawn, NJ). Mercury (II) chloride salt (ACS Reagent, 99.5+ %) used in biologically-inhibited experiments was obtained from Acros Organics (Morris Plains, NJ). All gases used in ampule preparation, sampling, and analyses were of ultra-high purity and obtained from Airgas (Radnor Township, PA).

2.1.1.b. Soils and humic materials

Eleven solids representing a range of total organic carbon (TOC) content and carbon structure were selected for use in the ampule incubation experiments (Table 2.1.1). The solids included Federal Fine Ottawa sand (US Silica Company, Berkeley Spring, WV); Appling soil (University of Georgia Agricultural Experiment Station, Eastville, GA); Webster soil (Iowa State University Agricultural Experiment Station, Ames, IA); Arkport soil; Hudson soil; and Marden soil (Cornell University, Ithaca, NY). Two soil samples (Fort Lewis, WA and Groveland, MA) were obtained from contaminated field sites prior to undergoing electrical resistive heating (ERH). Three reference soils were obtained from the International Humic Substances Society (IHSS, St. Paul, MN); Elliott silt loam soil (Joliet Army Ammunition Plant, Joliet, IL), Gascoyne Leonardite (Gascoyne Mine, Gascoyne, ND), and Pahokee Peat soil II (University of Florida Everglades Research & Education Center, Belle Glade, FL). Four freeze-dried humic and fulvic acid standard materials were also obtained from the IHSS; Suwannee River fulvic Acid Standard II, Pahokee Peat humic acid standard, Elliott Soil humic acid standard, and Gascoyne Leonardite humic acid standard.

Table 2.1.1. Properties and amounts of soils and humic materials used in the ampule incubation experiments.

Solid phase	OC (% weight)	COOH ($mmol/g_s$)	Solid mass per ampule in Set: #1	#2	#3	#4	#5
Federal Fine Ottawa sand	0.01	nd	15 g	15 g	-	-	15 g
Groveland aquifer material	0.01	nd	15 g	15 g	-	-	15 g
Appling soil	0.66	0.02[b]	10 g	10 g	-	-	10 g
Webster soil	1.97	0.08[b]	10 g	10 g	-	-	10 g
Arkport soil	0.32	nd	-	-	-	-	10 g
Hudson soil	1.14	nd	-	-	-	-	10 g
Mardin soil	1.42	nd	-	-	-	-	10 g
Suwannee River fulvic acid standard II	52.34[a]	5.81[a]	-	-	7 mg	-	-
Pahokee peat humic acid standard	56.37[a]	5.02[a]	-	-	8 mg	-	-
Elliott soil humic acid standard	58.13[a]	4.77[a] 4.51[b]	-	-	8 mg	-	-
Leonardite humic acid standard	63.81[a]	4.64[a] 4.16[b]	-	-	8 mg	-	-
Elliott silt loam soil	2.86	0.07[b]	-	-	-	8 g	8 g
Pahokee peat soil II	46.90[a]	nd	-	-	-	3 g	3 g
Gascoyne leonardite	50.11	1.14[b]	-	-	-	3 g	3 g

nd = not determined. Values determined at Tufts University unless specified otherwise: (a) International Humic Substances Society, (b) University of Georgia.

2.1.1.c. Preparation of batch reactors

Five sets of thermal incubation experiments were performed in 20 mL borosilicate glass ampules (Kimble-Chase, Vineland, NJ). Set #1 was designed to identify and quantify VFAs and hydrogen released during soil heating. Set #2 served as an abiotic control to assess VFA and hydrogen release when microbial activity was suppressed (i.e., $HgCl_2$-amended ampules). Sets #3 and #4 were designed to investigate the role of organic carbon structure in thermally induced VFA and hydrogen release. Set #5 was designed to identify and quantify VFA and hydrogen release following prolonged incubation at high temperature.

Prior to loading, the ampules were soaked overnight in a 10% by volume nitric acid solution, rinsed with 18.2 MΩ water, covered with aluminum foil, autoclaved at 121 °C for 30 minutes, and oven-dried overnight at 110 °C. To facilitate ampule loading, the solids (excluding humic and fulvic standard materials) were dried for at least 48 hours in a glass desiccator containing drierite desiccant (W.A. Hammond, Xenia, OH) under a 750 mm Hg vacuum. The solid phases were then passed through a sterilized #30 sieve (ASTM), with the exception of Fort Lewis soil, which was passed through a #5 sieve (ASTM). IHSS soils and standard materials were used as received.

Ampules used in sets #1 and #3-5 were loaded with porous media according to Table 2.1.1, followed by the addition of 10 mL of sterile (autoclaved), degassed 18.2 MΩ water. Ampules in set #2 were prepared similarly, except that the aqueous phase was supplemented with 2 mM $HgCl_2$ to inhibit microbial activity. Loaded ampules were then purged with filter-sterilized (0.22 μm) argon gas and flame-sealed using a Bernzomatic MAPP/oxygen torch (Worthington Industries, Columbus, OH) or a propane/air Twin Jet ampule sealer (Adelphi, West Sussex, UK). Method blanks containing no porous media were prepared for each ampule set. All batch experiments were prepared in triplicate or greater.

2.1.1.d. Reactor incubation and sampling

Sealed ampules were placed in a dark 30 °C constant temperature room, 60 °C water bath or incubator (Thermo Scientific, Waltham, MA), or at 90 °C in a recirculating water bath (VWR International, Westchester, PA) or oven (Fisher Scientific, Fair Lawn, NJ). Intact ampules were destructively sampled following an established procedure (Costanza et al., 2009) after incubation periods of: 28, 42, and 56 days (sets #1 and #2); 7, 14, 21, and 28 days (set #3); 7, 21, 42, and 70 days (set #4); or 180 days (set #5). The ampules were gently inverted and opened at the pre-scored neck. An argon stream (15 mL/min) was then directed toward the open neck of each ampule, while a 5 mL headspace sample was collected over 30 seconds in a gastight syringe (Hamilton Co., Reno, NV). Headspace samples were immediately injected into a gas chromatograph (GC) equipped with a thermal conductivity detector (TCD) for hydrogen analysis. The aqueous phase from each ampule was transferred to a sterile polypropylene microcentrifuge tube and placed in a -80 °C freezer for subsequent VFA analysis.

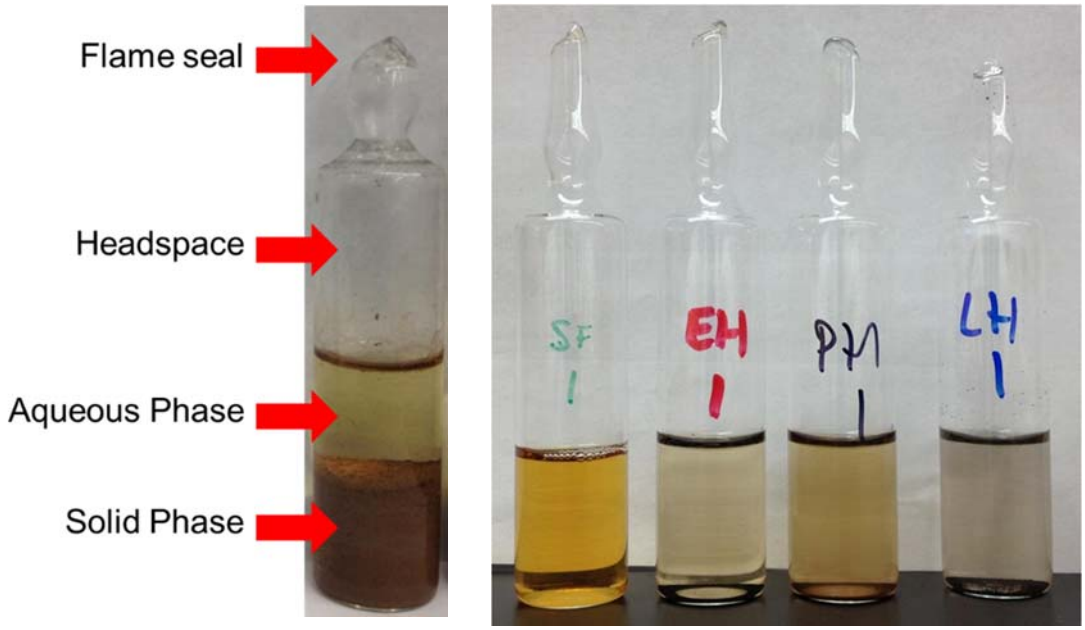

Figure 2.1.1. Images of flame-sealed glass ampules containing gas, aqueous and solid phases.

2.1.1.e. Analytical methods

Permanent gases (carbon dioxide, carbon monoxide, hydrogen, and methane) were measured using a Hewlett-Packard model 6890 GC-TCD (Agilent Technologies, Santa Clara, CA). Gas samples were manually injected to fill a 250 µL sample loop connected to a six port gas sampling valve operated at 120 °C. After 0.2 minutes, the gas sample was transferred to the inlet, operating at 200 °C with a 1:1 split ratio, then onto a Supelco Carboxen 1010 PLOT capillary column (Sigma-Aldrich, St. Louis, MO) with 320 µm mean outer diameter and 30 m length. The GC oven was held at an initial temperature of 30 °C for 4.5 minutes, followed by a +50 °C/min ramp to 130 °C, which was maintained for 3 minutes until the end of the run. Argon flowing at 2 mL/min was used as the carrier gas to optimize hydrogen sensitivity of the TCD, which was operated at 230 °C with argon reference and makeup flows of 20 and 7 mL/min, respectively. Calibration standards

for the GC-TCD were prepared by diluting a custom gas mixture containing 20% carbon dioxide, 5% carbon monoxide, 5% hydrogen, and 20% methane in a 100 mL gastight syringe (Hamilton Co., Reno, NV), using argon as the diluent. Method detection limits were determined according to the procedure described by Hubaux & Vos (1970), assuming a total confidence level of 99%. The method detection limits for carbon dioxide, carbon monoxide, hydrogen, and methane were 60, 70, 30, and 60 ppmv (mg/L by volume), respectively.

Organic acids (formate, acetate, propionate, butyrate, and lactate) in aqueous samples were measured using a Dionex ICS-2000 or Thermo Fisher ICS-2100 IC. The IC was equipped with a Dionex IonPac AS11-HC analytical column (Thermo Fisher Scientific, Waltham, MA) that was optimized for the separation of organic anions and held at a constant temperature of 35 °C, as well as an anion self-regenerating suppressor operated at 112 mA. The IC was operated with a constant flow rate of 1.5 mL/min and a variable potassium hydroxide eluent concentration that was held at an initial concentration of 1 mM for 25 minutes, ramped up to 30 mM from 25 to 54 minutes, then ramped down to 1 mM until the run ended at 56 minutes. IC calibration standards were prepared by diluting a stock solution containing 2 mM of each organic acid. The method detection limit for each organic acid was approximately 1 μM.

2.1.2. Abiotic Electrical Resistive Heating (ERH) Columns

A column study was completed to assess VFA mobility and availability down-gradient of a heated zone during thermal treatment. A borosilicate glass chromatography column was packed with Webster soil up-gradient and Federal Fine Ottawa sand down-gradient. The Webster soil zone was heated to imitate thermal treatment temperatures while aqueous and gas samples were collected from the down-gradient zone throughout the experiment.

2.1.2.a. Materials

IC standards were prepared with sodium lactate and sodium salts: acetate (≥99%; EMD); butyrate (≥98%; Alfa Aesar); formate (≥99%; Sigma); and propionate (≥99%; Sigma). GC standards used in hydrogen and methane analyses were of ultra-high purity and obtained from Airgas (Radnor Township, PA). Descriptions and properties of Webster soil and Federal Fine Ottawa sand are provided in Section 2.1.1.b.

2.1.2.b. Column design and preparation

The column experiment, designed to assess electron donor availability down-gradient of a heated soil zone, was completed using a horizontally-oriented borosilicate glass chromatography column (90 cm length × 5 cm i.d.; Ace Glass, Vineland, NJ). The up-gradient 30 cm was packed with Webster soil (30-mesh; Ames, IA), a silty clay loam with 1.97% OC content(Wang et al. 2010). The first 20 cm of this up-gradient segment made up the heated zone, which contained approximately 500 g of soil and had a pore volume (PV) of approximately 175 mL; all references to PV within this section are with respect to this value. The down-gradient 60 cm of the column was packed with sterile Federal Fine Ottawa sand (U.S. Silica, Frederick, MD), a 30 – 140 mesh quartz sand with <0.01% TOC content. Upper and lower sides of the down-gradient zone were equipped with six evenly distributed ports and fixed stainless steel needles to facilitate *in situ* sampling and temperature monitoring (Figure 2.1.2). Needles were installed in the upper ports to collect gas-phase samples and did not penetrate the sand. Needles placed in the lower ports extended 2.5 cm beyond the inner wall of the column to the center of the sand pack and were used

to collect aqueous-phase samples. Ports were sealed with Teflon Mininert syringe valves (Valco Instruments, Houston, TX) between sampling events.

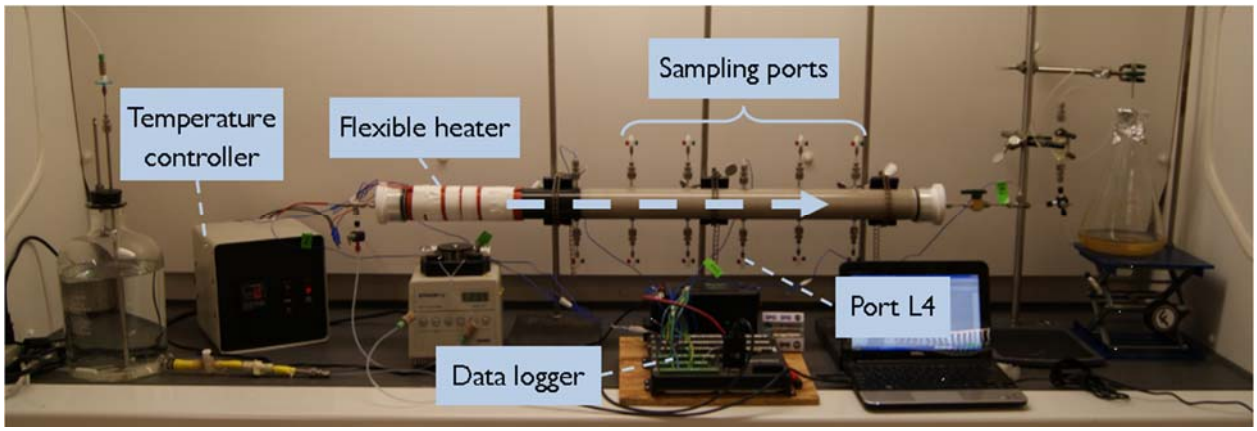

Figure 2.1.2. Experimental system setup of 90 cm thermal column experiment, which was designed to assess electron donor availability and mobility downgradient of a thermal treatment zone. The up-gradient heated portion of the column was packed with Webster soil and the down-gradient unheated section of the column was packed with Federal Fine Ottawa sand.

2.1.2.c. Operation and sampling of thermal columns

A sterile, argon-sparged solution containing 24 mM calcium chloride was pumped through the column at a pore-water velocity of v = 25 cm/day (Q ≈ 0.125 mL/min) for the duration of the experiment using a Rainin Dynamax RP-1 peristaltic pump (Mettler-Toledo; Columbus, OH). The system was initially operated at ambient temperature (approximately 22 °C) to establish steady flow conditions. Heating began after 3.3 PVs using a flexible silicone heater (Omega Engineering, Stamford, CT) wrapped around the column and covered with an insulating sleeve to minimize heat loss. A Watlow Series 965 feedback controller (Watlow Electric Manufacturing, St. Louis, MO) was used to regulate temperature, which was maintained within the set value ±0.5 °C. Temperatures were continuously monitored at multiple points throughout the system using Type K thermocouples (VWR) and were recorded to a CR1000 data logger (Campbell Scientific, Logan, UT). Unless otherwise specified, all temperature values reported herein were measured using a thermocouple located at the axial center of the Webster soil, 10 cm from the influent endplate. Temperature was increased in a stepwise manner between 3.3 and 21.4 PVs until reaching a maximum value of 82.7 °C, which was maintained for 6.2 PVs. The column temperature was then returned to ambient over the next 16.3 PVs and remained there until the conclusion of the experiment (Figure 2.1.3).

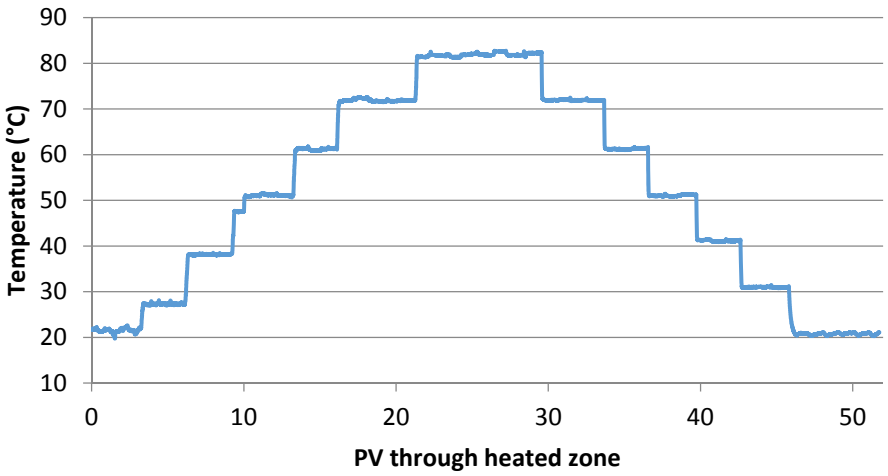

Figure 2.1.3. Temperature measured at the axial center of the Webster soil, 10 cm from the influent endplate over the course of the experiment.

Aqueous effluent samples were collected from a 20 mL glass sampling bulb approximately once per PV and immediately analyzed for oxidation-reduction potential and pH. Aqueous port samples (0.5 mL) were collected from ports L2 – L6 with similar frequency, though clogging in ports L2 and L3 prevented sampling during the latter half of the experiment. All aqueous samples were analyzed using an IC to identify and quantify VFAs released during heating of the Webster soil. Gas samples were collected from port U2 whenever gas accumulation was sufficient for analysis; gas samples of at least 3 mL were analyzed for hydrogen and other permanent gases using a GC equipped with a TCD.

2.1.2.d. Analytical methods

Organic acids: Organic acids were measured using a Thermo Fisher ICS-2100 IC according to the method described in Section 2.1.1.e.

Permanent gases: Permanent gases were measured using a Hewlett-Packard model 6890 GC equipped with a TCD according to the method described in Section 2.1.1.e.

Chlorinated ethenes: Chlorinated ethenes and ethene were measured using an Agilent 7890B GC equipped with a Teledyne Tekmar HT3 Headspace Analyzer and a flame ionization detector (FID). A 1 mL aqueous sample was loaded into a 20 mL headspace vial, which was then capped, allowed to equilibrate for 30 minutes at 70 °C, and pressurized to 10 psi. A 1 mL gas sample from the vial was then carried via a 110 °C transfer line to the GC inlet, which was operated at 200 °C in splitless mode, and injected onto an Agilent DB-624 capillary column with 320 µm mean outer diameter and 60 m length. The GC oven was held at an initial temperature of 60 °C for 4 minutes, followed by a +25 °C/min ramp to 200 °C, which was maintained for 2 minutes until the end of the run. Helium was used as the carrier gas at a flow rate of 3 mL/min, respectively. The FID was operated at 300 °C with air and hydrogen flows of 400 and 30 mL/min, respectively. Helium flowing at 30 mL/min served as the makeup gas. PCE, TCE, and *cis*-DCE calibration standards were prepared by diluting a concentrated stock solution (5,000 – 10,000 µg/mL) of each compound dissolved in

methanol. VC and ethene calibration standards were prepared by injecting a known volume of each gas into a sealed 160 mL culture bottle containing 100 mL of 18.2 MΩ water and allowing them to equilibrate overnight. The method detection limit for each chlorinated ethene and ethene was approximately 1 μM.

2.1.3. Biotic Electrical Resistive Heating (ERH) Columns

To assess the viability of the coupling ERH with bioremediation for more efficient cleanup of PCE contaminated soil an additional column experiment was performed using a PCE-to-ethene dechlorinating microbial consortium. No source of carbon or electron donor was provided to assess the ability of thermally-released substrates to support reductive dechlorination.

2.1.3.a. Microbial consortium

The column was bioaugmented with the well-characterized Bio-Dechlor INOCULUM (BDI-SZ), a non-methanogenic, PCE-to-ethene dechlorinating consortium that contains multiple dechlorinators, including three *Dhc* strains and *Geobacter lovleyi* strain SZ (*Geo*SZ) (Amos et al. 2009b). The three *Dhc* strains FL2, GT, and BAV1 harbor the *tceA, vcrA*, and *bvcA* RDase genes, respectively, and represent 46%, 54%, and < 0.001% of the *Dhc* population in BDI-SZ, respectively. The consortium was maintained for several months with periodic additions of 0.33 mM PCE as electron acceptor and 10 mM lactate as electron donor, and was sampled prior to inoculation for quantitative real-time polymerase chain reaction (qPCR) analysis that yielded initial abundances of $9.81 \pm 0.23 \times 10^7$ *Dhc* cells/mL and $3.66 \pm 1.24 \times 10^7$ *Geo*SZ cells/mL.

2.1.3.b. Field soil samples

PCE-contaminated soil was collected from a former dry cleaning facility located at the Naval Training Center Great Lakes (Site 22) located in Great Lakes, IL by personnel from TetraTech NUS, Inc. (Pittsburg, PA). Soil cores were collected from a single borehole (F3) between 10 and 12 feet below ground surface using a steel tube and then extruded into a plastic zip lock bag. The soil, classified as Ozaukee silty clay loam (fine, illitic, mesic Oxyaquic Hapludalfs), was gray, very sticky and plastic. The soil was 90% clay (<0.2 μm) and 10% silt (0.2 to 50 μm) by weight. The clay minerals present included kaolinite and illite based on Cu X-ray diffraction (XRD) analysis after dithionite-citrate-bicarbonate (DCB) treatment (Jackson, 2005). The total soil organic carbon content of Great Lakes soils ranged from 1.5 to 3.5% and extracts from the soil revealed the presence of fulvic acids at 60 mg/L and humic acids at 0.6 mg/L. The metals present included magnesium (1,210 mg/kg) and calcium (3,790 mg/kg) with minor amounts of potassium (12.5 mg/kg) and manganese (23.5 mg/kg). A strong effervescent reaction was observed upon addition of mild acid to the soil, indicating the presence of carbonates; magnesium and calcium were likely part of a carbonate soil fraction.

2.1.3.c. Electrical Resistive Heating (ERH) column design

The ERH treatment system consisted of a 5-cm inside diameter (ID) × 90 cm long glass chromatography column with total interior volume of 1.8 L (Ace Glass, Vineland, NJ; Figure III.1.3.a). Four sample collection ports were installed on the side of the column where each port was fitted with a 1/8-inch outside diameter (OD) × 6 cm long nickel-plated needle fitted with a Mininert value (VICI Valco Instrument Co. Inc., Houston, TX).

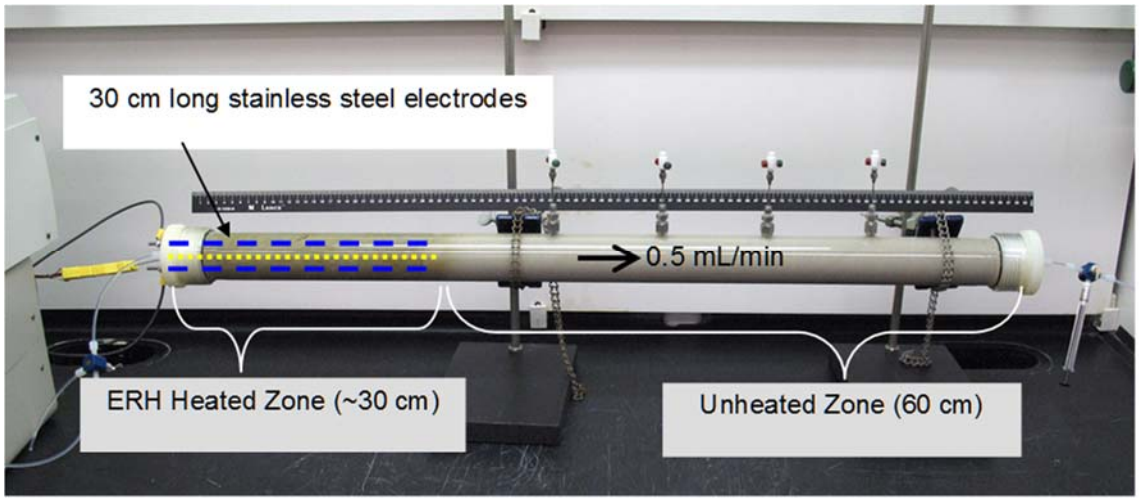

Figure 2.1.4. Picture of ERH treatment system consisting of a heated zone upgradient packed with Great Lakes soils and a downgradient unheated zone packed with Federal Fine Ottawa sand.

Two-thirds of the treatment cell volume was packed with Federal Fine Ottawa sand (US Silica, Berkeley, WV) to serve as the down-gradient section from which aqueous and gas phase samples were collected. The influent or up-gradient portion of the treatment cell volume was then filled with ca. 1 kg of PCE contaminated Great Lakes soil. The column ends were sealed with threaded nylon end-pieces fitted with fine mesh (100 μm) fiber filter disks (Ace Glass, Vineland, NJ) and 1/4-inch OD threaded adaptors. The influent end-piece was modified by installing two 1/8-inch OD × 18 inch long pieces of threaded stainless-steel stock (McMaster-Carr, Atlanta, GA), which served as electrodes, along with an electrically insulated K-type thermocouple (OMEGA Engineering Inc., Stamford, CT). The two stainless-steel electrodes were spaced approximately 4 cm apart on opposite sides of the column, and the thermocouple was placed directly between the electrodes. The two stainless-steel electrodes with automatic temperature feedback controller comprised the ERH system (Figure 2.1.4). The estimated pore volume (PV) of the combined Great Lakes and Federal Fine sand was 648 mL, based on the mass of solids added to the column and the porosity of the Great Lakes soil (0.4) and Federal Fine sand (0.35).

Once the column was fully assembled, synthetic groundwater was pumped upward through the electrode equipped end-piece at a flow rate of 0.5 mL/min to saturate the column. The column was then oriented horizontally and synthetic groundwater was pumped through the column at a flow rate of 0.11 mL/min, equivalent to a groundwater seepage velocity of approximately 25 to 30 m/day. After passing ca. 1.8 L of groundwater through the unheated column to establish baseline PCE concentrations, 12 to 24V DC power was applied to the electrodes using an automatic temperature feedback controller (Model 965, Watlow Electric Manufacturing Co., St. Louis, MO).

Initial aqueous concentrations of PCE were measured in the column effluent after flowing through the Great Lakes soil at 25°C, and then temperature was ramped up to 74°C. After heating the Great Lakes soil for one PV (approximately 2.8 days), 120 mL of the PCE-to-ethene-dechlorinating consortium (BDI) was introduced into the uncontaminated region of the column located 10 cm downgradient from the Great Lakes soil.

2.1.3.d. Sample collection and analytical methods

Aqueous samples were collected from the side ports and column effluent using a gas tight syringe to monitor changes in organic compounds including organic acids, methane, and chlorinated ethenes. The concentrations of aqueous-phase chloroethenes were determined by transferring 1 mL of aqueous sample into a sealed 22 mL headspace vial, which was analyzed using a Hewlett-Packard 6890 GC equipped with a Teledyne-Tekmar (Teledyne Technologies, Inc., Mason, OH) HT3 headspace autosampler and a 30 m long × 0.32 mm OD Agilent DB-5 column connected to an FID. The headspace autosampler was programmed to hold each sample at 70 °C for a period of 20 min prior to transferring the headspace gas to the GC injection port through silcosteel tubing heated to 140 °C. Calibration standards were prepared by injecting small volumes of a 10,000 mg/L chloroethene-methanol stock solution into 22 mL headspace vials filled with 1 mL of DI water.

After the completion of each experiment, solid samples were collected from every 10 cm along the column length to quantify the amount of PCE and degradation products. Solid samples were placed in 40 mL glass vials followed by 20 mL of methanol (Optima grade, Fisher Scientific). The vials were sealed with Teflon lined screw-top caps and placed on a vortex mixer. After 24 hr, the vials were centrifuged at 500 rpm and then a 1.5 µL of methanol was transferred using a gas tight syringe into a 2 mL GC autosampler vial. Each GC vial was crimp sealed and analyzed by a GC equipped with a DB-5 column connected to a micro electron capture detector (µECD) or an Agilent (Santa Clara, CA) 6890N GC a 30 m long × 0.25 mm OD Agilent DB-5ms column connected to an Agilent inert Mass Select Detector (MSD).

The concentration of organic acids, sulfate and chloride were determined by transferring 1 mL of aqueous sample into a 2 mL vial which was analyzed using a Dionex ICS-3000 IC equipped with an AS14 (4 mm × 250 mm) IonPac anion column connected to an ASRS-Ultra II suppressor and a conductivity detector. A 25 µL sample was automatically injected into a 3.5 mM Na_2CO_3 + 1.0 mM $NaHCO_3$ eluent flowing at 1.2 mL/min. Calibration standards for chloride (Cl^-), formate ($CHOO^-$), glycolate (COH_3COO^-), acetate (CH_3COO^-), oxalate ($COOHCOO^-$), and sulfate (SO_4^{2-}) were prepared over a concentration range of 0.02-0.50 mM. Calibration standards for formate and glycolate were prepared from 99% grade solids (ACROS Organics, Morris Plains, NJ), while acetate, oxalate, and sulfate solutions were prepared from ACS certified solids (Fisher Scientific, Fair Lawn, NJ). Chloride calibration standards were prepared by serial dilution of a 1,000 mg/L chloride solution (certified, SPEX CertiPrep, Metuchen, NJ).

Gas samples were collected periodically from the side ports using a gas tight syringe to monitor changes in chloroethenes, ethane, ethene, acetylene, hydrogen, carbon monoxide and carbon dioxide concentrations. Gas concentrations were determined using a Hewlett Packard 6890 GC equipped with a heated gas-sampling valve with a 250 µL sample loop. The gas sample in the 250 µL loop was injected into a GC inlet operated in the splitless mode for 45 s at 200°C. The sample passed through a 30 m × 0.32 mm OD Carboxen-1010 column (Supleco, Bellefonte, PA) connected to a TCD. Gas standards were prepared with high purity hydrogen, ethene, ethane or acetylene, while CO, CO_2, and methane standards were prepared from a certified mixture (Matheson Tri-Gas, Twinsburg, OH). Calibration standards were prepared using a 500 mL syringe (Hamilton Company, Reno, NV) with nitrogen as the dilution gas.

Select gas samples were injected into the inlet of a Varian Star 3600 GC equipped with a 30 m long × 0.32 mm OD Varian CP-Sil 8ms column connected to a Saturn 2000 Mass Spectrometer

(MS). Unknown compounds were identified using software (SaturnView ver. 5.41, Varian, Palo Alto, CA) that matched mass spectra to compounds in the NIST/EPA/NIH Mass Spectral Library (NIST98). The mass spectrometer was automatically tuned by adjusting the electron multiplier voltage to achieve a gain of 1×10^5 electrons per ion and by mass axis calibration to an internal reference compound (perfluorotributylamine) prior to each use. Gas calibration standards for PCE were prepared by injecting less than 6 μL of methanol stock into capped 21.3 mL headspace vials to span the PCE concentration range from 20 to 1,000 ppmv at 25 °C and 1 atm.

2.1.3.e. Biological sample preparation

Biomass was collected from 15 mL aqueous effluent samples by centrifugation at 4°C for 30 minutes at 4,000 rpm in a table top refrigerated centrifuge (Eppendorf 5810R, Hauppauge, NY). All but ca. 1 mL of the supernatant was decanted and the cell pellet was suspended in the remaining liquid. Centrifugation was repeated at 13,200 rpm for 15 minutes. From the side ports, 1-1.25 mL aqueous samples were collected using a 2.5 mL gas-tight syringe (Hamilton Co., Reno, NV) and centrifuged at 13,200 rpm at room temperature for 15 minutes. After removing the supernatant, the pellets were stored at -20°C until genomic DNA was extracted using the DNeasy® Blood and Tissue Kit (Qiagen, Valencia, CA) according the bacterial protocol, with modifications previously described by Ritalahti et al. (2006a). DNA was obtained in final volumes of 400 μL buffer AE (provided with the DNeasy® Blood and Tissue Kit) and stored at -80°C until qPCR analysis was performed. Soil was collected through destructive sampling at the termination of the experiment and prepared for DNA extraction according to described protocols (Cápiro et al. 2008). After homogenizing the samples, 1-3 g of the wet sample was placed in an aluminum weighing tray and dried overnight at 100°C to determine the sample water content. DNA was extracted from 0.27-0.33 g of wet sample (0.22-0.27 g dry weight) solid material using the PowerSoil™ DNA Isolation Kit (MoBio Laboratories, Inc., Carlsbad, CA) in accordance with the procedures provided by the manufacturer. A final volume of 100 μL DNA was collected in solution C6 (provided with the PowerSoil™ Isolation Kit) and stored at -80°C until qPCR analysis.

2.1.3.f. Quantitative real-time PCR (qPCR) analysis

Dhc strains and *Geo*SZ cell numbers were quantified using triplicate qPCR reactions targeting the 16S rRNA genes with an ABI 7500 Fast Real-Time PCR System (Applied Biosystems, Foster City, CA) using the standard operating modes. Primers and probes used were obtained from IDT Technologies (Coralville, IA). TaqMan-based qPCR analysis was used to quantify total *Dhc* 16S rRNA gene copies and associated reductive dehalogenase (RDase) genes (Ritalahti et al. 2006a), and quantification of *Geo*SZ 16S rRNA gene copies was performed using SYBR Green detection chemistry according to described protocols (Amos et al. 2007c, Duhamel and Edwards 2006) with the modifications introduced by Amos et al. (2009b).

Dhc cell numbers were expressed in terms of 16S rRNA gene copies or cell numbers per mL of fluid or per gram of solid, and used interchangeably because the known *Dhc* strains contain a single 16S rRNA gene copy per genome (Kube et al. 2005, Seshadri et al. 2005). The genome of *Geo*SZ contains two 16S rRNA gene copies (www.jgi.doe.gov) (Wagner et al. 2012); therefore, gene copy numbers were divided by a factor of two to yield the cell numbers that were reported per mL of fluid or per gram of solid. Standard curves were generated following the procedure outlined by Ritalahti et al. (2006a) using 10-fold dilutions of quantified plasmids (concentration determined spectrophotometrically at 260 nm) carrying a single copy of the 16S rRNA gene of either *Dhc* strain BAV1 or *Geo*SZ.

2.1.4. Low Temperature Thermal Columns

2.1.4.a. Chemicals and reagents

Sodium lactate (60% w/w syrup) and PCE (≥99% purity) used in low temperature column experiments were obtained from Sigma-Aldrich (St. Louis, MO). The PCE-to-ethene dechlorinating KB-1® culture, comprised of *Dehalococcoides mccartyi* sp., *Geobacter* sp., and *Methanomethylovorans* sp., was obtained from SiREM Labs. Gas chromatography standards were prepared with PCE, TCE (≥99.5%; Sigma-Aldrich), cis-1,2-dichloroethene (cis-DCE; 97%; Aldrich), vinyl chloride (VC; 99%; SynQuest Laboratories), and ethene (≥99.5%; Aldrich). Primers and probes used in qPCR analyses described in Section 2.1.3.f were obtained from IDT Technologies (Coralville, IA) or Thermo Fisher; TaqMan Universal PCR Master Mix was obtained from Applied Biosystems (Foster City, CA).

2.1.4.b. Column design and preparation

Transport and reactivity experiments were performed in borosilicate glass chromatography columns (15 cm length × 2.5 cm ID; Kimble-Chase) equipped with Teflon endplates (Figure III.1.4.a**)**. Each column was customized with three evenly spaced sampling ports sealed with rubber septa, with port 1 nearest the column influent. Columns (herein referred to as Column A and Column B) were packed under sterile conditions with Federal Fine Ottawa sand (30 – 140 mesh; U.S. Silica), a quartz sand with mean grain size of 0.32 mm, permeability of 4.2×10^{-11} m^2, and total organic carbon content of <0.01%. Initial aqueous pore volume (PV) in each column was 30.3 mL.

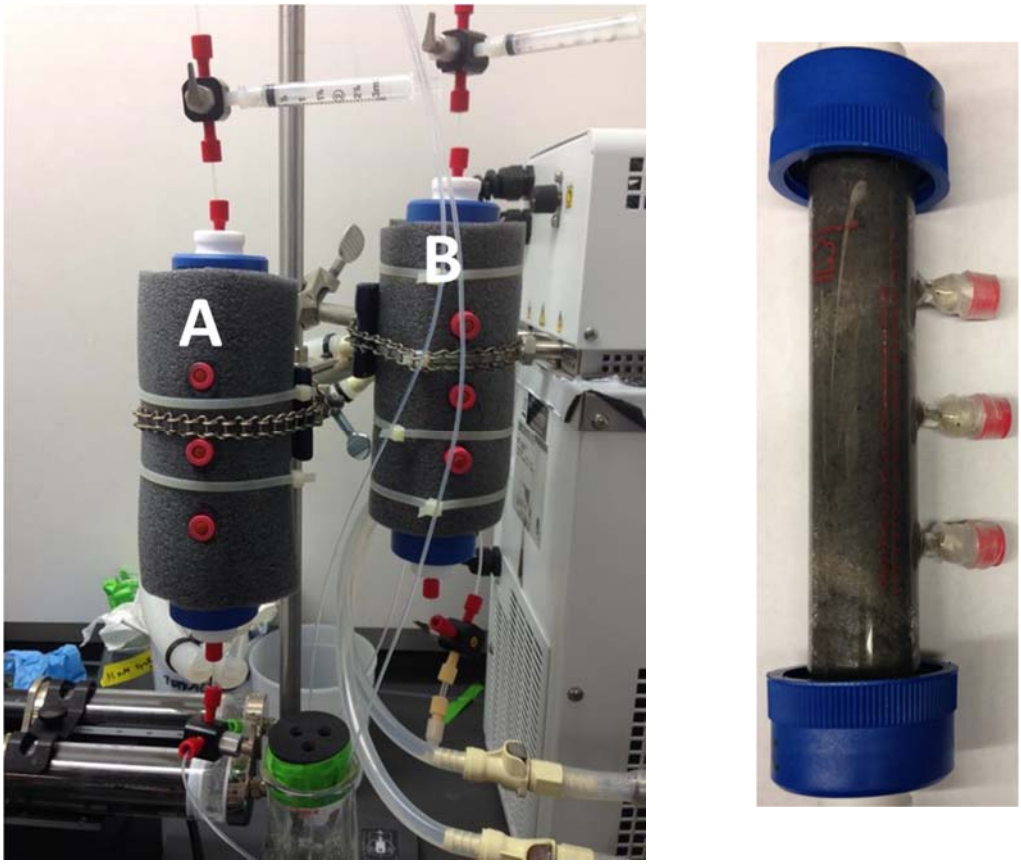

Figure 2.1.5. Images of low temperature thermal column system with and without insulation.

2.1.4.c. Synthetic groundwater preparation and delivery

A reduced, synthetic groundwater solution was prepared by making the following modifications to the low chloride mineral salt medium described by Amos et al. (2008): mineral salt and trace element concentrations were reduced by 90%; the $NaHCO_3$ concentration was reduced from 60 to 30 mM; and the N-Tris[hydroxymethyl]methyl-2-aminoethane-sulfonic acid (TES) buffer and vitamins were eliminated. Lactate (5 mM) was added as the electron donor. Synthetic groundwater was prepared in 1,500 mL batches, with 500 mL dispensed into each of three 1,000 mL media bottles (Chemglass Life Sciences) under an 80% nitrogen/20% carbon dioxide headspace. PCE (300 µL) was added to one bottle to serve as a PCE-saturated stock solution, then all three bottles were autoclaved. The column influent solution was prepared by diluting PCE-saturated stock in a sterile, 100 mL gastight syringe (SGE Analytical Science; Victoria, Australia) to an average PCE concentration of 283±33 µM using the unamended synthetic groundwater as diluent. Column influent was delivered via a PHD 2000 syringe pump (Harvard Apparatus) and syringes were refilled approximately every 3 PV.

2.1.4.d. Column operation and sampling

Columns A and B were operated similarly and in parallel throughout the experiment, except with respect to temperature. Bromide tracer tests were completed to determine initial aqueous pore volume, then recirculating water baths (Thermo Fisher or VWR International) were used to chill

Column A to 15 °C and heat Column B to 35 °C. Synthetic groundwater was introduced to each column at an initial pore water velocity of 15 cm/day (Q = 0.020 mL/min) for 17 PV to establish reduced conditions and ensure homogeneous distribution of dissolved PCE and lactate. Flow was then paused and 6 mL of the KB-1® culture obtained from SiREM (Guelph, Ontario, Canada) was injected via each column influent, sampling ports 1–3, and effluent, for a total of 30 mL per column. Flow was resumed after 48 hours and continued for 176 PV until experiment termination. Following bioaugmentation, the experiment was completed in four phases designed to assess microbial activity as a function of temperature (Table 2.1.2).

Table 2.1.2. Description of experimental sequence used in low temperature column studies.

Phase	Intent of experimental phase:	Action
I (0 – 52 PV)	Assess dechlorination activity at ambient versus elevated groundwater temperature	Columns A and B held at initial temperatures
II (52 – 95 PV)	Assess dechlorination activity in a system raised from ambient to elevated groundwater temperature	Column A temperature increased to 35 °C
III (95 – 112 PV)	Determine maximum temperature for *Dhc* activity	Column B temperature increased to 43 °C
IV (112 - 176 PV)	Determine maximum temperature for reductive dechlorination activity	Column B temperature increased to 74 °C

Effluent samples were collected every 2 – 3 PV to determine concentrations of chlorinated ethenes, ethene, organic acids, and monitor pH. Port samples were collected during each phase of the column experiments to determine the aqueous phase abundance of *Dehalococcoides mccartyi* sp., *Geobacter* sp., and RDase genes, which are responsible for microbial reductive dechlorination of cis-DCE and VC: *tceA*, *bvcA*, and *vcrA*. Columns were destructively sampled at the conclusion of the experiment to allow for determination of solid-phase bacterial and RDase abundance.

2.1.4.e. Sample preparation and DNA extraction

Aqueous samples (1 mL) collected from column ports for qPCR analysis were immediately placed in a sterile 1.8 mL microcentrifuge tube and centrifuged at 15,000 rpm (21,230 × g) for 15 minutes at ambient temperature. The supernatant was then discarded and cell pellets were stored at -20 °C until DNA extraction using the QIAGEN QIAamp DNA Mini Kit (QIAGEN, Hilden, Germany). Extractions were completed according to the protocol for Gram-positive bacteria. DNA was collected in 600 µL of Buffer AE and stored at -20 °C until qPCR analysis.

Immediately after terminating the experiment, 11 wet solid samples, weighing 6 – 18 g, were collected from each column under sterile conditions and placed in sterile 15 mL centrifuge tubes. Samples were homogenized using a flame-sterilized spatula, then approximately 2 g of each sample was placed in an aluminum dish and dried at 110 °C overnight to determine water content. Bacterial DNA was extracted from approximately 0.25 g of each wet solid sample using the PowerSoil DNA Isolation Kit (MO BIO Laboratories, Inc., Carlsbad, CA). DNA was collected in 100 µL of solution C6 and stored at -20 °C

2.1.4.f. Analytical methods

Chlorinated ethenes and ethene in aqueous samples were measured using an Agilent 7890B GC equipped with a Teledyne Tekmar HT3 Headspace Analyzer and a FID. A 1 mL aqueous sample was loaded into a 20 mL headspace vial, which was then capped, allowed to equilibrate for 30 minutes at 70 °C, and pressurized to 10 psi. A 1 mL gas sample from the vial was then carried via a 110 °C transfer line to the GC inlet, which was operated at 200 °C in splitless mode, and injected onto an Agilent DB-624 capillary column with 320 µm OD × 60 m length. The GC oven was held at an initial temperature of 60 °C for 4 minutes, followed by a +25 °C/min ramp to 200 °C, which was maintained for 2 minutes until the end of the run. Helium was used as the carrier gas at a flow rate of 3 mL/min, respectively. The FID was operated at 300 °C with air and hydrogen flows of 400 and 30 mL/min, respectively. Helium flowing at 30 mL/min served as the makeup gas. PCE, TCE, and cis-DCE calibration standards were prepared by diluting a concentrated stock solution (5,000 – 10,000 µg/mL) of each compound dissolved in methanol. VC and ethene calibration standards were prepared by injecting a known volume of each gas into a sealed 160 mL culture bottle containing 100 mL of 18.2 MΩ water and allowing them to equilibrate overnight. The method detection limit for each chlorinated ethene and ethene was approximately 1 µM. Lactate and its fermentation products were measured using a Thermo Fisher ICS-2100 IC as described in Section III.1.1.

Dhc and *RDase* abundances were determined by (qPCR) analysis using an Applied Biosystems StepOnePlus Real-Time PCR System (Applied Biosystems, Foster City, CA). Reactions targeting the *Dhc* 16S rRNA, *tceA*, *bvcA*, and *vcrA* genes were completed in triplicate according to the TaqMan-based qPCR protocol described in detail by Ritalahti et al. (2006). Standards were prepared by using the Qubit 2.0 Fluorometer (Thermo Fisher) to quantify and dilute plasmid DNA containing the gene of interest to 1 ng/µL, then performing 10:1 serial dilutions. The standard curve linear range was 10^2 – 10^8 gene copies/mL.

2.2. Effects of Metal Sulfide Formation and Dissolution on Aquifer Permeability (Task 2)

2.2.1. Abiotic Pump Driven Columns

A series of abiotic, 1-D column experiments was completed to assess the impacts of FeS precipitation on the aqueous pore volume and permeability of porous media. Anoxic solutions containing iron (II) and sulfide were introduced to the columns to induce abiotic precipitation of FeS. This evaluation was initially completed using porous media with a range of organic matter content and at flow rates up to 90 cm/day, and subsequent column experiments were completed at slower flow rates (ca. 20-15 cm/day) to assess the influence of groundwater velocity on the extent of precipitation. In cases where FeS precipitation was observed, selected columns were flushed with an oxygenated influent solution to evaluate the reversibility of the precipitation reaction and the effects of FeS oxidation on soil permeability.

2.2.1.a. Materials

Reagent grade iron (II) chloride tetrahydrate was purchased from Fisher Scientific (Fair Lawn, NJ), and sodium sulfide nonahydrate (>98%) was purchased from Sigma-Aldrich (St. Louis, MO) for use in column experiments. Chemicals used for colorimetric measurement of iron included ammonium acetate (Fisher Scientific, Fair Lawn, NJ), ferrozine reagent (Acros Organics, Morris

Plains, NJ), 99.999% hydroxylamine hydrochloride (Sigma-Aldrich, St. Louis, MO), and ammonium hydroxide (Fisher Scientific, Fair Lawn, NJ). Chemicals used in colorimetric measurement of sulfide included >98% N-N-dimethyl-p-phenylenediamine (Tokyo Chemical Industry Co., Tokyo, Japan), sulfuric acid (Fisher Scientific, Fair Lawn, NJ), 98% iron (III) chloride (Fisher Scientific, Fair Lawn, NJ), hydrochloric acid (EMD Millipore, Billerica, MA), and sodium hydroxide (EMD Millipore, Billerica, MA). Background electrolyte solutions were prepared using calcium chloride dihydrate obtained from EMD Millipore (Billerica, MA). Sodium bromide used in the non-reactive tracer tests was obtained from Fisher Scientific (Fair Lawn, NJ). Chemicals used for preparation of reduced medium solution are described by Sung et al. (2003) and Amos et al. (2008). All chemicals were of reagent grade or higher purity, and all solutions were prepared using 18.2 MΩ water (EMD Millipore; Billerica, MA).

Porous media used in column experiments were selected to provide a range of physical properties and organic carbon (OC) contents. The solid materials included Federal Fine Ottawa sand (US Silica Company; Berkeley Spring, West VA), Appling soil (University of Georgia Agricultural Experiment Station; Eastville, GA), Webster soil (Iowa State University Agricultural Experiment Station, Ames, IA) and aquifer material from the Groveland Wells Superfund site (Groveland Wells Superfund site; Groveland, MA). Federal Fine Ottawa sand is a quartz sand with < 0.01% OC, 0.32 mm mean diameter, and intrinsic permeability of 4.2×10^{-11} m^2 (Suchomel et al., 2007). Appling soil is a natural field soil with 0.66% OC, and is classified as a silty sand (Wang et al., 2010). Webster soil is another well-characterized soil with 2.2% OC that was obtained from the upper 30 cm (A horizon) and is characterized as fine-loamy, mixed, superactive, mesic Typic Endoaquoll. The Groveland Wells aquifer material passed through a number 30 sieve and has a 0.01% OC.

2.2.1.b. Column experiment design and preparation

Column experiments were performed using borosilicate glass chromatography columns (Kimble-Chase; Vineland, NJ) with a 4.8 cm ID × 15 cm length, except in the case of Federal Fine column #2, which was 60 cm in length. All column parts were sterilized by autoclaving for 30 minutes at 121 °C in the liquid cycle, or by thoroughly rinsing with methanol before packing. Federal Fine Ottawa sand was dry packed in approximately 2-cm increments. After the addition of each layer, the interface between the compacted sand and the new layer was mixed using a spatula to prevent stratification. The sand was then gently compressed using a tamping tool under gentle vibration before the next layer was added. Soils with higher organic contents and fine particles (Appling, Webster, and Groveland) were damp packed in a process similar to dry packing; however, these soils were lightly sprayed with 18.2 MΩ water before packing to minimize loss of fine particles, improve workability, and to prevent swelling or contracting of soils during column saturation. Once packed, columns were purged with carbon dioxide gas for 30 minutes to facilitate the dissolution of entrapped air, and then flushed with at least 10 pore volumes of a 24 mM (60 mM ionic strength) calcium chloride background electrolyte solution prepared with deoxygenated, 18.2 MΩ water (Oliviera et al., 1996; Wang et al., 2008; Lewis & Sjostrom, 2010). For constant flow column experiments the influent solution was delivered by a Rainin Dynamax RP-1 peristaltic pump (Mettler-Toledo; Columbus, OH) connected to an anoxic influent bottle and the column inlet (Figure III.2.1.a).

Based on the specific goals of each experiment, solutions containing iron (II) chloride, sulfide-containing medium, and oxygenated medium were flushed through the columns (Table 2.2.1). Abiotic pump-driven columns were divided into two groups: the first, consisting of two Federal

Fine columns, two Appling columns, and a Groveland column, were intended as a screening process to identify characteristics of porous media impacting the extent and severity of permeability loss due to FeS precipitation (Section 2.2.1.f); the second was focused on determining the influence of pore water velocity on precipitation in Federal Fine Ottawa sand (Section 2.2.1.g).

Table 2.2.1. Abiotic pump-driven column experimental parameters.

Column	**Influent phases**	**Pore velocity (cm/day)**	**Fe^{2+} (mg/L)**	**S^{2-} (mg/L)**	**Medium buffer** 10 mM TES +	**Ionic strength (mM)**
Federal Fine #1	Fe^{2+}/S^{2-}	80	250 (2.9)*	100 (2.2)*	10 mM $PO_4^{2-/3-}$	60
Federal Fine #2	Fe^{2+}/S^{2-}	80	250 (6.5)*	95 (6.5)*	10 mM $PO_4^{2-/3-}$	60
Appling #1	S^{2-}	25	na	140 (21.5)*	10 mM $PO_4^{2-/3-}$	60
Appling #2	$Fe^{2+}/S^{2-}/O_2$	70	250 (2.4)*	110 (45)*	10 mM $PO_4^{2-/3-}$	60
Groveland	$Fe^{2+}/S^{2-}/O_2$	90	210 (11)*	120 (31)*	10 mM $PO_4^{2-/3-}$	60
Federal Fine #3	S^{2-}	25	na	40-80 (46.6)*	2 mM $PO_4^{2-/3-}$ + 60 mM HCO_3^-	120
Federal Fine #4	S^{2-}	25	na	40-80 (81.6)*	2 mM $PO_4^{2-/3-}$ + 60 mM HCO_3^-	120
Federal Fine #5	S^{2-}	25	na	40-80 (83.6)*	2 mM $PO_4^{2-/3-}$ + 60 mM HCO_3^-	120

**Number of PV of solution introduced.*

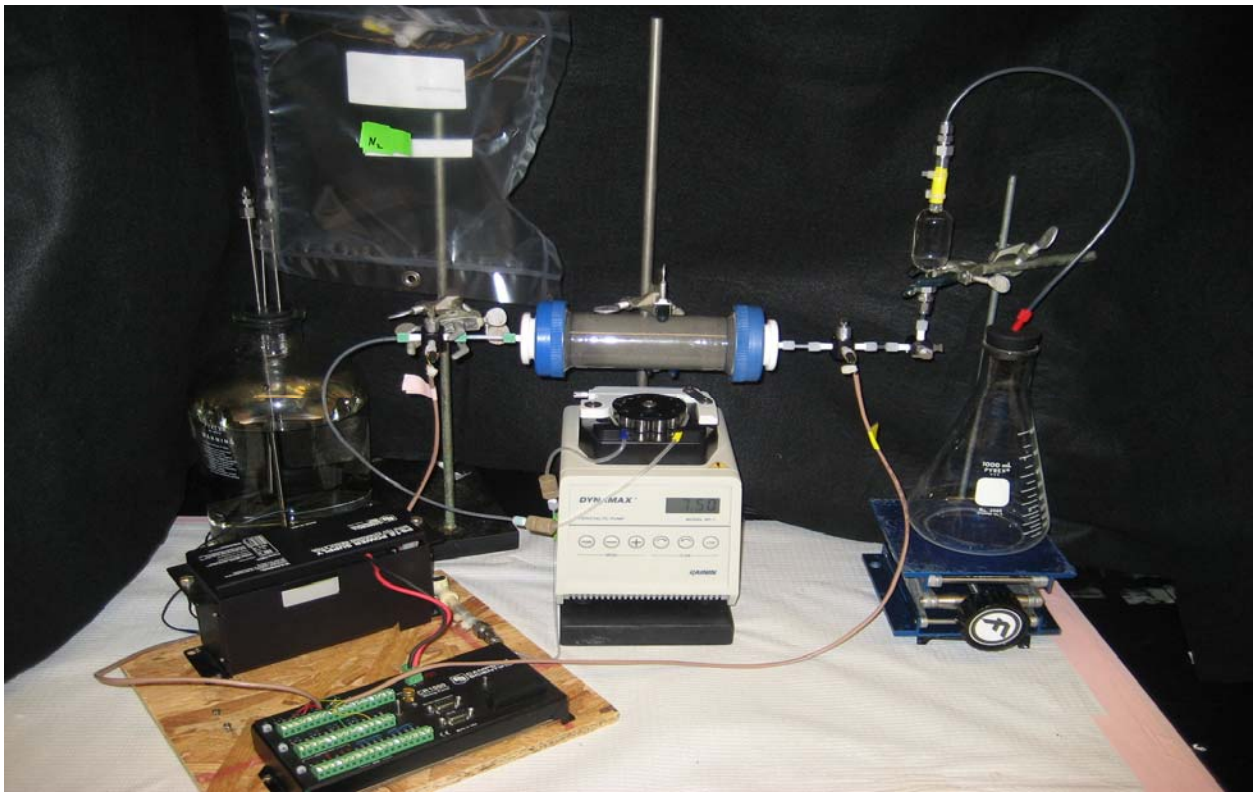

Figure 2.2.1. Pump-driven column experimental setup including anoxic influent bottle, data logger, pressure transducers, peristaltic pump, chromatography column, glass sampling bulb, and effluent bottle.

2.2.1.c. Anoxic influent system design

Influent solutions were prepared in a 4 or 9 L aspirator bottle (Ace Glass, Vineland, NJ). Each bottle was sealed with a 3-hole butyl rubber stopper equipped with three segments of stainless steel tubing and gas-tight Swagelok fittings to maintain anoxic conditions. Two segments of the tubing extended five to 10 cm from bottom of the bottle to allow for rapid, sterile nitrogen sparging or anoxic solution amendment. The third, shorter segment of tubing was positioned above the solution surface to allow for gas venting during sparging (Figure 2.2.2).

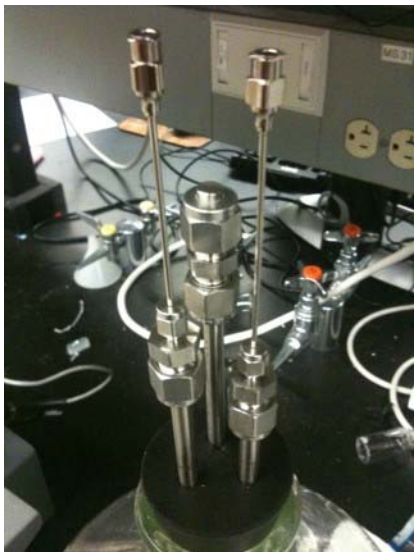

Figure 2.2.2. Butyl rubber stopper with tubing and Swagelok fittings for gastight closure of anoxic influent bottles.

2.2.1.d. Anoxic solution preparation

Sterile, anoxic influent solutions were prepared by sparging for at least 1 hour with argon or nitrogen gas, followed by autoclaving of the influent delivery system parts at 121 °C for 30 minutes on the liquid cycle. In order to avoid detrimental effects associated with changes in ionic strength (e.g. liberation of fine particles), all influent solutions for a given experiment were prepared with the same ionic strength, either 60 or 120 mM. Solutions were prepared in the anoxic influent bottles described previously, which were covered with aluminum foil during autoclaving to prevent solution contamination by water from the autoclave. Following autoclaving, the aspirator bottle was quickly sealed using the 3-hole butyl rubber stopper, and nitrogen lines with 0.22 μm sterile filters were attached to the two longer pieces of stainless steel tubing. The bottle was then placed in an ice bath with the nitrogen gas flush for approximately two hours. Any volatile or heat-labile influent solution components, such as sodium sulfide, were added after the solution had cooled to room temperature. During column operation, anoxic conditions were maintained in the system using an oxygen trap (Restek Corporation; Bellefonte, PA) and a gas sampling bag filled with ultra-high purity argon connected to the longest of the stainless steel lines. The gas sampling bag was refilled frequently with filter-sterilized, ultra-high purity argon to prevent a buildup of negative pressure in the system.

A reduced mineral salts medium was used as the primary column influent solution for abiotic column experiments. The medium was prepared as described previously (Amos et al. 2009a, Cápiro et al. 2015). A sterile potassium phosphate buffer (Sigma-Aldrich; St. Louis, MO) was added after the medium bottle was removed from the autoclave and cooled, resulting in a final concentration of 10 mM phosphate. In Federal Fine columns #3 – 5, the phosphate concentration was reduced from 10 to 2 mM, and 3 mM sodium bicarbonate was added. The phosphate and bicarbonate buffers were added after cooling to prevent the precipitation of insoluble compounds during heating. No vitamins or electron donors were added to the medium. Sulfide was added at concentrations ranging from 40 to 140 mg/L sulfide to imitate highly reducing conditions.

Iron (II) chloride solutions were prepared in a manner similar to the phosphate buffer in the reduced mineral salts medium. A concentrated stock solution of iron (II) chloride was prepared in one or more 200 mL culture bottles and sterilized by autoclaving. Once the solutions had cooled to room temperature, the sterile iron (II) chloride stock solution was quickly transferred into the aspirator bottle while the nitrogen flush was still in place, resulting in a final iron (II) concentration ranging from 210 to 250 mg/L.

Oxygenated medium solutions were prepared similarly to the reduced mineral salts medium described above, except that they did not include reducing agents (i.e., L-cysteine, sodium sulfide nonahydrate). Additionally, the oxygenated medium was gently sparged with filter-sterilized air throughout the oxygenated medium flush to maintain a dissolved oxygen concentration of approximately 5.5 mg/L.

2.2.1.e. Bromide tracer tests

Non-reactive tracer tests were performed for each column to characterize the initial hydraulic conditions, and after FeS precipitation and oxidation phases to quantify changes in pore volume. Tracer tests consisted of a 2 – 3 PV pulse of sodium bromide, followed by a 2 PV flush of calcium chloride dihydrate. Throughout each tracer test, a CF-2 fraction collector (Spectrum Labs, Rancho Dominguez, CA) was used to collect column effluent every 10 minutes. Bromide breakthrough concentration data was used to determine column pore volume using the CFITM model (van Genuchten 1981) as a part of Studio of Analytical Models (STANMOD) Version 2.2 (available through USDA-ARS U.S. Salinity Laboratory; http://www.ars.usda.gov). By fitting the one-dimensional form of the advective-dispersive transport equation (III.1) to the bromide tracer data (effluent concentration versus PV), one can obtain the aqueous pore volume, assuming a retardation factor (R_F) of 1.0, and the hydrodynamic dispersion coefficient (D_H) from the dimensionless Peclet number (Pe) as shown in equations 2.2.1 and 2.2.2 below.

$$R_F \frac{\partial C^*}{\partial PV} = \frac{1}{Pe}\frac{\partial^2 C^*}{\partial X^2} - \frac{\partial C^*}{\partial X} \qquad (2.2.1)$$

$$C^* = \frac{C}{C_0};\ PV = \frac{v_p t}{L};\ Pe = \frac{v_p L}{D_H};\ D_H = v_p \alpha;\ X = \frac{x}{L} \qquad (2.2.2)$$

where C is the aqueous concentration (M L^{-3}), C_0 is the influent or applied aqueous concentration (M L^{-3}), *PV* is the dimensionless pore volume, v_p is the pore-water velocity (L t^{-1}), *t* is time, *L* is the column length, *Pe* is the Peclet number, D_H is the hydrodynamic dispersion coefficient (L^2 t^{-1}), α is dispersivity (L), and *x* is the distance parallel to flow.

2.2.1.f. Column experiments with pressure transducers

In the first set of column experiments, differential pressure sensors (Figure 2.2.3) (Honeywell, Morristown, NJ) were used with a Campbell Scientific CR1000 data logger (Campbell Scientific, Logan, UT) to monitor and record pressure changes over the length of each soil column during FeS precipitation and subsequent oxidation. Sensors were attached to the influent and effluent sides of each column, allowing for the overall pressure drop to be calculated, which allowed in turn for permeability losses to be calculated using Darcy's law.

Figure 2.2.3. Image of a differential pressure sensor that was attached to the column influent and effluent to monitor changes in pressure and in turn, permeability due to FeS precipitation and subsequent oxidation, when applicable.

Pressure sensor outputs in millivolts were calibrated against a column of water with known elevation head; one port of each sensor was attached to the bottom of the water column while the other port was left open to the atmosphere. Pressure differentials were quantifiable to less than 1 cm of water. A representative pressure sensor calibration curve is presented below in Figure 2.2.4.

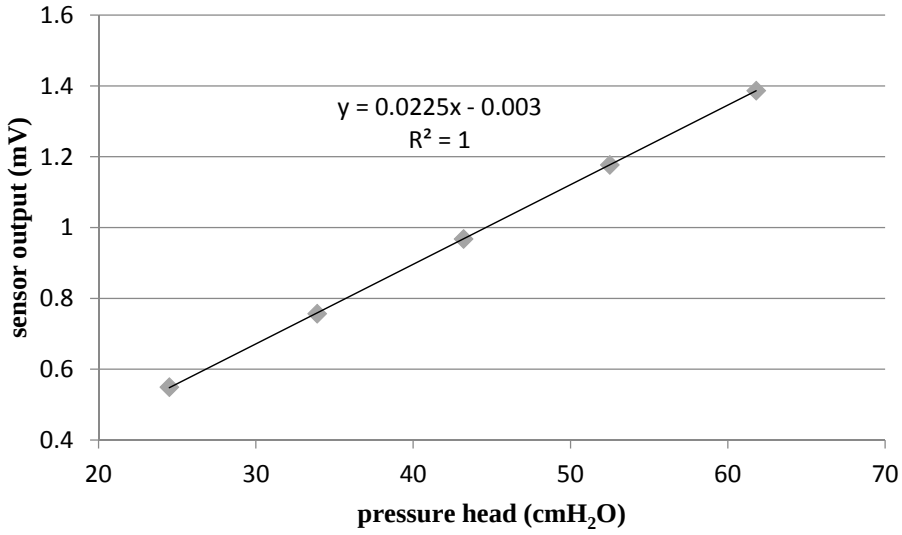

Figure 2.2.4. Example of pressure transducer calibration curve.

Throughout the Appling #1 and Groveland Wells column experiments, 4 mL effluent samples were collected from a 20 mL glass sampling bulb at least one time per PV and analyzed for sulfide, iron (II), and iron (III). A sampling bulb was used instead of an autosampler in an effort to minimize oxygen intrusion into effluent samples and to prevent potential loss of volatile analytes (e.g. sulfide). Oxidation reduction potential (ORP) and pH were measured using the remaining effluent sample volume. Effluent samples were not collected during the Appling #2 column or Federal Fine columns #1 and #2 in order to avoid inadvertent impacts on the pressure sensors and data logger during the brief (< 5 second) flow interruption required for sampling.

In the second group of column experiments, the use of pressure transducers was discontinued in favor of static head testing before and after FeS formation to determine permeability changes, as described by Hale & MacIver (1970). Briefly, the pump used to drive flow during the rest of the experiment and nonessential system components (e.g., sampling bulb) were disconnected, then the influent reservoir was raised to a known elevation above the effluent line, establishing a gravity-driven hydraulic gradient. Flow through the column was strictly monitored, allowing for permeability to be calculated using Darcy's law. This approach provided more reliable measurements of soil permeability over time relative to the pressure transducers due static head flow measurements more accurately distinguishing small variations in permeability at slower (<1m/day) seepage velocities.

2.2.1.g. Low flow column experiments

In the second set of abiotic pump-driven column experiments, three identical columns containing sterile Federal Fine Ottawa sand were used to quantify the effects of abiotically formed iron (II) sulfide precipitate on porous media intrinsic hydraulic properties under flow-rates that would be more conducive to microbial processes. Based on lessons learned from earlier column experiments, the first two centimeters of each column were packed with acid washed and sonicated Federal Fine sand to remove iron-oxides and prevent FeS precipitation. Static head permeability and non-reactive tracer tests were conducted immediately following column packing to determine the initial hydraulic parameters of the packed column. The influent solution delivered to the three columns was switched to the high sulfide medium immediately following the initial tracer test. To serve as a control for future biotic work, the flow rate of the high sulfide medium was maintained at 0.12 mL/min (equivalent to a pore-water velocity of 25 cm/day). This low flow rate also provided a long residence time for the sulfide to react with solid-bound iron and form iron (II) sulfide (FeS) precipitate. The goal for these column experiments was to allow the high sulfide medium flush continue until conditions became static and it appeared the column was no longer reacting with the influent sulfide. Then, a second tracer test would be conducted to quantify changes in the porosity and pore volume resulting from the formation of FeS.

For each column, several parameters at the influent and effluent were measured once every two days to determine when the high sulfide flush phase was complete. These parameters included sulfide concentration (mg S^{2-}/L), pH, and ORP. While the pH and ORP remained fairly stable throughout each column experiment, the influent and effluent sulfide concentrations gradually approached equivalent values, indicating that the column was no longer reacting with the influent sulfide. Influent samples were drawn from a purge line attached to a three-way valve connected to the influent solution and the column. These samples were withdrawn using a 15 mL syringe and were discarded into a 15 mL centrifuge tube where they were immediately sampled for sulfide concentrations, pH, and ORP. The effluent samples were collected from a 20 mL, air-tight, glass sampling bulb. A momentary flow interruption to the column allowed for withdrawal of a sample from the sample bulb where it could then be discarded in a 15 mL centrifuge tube and immediately sampled for sulfide concentrations, pH, and ORP. By sampling the effluent every other day, approximately 4 PV of high sulfide medium would flush through the column between samples.

Following the second tracer test, an aerated medium flush was used to determine the effects that oxidation of the iron sulfide precipitates would have on the porosity and permeability of the porous media. In this phase with the aerated medium, pH, ORP, and dissolved oxygen were measured at the influent and effluent. This phase of the experiment was considered complete when the influent and effluent parameters were stable for five sampling periods. Hydraulic conductivity

and porous media permeability was determined using the static head test as described previously (Hale and MacIver 1970).

2.2.1.h. Analytical Methods

Aqueous phase sulfide analysis: Sulfide concentrations were measured using a variation of the spectrophotometric methylene blue method (Haddad & Heckenberg, 1988). For this procedure, a 1 mL sample was added to a UV spectrophotometer cuvette, followed by the addition of 1 mL of a 25 mM solution of N-N-dimethyl-p-phenylenediamine in 1 M sulfuric acid to the same cuvette. A Pasteur pipette was used to add one drop of saturated iron (III) chloride to the cuvette to act as the oxidant, based on the following reaction:

$$2(CH_3)_2C_6H_4NH_2 + H_2S + 6Fe^{3+} \rightarrow 6Fe^{2+} + NH_4^+ + 4H^+ + C_{16}H_{18}N_3S^+ \quad (2.2.3)$$

The cuvette was then gently inverted to mix, minimizing oxygen introduction, and was placed in the dark for 5 minutes. After the color in the cuvette was fully developed, a 1:40 dilution of the solution was performed in a second cuvette using nitrogen-sparged MilliQ water as the diluent. This dilution step was required to reduce absorbance in the cuvette to a measureable level. The second cuvette was then gently inverted and placed in the dark for five minutes while color developed. Absorbance was then measured using a UV-1800 UV-Vis Spectrophotometer (Shimadzu Corp.; Kyoto, Japan) operated at a wavelength of 664 nm. A linear standard curve of sulfide concentration versus absorbance was attainable up to sulfide concentrations of approximately 100 mg/L. Calibration standards were prepared in nitrogen-sparged MilliQ water using a sodium sulfide nonahydrate salt. Concentrations higher than 100 mg/L required dilution prior to the addition of N-N-dimethyl-p-phenylenediamine and iron (III) solutions. The limit of quantitation and method detection limits were calculated to be 3.2 and 1.6 mg/L sulfide, respectively (Hubaux & Vos, 1970).

Acid volatile sulfide analysis: Solid phase sulfide concentrations were measured using a variation of EPA method EPA-821-R-91-100 using three 250 mL Erlenmeyer flasks instead of spherical reaction vessels (Allen et al., 1991). The a first flask contained 6 M hydrochloric acid, while the second and third flasks contained solutions of 0.5 M sodium hydroxide. Solid sulfide complexes reacted with hydrochloric acid in flask 1 to form hydrogen sulfide gas (equation 2.2.4), which was then purged and trapped in flasks 2 and 3 as deprotonated sulfide (equation 2.2.5). Nitrogen was used as the purge gas.

$$FeS + 2HCl \rightarrow FeCl_2 + H_2S \quad (2.2.4)$$

$$2OH^- + H_2S \rightarrow S^{2-} + 2H_2O \quad (2.2.5)$$

To determine the acid volatile sulfide content of solid samples, 100 mL of MilliQ water was first added to flask 1, and 100 mL of 0.5 M sodium hydroxide was added to flasks 1 and 2. The system was then purged with nitrogen for 10 minutes at approximately 100 mL/min to remove oxygen. Nitrogen flow was then reduced to 40 mL/min, measured using an Alltech model 4700 digital flow meter (Alltech Associates, Inc.; Deerfield, IL), and approximately 10 g of wet soil was

added to flask 1, using sulfide-free parafilm instead of a weighing dish. The system was once again purged for 10 minutes at a nitrogen flow rate of 10 mL/min. Nitrogen flow was then stopped and 10 mL of 6 M hydrochloric acid was injected through a septum into flask 1. Nitrogen flow was reestablished at 20 mL/min for 60 minutes. The methylene blue method for aqueous phase sulfide analysis was then used to determine sulfide concentration in the two traps, flasks 2 and 3.

Aqueous phase iron (II) and total iron analysis: Iron (II) and total iron concentrations were measured using a variation of the spectrophotometric ferrozine method (Stookey, 1970; Viollier et al., 2000; Costanza, 2005). Three reagents were prepared for the ferrozine analysis; Reagent A was a solution of 100 mM ammonium acetate and 10 mM ferrozine iron reagent; Reagent B was a reducing solution of 1.2 M hydroxylamine hydrochloride in 1.7 M hydrochloric acid; Reagent C was a buffering solution of 10 M ammonium acetate, adjusted to pH 9.55 using a 28% ammonium hydroxide solution. Reagent A (300 µL) was added to a UV spectrophotometer cuvette, followed by 25 µL of the sample to be analyzed. The cuvette was then inverted to mix and placed in a dark room for two minutes. MilliQ water (2.5 mL) was then added, and the cuvette was returned to the dark room for 10 minutes. Once the reaction was complete, an absorbance reading was taken using a UV spectrophotometer at a 562 nm wavelength to measure iron (II) concentration. Reagent B (200 µL) was then added to the cuvette before it was returned to the dark room for 10 minutes. Reagent C (50 µL) was then added to the cuvette and another absorbance reading was taken at 562 nm wavelength to measure total iron concentration. Linear standard curves of iron (II) and total iron concentrations versus absorbance were attainable up to total iron concentrations of approximately 30 mg/L. Samples with higher total iron concentrations required dilution prior to ferrozine analysis. Calibration standards were prepared using a stock solution of iron (II) chloride tetrahydrate at concentrations ranging from 1 to 30 mg/L iron (II).

Bromide, oxidation-reduction potential, pH, and dissolved oxygen measurement: Bromide concentrations were measured using an ion-selective conductivity probe (Cole-Parmer; Vernon Hills, IL) connected to an Orion model 420A+ conductivity meter (Thermo Scientific; Waltham, MA) or an Accumet Model 50 pH/ion/conductivity meter (Fisher Scientific; Fair Lawn, NJ). ORP was measured using an Accumet platinum pin Ag/AgCl combination electrode (Fisher Scientific; Fair Lawn, NJ) connected to an Orion model 420A+ conductivity meter. pH was measured using an Orion Triode Ag/AgCl combination pH/ATC electrode (Thermo Scientific; Waltham, MA) connected to an Orion 3-Star pH meter (Thermo Scientific; Waltham, MA). Dissolved oxygen was measured using self-filling CHEMets ampule kits K-7512 (1-12 mg/L) and K-7501 (0-1 mg/L) (CHEMetrics; Midland, VA).

2.2.2. Abiotic Head Driven Columns

In addition to the pump driven column experiments designed to quantify permeability loss due to FeS precipitation, four 15 cm, abiotic, head-driven column experiments were also completed. These head-driven column experiments were designed to simulate more realistic field conditions, since the lack of a pump as the driving force allows for flow through the columns to slow or stop entirely if sufficient FeS precipitation occurs.

2.2.2.a. Operation of abiotic head driven columns

The influent solutions used during abiotic head-driven column experiments were similar to those used in pump driven experiments, but there were some other limited changes to maximize the information gained from each experiment. Head-driven column experiments were completed

in pairs that were subjected to identical hydraulic gradients and influent solutions: the first pair, Federal Fine column #6 and Appling column #3 (Figure 2.2.4), was designed to provide a direct comparison of permeability loss between porous media with different amounts of organic carbon; the second pair included both Webster columns, but only Webster column #1 was exposed to iron (II) prior to the sulfide flush, in an effort to evaluate the impacts of excess iron (II) on FeS precipitation and soil permeability losses. A summary of head-driven column experiment parameters is shown in Table 2.2.2.

Table 2.2.2. Abiotic head-driven column experiment influent parameters. Initial velocity is the pore water velocity at the beginning of the column experiment.

Column	**Influent phases**	**Initial velocity (cm/day)**	**Fe^{2+} (mg/L)**	**S^{2-} (mg/L)**	**Medium buffer** 10 mM TES +	**Ionic strength (mM)**
Federal Fine #6	Fe^{2+}/S^{2-}	350	850 (15)	75 (76)	10 mM $PO_4^{2-/3-}$	60
Appling #3	Fe^{2+}/S^{2-}	300	850 (17)	75 (57)	10 mM $PO_4^{2-/3-}$	60
Webster #1	$Fe^{2+}/S^{2-}/O_2$	250	800 (4)	100 (73)	10 mM $PO_4^{2-/3-}$	60
Webster #2	S^{2-}/O_2	240	na	100 (44)	10 mM $PO_4^{2-/3--}$	60

Flow through each head-driven experiment was delivered by elevating the anoxic influent bottle above the effluent line, establishing a hydraulic gradient. Unlike during the pump-driven column experiments, flow rates gradually declined as FeS precipitation occurred, necessitating a higher initial pore water velocity. The flow rate of each column was monitored using a CF-2 fraction collector (Spectrum Labs, Rancho Dominguez, CA), allowing for calculation of permeability changes over time using Darcy's Law. Although influent chemistry was strictly monitored, according to the protocols outlined in section 2.2.1.h, effluent samples were not collected during head-driven experiments in order to avoid flow disturbances.

Figure 2.2.5. Head-driven column experiment setup with anoxic influent bottle above Federal Fine column #6 and Appling column #3 effluent line heights to establish gravity flow.

2.2.3. Abiotic Aquifer Cell Experiments

An aquifer cell experiment was completed to assess the effects of FeS precipitation and subsequent oxidation on soil permeability and development of hydraulically isolated zones (i.e., flow bypassing) in a 2-D, head-driven system. The aquifer cell consisted of two glass panes, Viton rubber gaskets, and an aluminum frame, with hydraulically active interior dimensions of 63.5 cm length × 1.4 cm width (thickness) × 38 cm height, and pore volume of 1,200 mL (Figure 2.2.6). The front glass pane was equipped with two injection ports and 16 sampling ports. A layer of F-70 quartz sand served as a low permeability lower boundary. The cell was packed under a 2-cm head of MilliQ water with a Federal Fine Ottawa sand background, and included a 17.5 cm × 3.7 cm lens of #30 mesh Appling soil (0.66% organic carbon). The Appling soil lens was included to assess the impacts of FeS precipitation in a more realistic soil, with lower permeability and moderate total organic carbon (TOC) content.

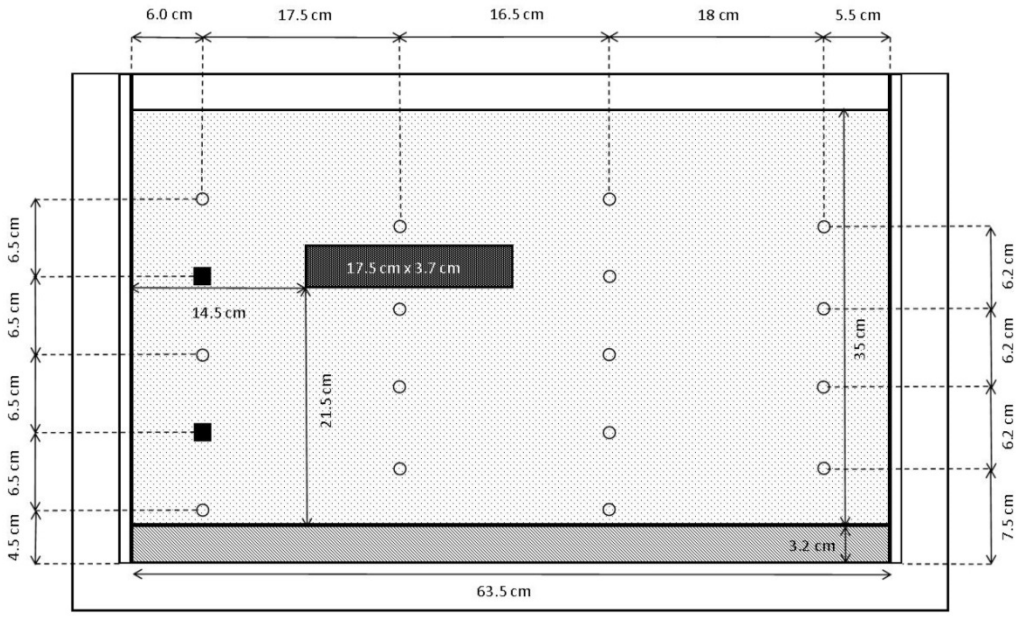

Figure 2.2.6. Diagram of 2-D aquifer cell showing locations and dimensions of the low permeability F-70 layer (bottom), Federal Fine Ottawa sand (background), Appling soil lens (dark rectangle), sampling port locations (empty circles), and injection port locations (filled squares).

Flow through the aquifer cell was maintained by establishing a constant differential head at the inlet and outlet chambers (Figure 2.2.7). Monometers located in both the influent and effluent well screens allowed for direct monitoring of differential head and calculation of overall hydraulic conductivity of the aquifer cell.

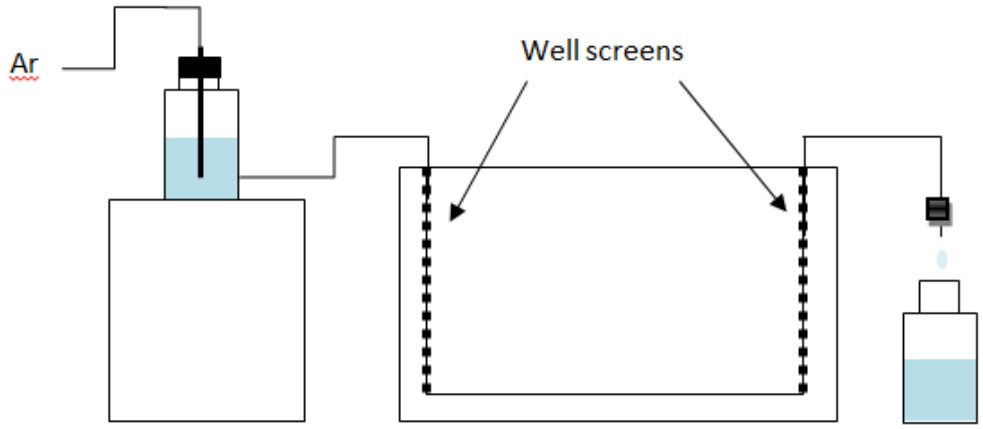

Figure 2.2.7. Diagram of 2-D aquifer cell showing locations of influent and effluent well screens, and operational setup.

2.2.3.a. Operation of the aquifer cell

Similar to the column experiments described previously, the aquifer cell experiment was completed in two phases: an abiotic FeS precipitation phase, followed by an aerobic phase. Non-reactive tracer tests were performed before and after each phase of the experiment to characterize changes in hydraulic conditions within the aquifer cell.

Throughout the FeS precipitation phase, 6.4 PV of $FeCl_2$ (600 mg/L Fe^{2+}) was flushed through the influent well of the aquifer cell at 1.2 mL/min (approximately 1.4 PV/day). After 2 PV of $FeCl_2$ had been flushed through the cell, high sulfide medium (0.77 PV; 70 mg/L) was simultaneously introduced through the two injection ports on the face of the aquifer cell at a flow rate of 0.1 mL/min to induce FeS precipitation. Photos were taken approximately every eight hours throughout the FeS precipitation phase.

Following the second tracer test, which was performed to evaluate changes in flow due to FeS precipitation, an oxygenated (5.5 mg/L DO) solution of 60 mM $CaCl_2$ was introduced to the aquifer cell through the influent well screen. In total, 32 PV of oxygenated solution were flushed through the aquifer cell at a flow rate of 2.5 mL/min. Photos were taken approximately every 24 hours throughout the oxidation phase.

2.2.4. Biotic Batch Reactors to Examine *Dhc* Sulfide Tolerance

Biotic batch reactor studies were completed to determine the sulfide concentrations that began to limit or prevent the dechlorination abilities of BDI-SZ. Results from the batch reactor studies can be used to guide the use of PCE-to-ethene dechlorinating consortiums in regions with high sulfate, and in turn, high sulfide concentrations following stimulation of sulfate-reducing bacteria due to electron donor additions.

2.2.4.a. Materials and microbial culture

For sulfide analysis, >98% N-N- dimethyl-p-phenylenediamine, sulfuric acid, 98% iron (III) chloride, hydrochloric acid, and sodium hydroxide were used as reagents (details can be found in Section 2.2.1.a). The reduced mineral salts medium, a recipe that has been described previously (Löffler et al. 2005, Loffler et al. 1996, Sanford et al. 2002, Thomas et al. 2010) was used.

The Bio-Dechlor INOCULUM (BDI-SZ) culture was a non-methanogenic PCE-to-ethene dechlorinating consortium evaluated in PCE dechlorination experiments. This inoculum was composed of several dechlorinating cultures including the PCE to *cis*-DCE dechlorinating species, *Dehalobacter* and *Geobactor lovelyi* SZ, as well as three *Dehalococcoides mccartyi* (*Dhc*) strains (FL2, GT, and BAV1) capable of the full PCE to ethene degradation. *Geobacter lovelyi* SZ also possesses the ability to reduce iron (III) to iron (II) (Sung et al. 2006). Optimal activity for this culture aligns with that of pure *Dhc* cultures that have been measured in the pH range of 7.2-7.4 (He et al. 2003, Löffler et al. 2013). BDI-SZ was maintained with 0.33 mM PCE and 10mM lactate at 35°C without shaking.

2.2.4.b. Biotic reactor experimental design

All batch reactor experiments were prepared in triplicate 160 mL serum bottles (Wheaton; Millville, NJ) capped with butyl rubber stoppers (Geo-Microbial Technologies, Inc.; Ochelata, OK) and an aluminum crimp cap (Wheaton) to assess reproducibility of results. Triplicate reactors

containing were prepared with 100 mL of the anoxic medium described previously (Löffler et al. 2005). PCE (3-5 µL) was then added through the rubber septa for a target final concentration of 50 mg PCE/L. These bottles were then autoclaved on the liquid cycle at 121°C for 30 minutes. The reactors were then amended with 5% by volume of BDI-SZ. Wolin vitamins (100 µL) were added last to each reactor (Wolin et al. 1963). Iron (II), total iron, and the PCE dechlorination byproducts were then measured with time.

To assess sulfide toxicity on the BDI-SZ consortium, reactors were prepared in 7 triplicate sets (1 of the 7 was an abiotic control containing 0.4 mM sulfide and no BDI-SZ). Each set of three reactors was designated a target sulfide concentration that corresponded to 0.4 mM, 1 mM, 5 mM, 8 mM, 12 mM, or 20 mM. Sulfide was added by filter sterilizing a known stock concentration of sodium sulfide nonahydrate to the reactors. Addition of the sodium sulfide nonahydrate to the reactors results in basic byproducts which can raise the pH. Hydrochloric acid (12.1 M) was used to adjust pH to circumneutral values prior to adding any microbial cultures, particularly for the reactors containing high levels of sodium sulfide nonahydrate. Lastly, the same culture of BDI-SZ was added to each reactor so the volume of inoculate was 5% of the total medium volume. Wolin vitamins (100 µL) were added last to each reactor (Wolin et al. 1963). PCE and its degradation products were monitored over time.

2.2.4.c. Analytical methods

The methods for the analysis of bromide, ORP, pH, DO, sulfide, and hydraulic conductivity are described in section 2.2.1. The two volatile fatty acids used as electron donors, lactate and acetate, were measured on a Dionex ICS-2100 IC equipped with an AS-11 HC isocratic column with an ID 4 mm and length of 250 mm. Potassium hydroxide (30 mM) was used as the eluent with a 4 mm ASRS suppressor operating at 112 mA. The IC cell and column temperatures were 35 °C, while the flow rate was 1.50 mL/min. To analyze the VFAs, the pump was set to a multi-step gradient for a run time of 56 minutes. To avoid degradation of IC components due to the chlorinated solvents present in the samples, samples were weighed and left open to the atmosphere in a hood overnight to reduce the concentration of volatile organic compounds. The following day, the samples were reweighed and water was added to each vial to make up for the differences in mass.

Concentrations of chlorinated ethenes were determined using an Agilent 7890A GC equipped with an FID and an Agilent J&W DB-624 capillary column (Agilent Technologies; Lexington, MA) with an HT3 headspace autosampler (Teledyne-Tekmar; Mason, OH). The column had an ID of 0.32 mm and was 60 m in length with a film thickness of 1.8 µm.

2.3. Impacts of Remedial Strategies on pH and Microbial Reductive Dechlorination

To evaluate the consequences of pH reductions on reductive dechlorination activity and microbial community structure, a series of experiments of increasing complexity were performed. First, batch culture experiments with a variety of dechlorinating pure and mixed cultures available in the Löffler lab were used to determine the pH boundary conditions for reductive dechlorination activity. The effects of fluctuating pH on dechlorination rates and the microbial community structure, including the abundance of key dechlorinators, was monitored. These experiments were designed to determine the effects of pH decrease on reductive dechlorination, and also evaluate the ability of the dechlorinators to tolerate pH fluctuations. In addition, we enriched bacteria that

could dechlorinate chlorinated ethenes at low pH. While numerous isolates are available that efficiently dechlorinate between pH 6.5 and 8, none of the currently known bacteria use chlorinated ethenes as respiratory electron acceptors at pH < 6. Since many contaminated groundwaters have pH values below 6.5, the paucity of microbes capable of reductive dechlorination in the lower pH range provided an opportunity to discover new organisms that perform in low pH environments.

2.3.1. Tolerance of Existing Isolates and Mixed Dechlorinating Cultures to pH Changes

A series of batch reactor tests were performed to assess the ability of existing isolates and mixed cultures available in the Loffler laboratory to dechlorinate PCE at pH 5.5, 6 and 7.2.

2.3.1.a. Chemicals

PCE and trichloroethene (TCE) were purchased from Acros Organics (VWR international, West Chester, PA, USA). cis-1,2-Dichloroethene (cDCE), vinyl chloride (VC) and ethene were obtained from Sigma-Aldrich Chemicals (St. Louis, MO, USA). HOMOPIPES (homopiperazine-1,4-bis(2-ethanesulfonic acid)) and MES (2-(N-morpholino)ethanesulfonic acid) were purchased from Acros Organics. Sodium bicarbonate was purchased from Fisher Scientific (Pittsburgh, PA, USA).

2.3.1.b. Medium preparation

Reduced mineral salts medium was prepared with deionized water following established protocols (Löffler et al. 2005). A filter-sterilized (0.22 μm) vitamin stock solution was added by syringe after the medium had been autoclaved (Löffler et al. 2005). Lactate (5 mM) and hydrogen gas (10 mL) were added to 160-mL serum bottles as carbon source and electron donor, respectively. The mineral salts medium contained 30 mM bicarbonate and the pH was adjusted to 7.2 with CO_2. For pH 4.5 mineral salts medium, 30 mM HOMOPIPES (pKa=4.84 at 20 °C) replaced bicarbonate. For pH 5.5 or 6 mineral salts medium, MES buffer (pKa=6.15 at 20 °C) was used. Culture bottles prepared with Good buffers (Good et al. 1966) were flushed with oxygen-free dinitrogen and following the distribution of medium, 1 mM sodium bicarbonate was added from a 1 M stock solution. The medium pH values were verified after autoclaving, after inoculation and after incubation. If necessary, pH adjustments were conducted by adding appropriate volumes of 1 M hydrochloric acid or 1 M sodium hydroxide from nitrogen-flushed anoxic and filtered-sterilized stock solutions.

2.3.1.c. Screening for dechlorinating isolates and mixed cultures as a function of pH

Several PCE-dechlorinating isolates (*Desulfuromonas michiganensis* strain BB1 (Sung et al. 2003), *Desulfitobacterium* sp. strains Viet1 (Tront et al. 2006), *Desulfitobacterium* sp. strain JH1(Fletcher et al. 2008), *Geobacter lovleyi* strain SZ (Sung et al. 2006), *Sulfurospirillum multivorans (*Scholz-Muramatsu et al. 1995*)*) and a *Dhc*-containing consortium BDI (Bio-Dechlor Inoculum) (Cápiro et al. 2014) were tested for PCE dechlorination at pH 5.5, 6 and 7.2. These dechlorinating isolates and mixed cultures were maintained in the lab fed with PCE (Löffler et al. 2005). *Desulfuromonas michiganensis* strain BB1, *Desulfitobacterium* sp. strains Viet1 and JH1, *Geobacter lovleyi* strain SZ, *Sulfurospirillum multivorans* and a *Dhc*-containing consortium BDI were pre-cultivated in 160 mL serum bottles containing 100 mL pH 7.2 mineral salts medium amended with 5 μL neat PCE, 10 mL hydrogen and 5 mM lactate. Screening experiments were conducted by inoculating triplicate serum bottles containing 100 mL of mineral salts medium (pH 5.5, 6 or 7) with 3 mL culture grown at pH 7.2.

2.3.1.d. Analytical methods

The pH of the bulk liquid phase was measured by transferring 1 mL liquid aliquots from a culturing vessel into a 2-mL plastic tube. After centrifuging the tube for 30 seconds at 14,000 rpm in a microcentrifuge, the pH of the supernatant was measured with Fisher Scientific Accumet Glass AgCl pH electrode (Pittsburgh, PA, USA).

Concentrations of chlorinated ethenes were measured by analyzing 100 µL headspace gas samples using an Agilent 7890A GC equipped with an Agilent DB624 column (30 m × 0.53 mm ID, 3 µm film thickness) with an FID. Gas samples (100 µL) were removed from the headspace of 160 mL serum bottles using a gas-tight 250 µL Hamilton SampleLock syringe and then injected into the GC manually. The concentrations of chlorinated ethenes were calculated by normalizing the peak area values to standard curves generated by adding known amounts of chlorinated ethenes to the bottles with same gas to liquid ratio. The total moles of chlorinated ethenes per bottle was calculated by the formula: total moles = (volume x density)/molecular weight. The retention times for different chlorinated ethenes and ethene were determined by injecting neat compounds into the GC, and used to assign peaks to PCE daughter products.

2.3.2. Effects of Fluctuating pH on Dechlorination in Batch Reactors

While it is established that *Dhc* perform best at circumneutral pH, information about the effects of low pH exposure on the ability of *Dhc* to recover reductive dechlorination activity is lacking. To address this knowledge gap, experiments were conducted to investigate the growth of Dhc under acidic conditions, and to study the recovery of Dhc after low pH exposure. The general procedures described in Section 2.3.1 were followed, with the modifications described below for preparation and handling of the batch reactors.

2.3.2.a. Reactor preparation

The consortium biomass, grown at pH 7.2 with PCE as electron acceptor (Step 1), was collected and suspended in pH 5.5 and pH 7.2 medium (Step 2). Following incubation of 8 (Step 3), 16 (Step 4), and 40 (Step 5) days at pH 5.5 and 7.2. The biomass was collected again and transferred to pH 7.2 medium amended with hydrogen (electron donor), lactate (carbon source) and PCE. Chlorinated ethenes and ethene were monitored to determine if reductive dechlorination activity recovered after exposure to low pH for 8-40 days. In addition, *Dhc* 16S rRNA gene copies were being enumerated with qPCR to evaluate *Dhc* cell growth. Reductive dehalogenase genes *tceA*, *vcrA* and *bvcA* were monitored to determine if different *Dhc* strains respond differently to low pH exposure (Figure 2.3.1). In addition, a qPCR assay was performed following established protocols (Ritalahti et al. 2006a).

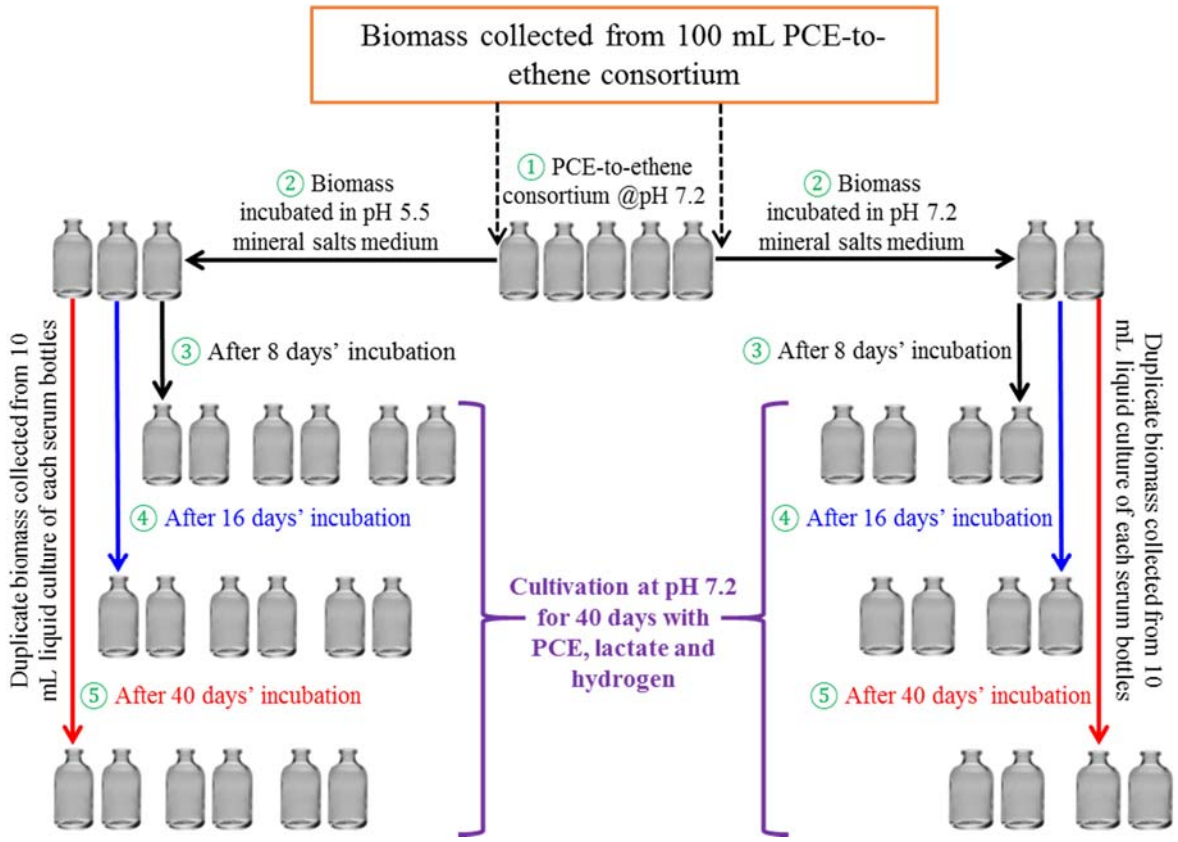

Figure 2.3.1. Experimental scheme used for recovery of a PCE-to-ethene consortium exposed to low pH stress; pH 7.2 incubation was used as the control group.

2.3.2.b. DNA extraction and PCR

Microbial biomass was collected from 2-mL liquid culture suspension by vacuum filtration through 0.22 µm membrane filters (Millipore GVWP025000). Filter-trapped microbial cells were suspended in the PowerSoil® bead tubes (Mo Bio Laboratories Inc., Carlsbad, CA) and ruptured with a high efficiency Bead Ruptor Homogenizer (Omni International, Kennesaw, GA, USA) at a speed of 3.25 m/s for 5 minutes. Genomic DNA was extracted using the PowerSoil® DNA Isolation Kit (Mo Bio Laboratories Inc., Carlsbad, CA) following the manufacturer's recommendations. DNA concentrations were quantified with a NanoDrop 1000 (NanoDrop Technologies, Wilmington, DE). DNA samples extracted from replicate cultures were pooled and stored at -20°C. Molecular tools, such as quantitative PCR have been used to investigate how low pH condition exposure affected dechlorinators and their functional genes.

2.3.2.c. Statistical analysis

All statistical analyses were performed using R Statistical Software (version 3.2.4., R Foundation for Statistical Computing, Vienna, Austria). Variance homogeneity of two pH intervals was tested by Bartlett test and Fligner-Killeen test with the default parameters. One-way t-test was used to compare the average of two pH intervals with the alternative parameter set as "less".

2.3.3. Microcosm Studies Conducted with Materials from Low pH Sites

The known dechlorinators are neutrophils limited to sustained dechlorination in neutral pH environments, and no microbes capable of growth with chlorinated ethenes at pH 5.5 have been described to date. To fill this knowledge gap, a series of experiments was conducted to enrich and isolate PCE dechlorinators from field sites in an effort to identify isolates capable of PCE dechlorination under low pH conditions.

2.3.3.a. Sampling site conditions

Soil and groundwater samples collected from a total of sixteen sites were used to establish microcosms for enriching PCE dechlorinators at pH 5.5 and pH 7.2 (Table 2.3.1). Groundwater, soil and sediment samples were transferred to the lab and stored at 4°C for no longer than 1 week prior to microcosm setup.

2.3.3.b. Microcosms setup and culture transfer

Before setting up the microcosms, groundwater, soil and sediment samples were transferred into glove box (filled with nitrogen and 3% hydrogen). After opening 160 mL serum bottles with 100 mL mineral salts medium in the glove box, soil or sediment samples (about 10 g wet weight) were added to the bottles with autoclaved spatulas; or 50 mL groundwater was mixed with 50 mL mineral salts medium. The serum bottles were closed with autoclaved black rubber stoppers (Geo-Microbial Technologies, Inc., Ochelata, Okla.) and crimped with aluminum caps. After removing the serum bottles from the glove box, neat liquid PCE (5 μL) were added into serum bottles by 5 μL Hamilton gas-tight micro-syringe (Hamilton Company, Rena, Nevada). All microcosms were established in duplicate or triplicate, and incubated at room temperature (21°C). Time zero measurements were conducted after a 24-hour equilibration period. After VC and ethene were detected in the original microcosms, the microcosms were shaken vigorously, and 3 mL of inoculum were removed with nitrogen-flushed 3-mL syringes. The withdrawn culture suspension was immediately injected into a new bottle with fresh mineral salts medium. To enrich microbes under different pH conditions, several buffer systems were used including 30 mM HOMOPIPES for pH 4.5, 30 mM MES for pH 5.5 or 6 mineral salts medium, and 30 mM bicarbonate for pH 7.2 mineral salts medium. Aseptic techniques were applied to all steps.

Table 2.3.1. Summary of soil and groundwater samples collected from low pH sites.

#	Sample sites ID	Locations	Sample Type	Carbon Source Electron Donor	Electron Acceptor	PCE Degradation End Product	
						pH 5.5	pH 7.2
1	Ft. Pierce	USA	Soil	Lactate + H_2	PCE	X	X
2	PNNL	USA	Soil	Lactate + H_2	PCE	X	X
3	DuPont Oakley	USA	Soil	Lactate + H_2	PCE	X	X
4	-	Brazil	Soil	Lactate + H_2	PCE	X	X
5	Third Creek	TN, USA	Sediment	Lactate + H_2	PCE	Ethene	Ethene
6	Neckar River	Germany	Sediment	Lactate + H_2	PCE	Ethene	Ethene
7	Rotenberg Trester	Germany	Soil	Lactate + H_2	PCE	VC, Ethene	VC, Ethene
8	Rotenberg Creek	Germany	Soil	Lactate + H_2	PCE	X	X
9	McGuire AFB	USA	Soil, GW	Lactate + H_2	PCE	X	X
10	-	USA	Soil, GW	Lactate + H_2	PCE	X	X
11	-	USA	Soil, GW	Lactate + H_2	PCE	Ethene	Ethene
12	Shady Valley	TN, USA	Soil, Sediment	Lactate + H_2	PCE	*c*DCE	*c*DCE
13	Axton Cross	USA	Soil, GW	Lactate + H_2	PCE	VC	Ethene
14	-	USA	Soil	Lactate + H_2	PCE	X	X
15	Tidal Flat	Korea	Soil	Lactate + H_2	PCE	X	TCE
16	Elkhart Rail Yard	USA	Soil, GW	Lactate + H_2	PCE	Ethene	Ethene

2.3.3.c. DNA extraction

Microbial biomass was collected from 2-mL liquid culture suspension by vacuum filtration through 0.22 μm membrane filters (Millipore GVWP025000). Filter-trapped microbial cells were suspended in the PowerSoil® bead tubes (Mo Bio Laboratories Inc., Carlsbad, CA) and ruptured with a high efficiency Bead Ruptor Homogenizer (Omni International, Kennesaw, GA, USA) at a speed of 3.25 m/s for 5 minutes. Genomic DNA was extracted using the PowerSoil® DNA Isolation Kit (Mo Bio Laboratories Inc., Carlsbad, CA) following the manufacturer's recommendations. DNA concentrations were quantified with a NanoDrop 1000 (NanoDrop Technologies, Wilmington, DE). DNA samples extracted from replicate cultures were pooled and stored at -20°C.

2.3.3.d. 16S rRNA gene amplicon sequencing and analysis

MiSeq 16S rRNA gene amplicon sequencing was performed to reveal the taxonomic compositions of the pH 5.5 and pH 7.2 dechlorinating enrichment cultures derived from the ACS site. Sequencing used a MiSeq desktop sequencer (Illumina, Inc., San Diego, CA, USA) available through the Center of Environment Biotechnology at the University of Tennessee and followed established protocols (Caporaso et al. 2012). Amplification was performed in 50 μL assays consisting of 5 μL DNA sample, 1 μL barcoded-primer (10 μM) targeting the V4 variable region of the 16S rRNA gene, and 44 μL of a mixture of 31 μL deionized molecular biology grade water (5 PRIME Inc., Gaithersburg, MD, USA), 5 μL Invitrogen Pfx50™ buffer (Invitrogen, Carlsbad,

CA, USA), 1 µL CAP 515F primer (10 µM), 1 µL dNTP, 1 µL Invitrogen Pfx50™ Polymerase and 5 µL of MgCl2 (25 mM) (Invitrogen, Carlsbad, CA, USA). The following temperature cycling program was applied: denaturation at 94°C for 3 min followed by 35 cycles at 94°C for 45 sec, annealing at 55°C for 60 sec, and extension at 72°C for 90 sec, and final extension at 72°C for 10 min. The amplicon quality (size) was checked using the High Sensitive DNA Kit on a model 2100 Bioanalyzer (Agilent, Santa Clara, CA, USA). The relative DNA concentrations of individual samples were estimated based on the peak height of the appropriate sized amplicons compared with the upper marker peak heights with samples with known DNA concentrations. Then, DNA of individual samples was pooled to contain equal quantities of DNA from each sample. Pooled samples were purified with solid-phase reversible immobilization (SPRI) magnetic beads (Beckman Coulter, Inc., Indianapolis, IN, USA). The purified samples were analyzed again with the High Sensitive DNA kit for quality assurance and verification of complete removal of primer dimers. The Illumina sequencing library was quantified using the quantitative PCR-based Illumina Library Quantification kit (KAPA Biosystems, Boston, MA, USA) following the manufacturer's protocol. The library concentration was diluted to 10 nM followed by Illumina sequencing. Forward and reverse sequence files were paired and analyzed using Mothur software using the analysis pipeline MiSeq SOP (Kozich et al. 2013). After quality control, 69,030 sequences (17,441,054 total base pairs) from the ACS pH 5.5 enrichment and 103,503 sequences (26,171,881 total base pairs) from ACS pH 7.2 enrichment were obtained. These trimmed and paired sequences were uploaded to the SILVAngs server for analysis based on high-quality SILVA alignment (Quast et al. 2013). A total of 83 sequences were rejected by SILVAngs and were not analyzed. The remaining sequences were analyzed using the SILVAngs data analysis service with the default parameters (www.arb-silva.de/ngs/service/file/?file=SILVAngs_User_Guide_15_12_15.pdf).

2.3.3.e. Isolation procedures for dechlorinators at low pH

Isolation efforts focused on the ACS PCE-dechlorinating enrichments that maintained dechlorinating activity for at least 10 consecutive transfers in pH 5.5 medium. Dilution to extinction series in liquid and semi-solid medium prepared with modified 1% (w/vol) low melting agarose (MP Biomedicals, LLC., Solon, OH, USA) with 5 mM lactate and 1 µL neat PCE were established as described (Löffler et al. 2005). Colony formation was monitored weekly by visual inspection. Eight white colonies with an estimated radius of approximately 0.5 mm were retrieved from the 10-4 and 10-5 dilution agar tubes using a nitrogen-flushed 1-mL plastic syringe with a 25G x 7/8 BD PrecisionGlide needle (BD, Franklin Lakes, NJ, USA) and transferred to 160-mL serum bottles with fresh pH 5.5 medium to test for PCE dechlorination.

2.3.3.f. Identification of isolates and construction of phylogenetic tree

PCR amplicons obtained with the 16S rRNA gene-targeted general bacterial primers set 8F/1541R (8F-AGA GTT TGA TCC TGG CTC AG and 1541R-AAG GAG GTG ATC CAG CCG CA) (Löffler et al. 2005) were treated with the DNA Clean & Concentrator™-5 kit (Zymo Research Corp., Irvine, CA, USA). Both strands of purified amplicons were Sanger sequenced, and nearly full-length 16S rRNA gene sequences were obtained by using DNA Baser software (Heracle BioSoft SRL, Romania) to pair both strands with default settings. The 16S rRNA gene sequences were then blasted against the NCBI NT database to identify phylogenetically related (>97% sequence similarity) sequences (Table 2.3.2). The sequences were imported into the Geneious software environment (Biomatters, Auckland, New Zealand), aligned with MAFFT (Katoh et al. 2002)., and a 16S rRNA gene phylogenetic tree was constructed with Tree Builder

using software's default settings. A Zeiss Axio Imager.A2 was used to visualize the liquid cultures for microscopic examination.

Table 2.3.2. 16S rRNA gene sequences used to build the *Sulfurospirillum* phylogenetic tree.

Name	Accession Number	Sequence Length
Desulfitobacterium dehalogenans strain ATCC 51507	NR_074128.1	1447
Desulfitobacterium dichloroeliminans	AJ565938.1	1467
Desulfitobacterium frappieri	U40078.1	1655
Desulfitobacterium hafniense strain DCB-2	NR_122068.1	1554
Escherichia coli str. K12	AP009048.1	1551
Sulfurospirillum alkalitolerans strain HTRB-L1	GQ863490.1	1437
Sulfurospirillum arcachonense strain F1F6	NR_026408.1	1433
Sulfurospirillum arsenophilum	U85964.1	1321
Sulfurospirillum arsenophilum strain MIT-13	NR_044806.1	1321
Sulfurospirillum barnesii SES-3	NR_102929.1	1497
Sulfurospirillum carboxydovorans strain MV	AY740528.1	1354
Sulfurospirillum cavolei	AB246781.1	1336
Sulfurospirillum cavolei strain Phe91	NR_041392.1	1336
Sulfurospirillum deleyianum strain DSM 6946	NR_074378.1	1497
Sulfurospirillum deleyianum strain Spirillum 5175	NR_026422.1	1431
Sulfurospirillum halorespirans strain PCE-M2	AF218076.1	1489
Sulfurospirillum multivorans strain DSM 12446	NR_121740.1	1498
Sulfurospirillum multivorans strain K	NR_044868.1	1464
Sulfurospirillum sp. C6	DQ228139.1	1201
Sulfurospirillum sp. EK7	AJ535704.1	1431
Sulfurospirillum sp. JPD-1	AY189928.1	1415
Sulfurospirillum sp. NO3A	AY135396.1	1300
Sulfurospirillum sp. strain PLC_{DCE}		1375
Sulfurospirillum sp. strain PLC_{TCE}		1015

2.3.4. Reactor Studies to Evaluate the Influence of Solids on pH Tolerance

To evaluate the effect of soil physical and chemical properties on microbial dechlorination activity at low pH conditions, an additional set of reactors studies was performed with the field soil samples (Table 2.3.1).

2.3.4.a. Preparation of soil reactors

Soils collected from contaminated sites were sterilized by autoclave (gravity cycle: 20 min 121°C and 15 min dry) and then oven-drying at 100°C for about 12 hours. Sterilized soil samples were cooled to room temperature and then moved into the glove box to remove the oxygen from the soil samples. Serum bottles with 100 mL pH 5.5 mineral salts medium were added with 20 g

sterilized soil in triplicate. The batch reactors were also amended with lactate (carbon source), hydrogen (electron donor) and PCE (electron acceptor). After batch reactors were removed from the glove box, 3 mL pre-grown BDI culture was inoculated into the reactors by a nitrogen-flushed 3 mL syringe. When the reactor systems were established, the pH of bulk liquid phase was measured by transferring 1 mL liquid aliquot from the culturing vessel into a 2-ml plastic tube. After centrifuging the tube for 30 seconds at 14,000 rpm, the pH of the supernatant was measured with Fisher Scientific Accumet Glass AgCl pH electrode (Pittsburgh, PA, USA). PCE dechlorination activities were monitored by injecting 100 μL gaseous samples from the headspaces of the batch reactors into GC as Section 2.3.1.d. After PCE was degraded into VC or ethene, the pH of the bulk liquid phase was measured again.

2.3.4.b. Analysis of soil physical and chemical properties

To obtain physical-chemical properties of the solid phase, soil samples (Table 2.3.1) were packed and sent to Soil, Plant, and Water Analysis Laboratory (SPW) in University of Georgia, Athens (UGA). For each soil sample, the laboratory performed the "S2" analysis, which includes pH, Ca, P, Lime Requirement, Zn, K, Mn, Na, Fe, Cu, Cr, Mo, Ni, Cd, Pb, Cation Exchange Capacity (CEC), and Percent Base Saturation.

CHAPTER 3

RESULTS AND DISCUSSION

3.1. IMPACTS OF THERMAL TREATMENT ON GROUNDWATER GEOCHEMISTRY AND COMBINED REMEDIES (TASK 1)

3.1.1. Ampule Experiments Evaluating the Release of Electron Donors from Heated Soils

The primary objective of this work was to determine the effects of thermal treatment of soils on the release of electron donors and fermentable electron donor precursors, which could potentially support microbial reductive dechlorination processes. A secondary objective of this work was to identify soil properties or heating conditions that could be used in a predictive manner to estimate the extent of electron donor release from natural soils and soil constituents. To achieve these objectives, five sets of thermal incubation experiments were performed in 20 mL flame-sealed glass ampules containing soils or reference humic materials (see Table 2.1.1.) with a range of organic carbon contents and structure. Set #1 was designed to identify and quantify VFAs and hydrogen released during soil heating. Set #2 served as abiotic controls to assess VFA and hydrogen release when microbial activity was suppressed (i.e., in $HgCl_2$-amended ampules). Sets #3 and #4 were designed to investigate the influence of organic matter structure on thermally induced VFA and hydrogen release. Set #5 was designed to identify and quantify VFA and hydrogen release following prolonged incubation at high temperature (180 days at 90 °C). The ampules were loaded with the solid phase, followed by 10 mL of DI water and an inert argon gas headspace, flame-sealed, and then incubated at 30, 60, or 90 °C for up to 180 days. Following each incubation period, the ampules were destructively sampled to obtain gas, liquid (water), and solid samples. Concentrations of VFAs in the aqueous phase were determined using ion chromatography, while H_2 in the gas phase were determined using gas chromatography.

In order to facilitate quantitative comparison between direct (i.e., H_2) and indirect (i.e., VFAs) electron donor sources, release is expressed as the maximum theoretical reducing equivalents per gram solid (e^-/g_s) that would result from the complete oxidation of each compound to CO_2 (Table 3.1.1.), unless specified otherwise.

Table 3.1.1. Maximum theoretical reducing equivalents (e^-) resulting from oxidation of VFAs to carbon dioxide.

Generic formula	$C_xH_yO_z + (2x - z)H_2O \rightarrow \left(\frac{y}{2} + 2x - 2\right)H_2 + xCO_2$	(1)
Hydrogen oxidation	$H_2 \rightarrow 2H^+ + \mathbf{2}e^-$	(2)
Eqn. (1) + (2)	$C_xH_yO_z + (2x - z)H_2O \rightarrow (y + 4x - 4)(H^+ + e^-) + xCO_2$	(3)
Formic acid oxidation	$HCOOH \rightarrow 2H^+ + \mathbf{2}e^- + CO_2$	(4)
Acetic acid oxidation	$CH_3COOH + 2H_2O \rightarrow 8H^+ + \mathbf{8}e^- + 2CO_2$	(5)
Propionic acid oxidation	$C_2H_5COOH + 4H_2O \rightarrow 14H^+ + \mathbf{14}e^- + 3CO_2$	(6)
Butyric acid oxidation	$C_3H_7COOH + 6H_2O \rightarrow 20H^+ + \mathbf{20}e^- + 4CO_2$	(7)

3.1.1.a. Identification and quantification of electron donors released during soil heating

The first thermal treatment experiment (Set #1) consisted of 111 non-blank ampules (i.e., containing a solid phase) and was designed to assess VFA and H_2 release during heating of Federal Fine Ottawa sand, Groveland aquifer material, Appling soil, and Webster soil (<0.01 – 1.97% OC) incubated 30, 60, or 90 °C for 28 to 56 days. Analysis of aqueous samples confirmed the release of VFAs, with at least acetate, formate, propionate, or butyrate detected above the 1 μM detection limit in all 111 ampules. H_2 was also measured above the 30 ppmv detection limit in the headspace of 30 ampules. VFA and H_2 concentrations were consistently below the detection limit in blanks containing no solid phase in Set #1 and all subsequent sets. Acetate and formate were the most frequently detected and abundant VFAs in Set #1, appearing in all 111 ampules and accounting for 68 and 18% of total reducing equivalents, respectively (Figure 311.1.a). Propionate was detected in 33 ampules and accounted for 13% of reducing equivalents. Butyrate was detected in only 7 ampules and accounted for 1% of reducing equivalents. Total VFA release (i.e., formate + acetate + propionate + butyrate) was lowest in ampules containing Federal Fine Ottawa sand (<0.01% OC), never exceeding 157×10^{-9} mol e^-/g_s for any replicate (Figure 3.1.1.a-c). The greatest VFA formation occurred in Webster soil (1.97% OC) ampules incubated for 56 days at 60 and 90 °C, with total releases of $75{,}336 \pm 16{,}821 \times 10^{-9}$ mol e^-/g_s and $71{,}892 \pm 6{,}761 \times 10^{-9}$ mol e^-/g_s, respectively (Figure 3.1.1.k,l). In general, an increase in incubation temperature or soil OC content corresponded to an increase in total VFA release. Additionally, total VFA accumulation increased over time for the majority of the soils, and most notably for Webster soil incubated at 60 and 90 °C, which is consistent with time-dependent release of VFAs.

Concentrations of hydrogen detected in ampules containing Federal Fine Ottawa sand were negligible over the 56-day incubation period at all of the temperatures evaluated (Figure 3.1.1.a-c). Hydrogen concentrations in 90 °C Groveland aquifer material and Appling soil ampules were low and stable for the duration of the experiment, with maximum concentrations of $9.8 \pm 2.7 \times 10^{-9}$ and $6.6 \pm 0.4 \times 10^{-9}$ mol e^-/g_{solid}, respectively. Negligible levels of hydrogen were detected in 30 and 60 °C ampules of both soil types (Figure 3.1.1.d-i). These data indicate that for the relatively low OC soils, hydrogen formation was minimal below 90 °C and, when produced, did not increase with incubation time. In contrast, elevated concentrations of hydrogen were detected in ampules containing Webster soil incubated at 60 °C, where levels increased from $8.0 \pm 0.4 \times 10^{-8}$ to $1.4 \pm 0.2 \times 10^{-7}$ mol e^-/g_{solid} over the course of the experiment (Figure 3.1.1.k). Low levels of hydrogen were detected in Webster ampules incubated at 30 °C (Figure 3.1.1.j), consistent with the other soils tested. Interestingly, hydrogen was not detected in any of the Webster ampules incubated 90 °C (Figure 3.1.1.l), which suggests that hydrogen formation may have been microbially-mediated in heated Webster soil, but that this activity was inhibited at 90 °C. To further investigate the potential for microbially-driven hydrogen formation, a second set of ampule experiments (Set #2) was conducted with 2 mM mercury (II) chloride ($HgCl_2$) added to the ampule aqueous phase to inhibit microbial activity.

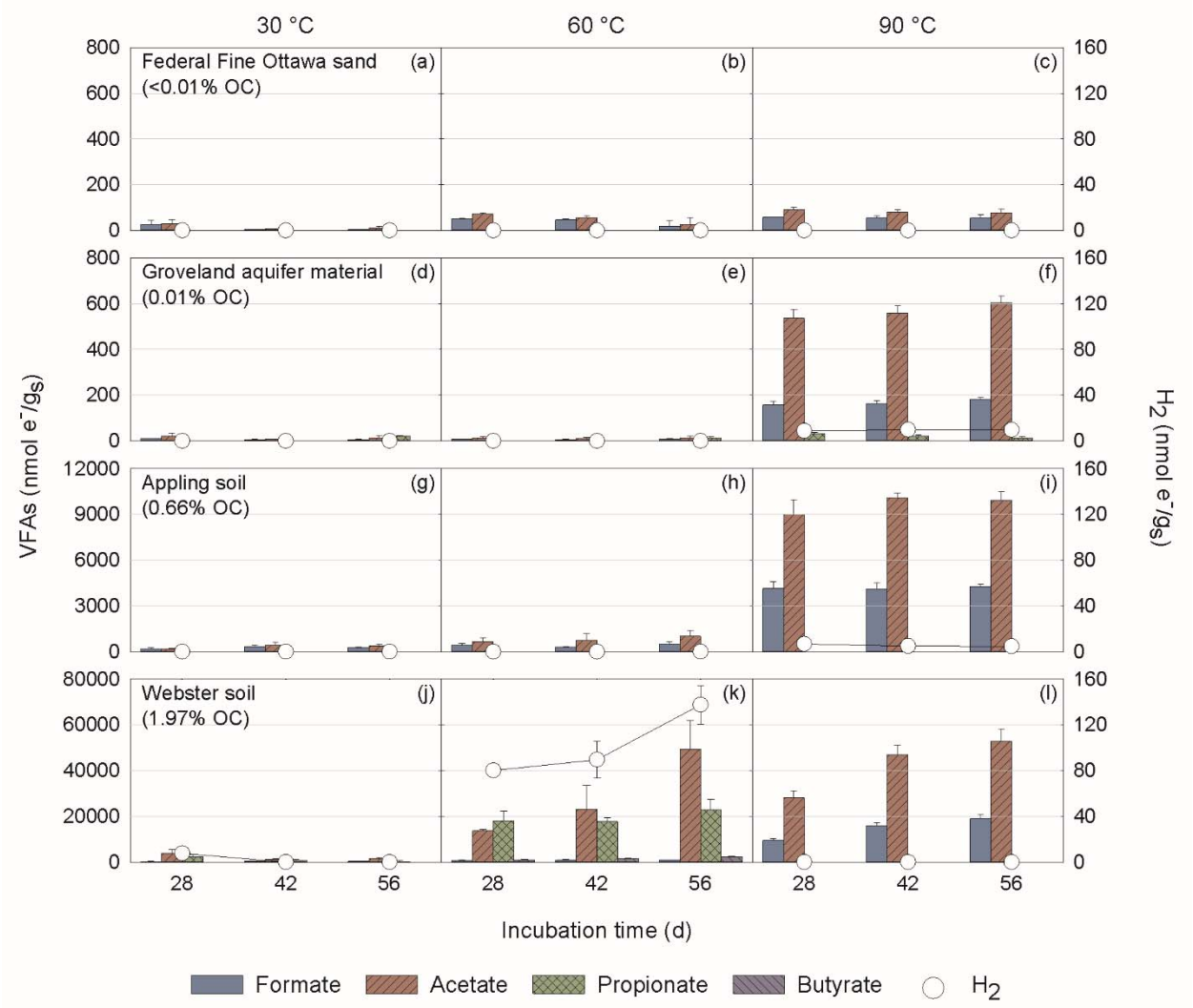

Figure 3.1.1. Concentrations of VFAs and hydrogen in ampules (Set #1) containing Federal Fine Ottawa sand, Groveland aquifer material, Appling soil or Webster soil incubated 30, 60, and 90 °C for up to 56 days (Set #1). Error bars represent one standard deviation.

3.1.1.b. Electron donor release during microbial inhibition

The second thermal treatment experiment (Set #2) consisted of 43 non-blank ampules amended with 2 mM $HgCl_2$, and was intended to determine whether the hydrogen measured in Set #1 resulted from heat-induced abiotic reactions or from the fermentation of compounds released during heating. Following incubation at 60 or 90 °C for up to 56 d, VFAs were detected in all 43 ampules (Figure 3.1.2) at magnitudes similar to those measured in the absence of $HgCl_2$ (Set #1). However, hydrogen was not detected in the presence of 2 mM $HgCl_2$ except in ampules containing Webster soil incubated at 60 °C (Figure 3.1.2.g). Among the Webster soil ampules in which hydrogen was detected, mean release was at least 76% lower than in Set #1 counterparts containing no $HgCl_2$ (Figure 3.1.2.g versus 3.1.1.k). These data indicate that hydrogen production observed in Set #1 Webster ampules at 60 °C was primarily the result of microbial activity.

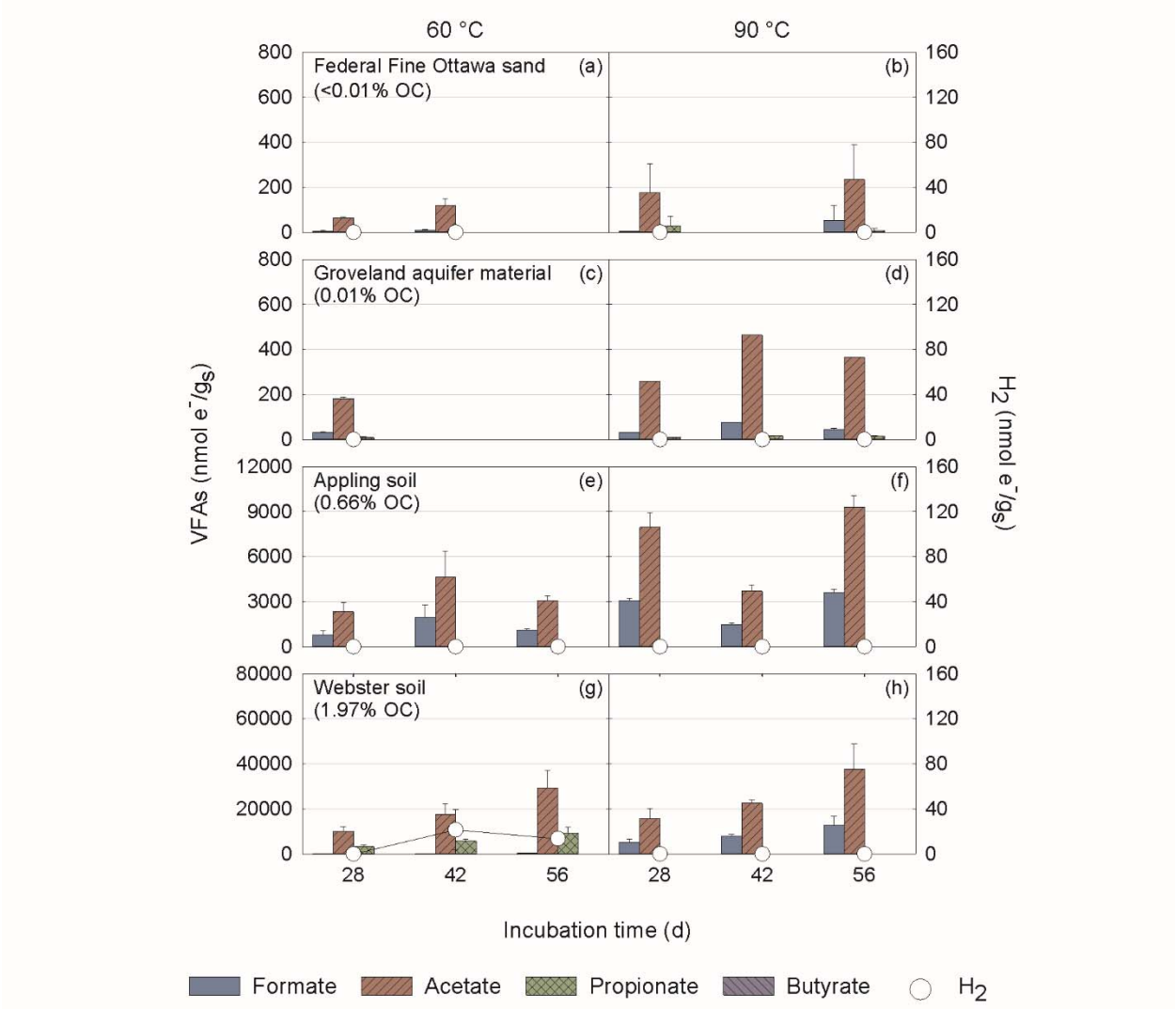

Figure 3.1.2. Concentrations of VFAs and hydrogen detected in biologically-inhibited ($HgCl_2$) ampules (Set #2) containing Federal Fine Ottawa sand, Groveland aquifer material, Appling soil, and Webster soil incubated at 60 and 90 °C (Set #2). Error bars represent one standard deviation.

3.1.1.c. Volatile fatty acid release during thermal treatment of humic materials

The third thermal treatment experiment (Set #3) consisted of 161 ampules, and was designed to elucidate the role of organic constituents in VFA and H_2 release during thermal treatment. Four humic and fulvic acid standards, Suwannee River fulvic acid standard II, Pahokee peat humic acid standard, Elliott soil humic acid standard, and Leonardite humic acid standard (52.34 – 63.81% OC) were used as the ampule solid phases. These well-characterized materials were intended to confirm VFA release trends (i.e., dependence on incubation temperature, time, OC content) observed in Sets #1 and #2, and to explore the influence of organic matter functional groups on the extent of VFA release. Hydrogen was not detected in any ampule in Set #3 (Figure 3.1.3), but VFAs were detected at similar relative ratios to those in Sets #1 and #2 (Figures 3.1.1 and 3.1.2). Total VFA release was orders of magnitude greater in ampules containing humic and fulvic acid standards (52.34 – 63.81% OC) compared to ampules containing soils and aquifer materials (<0.01

– 1.97% OC), supporting the positive correlation between VFA release and OC content of the solid phase observed in Sets #1 and #2. However, when considering only results from Set #3 (i.e., ampules containing humic and fulvic acid standards), VFA release was negatively correlated to OC content. For example, despite containing 63.81% OC, total VFA release in Leonardite humic acid standard ampules incubated at 90 °C reached only 632 ± 35 × 10^{-6} mol e^-/g_s after 28 days of incubation (Figure 3.1.3.l). In contrast, VFA release in Elliott soil humic acid standard (58.13% OC) ampules reached 2,687 ± 171 × 10^{-6} mol e^-/g_s under the same incubation conditions (Figure 3.1.3.i). Furthermore, release of VFAs in ampules containing Suwannee River fulvic acid standard II (52.34% OC) reached 2,652 ± 244 × 10^{-6} mol e^-/g_s after only 21 days at 90 °C (Figure 3.1.3.c). The observed differences in total VFA release from these high OC humic materials indicates that OC content alone may not provide accurate predictions of VFA release, and suggest that OC structure also plays a role in VFA release at elevated temperatures.

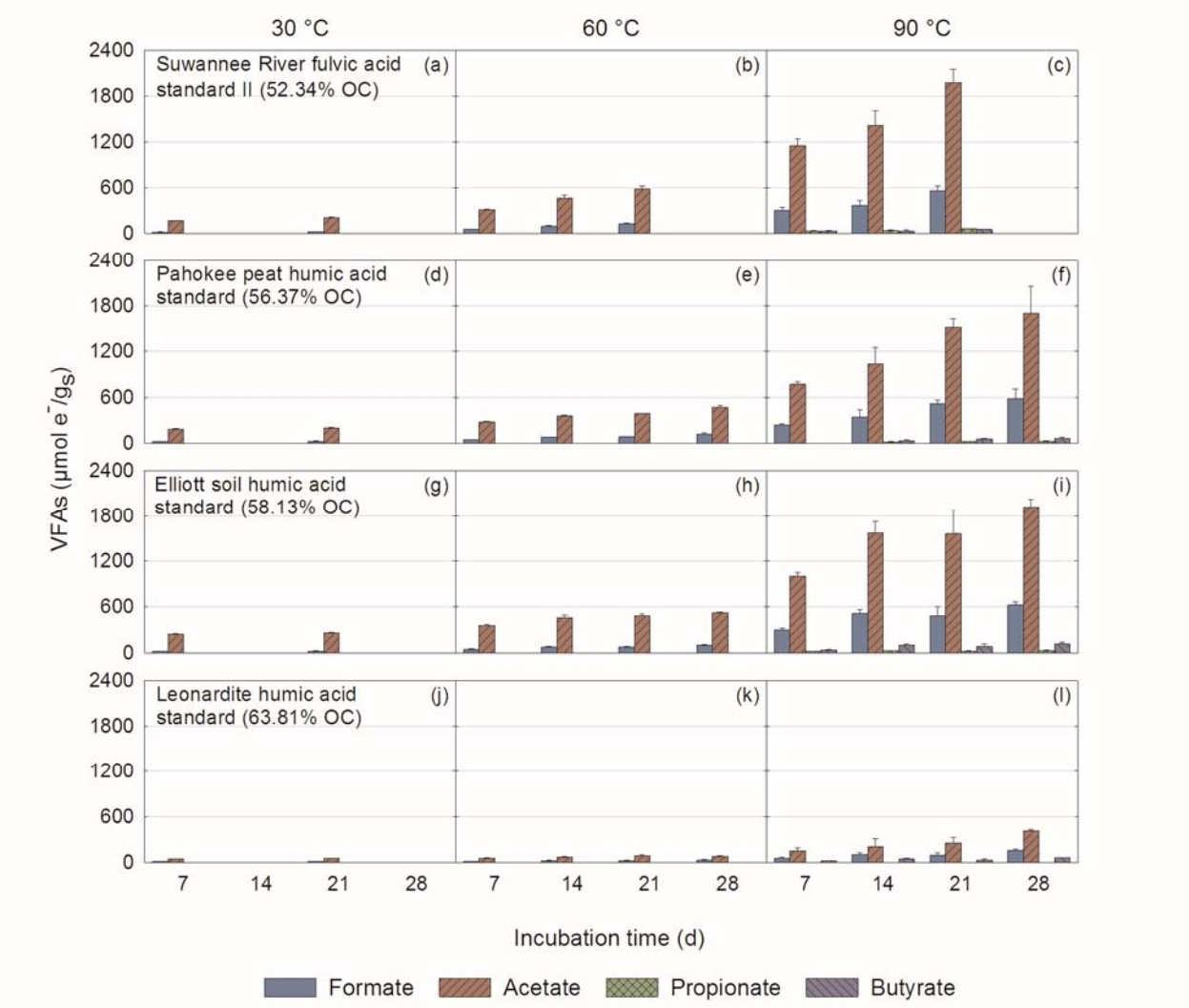

Figure 3.1.3. Concentrations of VFAs detected in ampules containing freeze-dried reference humic materials (Suwannee River fulvic acid standard II, Pahokee peat humic acid standard, Elliott

humic acid standard, and Leonardite humic acid standard) incubated at 30, 60 and 90 °C for up to 28 days (Set #3). Error bars represent one standard deviation.

3.1.1.d. Electron donor release during thermal treatment of high organic carbon content soils

The fourth experiment (Set #4) consisted of 179 ampules containing three bulk IHSS solids (Elliott silt loam soil, Pahokee peat soil II, and Gascoyne leonardite) from which the humic acid standards in Set #3 were originally extracted. Set #4 was intended to further investigate the influence of organic matter functional groups on VFA release, and to explain the negative relationship between VFA release and OC content observed in Set #3 ampules. VFA release trends among the bulk IHSS solids (Figure IV.1.1.d) were similar to those observed for humic and fulvic acid standards (Figure IV.1.1.c). This finding supports the hypothesis that solids containing abundant OC have a high potential for VFA release, but also that the structure of organic matter can impact VFA release. Total VFA release was unexpectedly lower in 90 °C Elliott soil ampules than in all other soils except Gascoyne leonardite, but still increased over time (Figure IV.1.1.d:c). Hydrogen production also occurred in ampules containing all three IHSS soils. The highest hydrogen levels were measured in Elliott soil ampules incubated at 60 °C ($357 \pm 203 \times 10^{-9}$ mol e^-/g_s; Figure IV.1.1.d:b), with lower concentrations measured following 30 and 90 °C incubation of each soil type (Figure IV.1.1.d). There was no significant increase (t-test, $p = 0.05$) in hydrogen production between sampling events for any soil type or incubation condition.

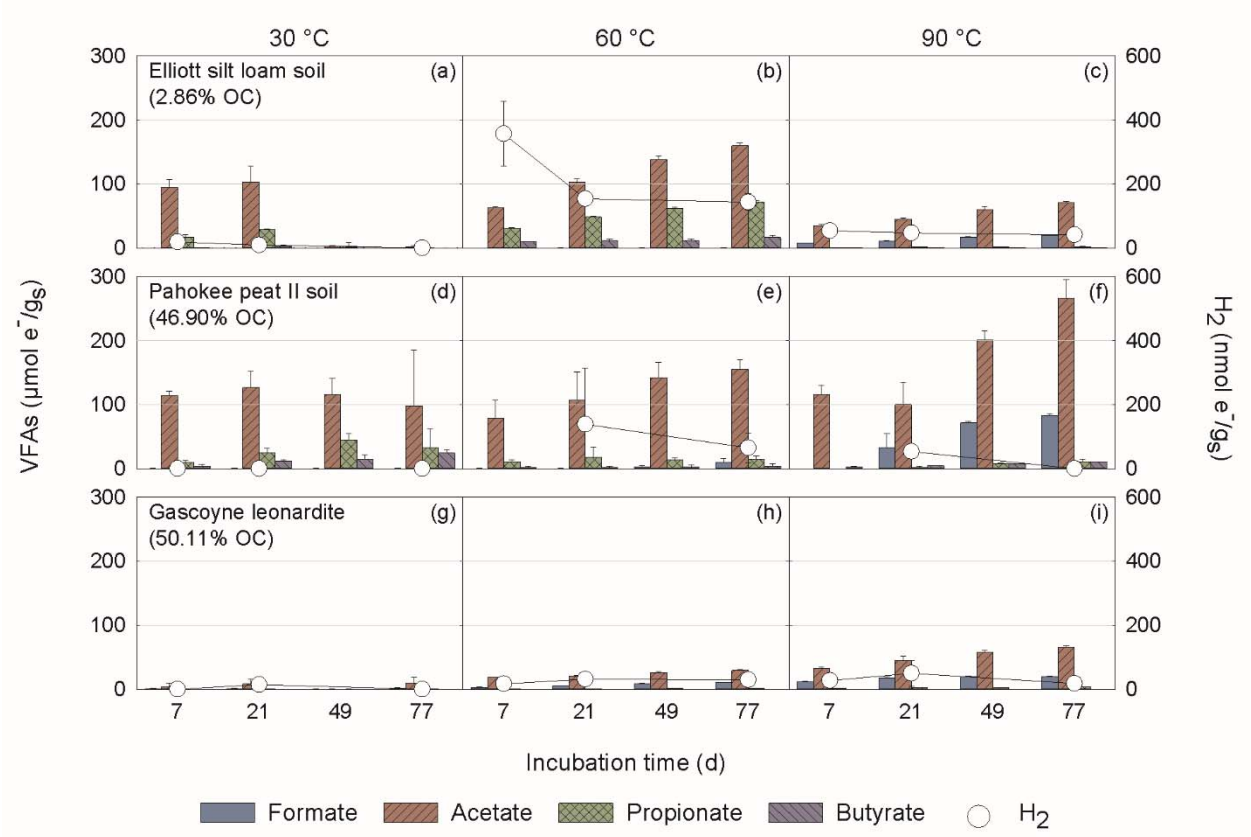

Figure 3.1.4. Concentrations of VFAs and hydrogen detected in ampules containing IHSS reference soils (Elliott soil, Pahokee soil, and Gascoyne leonardite) incubated at 30, 60 and 90 °C for up to 77 days (Set #4). Error bars represent one standard deviation.

3.1.1.e. Electron donor release during long-term, high temperature soil heating

The fifth experiment (Set #5) consisted of 49 non-blank ampules containing 10 soils and aquifer materials, and was designed to quantify VFA and H_2 release following long-term (180 days) incubation at 90 °C, similar to conditions that would occur at an ERH field site. VFA release occurred in all ampules and, with the exception of Gascoyne leonardite, increased with solid phase OC content (Figure 3.1.5). The highest VFA release was $631 \pm 10 \times 10^{-6}$ mol e^-/g_s, measured in ampules containing Pahokee peat soil II. Low levels of hydrogen were also detected in all ampules except for those containing Federal Fine Ottawa sand, with a range of $7 \pm 0 \times 10^{-9}$ mol e^-/g_s in Appling soil ampules to $54 \pm 4 \times 10^{-9}$ mol e^-/g_s in ampules containing Elliott soil. Results from Set #5 reinforce those from Sets #1 – 4, particularly that the capacity for VFA release is primarily governed by the OC content of the solid phase.

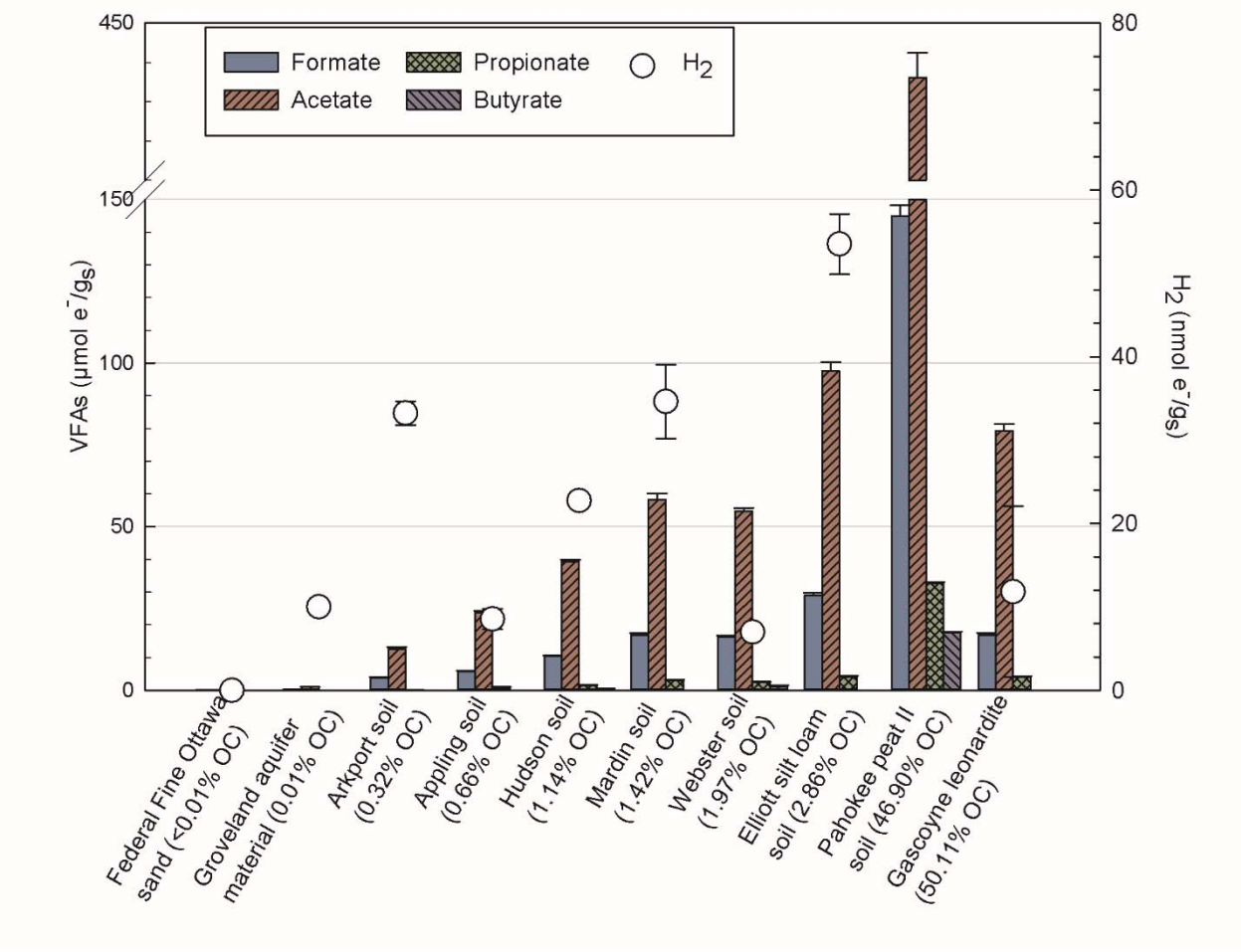

Figure 3.1.5. Concentrations of VFAs detected in ampules containing reference soils, field material, and IHSS reference soils incubated at 90 °C for 180 days (Set #5). Error bars represent one standard deviation.

3.1.1.f. Hydrogen production during soil heating

Results obtained from ampule experiments indicated that hydrogen was produced during thermal treatment of soils. However, in terms of reducing equivalents, hydrogen production was minimal relative to VFA release. For example, incubation of Elliott soil at 60 °C yielded the highest overall production of hydrogen ($357 \pm 203 \times 10^{-9}$ mol e^-/g_s; Figure 3.1.5.b), but that hydrogen represented only 0.3% of reducing equivalents measured following heating, while the remaining 99.7% were associated with VFAs. The lack of a consistent correlation with incubation parameters or soil properties suggests that H_2 production was likely the result of microbial activity, rather than a direct consequence of thermal treatment. The reduced hydrogen concentrations measured in Set #2 ampules containing 2 mM $HgCl_2$ as microbial inhibitor (Figure 3.1.2) support this conclusion, as does the complete lack of hydrogen in Set #3 ampules prepared with humic and fulvic acid standards (Figure 3.1.3), which are rendered essentially sterile during the extraction and ampule preparation process due to repeated hydrofluoric acid exposure, freeze-drying, and desiccation (Swift 1996). Furthermore, eight of the ten conditions that yielded the greatest H_2 production involved 60 °C incubation of soils with moderate to high OC content (1.97%),

providing an environment heated enough to induce release of fermentable VFAs from the soil, yet cool enough to permit microbial activity (Wang and Wan 2009).

3.1.1.g. Volatile fatty acid release from heated soils

Volatile fatty acids (i.e., formate, acetate, propionate, and butyrate) were released to the aqueous phase during thermal treatment of 14 different solids, including aquifer materials, natural soils, and humic and fulvic acid standards. The extent of VFA release was, to varying degrees, a function of incubation temperature, incubation time, and OC content of the solid phase. The carbonaceous nature of VFAs necessitates the presence of carbon in a solid in order for VFA release to occur, and sets an upper limit on potential VFA release during heating. Assuming that a soil contains the OC, results obtained from incubation experiments demonstrated a generally positive relationship between incubation temperature and VFA release. The notable exception to this trend was Elliott soil incubated at 90 °C (Figure 3.1.4.c), where the total average VFA release at each time point was 36 – 43% less than that measured in corresponding 60 °C ampules (Figure 3.1.4.b). After 77 days of incubation, headspace CO_2 levels were slightly lower in 90 °C ampules (25.7 ± 1.1% volume) compared to the 60 °C ampules (30.8 ± 2.0% volume). CO_2 is a product of both decarboxylation and microbially-catalyzed oxidation of organic matter. Therefore, this decrease in CO_2 concentration with increasing temperature indicates that neither decarboxylation nor microbial consumption was a likely cause of the discrepancy in VFA release between Elliott soil ampules incubated 60 and 90 °C.

Longer incubation times were associated with greater release of VFAs, particularly when solids were incubated at 60 or 90 °C. This temporal dependence is indicative of a rate-limited process, and is best exemplified by analyzing results from Set #3, in which only the humic and fulvic acid fractions of IHSS soils were heated. Dissolved organic carbon (DOC) concentrations remained constant or declined slightly between 7 and 28 days for most incubation conditions, suggesting that most, or all, of the organic compounds that could dissolve did so within the first 7 days (Table 3.1.2). Despite this rapid dissolution, the concentrations of DOC identifiable as VFAs increased over time, indicating that the rate-limiting step was not dissolution, but instead the breakdown of larger dissolved organic compounds to VFAs. This breakdown occurred in the aqueous phase and proceeded more rapidly at higher temperatures, suggesting that thermal decomposition of organic matter was the dominant mechanism for VFA formation, rather than microbial degradation.

Table 3.1.2. Mean dissolved organic carbon (DOC) and mean total volatile fatty acids (VFAs) measured in the aqueous phase of heated ampules (Set #3).

Solid phase	Temperature (°C)	DOC (mol % of initial ampule OC)				VFAs (mol % of DOC)			
		Time (d)				Time (d)			
		7	14	21	28	7	14	21	28
Suwannee River	30	84	-	▼ 72	-	0.1	-	▲ 0.2	-
fulvic acid	60	69	▼ 61	▲ 62	-	0.4	▲ 0.6	▲ 0.8	-
standard II	90	64	▼ 60	60	-	1.6	▲ 2.1	▲ 3.1	-
Elliott soil	30	12	-	▲ 16	-	1.2	-	▼ 1.0	-
humic acid	60	18	▲ 20	▼ 18	▲ 19	1.3	▲ 1.6	▲ 1.8	▲ 2.0
standard	90	23	▲ 26	▼ 23	▲ 25	3.6	▲ 5.4	▲ 5.8	▲ 6.8
Pahokee peat	30	29	-	▲ 35	-	0.4	-	0.4	-
humic acid	60	41	▼ 40	40	▲ 41	0.5	▲ 0.7	0.7	▲ 0.9
standard	90	60	▼ 51	▲ 53	▼ 50	1.1	▲ 1.9	▲ 2.6	▲ 3.2
Leonardite	30	7	-	▲ 9	-	0.5	-	▼ 0.4	-
humic acid	60	14	14	▲ 16	▼ 15	0.3	▲ 0.4	0.4	▲ 0.5
standard	90	16	▲ 22	▼ 20	▼ 18	0.8	▲ 0.9	▲ 1.1	▲ 2.0

▲ = increase from previous, ▼ = decrease from previous.

While incubation parameters influenced VFA release from each soil, aquifer material, and humic and fulvic acid standard tested, the greatest variations were observed when comparing different solids to one another. The relative magnitude of VFA release was strongly impacted by the OC content of the solid phase, presumably because OC content sets a maximum capacity for release. Furthermore, average VFA release corresponded to less than 3% of total available OC for all 140 incubation conditions, regardless of solid phase or OC content. The result was a generally positive correlation between VFA release and OC content. This relationship can be demonstrated using linear regression models of $VFAs_1$ (μmol e^-/g_s) in Set #5 ampules (180 d at 90 °C; Figure 3.1.4) as a function of OC (% weight) content (Equation 3.1.1; Figure 3.1.6; adjusted $R^2 = 0.47$).

$$\widehat{VFAs_1} = 6.5 \times OC + 43.9 \quad (3.1.1)$$

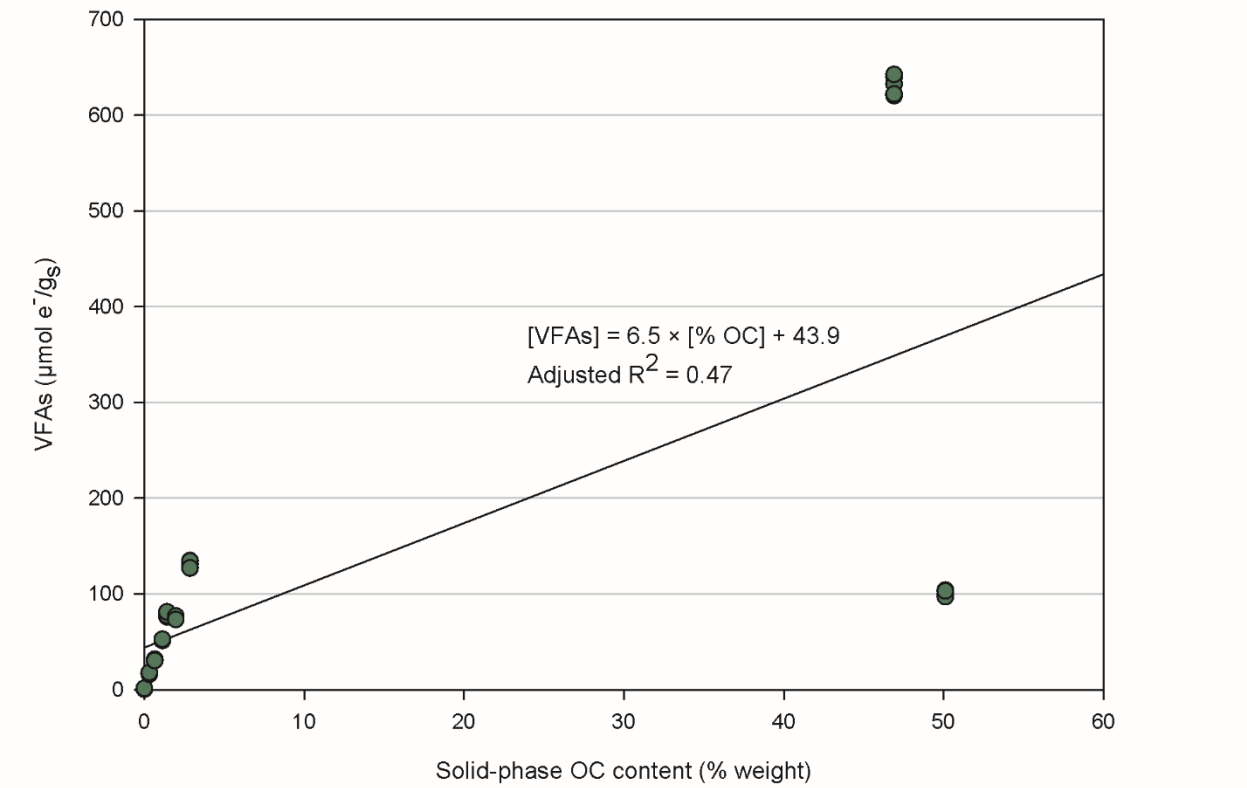

Figure 3.1.6. Linear regression of total average VFA release from porous media with OC content between <0.01 and 50.11% by weight following incubation at 90 °C for 180 days.

When ampules containing the high-OC Pahokee peat soil II (46.90% OC) and Gascoyne leonardite (50.11% OC) are excluded, the adjusted R^2 value increases to 0.97 (Equation 3.1.2; 3.1.7) and the intercept term (i.e., + 1.8) is no longer differentiable from zero ($p = 0.33$).

$$\widehat{VFAs_2} = 44.1 \times OC + 1.8 \quad (3.1.2)$$

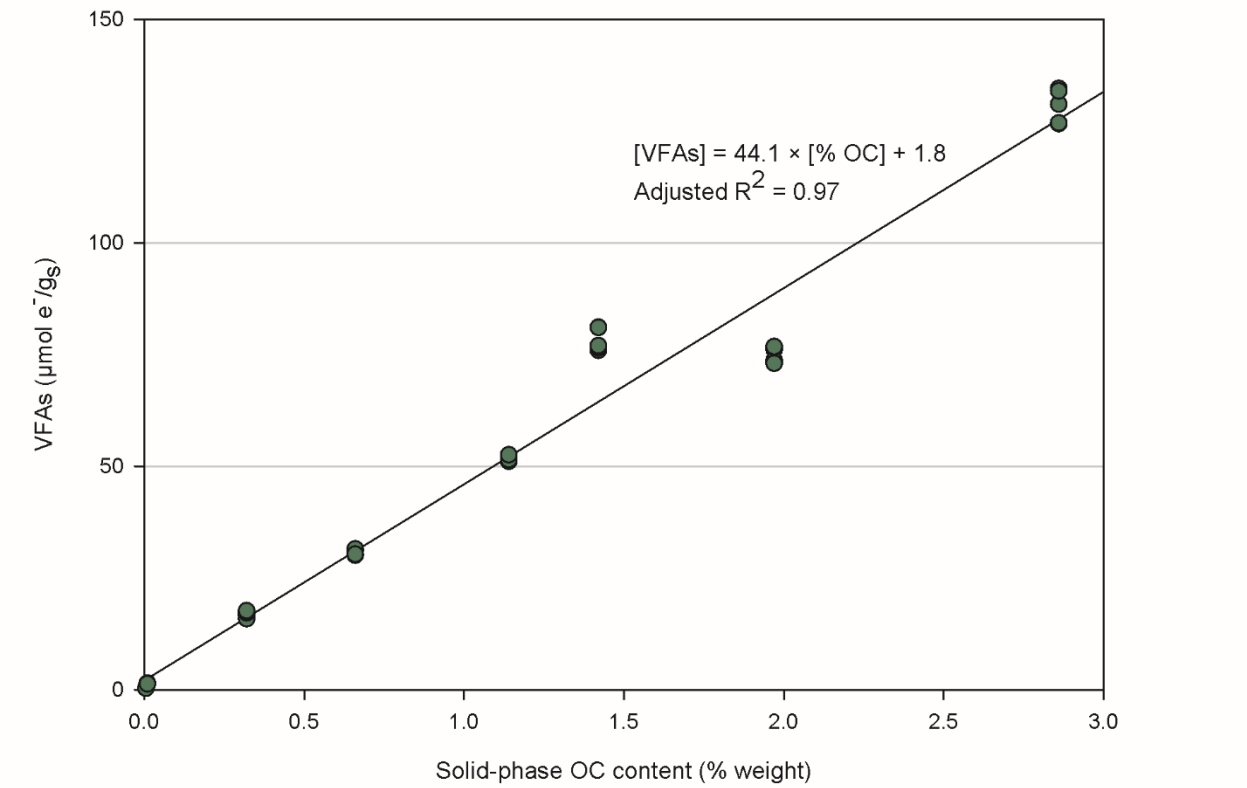

Figure 3.1.7. Linear regression of total average VFA release from porous media with OC content between <0.01 and 2.86% by weight following incubation at 90 °C for 180 days.

The dramatic improvement in model fit highlights an important distinction between the eight solids with <0.01 – 2.86% OC content and those IHSS materials with abundant OC (46.90 – 63.81%): VFA release from the high-OC materials generally decreases with increasing OC content. This relationship is illustrated in Equation 3 (adjusted $R^2 = 0.72$), a multivariable linear regression of $VFAs_3$ (µmol e^-/g_s) in humic and fulvic acid standard ampules (Set #3) as a function of OC (% weight) content, incubation time (d), and incubation temperature ($[T_1] = [T_2] = 0$ during 30 °C incubation; $[T_1] = 1$ and $[T_2] = 0$ during 60 °C incubation; $[T_1] = 0$ and $[T_2] = 1$ during 90 °C incubation).

$$\widehat{VFAs_3} = -89.4 \times OC + 26.7 \times Time + 190.7 \times T_1 + 1291.6 \times T_2 + 4970.6 \quad (3.1.3)$$

The negative coefficient associated with the OC term indicates that every 1% increase in solid phase OC content should be associated with an approximately 89.4 µmol e^-/g_s decrease in total VFA release, in direct contrast to the results of Sets #1, #2, #5 (Figures 3.1.1, 3.1.2, 3.1.5), and Set #5 regression models (Equations 3.1.1 and 3.1.2). However, these conflicting relationships can be explained by examining the structure of the OC in the humic and fulvic acid standards. Each humic and fulvic acid standard contains a known COOH abundance accounting for a portion of the total OC content (Table 3.1.1). These functional groups are a characteristic feature of all VFAs, and thus a prerequisite for abiotic VFA release. Regression of $VFAs_4$ (µmol e^-/g_s) in Set #3 as a function of COOH abundance (mmol/g_s), incubation time (days), and incubation temperature

(Equation 3.1.4; adjusted $R^2 = 0.60$) demonstrates a positive correlation between VFA release and COOH abundance.

$$\widehat{VFAs_4} = 545.8 \times COOH + 26.0 \times Time + 180.3 \times T_1 + 1281.8 \times T_2 - 2940.3 \quad (3.1.4)$$

Although Equation 3.1.2 indicates that OC content can be a suitable predictor of VFA release from solids, stoichiometry dictates that this linear relationship cannot be maintained for solids with very high OC content. On a mass basis, the OC content of each VFA ranges from 27% for formate to 55% for butyrate, so any solid with OC content greater than 55% must include additional carbon that is unassociated with VFAs, such as highly stable phenol groups. However, since such high OC concentrations are rare, the Equation 3.1.2 regression model provides a tool to estimate reductive capacity following thermal treatment at most sites. As an example, heating a 1 m^3 volume of aquifer material with bulk density of 1.6 g/cm^3 and 0.5% weight OC content could provide sufficient reductive capacity to dechlorinate 4.77 mol (791 g) of PCE to non-toxic ethene. Although this level of dechlorination would require nearly complete conversion of liberated VFAs to reducing equivalents and minimal consumption by non-dechlorinating microorganisms, the example highlights the potential capacity for VFA release to support the reductive dechlorination process, and supports the consideration of coupled thermal and microbiological technologies during remedial design.

3.1.2. Abiotic Electrical Resistive Heating Column Studies

The results of batch reactor experiments described above (Section 3.1.1.) demonstrated that VFAs are released to the aqueous phase during thermal treatment of soils. Building upon this result, an abiotic column study was undertaken to assess VFA release and availability down-gradient from the heated zone during thermal treatment. The horizontal, 90 cm long borosilicate glass column, which was equipped with side-ports to allow for internal sample collection, was packed with Webster soil (silty clay loam, 1.97 % OC) in the heated zone (0-30 cm) and Federal Fine Ottawa sand (30-90 cm) in the down-gradient zone. The Webster soil zone was heated in incremental steps (20 °C to 82 °C) to simulate the gradual heating process that occurs during field-scale thermal treatment. Aqueous and gas phase samples were collected from the down-gradient zone throughout the experiment. A sterile, argon-sparged solution containing 24 mM calcium chloride was pumped through the column at a pore-water velocity (v) of 25 cm/day ($Q \approx 0.125$ mL/min) for the duration of the experiment. Aqueous samples were analyzed for VFAs by IC and gas samples were analyzed for hydrogen and methane by GC.

3.1.2.a. Effect of heating regime on volatile fatty acid release from soil columns

The temperature ramp for the heated portion of the 90 cm column involved a step-wise increase in temperature of approximately 10 °C at 3-4 PV intervals until the temperature reached 82 °C at approximately 22 PVs (Figure 3.1.8). The temperature of the heated zone was maintained at 82 °C for approximately 6 PVs, and then incrementally decreased to 20 °C in a manner similar to the temperature increase. For this system, 1PV represents a residence time in the heated zone (0-30 cm) of approximately 1.2 days based on the pore-water velocity of 25 cm/day. Aqueous samples collected from Port L4, located approximately 60 cm from the column inlet, or approximately 30 cm from the end of the heated Webster soil, contained acetate, propionate, butyrate, and some formate (Figure 3.1.8). Production of VFAs increased rapidly once the temperature reached 50 °C

in the heated zone (approximately 12 PVs), and existed at ratios similar to those measured in aqueous samples from ampules containing Webster soil incubated to 60 °C (Figure 3.1.2.k). Acetate was the most abundant VFA measured in port samples and reached a peak concentration of 12.9 mmole e^- shortly after the Webster soil zone was increased to 72 °C.

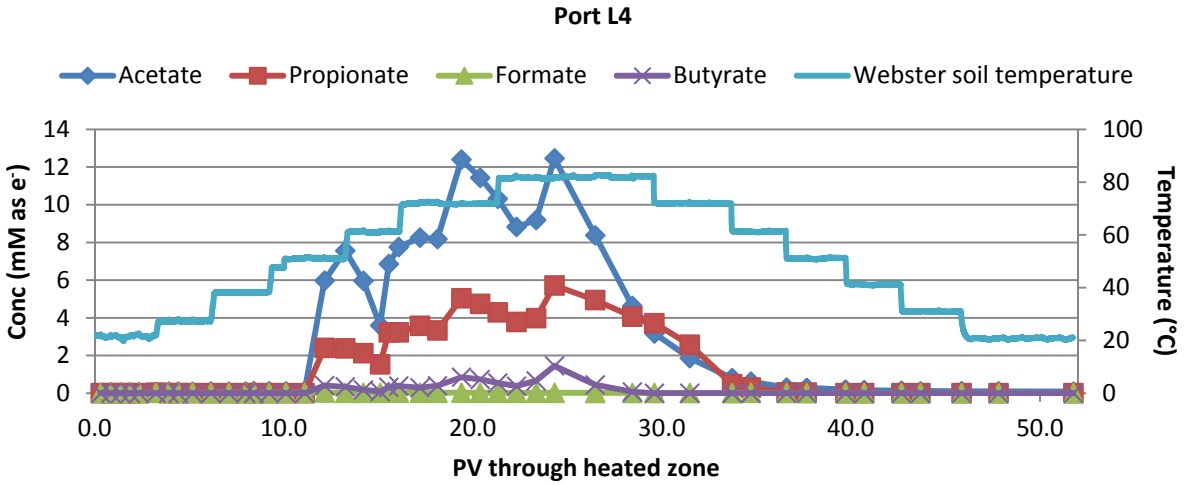

Figure 3.1.8. Temperature profile in heated zone of the column containing Webster soil, and the resulting concentrations of VFAs measured in down-gradient Port L4, expressed in terms of maximum potential reducing equivalents (as noted in Table 3.1.1).

The stepwise nature of the column heating ramp revealed VFA release patterns that were not readily apparent from previous batch studies. Concentrations of VFAs detected in aqueous samples collected from the down-gradient unheated zone (Ottawa sand) remained low for approximately the first 10 PV of the experiment, but pronounced spikes in acetate and propionate concentrations were observed once the temperature of the Webster soil exceeded approximately 50 °C. All subsequent temperature increases led to similar spikes in VFA concentrations, indicating that release of OC from the soil to the aqueous phase occurs rapidly once a threshold temperature is reached. These data suggest that VFA release would occur gradually and in a controlled manner during field-scale thermal treatment, since the subsurface is not typically subject to sudden temperature changes, and instead would increase in temperature slowly in response to heating over the course of weeks or months (Bakke et al. 2007, McGuire et al. 2006). Additionally, as the temperature of the Webster soil increased, the more complex VFAs (e.g., propionate and butyrate) represented a larger fraction of the total available reducing equivalents. Fermentation of propionate and butyrate with associated hydrogen formation is a slow processes that is thermodynamically favorable only when hydrogen concentrations are very low (10^{-4} – 10^{-5} atm) (Schink and Friedrich 1994). These results illustrate the potential for thermal treatment to provide a sustained source of reducing equivalents to dechlorinating bacteria, which are capable of utilizing very low concentrations of hydrogen, while minimizing consumption by competing microorganisms such as methanogens (Fennell et al. 1997, Löffler et al. 1999).

3.1.2.b. Reducing capacity of volatile fatty acids released during soil column heating

Assuming linear interpolation between the measured VFA concentrations shown in Figure 3.1.8, a total of 43.7 mM of e^- were detected in aqueous samples collected from Port L4 over the course of the entire experiment. On a stoichiometric basis, this quantity of reducing equivalents is theoretically sufficient to drive the microbial reductive dechlorination of 5.5 mmol (905 mg) of PCE to nontoxic ethene. Such high efficiency dechlorination is unlikely as it would require consumption of all reducing equivalents exclusively by dechlorinating bacteria. Nevertheless, the extent of VFA release (reducing equivalents) resulted from heating only 500 g of soil to a maximum of 82 °C. Even a relatively small zone (e.g., 1 m × 1 m × 1 m) of contaminated Webster soil (1.97% OC) would have a solid-phase mass of approximately 1.4×10^6 g. Assuming that reducing equivalents released during heating are used by dechlorinating bacteria at only 1% efficiency (9.05 mg_{PCE} reduced per 500 g_{soil}), this would still provide sufficient reductive capacity to convert 25.5 g of PCE to ethene, or the equivalent of complete remediation of the column saturated zone ($V_w \approx 450$ L) assuming an initial PCE concentration of 57 mg/L.

Results from the ampule incubation experiments (Section 3.1.1) demonstrated that soil heating can lead to the release of bioavailable VFAs to the aqueous phase. In addition, the data presented here for the 90 cm column experiment serve to further demonstrate that thermal treatment of soils can provide a source of reducing equivalents for dechlorinating bacteria. In the next section of the report, we extend this work to a biotic column system to determine whether VFAs released during soil heating are sufficient to stimulate and sustain microbial reductive dechlorination in the absence of an external electron donor source (e.g., lactate).

3.1.3. Biotic Electrical Resistive Heating Column Studies

A treatment train approach was established to examine the potential of organic acids released following soil heating to support organohalide respiration without the addition of electron donor or a carbon source. The upgradient 0 – 30 cm of a 90 cm column was packed with soil from the Naval Training Center Great Lakes (Site 22) and heated by ERH, and the 30 – 90 cm downgradient zone was packed with Federal Fine Ottawa sand and was unheated. The unheated zone was bioaugmented with the PCE-to-ethene dechlorinating microbial consortium (BDI-SZ) as described Section 2.1.3.

3.1.3.a. Microbial reductive dechlorination following ERH in soil columns

During the initial water flushing period (0.8 L) through the contaminated Great Lakes soil, baseline PCE concentrations of 22±9 µM were detected in the column effluent at room temperature (25 °C) (Figure 3.1.9). Following heating to 74 °C, aqueous PCE concentrations spiked to 189 µM. After injecting an additional 0.3 L (1.13 L cumulative volume), TCE and cis-DCE were also measured in the effluent at concentrations of 72 µM, while the parent compound PCE decreased to 79 µM. After 1.3 L of flushing, the temperature was increased to 84 °C, at which point PCE and TCE concentrations rapidly decreased and cis-DCE concentration increased to 339 µM within 0.2 L of flushing after the temperature increase (Figure 3.1.9). The formation of PCE dechlorination byproducts following heating indicates that the native microbial community associated with the Great Lakes field material was utilizing an electron donor and/or carbon source that was not available prior to heating.

After 2.3L of water flushing, the downgradient 60 cm section packed with Federal Fine sand was bioaugmented the BDI-SZ culture through the column sampling ports and within 0.5 L (approximately the pore volume of the sand region) of additional flushing (2.8 L of total water), VC and ethene were measured in the effluent (Figure 3.1.9). This more complete dechlorination following bioaugmentation demonstrates that the appropriate strains of *Dehalococcoides mccartyi* needed to carry out the transformation of PCE beyond cis-DCE were absent or present in insufficient quantity in the native community.

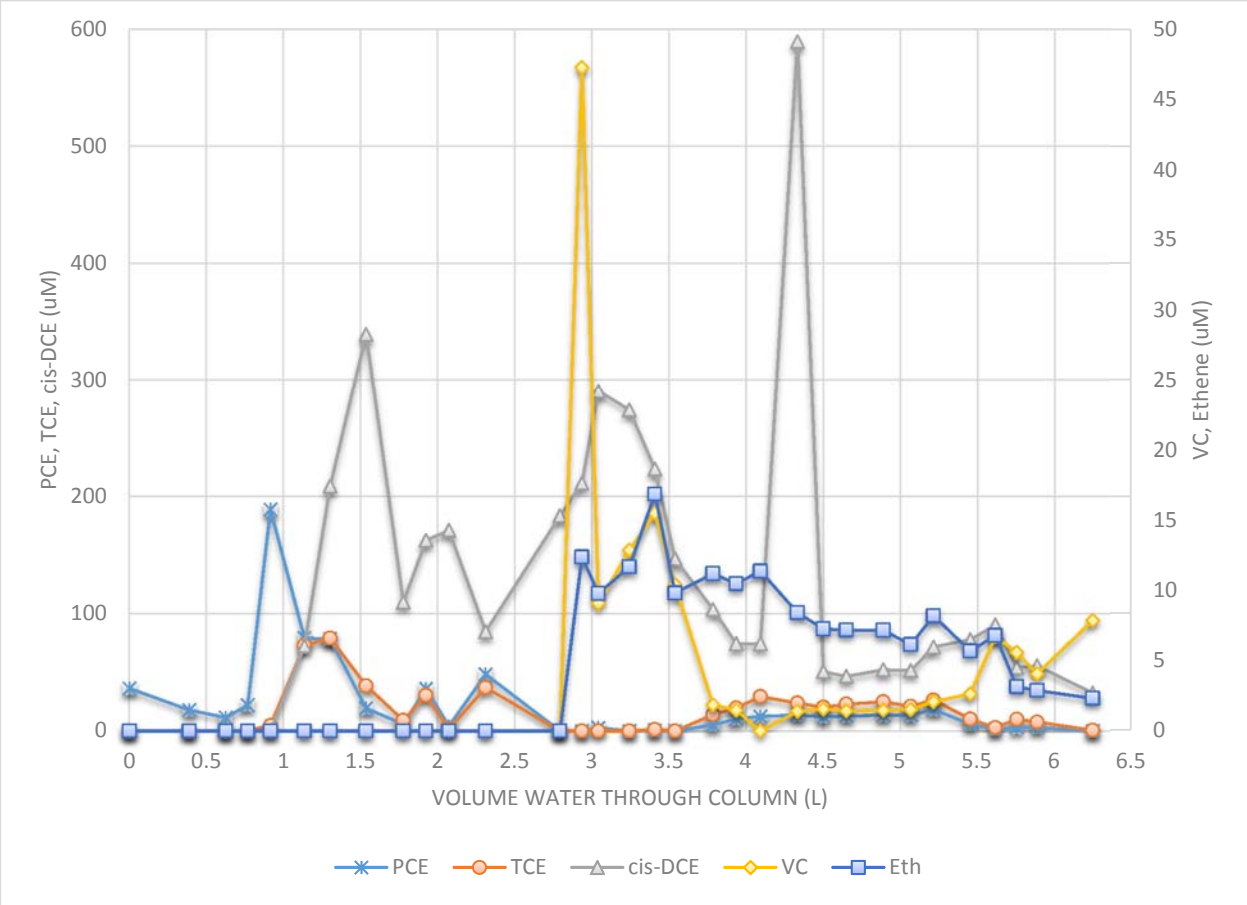

Figure 3.1.9. Concentrations of chlorinated ethene and ethene measured in column effluent samples following heating to 74 °C and 84 °C after 0.8 L and 1.3 L of water flushing, respectively, and bioaugmentation with the PCE-to-ethene BDI consortium after 2.3 L of flushing.

3.1.3.b. Ability of released organic acids to support of dechlorination to ethene

While the column was unheated (25 °C) and at the 74 °C set point temperature, organic acids were not detected in the column effluent. However, upon heating the Great Lakes soil to 84°C, acetate and propionate were immediately measured in the effluent (Figure 3.1.10). As seen in the ampule experiments with Groveland and Appling porous media (described in Section 3.1.1.a), this result demonstrates that the Great Lakes soil requires a higher temperature for organic acids release. In contrast to the Groveland and Appling materials that have organic carbon contents of 0.01% and 0.66% by weight, respectively, the Great Lakes soil has an organic carbon content (1.5

to 3.5% by weight) comparable to Webster soil (1.96% by weight), which released elevated organic acids at both 60°C and 90°C. This finding further supports the conclusion that organic carbon content coupled with heating regime is not always sufficient to predict organic acid release.

Speciation of organic acids measured during heating is another difference between the ampule batch experiment and ERH column results. In the ampule experiments, the simplest organic acids (i.e., formate and acetate) were detected in all cases except for blanks containing no solid phase. However, acetate and propionate were measured in the ERH column, which is similar to the ampule sets filled with Webster soil, Elliott soil, Pahokee soil, Mardin soil, and Hudson soil, which all have organic carbon contents above 1% (Section 3.1.1), suggesting that these soils harbor more organic compounds that are degraded to a greater diversity of products, including organic acids.

Despite the short period over which organic acids were detected in the column effluent, the activity of organohalide respiring bacteria was supported, and the reductive dechlorination to vinyl chloride and ethene was carried out without the addition of external electron donor or carbon sources. Analysis of biomass samples also revealed that the released organic acids supported the growth of *Dehalococcoides mccartyi* by more than two orders of magnitude. It is likely that organic acids released from the heated Great Lakes soil were fermented and the hydrogen generated supported *Dehalococcoides mccartyi* dechlorination activity. In addition, the organic acids could directly support PCE to cis-DCE dechlorinators or non-dechlorinating microbial species prior to transport and measurement in effluent aqueous samples. Overall, these findings demonstrate that thermally-released byproducts served as the sole electron donor source, either directly or following fermentation, to support a PCE-to-ethene dechlorinating consortium downgradient from the heated zone in a treatment train remedy approach.

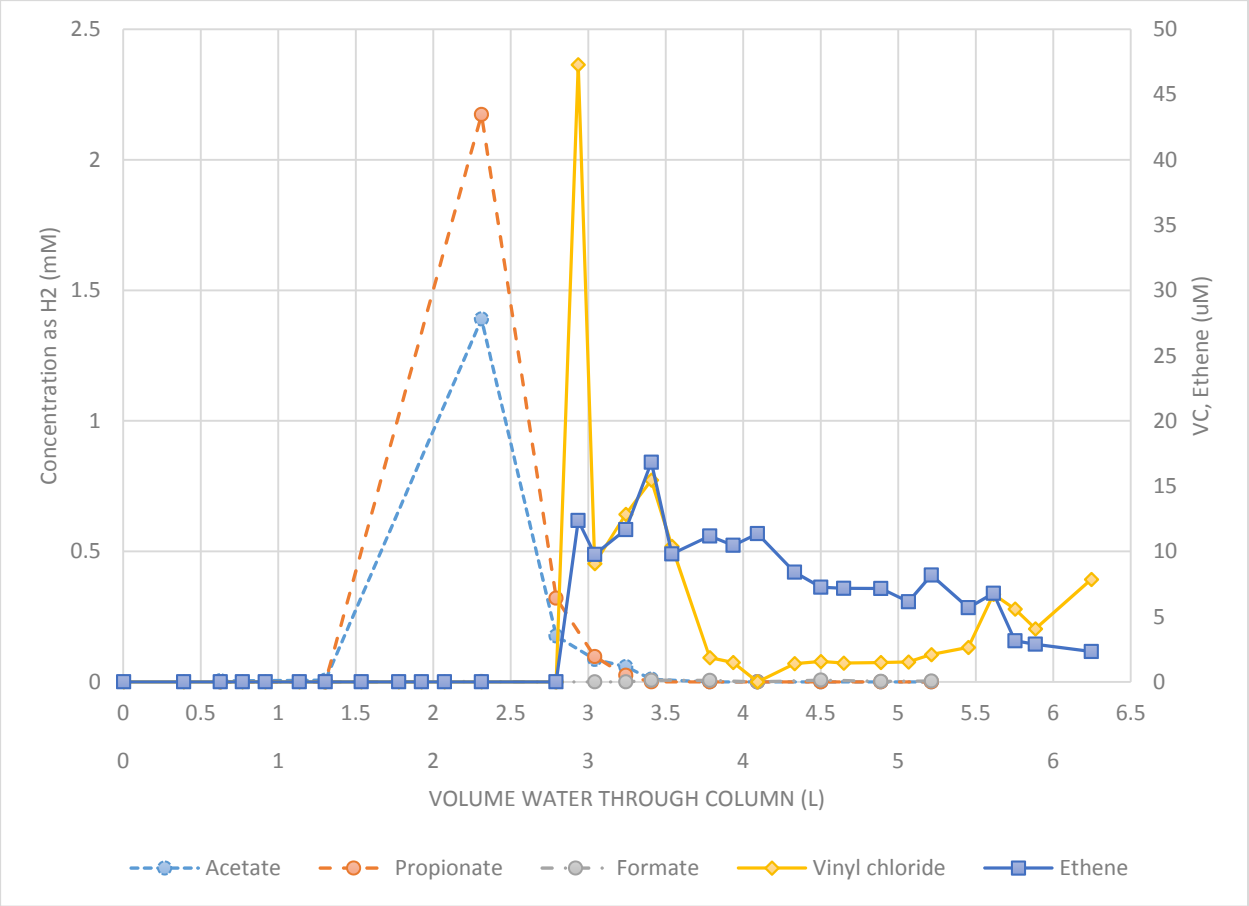

Figure 3.1.10. Flux-averaged effluent VFA concentration detected in column effluent after heating Great Lakes soil to 84 °C (at 1.3 L). Measurement of flux-averaged effluent vinyl chloride and ethene immediately following bioaugmentation (at 2.3 L) and approximately 0.5 L of additional water flushing.

3.1.4. Microbial Reductive Dechlorination in Low Temperature Thermal Columns

The coupled implementation of *in situ* thermal treatment and microbial reductive dechlorination has been proposed as a combined remedial approach to achieve cleanup goals at sites contaminated with chlorinated solvents. The average groundwater temperature in the United States ranges from 3 °C in parts of Maine and Minnesota to 25 °C in southern Florida and Texas (EPA 2016), but all characterized dechlorinating bacteria are mesophilic, with optimal growth temperatures ranging from 22 to 38 °C (Fletcher et al. 2011a, Friis et al. 2007, Gerritse et al. 1996, Holliger et al. 1993, Löffler et al. 2013). Although laboratory studies suggest that soil heating can enhance the activity of dechlorinating bacteria, a narrow optimal range of 25 to 30 °C has been identified for strictly hydrogenotrophic *Dehalococcoides mccartyi* (*Dhc*), the only known species capable of reducing vinyl chloride (VC) to nontoxic ethene (Löffler et al. 2013). In one study, dechlorination of trichloroethene (TCE) to ethene occurred very slowly when the tetrachloroethene (PCE)-to-ethene dechlorinating Bio-Dechlor INOCULUM (BDI) was incubated at 40 °C (Fletcher et al. 2010), representing the highest temperature permissive of sustained *Dhc* activity available in the literature. Thus, the objective of these experiments was to determine if low temperature heating (e.g., 35 °C) enhances the microbial reductive dechlorination of PCE in dynamic column systems.

Although microbial reductive dechlorination has been studied extensively in batch experiments, few studies have incorporated the simultaneous effects of flow through a porous medium and variable temperature. In a study designed to compare dechlorination in column experiments to culture and microcosm batch experiments at room temperature, dechlorination by *Dhc* was approximately 200-times greater in columns (Schaefer et al. 2009), highlighting the potential for flow conditions to dramatically affect microbial activity. Similarly, the PCE- and TCE-dechlorinating *Dehalobacter restrictus* strain PER-K23 did not grow in batch studies at 10 °C,(Holliger et al. 1993) despite reaching PCE transformation rates of 3.7 μmol L^{-1} h^{-1} in an anoxic column operated at the same temperature (De Bruin et al. 1992). While the causes of these discrepancies are unclear, geochemical conditions are known to have differential impacts on *Dhc* behavior at the strain level, potentially leading to outcome variability even when total *Dhc* abundance is similar between two systems. For example, of the five known *Dhc* strains capable of *cis*-DCE and VC reduction, strains 195 and FL2 possess the *tceA* gene, strains VS and GT possess the *vcrA* gene, and strain BAV1 possesses the *bvcA* gene (Löffler et al. 2013). The *vcrA* gene is often targeted during qPCR analysis because of its frequent detection at contaminated sites following bioaugmentation (Scheutz et al. 2008). However, even though *vcrA* abundance is correlated to VC and ethene formation under highly reducing conditions, the *bvcA* and *tceA* genes may play an increasingly important role in dechlorination under more oxidizing conditions (van der Zaan et al. 2010). Similarly, abundance of *tceA* and *bvcA* increased following thermal treatment of a field site in Fort Lewis, WA (Macbeth et al. 2012).

During field application of *in situ* thermal remediation, temperatures of 80 – 110 °C are typically targeted for the treatment zone in order to volatilize and recover organic contaminants in the gas phase (Triplett Kingston et al. 2010). Laboratory-scale microcosm studies show that these conditions reduces viability of most species involved in reductive dechlorination (Fletcher et al. 2011a, Friis et al. 2007), but microbial activity could be retained or even increased in peripheral and downgradient zones that experience lower temperatures. Alternatively, *in situ* thermal treatment could be specifically designed to achieve subsurface temperatures of 35 – 40 °C, with the goal of stimulating microbial reductive dechlorination. This strategy has the potential to greatly reduce energy costs by eliminating the need for extensive gas phase extraction and above-ground treatment systems currently employed for conventional *in situ* thermal remediation. Thus, the objectives of this study were a) to investigate the impacts of low-temperature heating on the rate and extent of microbial reductive dechlorination of PCE, and b) to quantify changes in microbial community structure in response to increasing temperature.

Briefly, two columns (A and B) were operated similarly and in parallel throughout the experiment, except with respect to temperature. Initially, Column A was chilled to 15 °C, while Column B was heated to 35 °C. After 17 PVs of synthetic groundwater had been flushed through each column at a pore-water velocity of 15 cm/day, approximately 30 mL of KB-1 culture was introduced into each column. Following bioaugmentation, the columns were maintained at 15 °C and 35 °C, respectively, until PV 52. The temperature of the columns was then increased incrementally to assess microbial activity as a function of temperature (see Table 2.1.2). Effluent samples were collected every 2–3 PVs to determine concentrations of chlorinated ethenes, ethene, organic acids, and pH. Side-port samples were collected during the temperate regime to assess abundance of *Dehalococcoides mccartyi*, *Geobacter* sp., and RDase genes responsible for reductive dechlorination of cis-DCE and VC: *tceA*, *bvcA*, and *vcrA*. The columns were destructively sampled at the conclusion of the experiment to allow for determination of solid-phase

bacterial and RDase gene abundances. Further details of the experimental methods are provided in Section 2.1.4.

3.1.4.a. Bioaugmentation and microbial elution

The KB-1 culture contained 1.4±0.2 × 10^7 *Dhc* cells/mL, approximately 32% of which were immediately washed out during bioaugmentation of Columns A and B, resulting in initial *Dhc* abundances of 2.9 × 10^8 cells per column. Greater than 99% of *Dhc* cells retained in each column immediately post-bioaugmentation possessed the *vcrA* gene.

3.1.4.b. Effects of heating on dechlorination activity

Within the first 20 PV following bioaugmentation, PCE and TCE in the effluent of Column A (15 °C, Figure 3.1.11) gave way primarily to *cis*-DCE (151±2 μM), with lower levels of VC (51±0 μM) and ethene (19±0 μM). In contrast, PCE and TCE were never detected in the effluent of Column B (35 °C, Figure 3.1.12) after bioaugmentation, and the relatively low concentration of *cis*-DCE (98±10 μM) initially detected in the Column B effluent was rapidly degraded to VC and ethene within the same period. These results indicate that a moderate temperature differential can dramatically improve dechlorination rates in a flow-through column system, even when dechlorinating bacteria are initially present in comparable numbers. Furthermore, *cis*-DCE concentrations measured in the effluent of Column A decreased from 102±1 to 58±1 μM between 53 and 61 PVs as temperature was gradually increased from 15 to 35 °C, and fell below the detection limit within the next 17 PVs at 35 °C. This near-immediate decrease in *cis*-DCE concentration was concurrent with an increase in effluent VC concentration from 34±0 to 85±2 μM, indicating that the *Dhc* strain(s) primarily responsible for *cis*-DCE-to-VC dechlorination were present prior to the temperature increase, but were not yet dechlorinating *cis*-DCE. The temperature increase had little immediate impact on ethene formation, but after 58 PVs and 48 PVs at 35 °C in Columns A and B, respectively, effluent ethene concentrations began to rise exponentially, and in both cases surpassed VC as the dominant dechlorination product after 73 PVs at 35 °C. The observed lag in ethene formation suggests that the *Dhc* strains responsible for the majority of VC-to-ethene dechlorination at 35 °C required additional growth time to reach adequate abundance to effectively degrade VC. Effluent VC concentrations from Columns A and B continued to decline during this period of rapid ethene formation, but the reductions in VC mass did not account for all of the increased ethene mass in either column. These mass balance discrepancies likely resulted from equilibration of the aqueous phase with a gas phase that developed in each column during rapid ethene formation, which artificially inflated subsequent ethene concentrations in the effluent of each column.

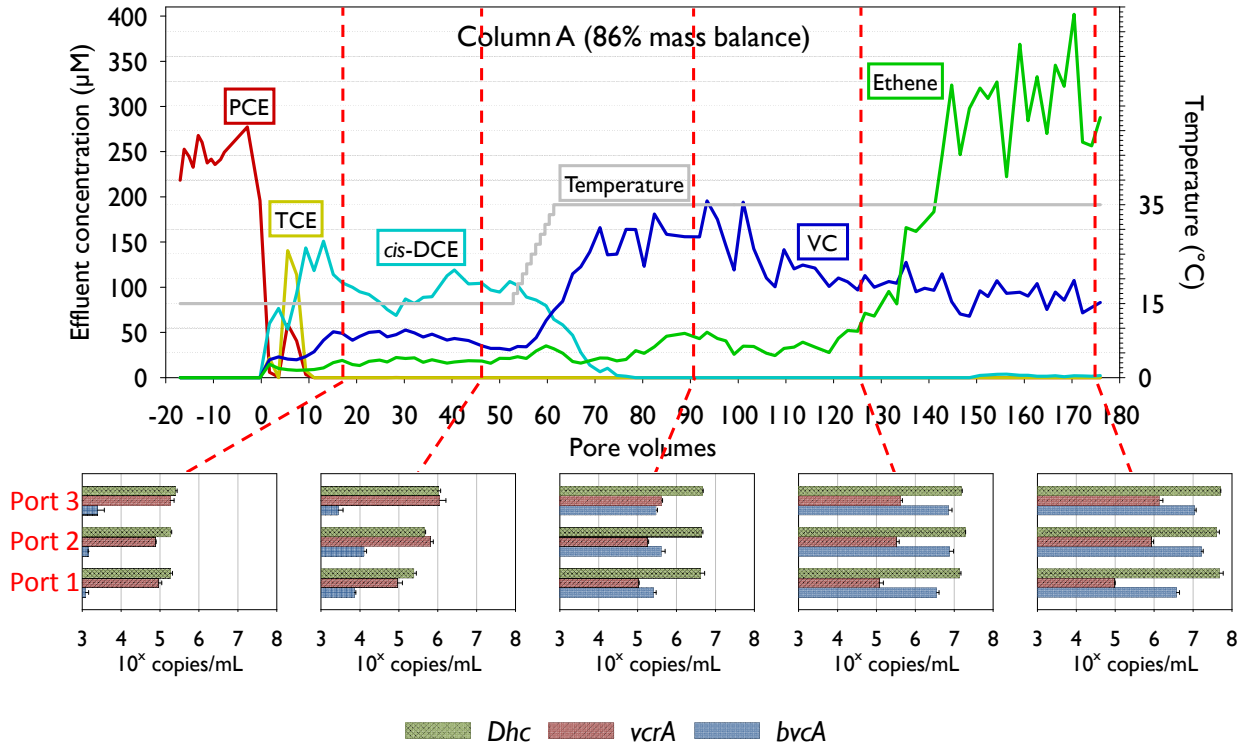

Figure 3.1.11. Effluent concentrations of PCE and daughter products measured in Column A. Bioaugmentation occurred at PV = 0. Dashed lines link *Dhc* 16S rRNA gene and RDase gene abundances (bar charts) in aqueous port samples (P1 – P3) to corresponding pore volume.

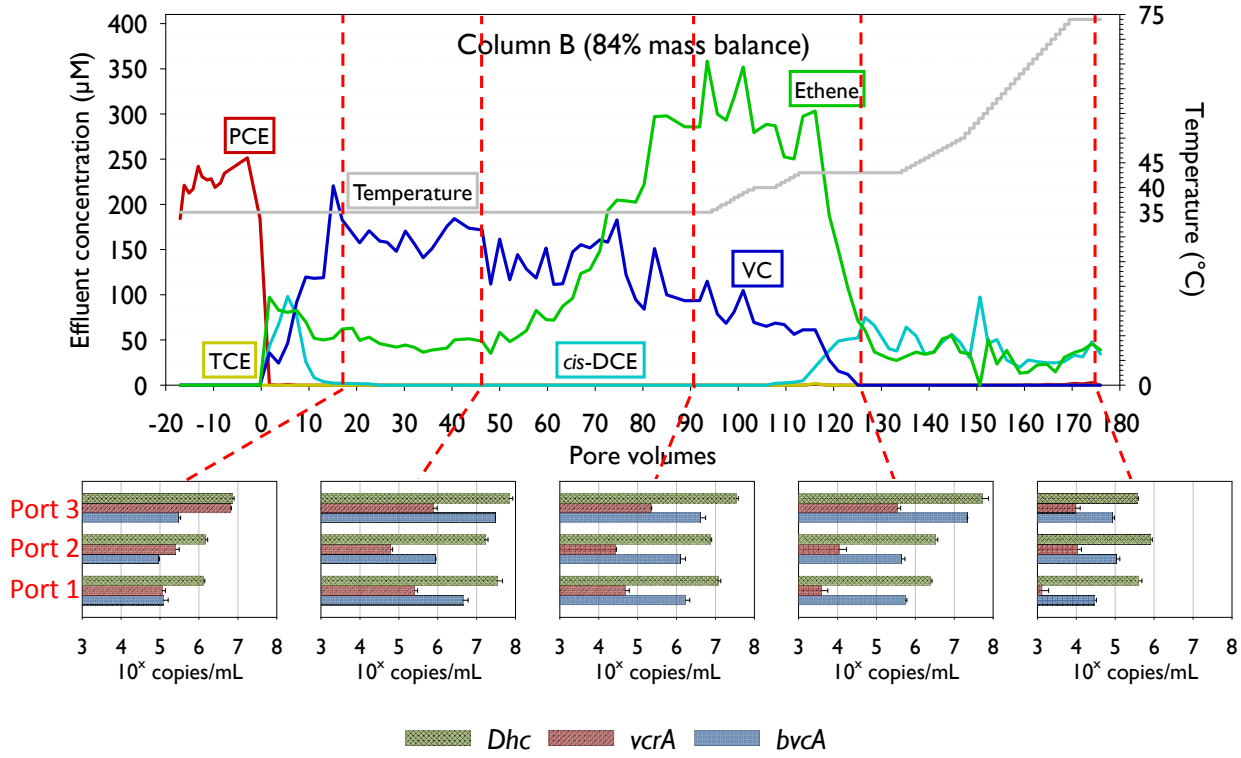

Figure 3.1.12. Effluent concentrations of PCE and daughter products measured in Column B. Bioaugmentation occurred at PV = 0. Dashed lines link *Dhc* 16S rRNA gene and RDase gene abundances (bar charts) in aqueous port samples (P1 – P3) to corresponding pore volume.

3.1.4.c. Optimal temperature for *Dehalococcoides mccartyi* mediated reductive dechlorination

Between 95 and 113 PVs, the temperature of Column B was gradually increased to determine whether the optimal temperature identified for *Dhc* in batch studies (25 to 30 °C (Löffler et al. 2013)) remains valid in a flow-through column system. During this period, the effluent VC concentration continued to decrease from 115±3 to 61±1 µM and ethene concentration remained high (>250 µM), indicating continued *Dhc* activity. Once the temperature reached 40 °C, *cis*-DCE was again detectable in effluent samples at very low concentrations (2 – 3 µM), despite continued ethene production. However, when the temperature of Column B reached 43 °C, effluent VC and ethene concentrations declined and *cis*-DCE concentrations quickly rebounded to 75±1 µM, suggesting that a maximum temperature permissive of *Dhc* activity had been reached. Aqueous abundances of *Dhc* measured in port samples (bar charts, Figure 3.1.12) support this conclusion: *Dhc* abundance increased with temperature up to approximately 43 °C, then remained steady or declined with further temperature increases (125 – 175 PVs, Figure 3.1.12). Collectively, these results indicate that *Dhc* are able to withstand and benefit from higher temperatures (<43°C) in flow-through systems than previously reported for batch studies (35 °C) (Löffler et al. 2013).

3.1.4.d. Impacts of temperature on *Dehalococcoides mcartyi* strains in heated soil columns

While column effluent data demonstrate a clear connection between system temperature and overall dechlorination activity, results from qPCR analyses performed on aqueous port samples also indicate that individual *Dhc* strains respond differently to temperature changes. As noted previously, *Dhc* strains possessing the *vcrA* RDase gene accounted for virtually all *Dhc* cells in the bioaugmenting KB-1 culture. This predominance was maintained throughout the entire 15 °C phase of Column A (bar charts, Figure 3.1.11). Following a temperature increase to 35 °C, however, *vcrA* abundance remained static or declined, despite increases in total *Dhc* and particularly *bvcA* abundance. Over the remainder of the experiment, aqueous *vcrA* abundance slowly began to increase again, but still lagged behind *bvcA* by an order of magnitude or greater. This trend was confirmed following destructive sampling and analysis of *Dhc* cells and RDase genes associated with the solid phase, where *bvcA* abundance was again greater than *vcrA* abundance (Figure 3.1.13).

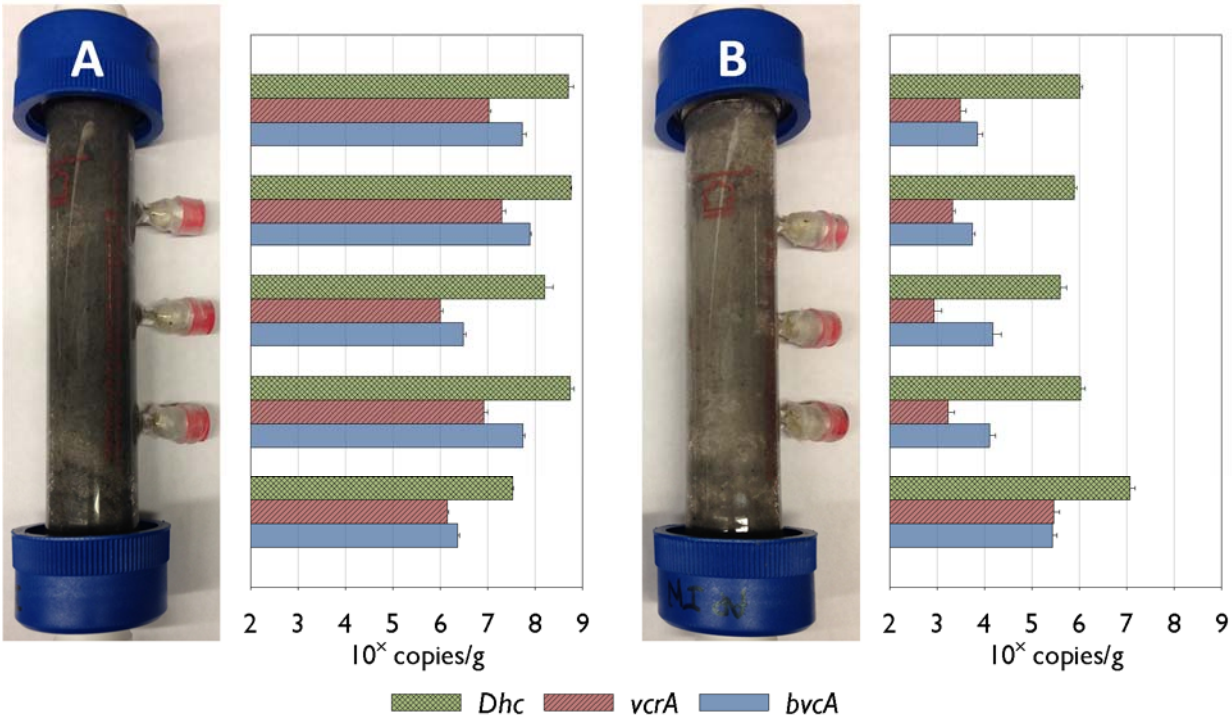

Figure 3.1.13. Spatial distribution of *Dhc* 16S rRNA and RDase genes associated with the solid phase of Column A (left) and Column B (right) following experiment completion and column dissection. Note that the direction of water flow during each column experiment was upward, from bottom to top in the images shown here.

Analyses of Column B port samples yielded similar results, with total *Dhc* 16S rRNA gene and *bvcA* abundances reaching 5.5±2.1 × 10^7 and 2.2±0.0 × 10^7 copies/mL, respectively, at 43 °C. The apparent proclivity for *bvcA*- and *tceA*-containing *Dhc* strains to play an increased role in ethene production at super-ambient temperatures is in agreement with results from the field-scale study completed by Macbeth et al. (2012), and supports the need to use of additional biomarkers

when assessing microbial reductive dechlorination performance at sites with elevated subsurface temperatures.

3.2. Effects of Metal Sulfide Formation and Dissolution on Aquifer Permeability (Task 2)

3.2.1. Permeability Alterations in Abiotic Pump-Driven Columns

A series of abiotic column experiments was completed to investigate the extent to which abiotic mechanisms contribute to FeS formation, and the consequences of this solid precipitation on aquifer permeability. The primary objective of this subtask was to assess permeability reductions in porous media with different organic carbon content due to iron (II) sulfide (FeS) precipitation prior to further studies conducted in biotic systems under Section 3.2.2. The following experimental conditions were investigated: (i) solid phase (e.g., well-characterized soils and aquifer materials of varying organic carbon content), (ii) hydrogen sulfide concentration, and (iii) dissolved ferrous iron concentration. Assessments of water flow and permeability changes were accomplished by utilizing the following approaches as either stand-alone or combined measurements: (a) monitoring the pressure differential in a constant flow system, (b) measuring changes in pore volume using non-reactive tracer tests, and (c) monitoring the flow rate in a constant head (pressure) system and subsequent calculations of hydraulic conductivity.

3.2.1.a. Impacts of FeS precipitation on hydraulic properties in a low organic carbon content sand (Federal Fine Column #1)

An initial 15 cm Federal Fine Ottawa sand column experiment was performed to establish baseline effects of FeS precipitation on hydraulic parameters (i.e., permeability, porosity, dispersivity) in a system with low organic carbon (OC) content (<0.01% OC). Following the introduction of 2.5 PVs of an iron (II) chloride solution (250 mg/L Fe^{2+}) and 3.5 PVs of a high sulfide (100 mg/L S^{2-}) medium solution to the 15 cm, horizontally-oriented column packed with Federal Fine Ottawa sand, black FeS precipitate was visible in the first 3 cm of the column inlet (Figure 3.2.1, top). After injecting only 1 PV of iron (II) chloride solution, effluent iron (II) concentrations were equal to influent concentrations. While a small mass of iron (II) was likely retained in the column after the introduction of the iron (II) chloride solution, the iron (II) analytical method (i.e., ferrozine method, Section 2.2.1.h) was not sensitive enough to calculate the retained mass. After a 24-hour flow interruption (i.e., no flow), another 2.9 PVs of 100 mg/L sulfide medium was flushed through the column, during which time the measured differential pressure (i.e., inlet pressure minus outlet pressure) remained constant at 5.5 cm H_2O. The corresponding permeability was calculated according to Equation 1, where k = intrinsic permeability of the system, μ = dynamic viscosity of the fluid (i.e., water), Q = volumetric flow rate, L = column length, γ = specific weight of the fluid, A = column cross-sectional area, and $h_1 - h_2$ = pressure drop over the column length. The calculated permeability of 1×10^{-8} cm^2 was consistent with literature values for clean sand (Freeze and Cherry 1979).

$$k = \frac{\mu \times Q \times L}{\gamma \times A \times (h_1 - h_2)} \tag{3.2.1}$$

Another flow interruption was then performed for 18 hours, after which extensive precipitation prevented further aqueous flow through the column (Figure 3.2.1., bottom).

Figure 3.2.1. Federal Fine Ottawa sand 15 cm column (horizontally-oriented, flow left to right) after 3.5 PVs of high sulfide (100 mg/L sulfide) medium solution (top); Federal Fine Ottawa sand 15 cm column after 24-hour flow interruption, 3 additional PVs of high sulfide medium, and a second 18 hour flow interruption (bottom).

3.2.1.b. Impacts of FeS precipitation on hydraulic properties of a natural soil with intermediate organic carbon content (Appling Soil Column #1)

The first Appling soil column was completed to assess permeability reduction due to FeS precipitation in a natural soil with intermediate organic carbon content (0.66% OC). While flushing reduced medium solution (11 PVs of 3 mg/L sulfide, then 22 PVs of 140 mg/L sulfide) through the first of two 15 cm column packed with Appling soil, black precipitate (FeS) became visible after 15 PVs, but differential pressure measured between the influent and effluent remained constant for the first 28 PVs. Because the system was driven by a peristaltic pump and the flow rate was controlled throughout the experiment, this lack of change in differential pressure, and by extension differential head, indicates that the permeability of the system remained relatively unchanged during this period. However, from PV 28 to experiment termination at 32.5 PVs, the permeability decreased rapidly from 6×10^{-10} to 2×10^{-10} cm^2, representing an overall reduction of 57.5% (Figure 3.2.2). At the conclusion of the experiment, approximately 4 cm of the influent end column was visibly black presumably due to the formation of FeS precipitate, as shown in Figure 3.2.3.

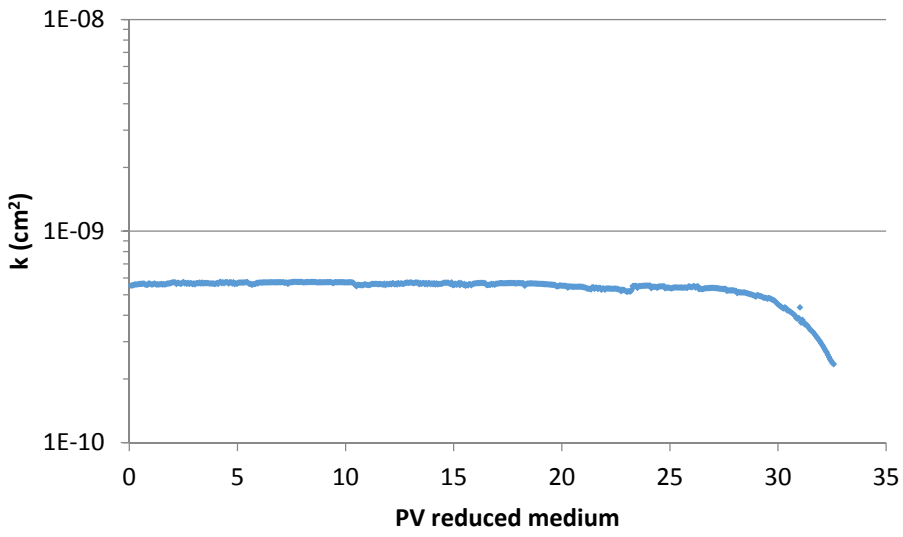

Figure 3.2.2. Permeability of Appling soil column #1 (15 cm) during infusion of 3 mg/L (0-11 PVs) and 140 mg/L (11-32.5 PVs) sulfide reduced medium.

Figure 3.2.3. Appling soil column (15 cm) after reduced medium (11 PV of 3 mg/L sulfide, then 22 PV of 140 mg/L sulfide) was injected (flow direction from bottom to top), with black precipitate (FeS) evident in the first 5 cm of the column. Pictured from left to right: 0 PV, 15 PVs, 26 PVs, 33 PVs.

3.2.1.c. Impacts of FeS precipitation on hydraulic properties of a fine textured, low organic carbon content soil (Groveland Field Site Column)

The most dynamic column experiment results occurred in a 15 cm column packed with Groveland field site material, which was completed to assess the impacts of FeS precipitation on a field material with high content of fine particles, but low OC content (0.01% OC). The experiment included an 11 PV infusion of $FeCl_2$ (210 mg/L Fe^{2+}), followed by 31 PVs of high sulfide reduced medium (140 mg/L S^{2-}), and 60 PVs of oxygenated medium (5.5 mg/L DO). Figure 3.2.4 shows the progression of the FeS precipitation front throughout the reduced medium infusion.

In the Groveland column, the initial decrease in soil permeability from 8×10^{-10} to 7×10^{-10} cm^2 during the reduced medium infusion was followed by an increase to 9×10^{-10} cm^2 (Figure 3.2.5). This temporary increase in permeability from 16 to 21 PV was possibly the result of pressure buildup within the column forcing pore throats to expand and restoring permeability. After this restoration, the permeability gradually decreased once again, but never reached the low permeability measured earlier in the experiment.

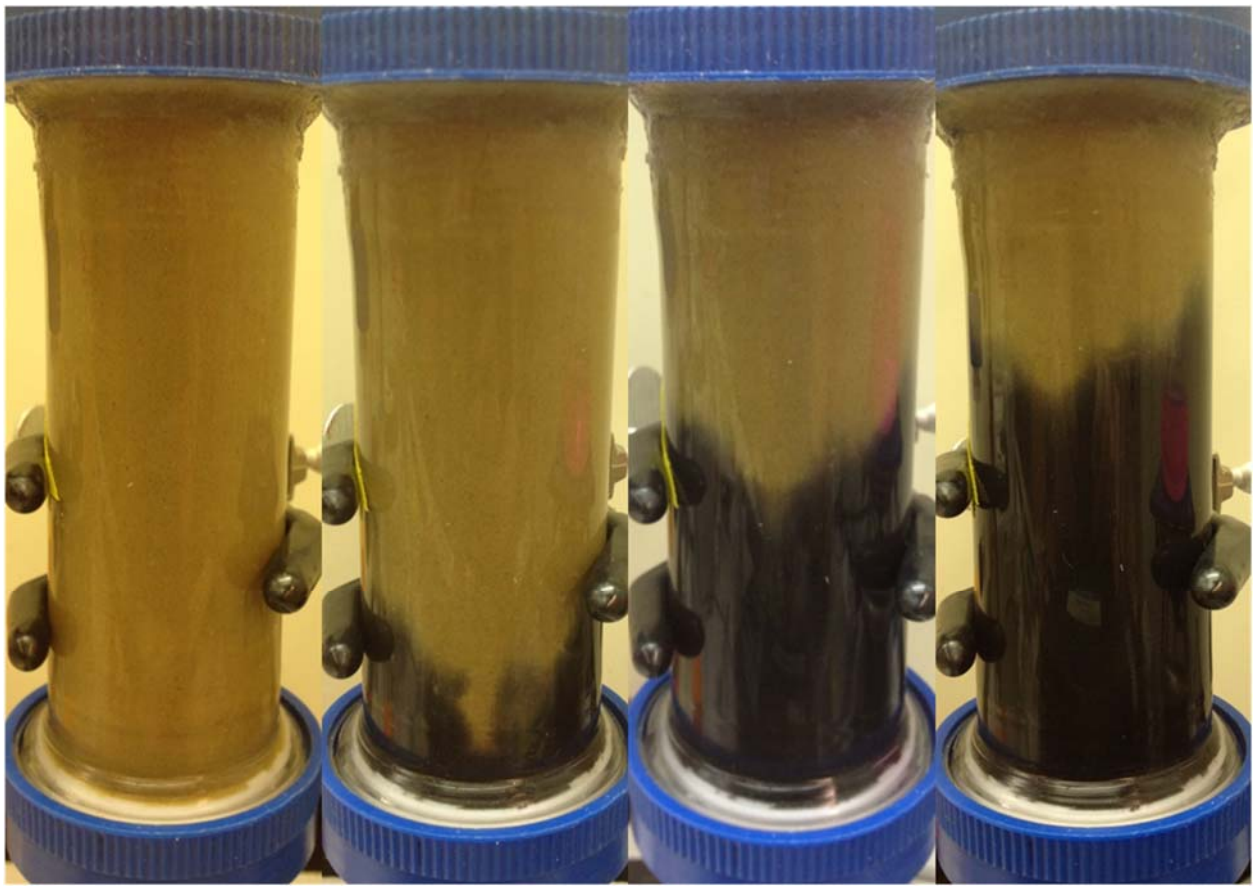

Figure 3.2.4. Pictures of the Groveland field material column after reduced medium infusion (11 PV of 120 mg/L sulfide, flow direction from bottom to top), with black precipitate (FeS) visible. Shown from left to right: 0 PV, 23.5 PVs, 37.9 PVs, 44.7 PVs.

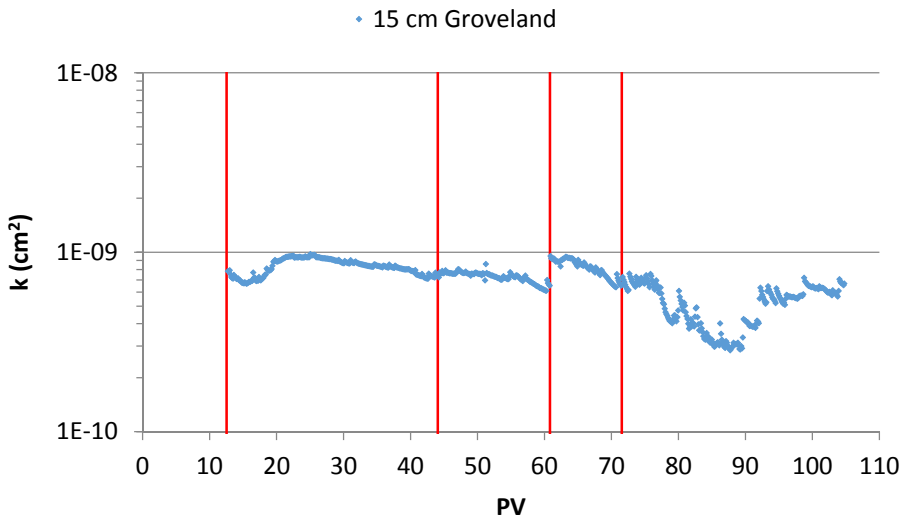

Figure 3.2.5. Permeability changes measured in Groveland column; 210 mg/L Fe^{2+} (0-12.3 PVs); 110 mg/L S^{2-} reduced medium (12.5-44 PVs); 5.5 mg/L DO oxygenated medium (44-106 PVs). Vertical lines indicate replacement of the influent bottle.

The largest permeability reduction occurred during the infusion of oxygenated (5.5 mg/L DO) medium following the high sulfide phase. At its lowest point, the permeability dropped to 2×10^{-10} cm^2, approximately 78% lower than the peak value of 9×10^{-10} cm^2 earlier in the experiment (i.e., 64 PVs, Figure 3.2.5). This effect was attributed to the oxidation of FeS and the formation of insoluble iron (III) oxides and iron (III) hydroxides (Figure 3.2.6). However, the observed decrease in permeability during the introduction of the oxygenated medium was followed by an equally steep increase; one hypothesis potentially explaining this increase (and thus restoration of effective column permeability) is that pore throats already clogged with FeS were once again forced to expand due to pressure buildup in the pump-driven system. Expansion of pore throats may have created new, preferential flow paths, which acted to restore the overall permeability lost due to FeS precipitation.

In addition to the permeability changes measured throughout the sulfide exposure and subsequent oxidation, bromide tracer tests performed prior to the FeS precipitation phase and after the oxygenated medium flush (Figure 3.2.6) showed that the initial column porosity of 0.42 had decreased by approximately 1% by the conclusion of the experiment. Furthermore, the initial dispersivity of 0.15 cm increased to 0.23 cm following FeS precipitation and oxidation, meaning that the relative role of diffusive transport increased throughout the experiment. This increase in dispersivity indicates that the FeS precipitation and subsequent oxidation caused flow conditions within the Groveland column to become more heterogeneous, which is consistent with the variations in permeability and decrease in porosity.

Figure 3.2.6. Inlet end of 15 cm column packed with Groveland field material after injection of oxygenated (5.5 mg/L DO) medium.

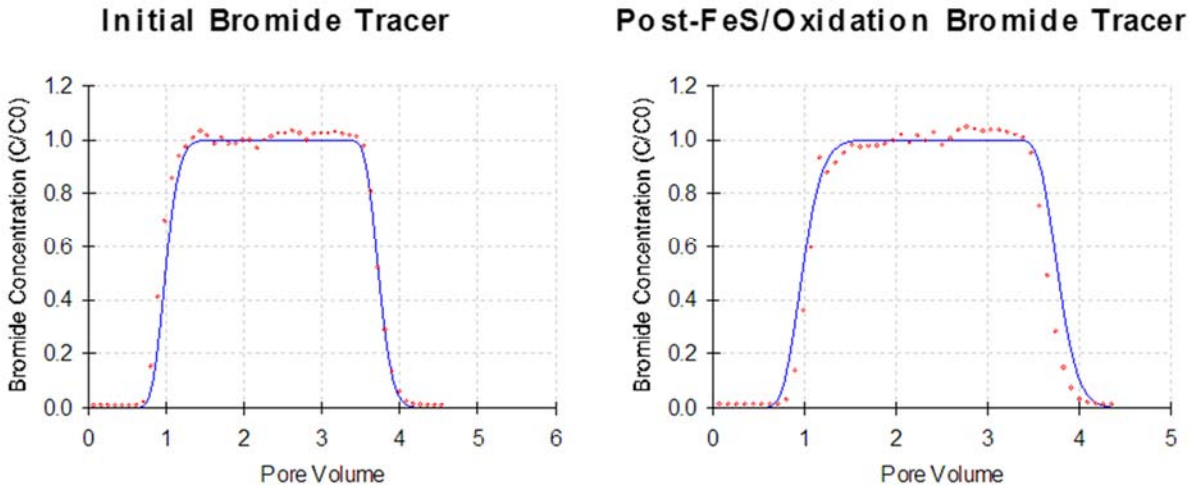

Figure 3.2.7. Measured (data points) and fitted (solid line) bromide tracer breakthrough curves (BTCs) for Groveland column before (left) and after (right) FeS precipitation and oxidation, showing increased spreading consistent with increased dispersivity.

3.2.1.d. Impacts of excess iron on FeS precipitation in a soil with intermediate organic carbon content (Appling Soil Column #2)

A second Appling soil column was completed to determine whether exposure to abundant iron (II) prior to sulfide exposure had any impact on the extent of permeability reduction. Unlike the first Appling soil column experiment, no change in permeability was detected following the injection of 2.4 PV of an iron (II) chloride solution (250 mg/L Fe^{2+}) and 45 PVs of high sulfide (110 mg/L S^{2-}) medium solution. The lack of permeability change throughout the reduced medium injection was unexpected because the entire column turned visibly black with FeS precipitate. Furthermore, bromide tracer tests performed before and after the precipitation phase showed that FeS precipitation caused a decrease in column porosity from 0.49 to 0.48, representing a decrease of approximately 2.8%. Dispersivity remained constant at approximately 0.06 cm before and after FeS precipitation. These results may be due in part to the fact that flow in the first 15 cm Appling column was stopped periodically for approximately 5 seconds at a time to allow for effluent sampling, and the second column was not. These short flow interruptions may have allowed colloidal FeS precipitate to more efficiently attach to soil grains than they would while the column was flowing, causing more drastic pore clogging. Furthermore, the higher pore water velocity used in the second Appling soil column experiment (v = 70 cm/d) compared to that in Appling soil column #1 (v = 25 cm/d) may have prevented FeS precipitate from depositing in the soil pore space.

During the 50.5 PV oxygenated medium (5.5 mg/L DO) infusion following the FeS precipitation phase, column permeability decreased from 1×10^{-9} to 6×10^{-10} cm^2 (Figure 3.2.8) equivalent to a 58% reduction in overall permeability. This reduction was similar to that measured during the oxygenated medium flush in the 15 cm Groveland column, and was likely due to the formation and precipitation of iron (III) oxides and iron (III) hydroxides. The fact that permeability was more highly impacted during the oxygenated medium phase than the reduced phase was not expected, and suggests that oxidized iron mineral phase formation may have a more significant impact on column permeability than FeS precipitation.

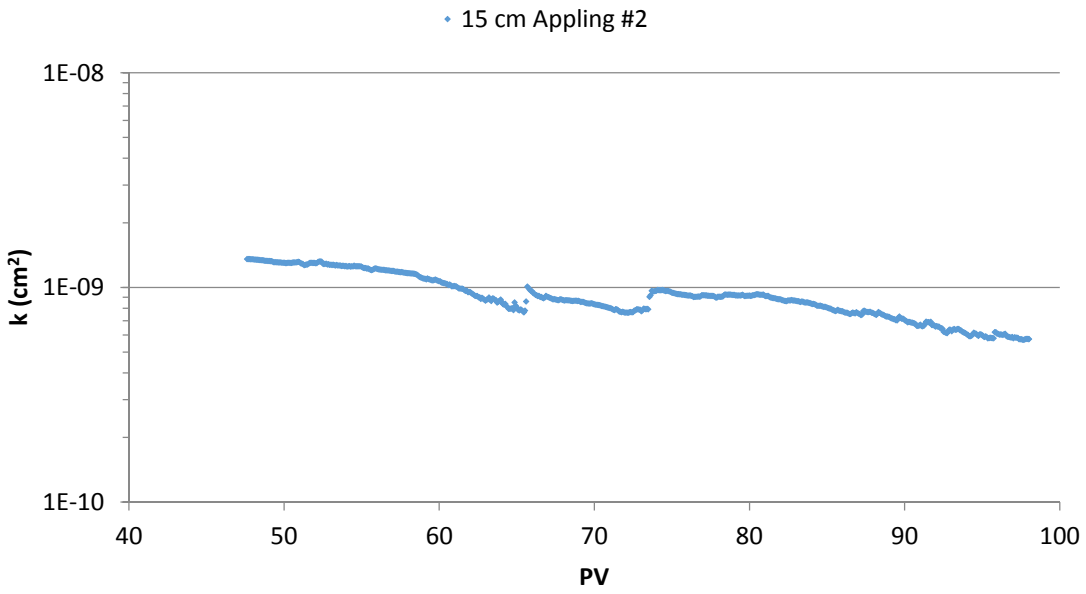

Figure 3.2.8. Permeability changes measured in Appling soil column #2 during injection of 5.5 mg/L DO oxygenated medium mg/L (45-50.5 PVs) followed by the injection of 45 PVs of reduced medium (110 mg/L S^{2-}).

3.2.1.e. Spatial variability in permeability loss during FeS precipitation (Federal Fine Sand Column #2)

A 60 cm column experiment was completed using Federal Fine Ottawa sand to quantify spatial variability in permeability loss due to FeS precipitation. However, bromide tracer tests revealed that the total column porosity decreased by only 0.05% from its initial value of 0.39 during the FeS precipitation phase. Furthermore, no change in permeability was detected after the introduction of 6.5 PV iron (II) chloride (250 mg/L Fe^{2+}) and 6.5 PVs high sulfide (95 mg/L S^{2-}) medium. However, formation of FeS precipitate was clearly visible within the first PV of sulfide medium injected. The column became gray in color due to FeS formation, and gradually darkened until the high sulfide injection was stopped (Figure 3.2.9). Pressure measurements taken from the side ports, which were intended to evaluate the spatial variability of permeability losses due to FeS precipitation, also did not indicate that column permeability was being affected. A subsequent 7-day flow interruption period during the high sulfide phase had no measurable impact on the differential pressure across the column. The results obtained in the 60 cm column were in stark contrast to those from the initial Federal Fine Ottawa sand column, which became clogged with precipitate to the point that column flow stopped entirely. However, despite the relatively steady permeability and porosity values in the 60 cm Federal Fine sand column, tracer tests completed before and after introduction of the high sulfide medium revealed that the dispersivity increased approximately +39.6%, from 0.08 to 0.11 cm, indicating that the FeS precipitation caused the system to become more heterogeneous. Thus, the absence of measurable changes in permeability and the minimal decrease in porosity in the 60 cm column may be due to location of the pressure transducers and the larger scale of the system, which could allow for flow bypassing and the formation of preferential flow paths.

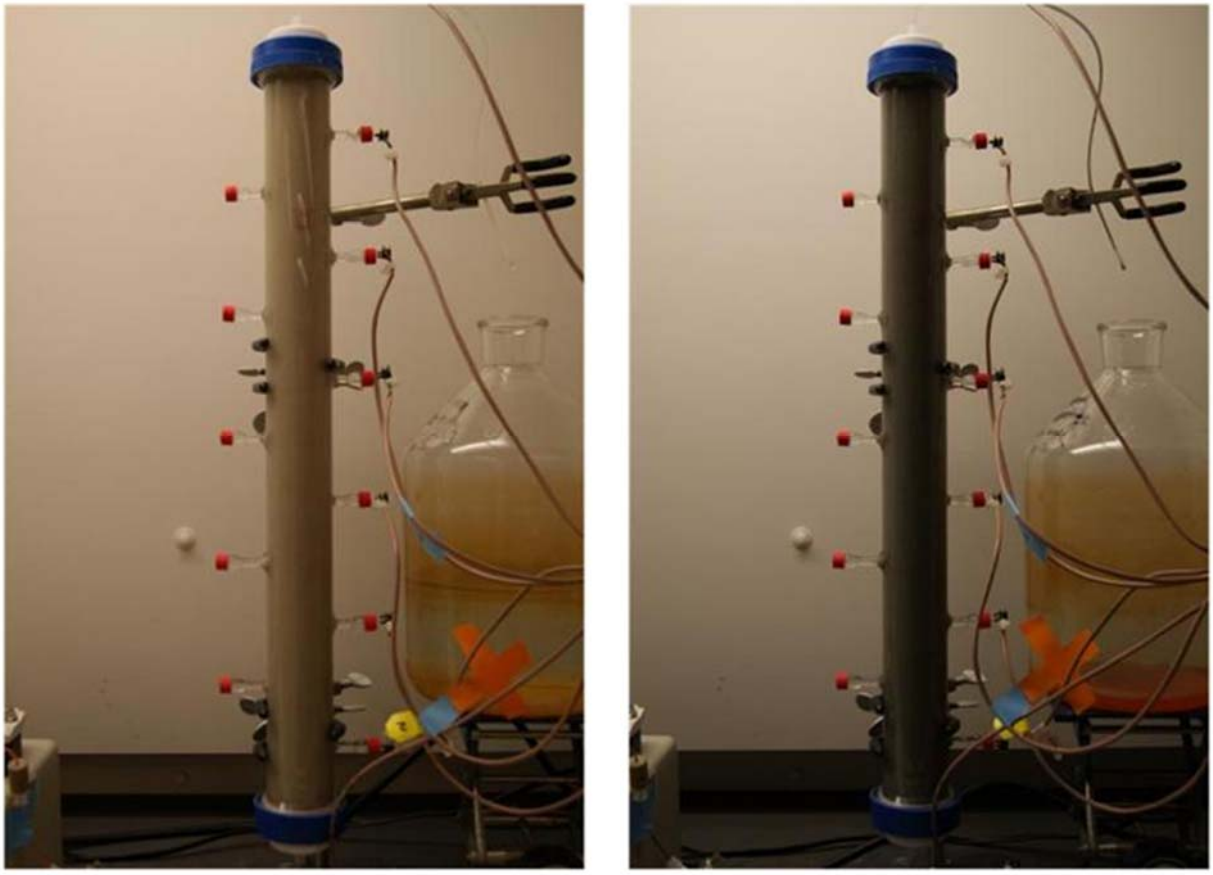

Figure 3.2.9. Pictures of a 60 cm column packed with Federal Fine Ottawa sand before (6.5 PVs, left) and after (13 PVs, right) introduction of reduced medium (95 mg/L S^{2-}). The direction of water flow is upward, from bottom to top.

3.2.1.f. Acid volatile sulfide analysis of Appling Soil Column #1 and Groveland field material

Acid volatile sulfide (AVS) analysis performed on the first 15 cm Appling soil column and the 15 cm Groveland field soil column yielded results that coincided with the visible FeS precipitation profiles (i.e., spatial deposition) for each column (Figure 3.2.10). Sulfide distribution in the Appling column was heavily skewed toward the influent end of the column, with 90.3% of sulfide mass recovered from the first 4 cm of the column. AVS analysis of the Groveland column showed that 86.4% of the sulfide mass was recovered between 3 and 9 cm from the column inlet; this distribution agreed with the visual FeS precipitation profile within the column (Figures 3.2.4 and 3.2.5), and also reflected the loss of FeS precipitate in the first 2 cm of the column due to the oxygenated medium flush.

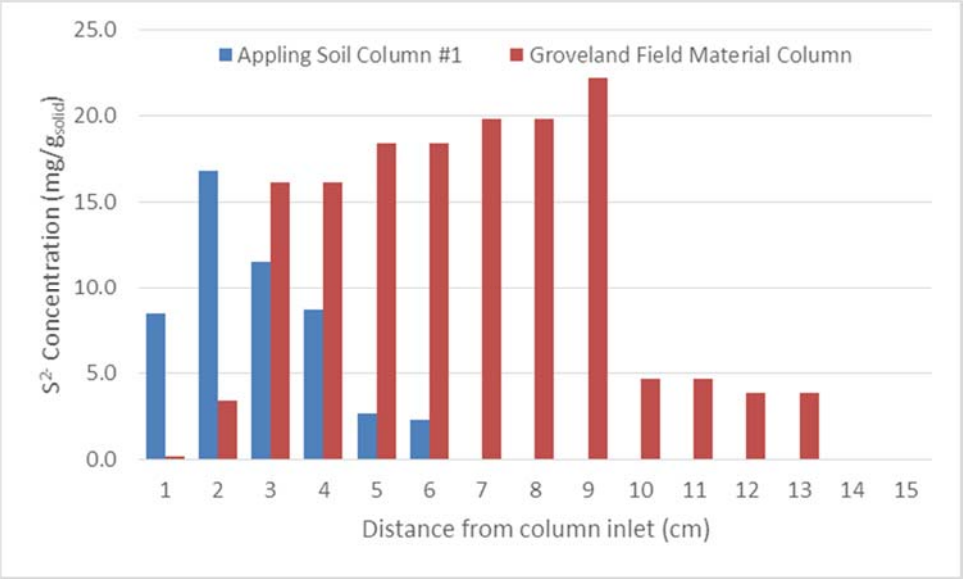

Figure 3.2.10. Sulfide mass distribution following destructive sampling and acid volatile sulfide analysis of Appling soil column #1 and the Groveland field material column.

Despite the apparent agreement between AVS and visible FeS profiles in each column, sulfide mass balances were only 13.9 and 38.7% for the Appling and Groveland columns, respectively. Given that no sulfide was measured in the effluent of either column, these low recoveries indicate that changes in the oxidation state of the sulfide could have occurred within the column during the column experiments, or that sulfide may be forming acid insoluble complexes. Strictly controlled batch experiments designed to test the efficiency of the AVS method resulted in a maximum of 49.5% sulfide mass recovery, indicating that the method is unlikely to yield complete sulfide recovery.

3.2.2. Influence of Flow Rate on FeS Precipitation in Pump-Driven Column Experiments

Following the completion of abiotic column experiments described above (Section IV.2.1), an additional set of abiotic column experiments was performed at a lower pore-water velocities of 25 cm/day.

The results of three abiotic, low-flow, pump driven column experiments are presented below. All three columns were subject to initial tracer and hydraulic conductivity tests to determine the background hydraulic parameters of each column. This was then followed with a high sulfide medium flush, which continued until column conditions appeared static and the influent medium was no longer reacting with the material in the column. A second round of tracer and hydraulic conductivity tests were then conducted to determine changes in the hydraulic parameters in each column. Finally, for one of the columns (Federal Fine #5), an aerated medium was used as the influent to determine the effects of oxidation on FeS precipitates. A third round of tracer and hydraulic conductivity tests was completed to measure the effects of oxidation on the hydraulic properties. One column was run individually, Federal Fine #3, while the other two columns, Federal Fine #4 and #5, were run simultaneously with a single influent to allow for direct comparisons.

3.2.2.a. Impacts of flow rate on permeability during FeS precipitation (Federal Fine Sand Column #3)

Federal Fine Ottawa sand column #3 was completed to determine whether pore clogging due to FeS precipitation is more significant at low pore water velocities (i.e., 25 cm/d). Following the introduction of 46.6 PV of high sulfide medium (40-80 mg/L sulfide) the influent and effluent concentrations of Federal Fine Ottawa sand column #3 were approximately equal, indicating that no additional sulfide from the influent solution was being retained within the column (see Figure 3.2.11). After analyzing the hydraulic properties with a second tracer test, it was determined that there was a net decrease in porosity and hydraulic conductivity of 2.04% and 95.8%, respectively. Dispersivity also decreased by 26.9%, indicating that mixing was decreased as a result of the FeS precipitate formation (Figure 3.2.12).

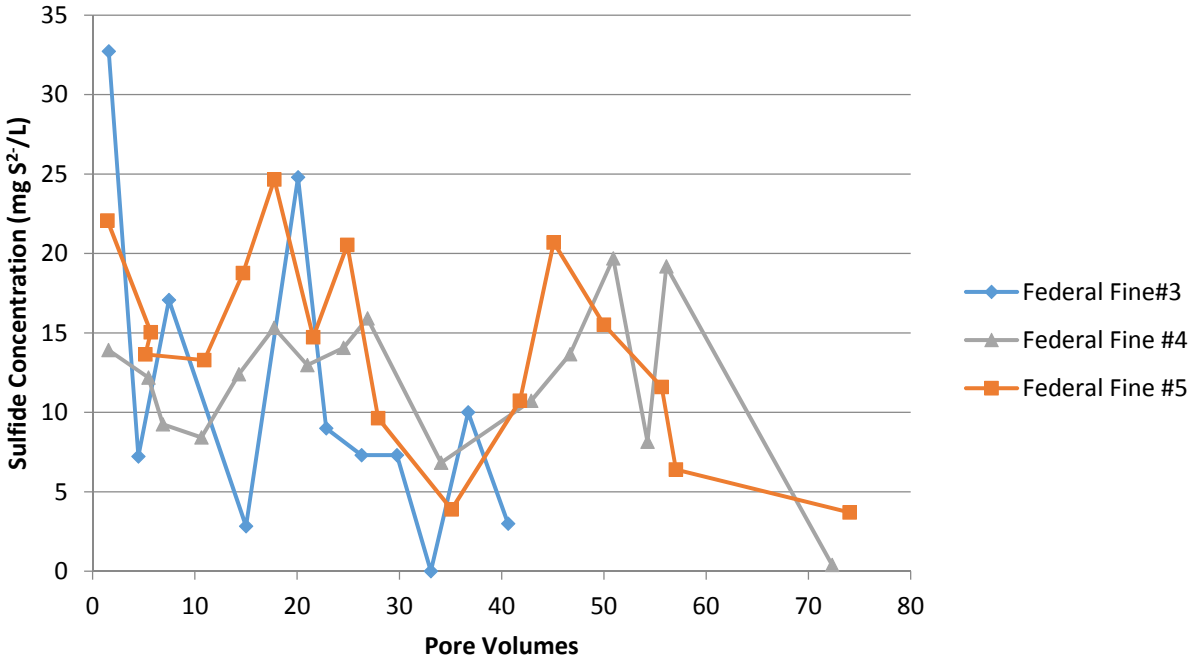

Figure 3.2.11. Differences between in influent and effluent sulfide concentrations as a function of PVs injected indicated when to cease column operation (i.e., when the difference approached zero).

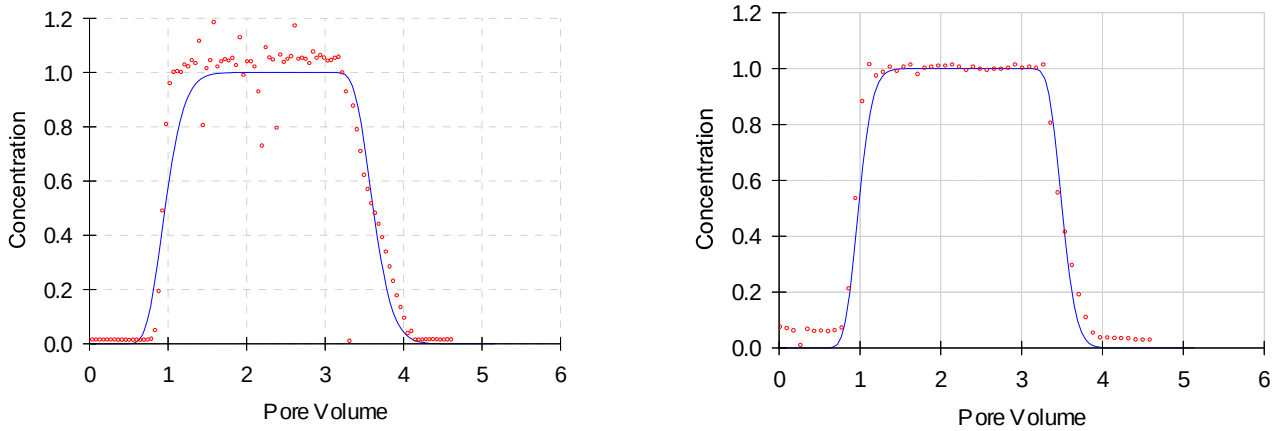

Figure 3.2.12: Measured (data points) and fitted (solid line) bromide tracer test breakthrough curves for pump-driven Federal Fine Column #3, before (left) and after (right) FeS precipitation, showing decreased spreading consistent with decreased dispersion.

3.2.2.b. Impacts of flow rate on permeability during FeS precipitation and oxidation Federal (Fine Ottawa Columns #4 and #5)

Two columns packed with Federal Fine Ottawa sand (Columns #4 and #5) were prepared in the same manner as Federal Fine Column #3, but were run simultaneously. Separate influent lines were used for the first tracer test before combining influent lines to maintain the same influent solution for the high sulfide flush. Given that flow through each column was driven by a separate pump, the flow rates differed slightly (0.11 to 0.15 mL/min), leading to minor differences in the number of PVs injected (i.e., 83.6 PVs for Federal Fine #4 and 81.6 PVs for Federal Fine #5) of high-sulfide medium. Following the injection of 1 PV of reduced medium (60 mg/L S^{2-}), black precipitate began to form in both columns between 2 and 15 cm. Minimal precipitate formed in the first 2 cm of each column, which was packed with acid-washed sand, indicating that the influent sulfide was reacting with iron in the sand between 2 and 15 cm (Figure 3.2.13).

Figure 3.2.13. Difference in color between the inlet 2 cm (bottom) in Federal Fine Ottawa sand column #4 (right) and Federal Fine Ottawa sand column #5 (left) and the remainder of the column (above) indicating FeS precipitate. The direction of water flow was upward, from bottom to top.

Due to the formation of precipitate in the influent bottle, which led to clogging in the influent lines, an alternative approach was taken to flushing the high sulfide medium through the columns. Rather than using one 9 L medium vessel to feed both columns, two separate 4 L high-sulfide medium solutions (60 mg/L S^{2-}) were prepared for each column. The smaller bottles provided a better seal against oxygen intrusion and limited precipitation prior to entering the columns. Both sets of influent and effluent solutions were then monitored for sulfide concentration, pH, and ORP. The high concentration sulfide media were flushed through Federal Fine Ottawa sand columns #4 and #5 until influent and effluent sulfide concentrations were approximately equal (Federal Fine #4: C_{in} = 39.5 mg/L S^{2-}, C_{out}=39.1 mg/L S^{2-}; Federal Fine #5: C_{in}=51 mg/L S^{2-}, C_{out} = 48 mg/L S^{2-}) (see Figure IV.2.1). The similar influent and effluent sulfide concentrations indicated that the columns were saturated with sulfide, and that sulfide introduced in the column influent solutions was no longer reacting with the systems. Tracer tests following the high sulfide flushes revealed decreases in porosity of 19.2% and 15.9% and increases in dispersivity of 270% and 213% for Federal Fine #4 and Federal Fine #5, respectively. The influent solution of Federal Fine Ottawa sand column #5 was then switched to a medium solution containing approximately 5.5 mg/L dissolved oxygen (DO). Almost immediately after beginning the oxygenated medium flush, the black FeS precipitate became darker in color and the dark color extended toward the column effluent (Figure 3.2.14).

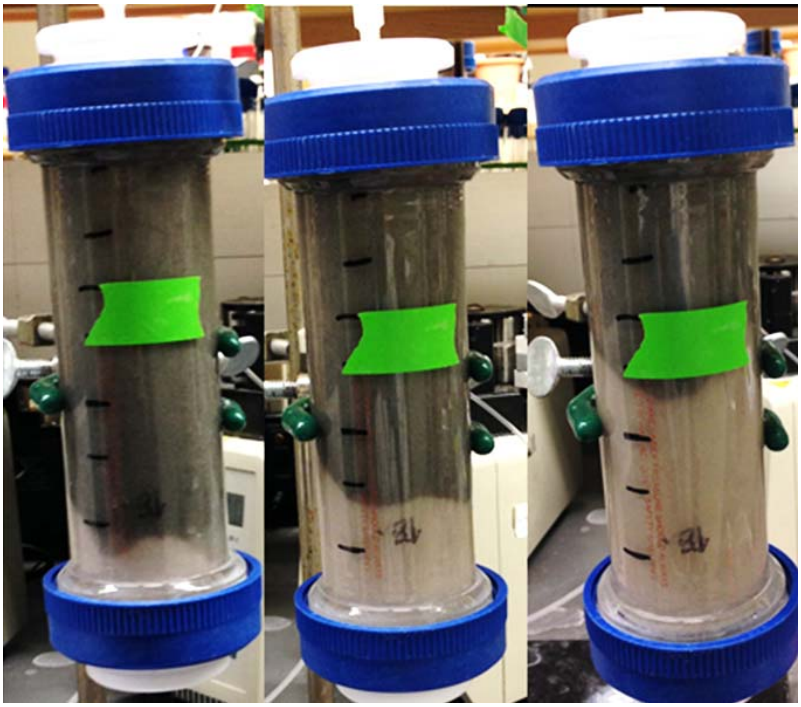

Figure 3.2.14. Pictures illustrating the darkening of FeS precipitate and migration toward the effluent after the introduction of the oxygenated medium in Federal Fine Ottawa sand column #5 after 1, 5 and 10 PVs post injection in the images from left to right, respectively. The direction of water flow is upward, from bottom to top.

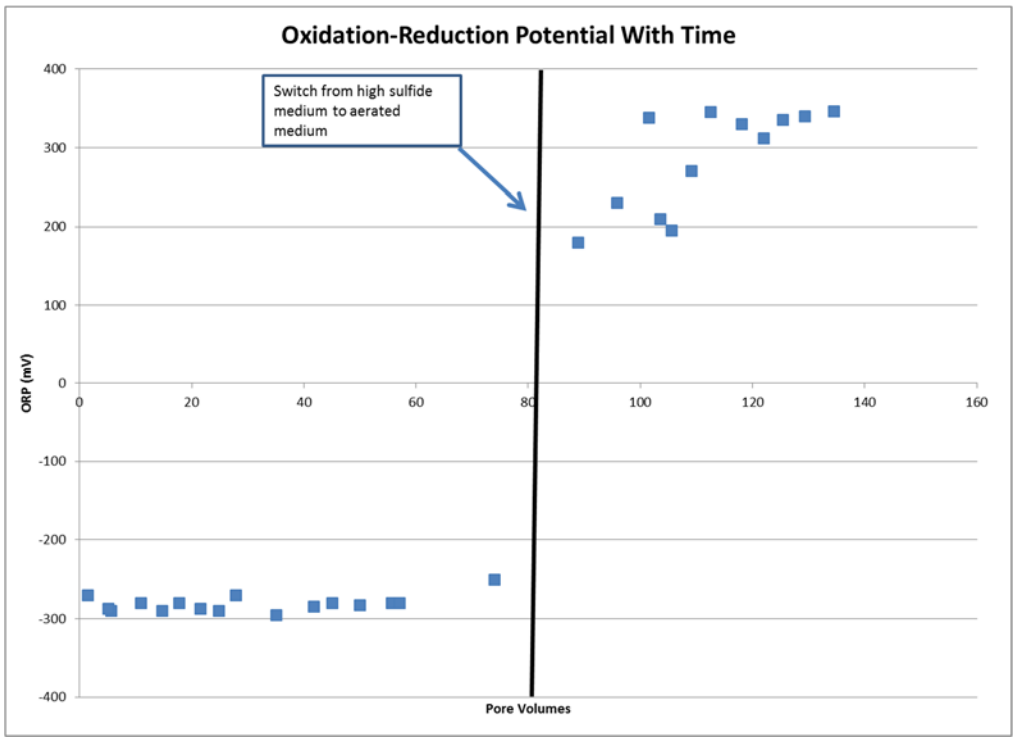

Figure 3.2.15. Change in the ORP between influent solutions in Federal Fine Column #5.

The oxygenated medium influent solution (≈ 5.5 mg/L DO) was introduced to Federal Fine Ottawa sand column #5 for 56 PVs before the influent and effluent DO, ORP, and pH were stable enough so that no further changes in hydraulic parameters were anticipated. Figure 3.2.14 shows the change in the influent ORP between the high sulfide medium and oxygenated medium solutions. For the final 14 PVs of the oxygenated medium injection, the influent parameters remained stable with DO = 5.5 mg/L, ORP = +310-340, and pH = 7.3, while the effluent parameters remained stable with DO =2 mg/L, ORP +300-330, and pH = 7.3 (Figure 3.2.15). The third and final tracer test of the Federal Fine Ottawa sand column #5 revealed that the system porosity increased by approximately +21.2% during the oxygenated medium injection, indicating that the porosity of the system had been restored to its initial value. Similarly, the dispersivity also recovered to the original value (i.e., pre-sulfide flush).

3.2.3. Permeability Alterations in Abiotic Head-Driven Soil Columns

Following the series of pump-driven column experiments, two sets of abiotic, head-driven column experiments were performed to evaluate the impacts of FeS precipitation under conditions that more closely resemble the natural flow in an aquifer system. Each set of two column experiments utilized the same influent bottle to minimize differences between parallel column experiments. The first set compared materials of contrasting OC content, Federal Fine Ottawa sand and Appling soil, which contain <0.01% and 0.54% OC by weight, respectively. The second set of columns was undertaken to compare the influence of pre-treatment with ferric chloride in columns packed with Webster soil, which contains approximately 2.36% OC.

3.2.3.a. Coupled effects of organic carbon content and head-driven flow on hydraulic properties (Federal Fine Sand Column #6 and Appling Soil Column #3)

Constant head column experiments were performed in parallel to simulate more realistic field conditions, while directly comparing the effects of FeS precipitation in porous media with different OC contents (<0.01% OC and 0.54% OC for Federal Fine Ottawa sand and Appling soil, respectively). Results from the first pair of head-driven column experiments, one packed with Federal Fine Ottawa sand and the other with Appling soil, demonstrated that overall permeability loss was more gradual when flow was head-driven, compared to pump-driven, constant flow systems. During the reduced medium injection, permeability decreased by 53 and 61% in the Federal Fine and Appling columns, respectively. Additionally, the higher OC Appling soil experienced more rapid permeability loss than Federal Fine Ottawa sand, and was less susceptible to sudden changes in flow (Figure 3.2.16).

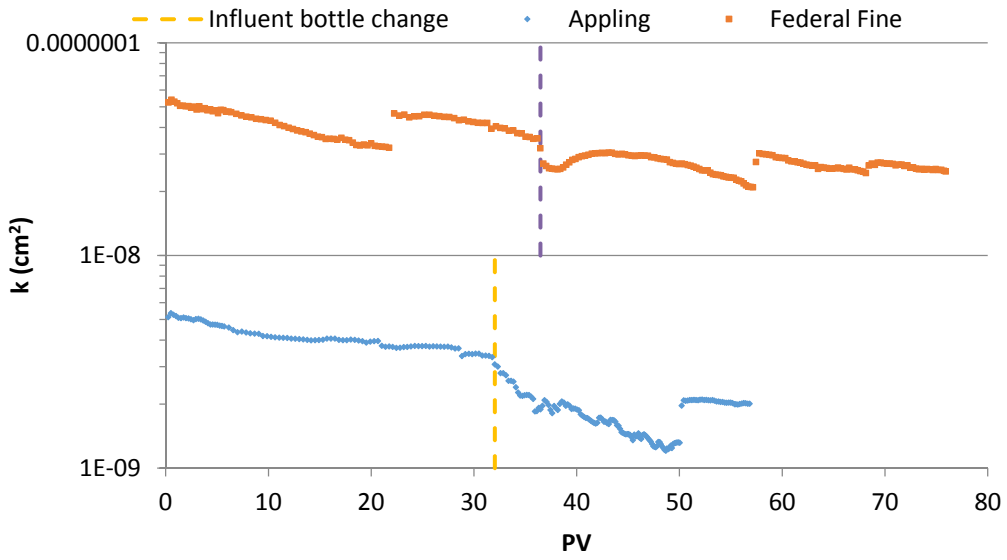

Figure 3.2.16. Permeability versus pore volumes of high sulfide (75 mg/L S^{2-}) reduced medium injected into head-driven Appling and Federal Fine Ottawa sand columns.

In addition to permeability losses in both the head-driven Federal Fine Ottawa sand and Appling soil columns, bromide tracer tests performed before and after FeS precipitation revealed decreases in overall porosity for both porous media. In the Federal Fine Ottawa sand column #6, FeS precipitation caused pore volume to decrease by 1.9%. In the Appling soil column #3, FeS precipitation caused a 7.5% reduction in porosity, representing the greatest porosity loss measured during any of the column experiments. Furthermore, the dispersivity increased dramatically in both columns following FeS precipitation. The dispersivity in the Federal Fine sand column #6 increased slightly from 0.05 cm to 0.08 cm, or +52.1%. The dispersivity in the Appling soil column #3 increased by +49.1%. However, since the initial dispersivity of the Appling soil column was significantly higher (0.18 cm) than that in the Federal Fine column #6, the increase was more dramatic, as shown graphically in Figure 3.2.17.

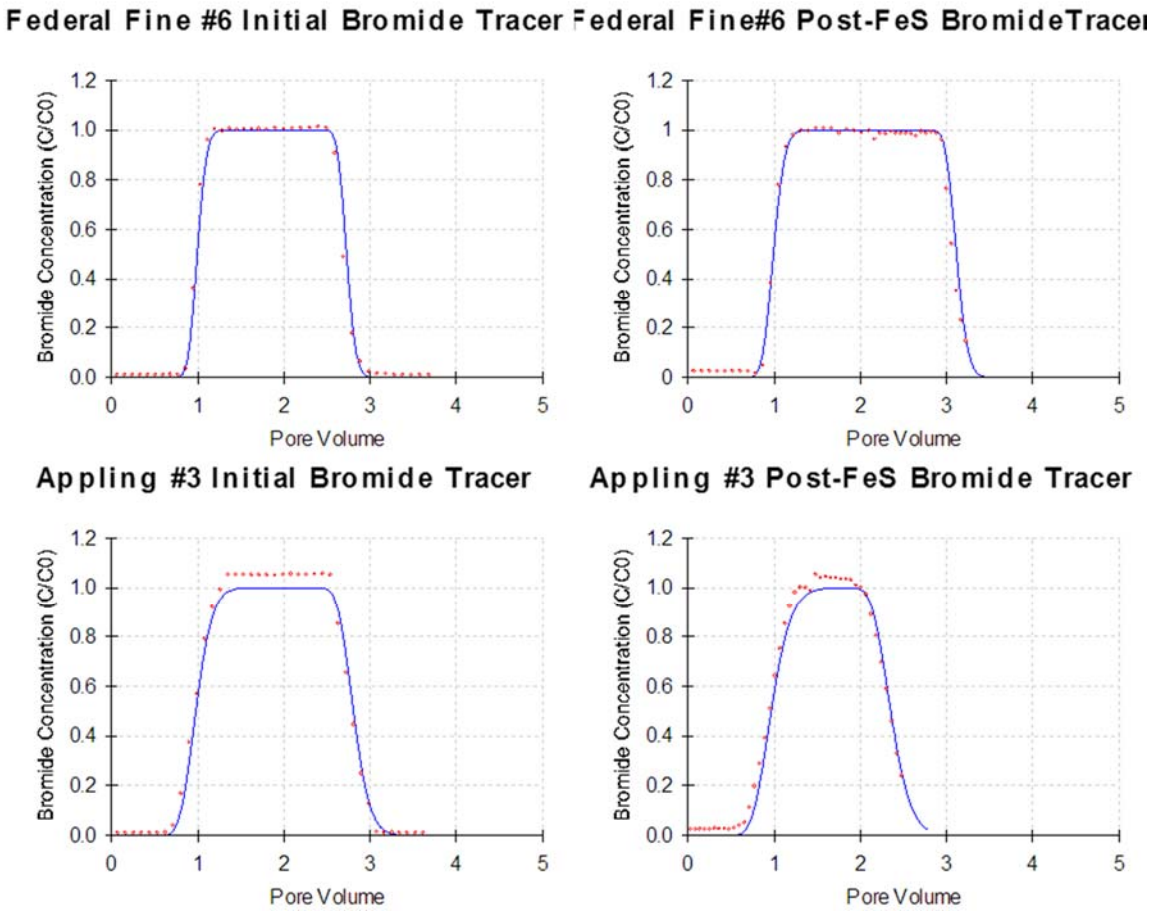

Figure 3.2.17. Measured (data points) and fitted bromide tracer test breakthrough curves for head-driven Federal Fine Column #6 (top row) and Appling soil column #3 (bottom row), before (left) and after (right) FeS precipitation.

While changes in permeability, porosity, and dispersivity were more apparent, and perhaps more realistic, in the head-driven column experiments, the variability measured in the pump-driven column experiments was not entirely eliminated: both the Federal Fine and Appling head-driven columns experienced at least one sharp increase in permeability throughout the reduced medium injection phase, possibly indicating the reopening of flow paths that had been partially or entirely clogged due to FeS precipitation.

3.2.3.b. Coupled effects of excess iron and head-driven flow on hydraulic properties of a high organic carbon content soil (Webster Soil Columns #1 and #2)

Similar to the first pair of head-driven column experiments, dual Webster soil column experiments were performed in parallel to assess permeability loss due to FeS precipitation in a high OC soil (2.36% OC). The two Webster soil columns were prepared similarly, but 4 PVs of iron (II) chloride (800 mg/L Fe^{2+}) was introduced to Webster soil column #1 prior to sulfide exposure in order to determine whether excess iron (II) availability has any impact on the extent of permeability and porosity reductions during FeS precipitation. Webster soil column #2 was not exposed to iron (II) prior to the injection of the reduced medium, and all iron in the system was associated with the soil.

Throughout the reduced medium (100 mg/L S^{2-}) injection phase, both head-driven Webster soil columns exhibited steady decreases in permeability (Figure 3.2.18). Permeability in Webster column #1, which had previously been flushed with 800 mg/L iron (II), decreased from 1×10^{-8} to 7×10^{-9} cm^2 over 73 PV. Unexpectedly, Webster column #2, which was not exposed to iron (II) prior to reduced medium injection, exhibited decreased flow rate and faster permeability loss, 1×10^{-8} to 3×10^{-9} cm^2 over only 40 PV. The relatively slow permeability decrease in Webster column #1 indicates that prior exposure of a soil to excess iron (II) did not enhance FeS precipitation rate or severity, and may in fact slow or prevent FeS-based permeability loss. A visible FeS precipitation front advanced through both Webster soil columns at approximately the same rate (Figure 3.2.19), which supports the reasoning that excess iron (II) has limited impact upon FeS precipitation.

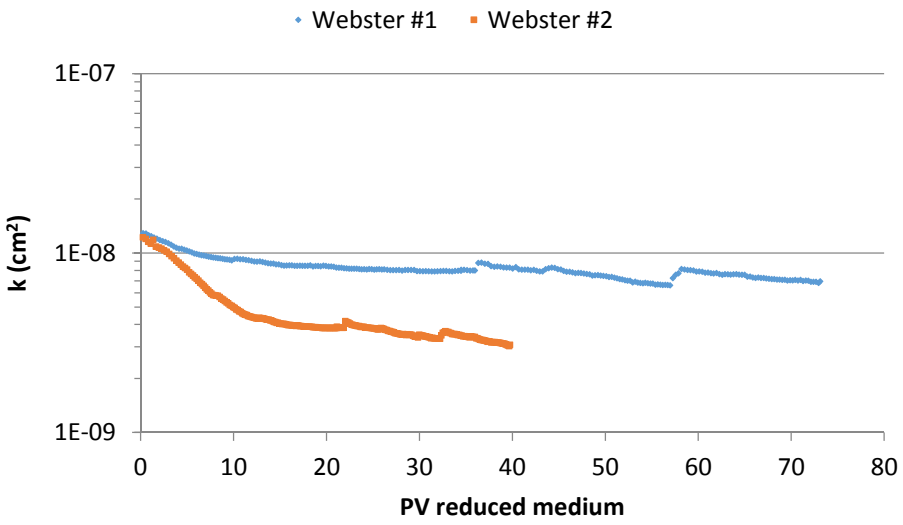

Figure 3.2.18. Permeability versus pore volumes of high sulfide (100 mg/L S^{2-}) reduced medium injected into head-driven Webster soil columns.

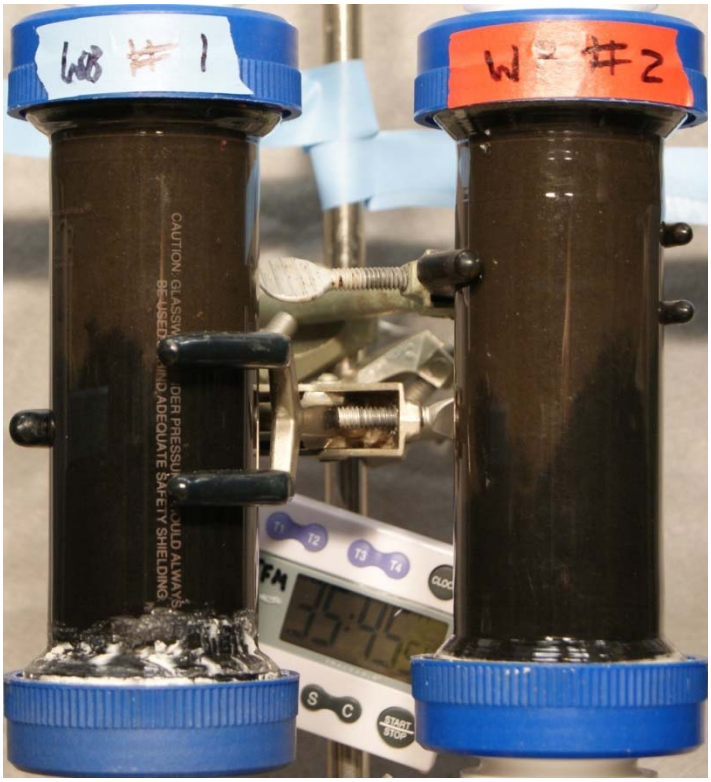

Figure 3.2.19. Head-driven columns packed with Webster soil after injecting 4 PVs of 800 mg/L iron (II) chloride and 73 PVs of reduced medium containing 100 mg/L S^{2-} (left, Webster soil column #1) or 44 PVs of reduced medium containing 100 mg/L S^{2-} (right, Webster soil column #2). The direction of water flow is upward, from bottom to top.

Following the introduction of reduced medium (i.e., FeS precipitation), the two head-driven Webster soil column experiments showed overall reductions in permeability of 46.1 and 74.8% in Webster soil columns #1 and 2, respectively. The observed reductions in permeability corresponded to overall porosity reductions of 2.97% and 4.72% for Webster columns #1 (exposed to Fe (II)) and #2 (unexposed), respectively, following the sulfide flush. Dispersivity was unchanged in Webster column #1 and decreased by 13.6% in Webster column #2. Reductions in permeability of Webster columns #1 and #2 continued throughout the oxygenated medium (5.5 mg/L DO) phase as well, with the permeability of both columns reaching 2×10^{-9} cm^2 upon experiment termination (Figure 3.2.18). In Webster column #1that was pre-flushed in Fe (II), the porosity recovered slightly (0.26%), and the dispersivity decreased by 28.6% following oxidation. Conversely, in Webster column #2 that was not pre-treated with Fe (II), the porosity and the dispersivity further decreased by 0.61% and 41%, respectively, following oxidation. These findings indicate that iron (II) pre-treatment of soils had no minimal impact on the extent of FeS precipitation, and instead, the Webster column #2 that was not pre-flushed with Fe (II), experienced greater impacts in dispersivity, permeability and porosity resulting from the precipitation of FeS.

Table 3.2.1 provides a comparison of all abiotic columns run under section IV.2, which were completed to determine the impacts of iron (II) sulfide precipitation on the permeability of porous media. Slow flow rates (i.e., higher residence time) and head-driven flow, and high soil OC content were generally associated with the greatest decreases in permeability and porosity due to FeS precipitation and subsequent oxidation. These decreases in permeability and porosity were typically associated with increased dispersivity, indicating that the FeS precipitation and oxidation caused the systems to become more heterogeneous. These findings suggest that changes in hydraulic parameters resulting from FeS formation are likely to be most pronounced in aquifer formations with low-flow conditions and moderate to high OC content.

Table 3.2.1. Summary of abiotic FeS column experiments described in Sections 3.2.1, 3.2.2, and 3.2.3.

Column	Driven by	Description	seepage velocity (cm/day)	Initial conditions α (cm)	k (cm²)	n (v_v/v_T)	Post-S^{2-} flush α (cm)	k (cm²)	n (v_v/v_T)	Post-O_2 flush α (cm)	k (cm²)	n (v_v/v_T)
							[% change from previous]			*[% change from previous]*		
Federal Fine #1	Pump	15 cm Fe^{2+}/S^{2-}	80	0.04	1E-08	0.39	- *[-]*	0E+00 *[-100]*	- *[-]*	- *[-]*	- *[-]*	- *[-]*
Federal Fine #2	Pump	60 cm Fe^{2+}/S^{2-}	80	0.08	7E-09	0.39	0.11 *[+39.6]*	7E-09 *[0]*	0.38 *[-0.05]*	- *[-]*	- *[-]*	- *[-]*
Federal Fine #3	Pump	15 cm Fe^{2+}/S^{2-}	25	0.29	9E-08	0.40	0.21 *[-26.9]*	4E-09 *[-95.8]*	0.39 *[-2.04]*	- *[-]*	- *[-]*	- *[-]*
Federal Fine #4	Pump	15 cm Fe^{2+}/S^{2-}	25	0.13	4E-08	0.39	0.48 *[+270.2]*	4E-08 *[-6.9]*	0.31 *[-19.2]*	- *[-]*	- *[-]*	- *[-]*
Federal Fine #5	Pump	15 cm Fe^{2+}/S^{2-}	25	0.24	4E-08	0.39	0.75 *[+212.5]*	3E-08 *[-6.5]*	0.33 *[-15.9]*	0.24 *[-68.0]*	5E-08 *[+47.9]*	0.40 *[+21.2]*
Federal Fine #6	Head	15 cm Fe^{2+}/S^{2-}	350	0.05	5E-08	0.38	0.08 *[+52.1]*	2E-08 *[-52.7]*	0.38 *[-1.91]*	- *[-]*	- *[-]*	- *[-]*
Appling #1	Pump	15 cm S^{2-}	25	0.13	6E-10	0.43	- *[-]*	2E-10 *[-57.5]*	- *[-]*	- *[-]*	- *[-]*	- *[-]*
Appling #2	Pump	15 cm $Fe^{2+}/S^{2-}/O_2$	70	0.06	1E-09	0.49	0.06 *[+8.6]*	1E-09 *[0]*	0.48 *-2.78*	- *[-]*	6E-10 *[-57.6]*	- *[-]*
Appling #3	Head	15 cm Fe^{2+}/S^{2-}	300	0.18	5E-09	0.43	0.26 *[+49.1]*	2E-09 *[-60.9]*	0.40 *[-7.52]*	- *[-]*	- *[-]*	- *[-]*
Webster #1	Head	15 cm $Fe^{2+}/S^{2-}/O_2$	250	0.21	1E-08	0.58	0.21 *[0]*	7E-09 *[-46.1]*	0.56 *[-2.97]*	0.15 *[-28.6]*	2E-09 *[-76.3]*	0.57 *[+0.26]*
Webster #2	Head	15 cm S^{2-}/O_2	240	0.29	1E-08	0.57	0.25 *[-13.6]*	3E-09 *[-74.8]*	0.54 *[-4.72]*	0.15 *[-41.0]*	2E-09 *[-50.4]*	0.54 *[-0.61]*
Groveland	Pump	15 cm $Fe^{2+}/S^{2-}/O_2$	90	0.15	8E-10	0.42	- *[-]*	- *[-]*	- *[-]*	0.23 *[+58.5]*	7E-10 *[-14.6]*	0.42 *[-0.88]*

3.2.4. Effects of FeS Precipitation on Hydraulic Properties in an Abiotic Aquifer Cell

An aquifer cell experiment (Figure 3.2.20) was performed to extend the results obtained from 1-D column studies (Sections 3.2.1, 3.2.2 and 3.2.3) to a larger-scale, multi-dimensional, heterogeneous system that is more representative of a natural aquifer formation.

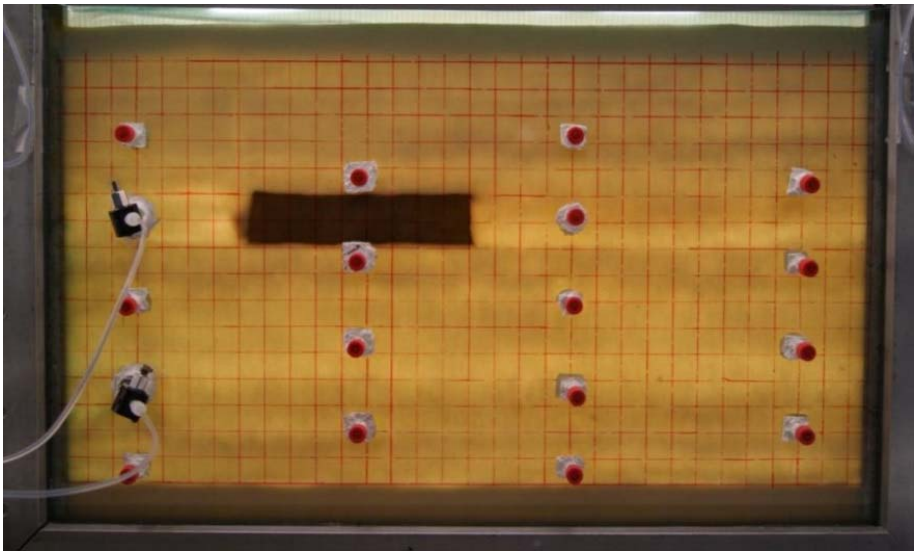

Figure 3.2.20. Picture of the aquifer cell packed with Federal Fine Ottawa sand and a rectangular lens of Appling soil (dark region) prior to introduction of iron (II) and high sulfide solution.

The first tracer test verified that there were no areas of preferential flow within the background medium of the aquifer cell (40-50 mesh Ottawa sand, lighter region) prior to the introduction of iron (II) and high sulfide solution (Figure 3.2.21). However, the tracer front (blue dye) showed that the tracer solution preferentially flowed around the Appling soil lens (darker region), consistent with its 50% lower permeability relative to the background Federal Fine Ottawa sand.

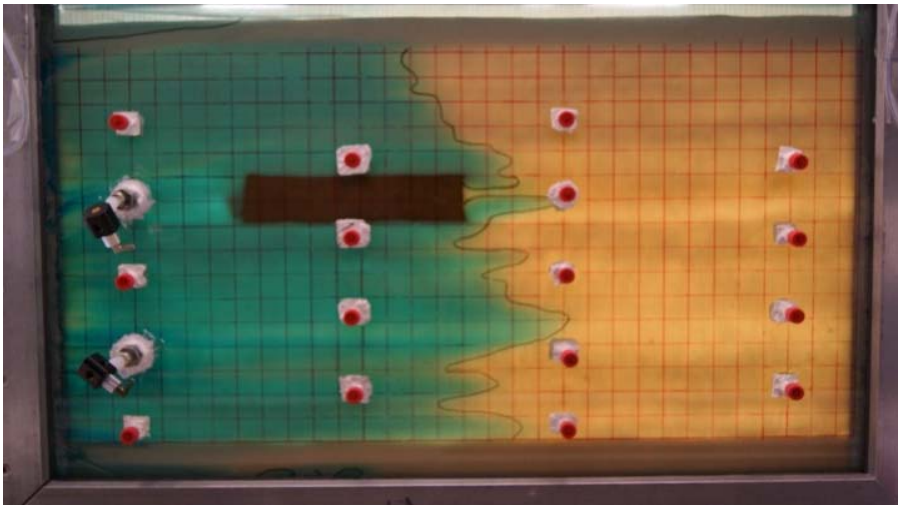

Figure 3.2.21. Initial tracer test (blue dye) conducted in the aquifer cell demonstrating preferential flow around the low permeability lens of Appling soil (dark region).

After introducing the high concentration sulfide medium (70 mg/L sulfide) through two injection ports on the left-hand side of the aquifer cell, sulfide began to react with the aqueous iron (II) background influent solution, forming a black FeS precipitate (Figure 3.2.22). The FeS precipitation front initially developed in the direction of flow through the aquifer cell, in agreement with the tracer test results; however, the precipitation front down-gradient from the upper injection port bypassed the low permeability Appling soil lens. As anticipated, the FeS precipitation front down-gradient from the lower injection port developed without any deviation in flow path (Figure 3.2.22).

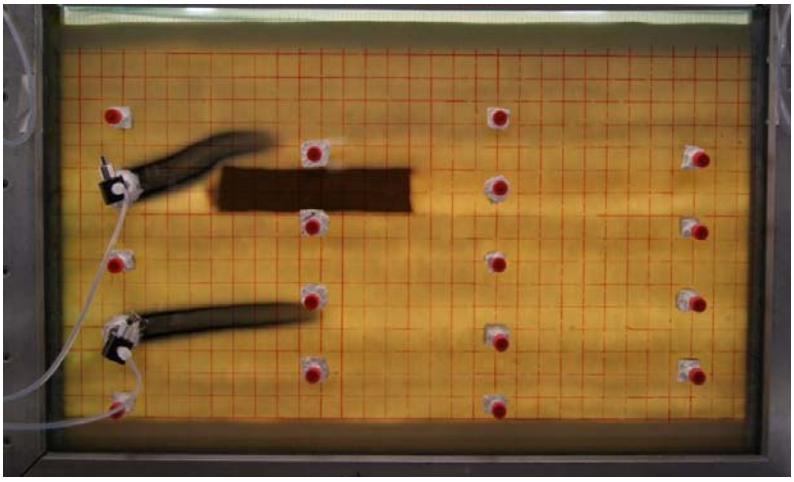

Figure 3.2.22. Picture of the aquifer cell showing visual evidence of FeS precipitation following the introduction of the high concentration sulfide medium (70 mg/L sulfide).

As the high sulfide medium injection continued, the formation of FeS precipitate caused reductions in permeability, which resulted in preferential flow beneath the Appling lens over time (Figure 3.2.23). In addition, the FeS precipitation front gradually expanded (i.e., lighter gray zones) to avoid the lower permeability zones (darker black zones). In the absence of an Appling soil lens, a narrower FeS precipitation zone formed, but still resulted in an expansion of the FeS precipitation front near the injection port over time (Figure 3.2.23).

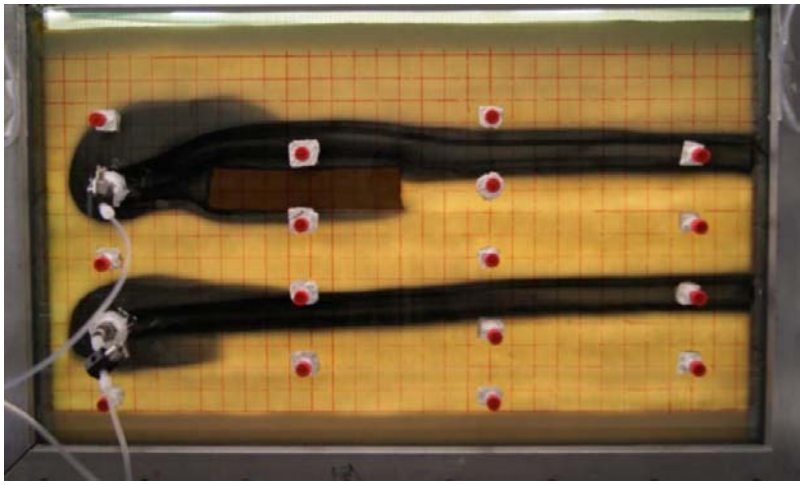

Figure 3.2.23. Picture of aquifer cell showing the FeS precipitation and preferential flow beneath the Appling lens, and expansion of the precipitation front at the injection ports.

Flow through the aquifer cell following FeS precipitation was variable and difficult to control, which was indicative of changes in the hydraulic conductivity within the cell. However, the clearly visible shift in flow paths following FeS precipitation clearly demonstrates that FeS precipitation can cause the development of preferential flow paths and zones of hydraulic isolation within the heterogeneous flow field. Furthermore, subsequent tracer tests revealed that the FeS precipitation caused a 1.5% decrease in aqueous porosity, and that the introduction of oxygenated water caused a further decrease in porosity of 2.2% (Figure 3.2.24), consistent with the results obtained from the 1-D column experiments completed under Sections 3.2.1, 3.2.2, and 3.2.3.

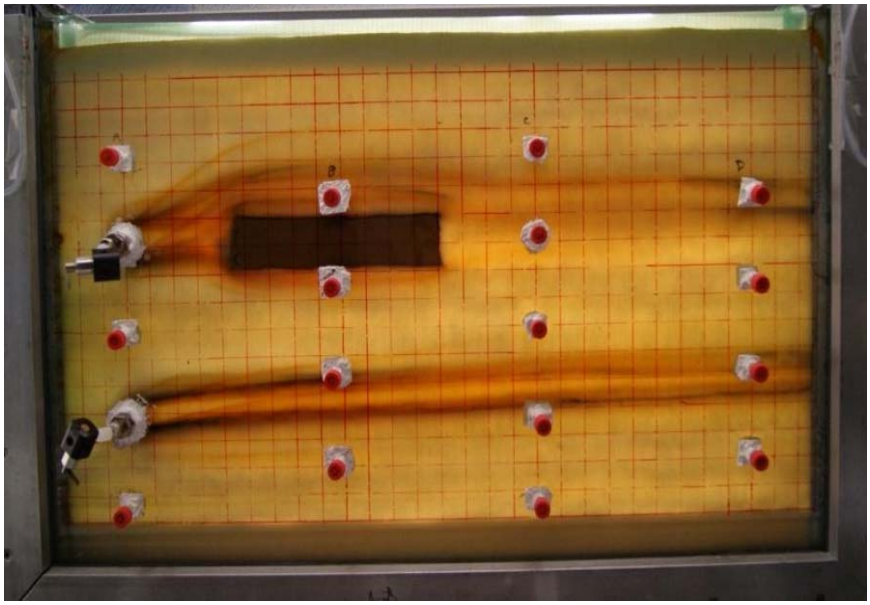

Figure 3.2.24. Picture of aquifer cell following the introduction of oxygenated medium (6-7 mg/L DO) for 30 PV.

Although fluctuations in the hydrogeology of a site are to be expected, especially when remediation takes place over the course of months or years, unanticipated changes in flow conditions could impact the efficacy of *in situ* treatment technologies. The experimental results presented in Sections 3.2.1, 3.2.2 and 3.2.3 demonstrate that iron (II) sulfide precipitation can cause changes to the hydrogeology of a porous medium when iron (II) and sulfide react to form insoluble FeS precipitates. In a heterogeneous, multi-dimensional aquifer cell, preferential flow paths were evident following FeS precipitation. Site managers and practicing environmental remediation engineers should incorporate strategies to address potential reductions in soil permeability and the creation of preferential flow paths in order to minimize negative impacts on remedial performance and the successful implementation long-term site management strategies.

3.2.5. Sulfide Tolerance of a PCE-to-Ethene Dechlorinating Consortium

A set of biotic batch reactors was used to determine the concentration of sulfide that decreased or inhibited PCE to ethene dechlorination activity of the BDI-SZ consortium. Reactors were

prepared in triplicate sets at the concentrations of 0.4, 1, 5, 8, 12, and 20 mM sulfide in defined DCB-1 mineral salts medium with 5mM lactate and 5mM acetate provided as fermentable electron donor sources and carbon sources, respectively. Actively dechlorinating BDI-SZ culture was then introduced (5% by volume). A seventh triplicate set of sterile 0.4 mM sulfide in medium was prepared as abiotic control to account for any abiotic PCE loss.

To evaluate the extent to which sequential degradation of PCE was occurring, the chlorine number metric (Leeson et al. 2004) was used as a means of comparison of dechlorination performance in reactors. The chlorine number was plotted versus time to compare the activity of BDI-SZ as a function of sulfide concentration (Figure 3.2.25). The chlorine number is calculated as:

$$\text{Chlorine \#} = \frac{4[\text{PCE}] + 3[\text{TCE}] + 2[\text{DCE}] + [\text{VC}]}{[\text{PCE}] + [\text{TCE}] + [\text{DCE}] + [\text{VC}] + [\text{ethene}] + [\text{ethane}] + [\text{acetylene}]} \qquad [3.2.2]$$

where "[ ]" denotes the concentration of the compound in mM. PCE has 4 chlorines; therefore, a chlorine number of four signifies that no dechlorination has occurred. Likewise, TCE has three chlorines, cis-DCE has two chlorines, and VC has one chlorine. The lower the chlorine number, the more degradation that has occurred within the batch reactor. Error bars were used to mark the standard error (standard deviation/ number of samples) in chlorine number for each triplicate set of reactors.

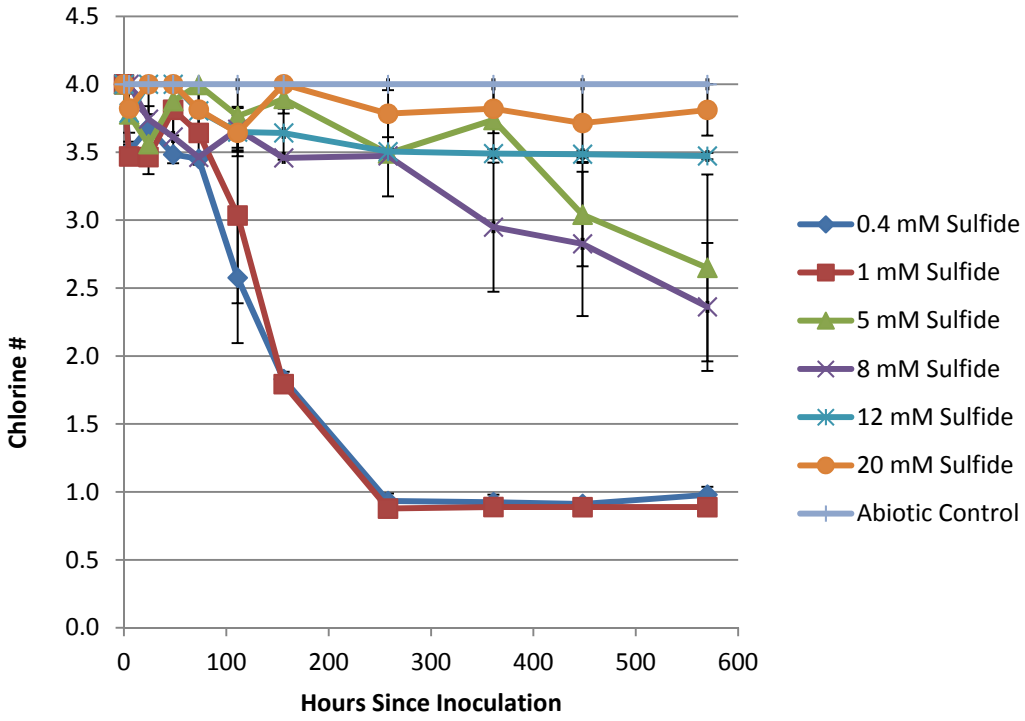

Figure 3.2.25. Activity of BDI-SZ in varying sulfide concentrations. Chlorine # is used as a measure of activity, as it is a metric for assessing how much degradation has occurred within each reactor. The lower the chlorine #, the more degradation of PCE has occurred.

Reactors with 0.4mM and 1 mM sulfide nearly mirrored each other in terms of extent and rates (-0.003 $days^{-1}$ for PCE transformation) of dechlorination over the 600 hours (25 days) of monitoring (Figure 3.2.26), indicating BDI-SZ dechlorination activity was not negatively impacted by sulfide concentrations up to 1 mM. This is consistent with prior observations with *Dehalococcoides mccartyi* strain FL2 (He et al. 2005). However, incomplete dechlorination to ethene was evident above 1mM sulfide, and PCE remained in the reactor prepared with 5 mM sulfide throughout the experimental monitoring period with cis-DCE and VC being the primary degradation products. In Figure 3.2.27, the chlorine numbers of the 5 and 8 mM sulfide reactors appear stagnant before the 448 hr sample and 378 hr sample, respectively. This delay in dechlorination activity indicates the sulfide may have impeded the initial dechlorinating efforts of BDI-SZ, but after an acclimation period, the cultures were able to dechlorinate to PCE to cis-DCE and VC. An alternate explanation is that sulfide impeded the fermentation of lactate and acetate (the provided electron donor sources) and delayed production of hydrogen, the required electron donor for *Dehalococcoides mccartyi*. The large standard error associated with each measurement in both systems indicate the kinetics of the 5 and 8 mM sulfide reactors were more variable, and more time may be required for clear trends to appear (Figure 3.2.27).

As can be seen from the small changes in chlorine number in Figure 3.2.25, and the lack of formation of any daughter products (see Figure 3.2.28), no dechlorination activity was detected in the reactors containing 12 mM sulfide and 20 mM sulfide during the 25 day monitoring period. While the 12mM and 20mM sulfide reactor sets reactors contained vinyl chloride, this was likely added with the inoculum. The concentrations of volatile organic carbon (VOC) compounds in the inoculum revealed no PCE, TCE, or *c*-DCE, but 0.455 mM VC, and 0.134 mM ethene. Thus, 0.023 mM VC and 0.007 mM ethene were introduced with the inoculum. The measured values of 0.015 mM VC in the 12 and 20 mM sulfide reactors can thus be explained by carry over from the inoculum. The maximum concentration of VC for all other reactors at the start of the experiment was 0.024 mM, which is within 5% of the VC concentration introduced with the inoculum. Additionally, ethene concentrations added to the batch reactors were more than an order of magnitude less than the VC concentrations and no ethene was detected in the initial GC analysis after inoculation.

As in other instances of perturbation (See section 3.3) and non-ideal growth conditions for *Dhc*, the final VC to ethene dechlorination step carried out by *Dhc* strains harboring the *bvcA* and *vcrA* genes is often incomplete, leading to the formation of VC (Ritalahti et al. 2006b). In contrast, *Dhc* harboring the *tceA* gene (TCE to VC) and *Geobacter lovleyi* strain SZ (PCE to cis-DCE and also a component of the BDI-SZ consortium) are more resilient to elevated temperatures (as observed in Section 3.1.4) or low pH (as described in Section 3.3). Exposure to sulfide was no exception, with cis-DCE formation likely carried out by *Geobacter* and transformation to VC carried out by *Dhc* strain FL2 harboring the *tceA* gene. Similarly, studies by Berggren et al. (2013) also suggested that different *Dhc* strains have different tolerances of sulfide concentrations. However, work done by He et al. (2005) showed complete halt of dechlorination activity by pure strain FL2 at 5 mM sulfide. The findings of the work presented here reinforce the benefits of *Dhc* being a component of a more robust consortium rather than a pure strain in terms of activity and tolerance to elevated concentrations of not just sulfide, but surfactants (Amos et al. 2007b) and other biogeochemical perturbations. Determining the maximum tolerable sulfide concentration not affecting chlorinated ethene-dechlorinating consortia is relevant to practitioners working at sites containing high sulfate concentrations. From the batch reactors discussed in this section, the

maximum level of sulfide, at which BDI-SZ still demonstrates at least partial dechlorination of chlorinated ethenes, lies between 8 and 12 mM sulfide.

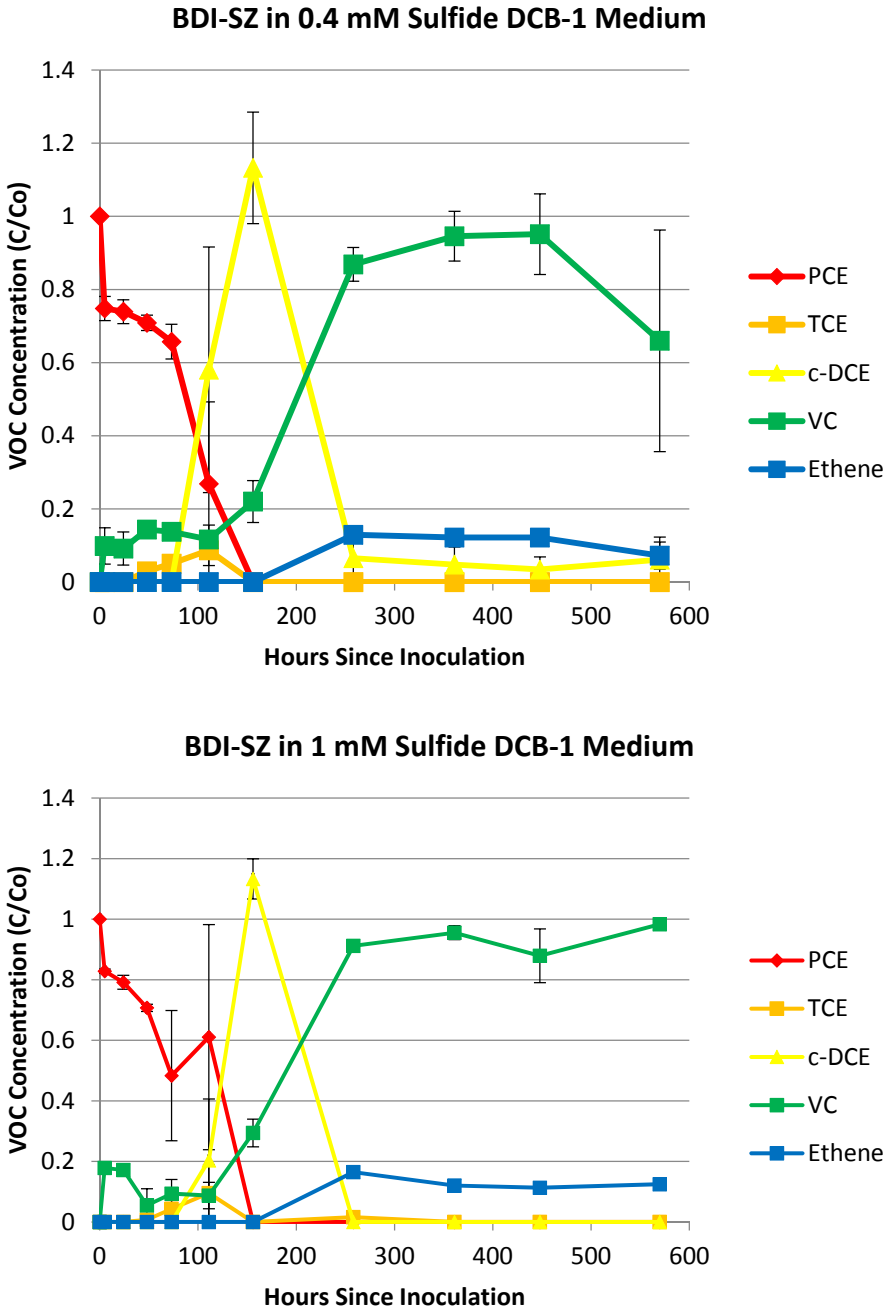

Figure 3.2.26. Comparison of BDI-SZ PCE dechlorination in batch reactors prepared with 0.4 mM and 1 mM sulfide. All results were normalized to their initial PCE concentration (mM) and then averaged across the triplicate reactors.

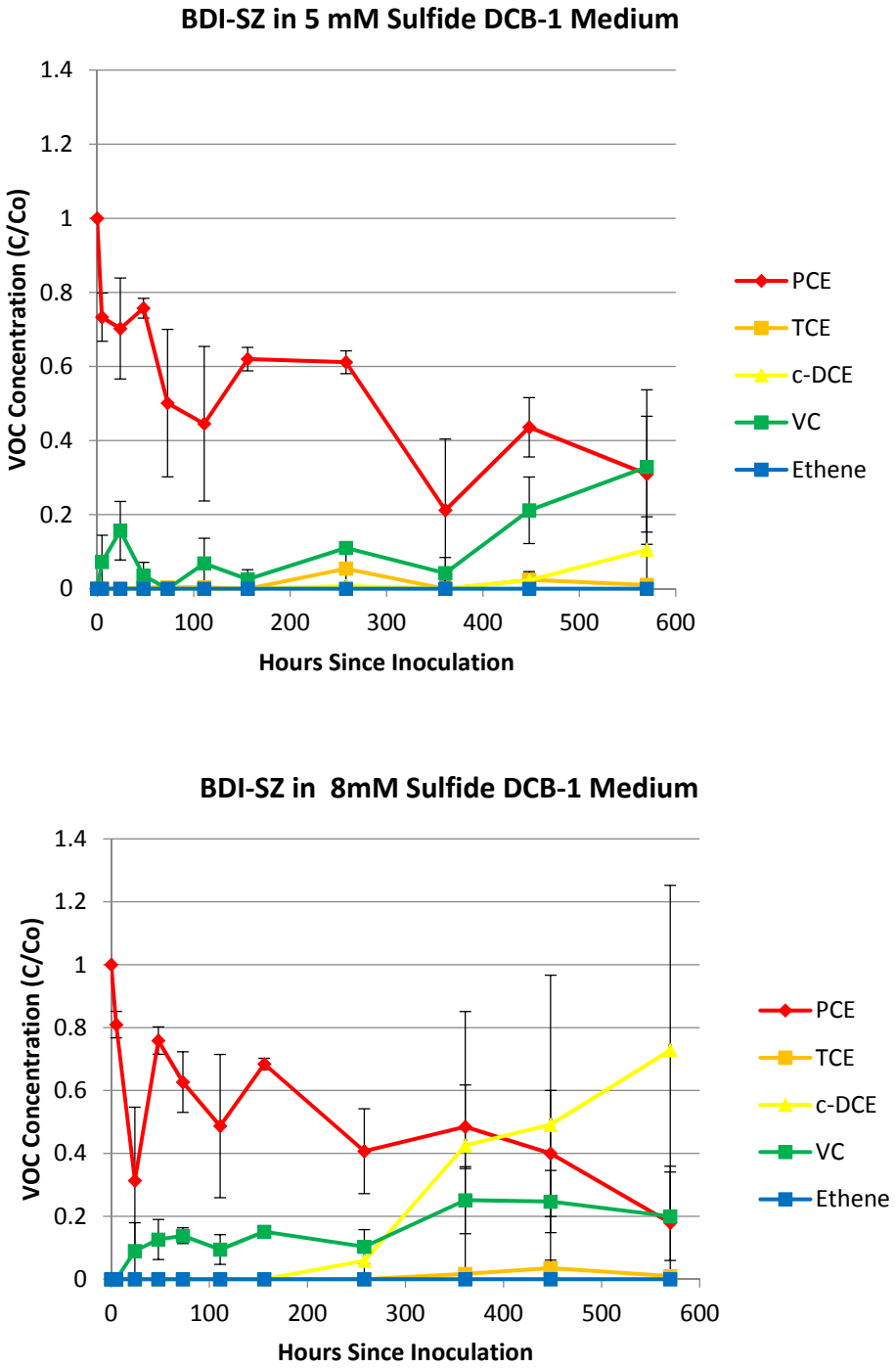

Figure 3.2.27. Comparison of BDI-SZ PCE dechlorination in batch reactors prepared with 5 mM and 8 mM sulfide. All results were normalized to their initial PCE concentration (mM) and then averaged across the triplicate reactors.

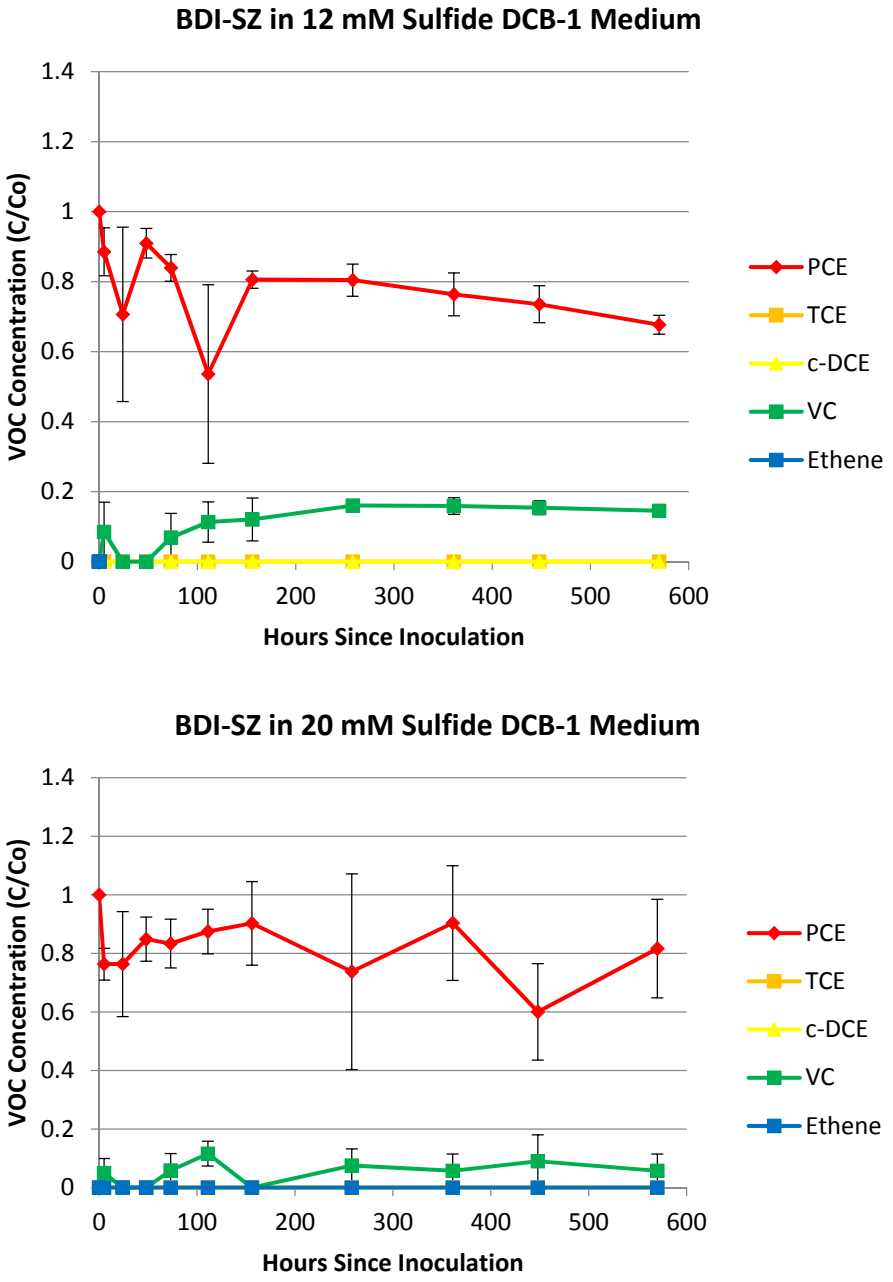

Figure 3.2.28. Comparison of BDI-SZ PCE dechlorination in batch reactors prepared with 12 mM and 20 mM sulfide. All results were normalized to their initial PCE concentration (mM) and then averaged across the triplicate reactors.

3.3. Impacts of Remedial Strategies on Groundwater pH and Microbial Reductive Dechlorination Performance (Task 3)

3.3.1. Batch reactor studies to examine pH tolerance of existing cultures

To determine the lower pH limits for available PCE-dechlorinating isolates and the *Dhc*-containing consortium BDI, a series of batch reactor experiments were conducted in defined mineral salts medium with pH values adjusted to 5.5, 6.5 and 7.2. All cultures showed the expected dechlorination activities in pH 7.2 medium, but the organisms showed variable responses to lower pH conditions. Both *Desulfitobacterium* sp. strain Viet1 (PCE→TCE) and *Desulfitobacterium* sp. strain JH1 (PCE→*c*DCE) showed no dechlorination activity in pH 6.0 medium. In contrast, *Desulfuromonas michiganensis* strain BB1, *Geobacter lovleyi* strain SZ, and *Sulfurospirillum multivorans* sustained PCE→*c*DCE dechlorination at pH 6.0; however, both strain BB1 and strain SZ cultures showed no reductive dechlorination activity in pH 5.5 medium. Among the cultures included in the screening, only *Sulfurospirillum multivorans* dechlorinated PCE to *c*DCE at pH 5.5. Consortium Bio-Dechlor INOCULUM (BDI) (PCE→ethene) produced ethene at pH 7.2, but *c*DCE and VC were the major dechlorination products at pH 6.0, and dechlorination was not sustained at pH 5.5. Of note, some residual reductive dechlorination activity was observed in low pH medium following the inoculation of culture suspension derived from actively dechlorinating cultures grown in pH 7.2 medium. All initial cultures were transferred to medium with the same pH to judge if the observed reductive dechlorination activity was lost or maintained upon repeated transfers in low pH medium. Limited PCE reductive dechlorination observed in the initial low pH transfer cultures, but not in 2nd generation transfer cultures prepared in the same medium, was attributed to residual activity of the pH 7.2-grown biomass introduced with the inoculum to low pH medium culture vessels. Sustained reductive dechlorination activity under low pH conditions in subsequent transfer cultures indicated growth of the dechlorinator(s). Table 3.3.1 lists the dechlorination end product(s) in cultures maintained under different pH conditions over at least two subsequent transfers.

Table 3.3.1. Sustained PCE reductive dechlorination activity of isolates and consortium BDI at different pH values. Shown are the major dechlorination end products, which were also generated in transfer cultures at the respective pH values.

Culture	pH 5.5	pH 6.0	pH 7.2
Consortium BDI	-	*c*DCE, VC	Ethene
Geobacter lovleyi SZ	-	*c*DCE	*c*DCE
Desulfuromonas michiganensis BB1	-	*c*DCE	*c*DCE
Sulfurospirillum multivorans	*c*DCE	*c*DCE	*c*DCE
Desulfitobacterium sp. JH1	-	-	*c*DCE
Desulfitobacterium sp. Viet1	-	-	TCE

A dash "–" indicates that no dechlorination was observed within the 50-day monitoring period

Sulfurospirillum multivorans was originally reported to grow between pH 7 and 7.5 (Scholz-Muramatsu et al. 1995) but our efforts demonstrated that the organism dechlorinated PCE to *c*DCE at pH 5.5 (Table 3.3.2). Following transfer of a *Sulfurospirillum multivorans* culture to vessels with pH 5.5, 6.0 and 7.2 medium, PCE was rapidly dechlorinated to *c*DCE (Table 3.3.2).

Table 3.3.2. PCE dechlorination by *Sulfurospirillum multivorans* in pH 5.5, 6.0 and 7.2 medium that received an inoculum from a pH 7.2-grown culture. All incubations were conducted in triplicates.

pH	Days	PCE (µmol/bottle)	*c*DCE (µmol/bottle)
pH 5.5	Day 1	31.6 ± 4.3	0
	Day 4	0	25 ± 1.3
pH 6.0	Day 1	30.1 ± 4.0	0
	Day 4	0	27.3 ± 2.1
pH 7.2	Day 1	29.9 ± 7.3	0
	Day 4	0	29.2 ± 1.6

PCE to *c*DCE dechlorination was sustained in pH 5.5 transfer cultures although the time period required for complete PCE dechlorination to *c*DCE increased compared to cultures maintained at pH 7.2. An apparent difference between pH 7.2 and pH 5.5 *Sulfurospirillum multivorans* cultures is the lag phase before PCE dechlorination commenced following a 3% (vol/vol) inoculum transfer from a culture maintained under the same growth conditions. At pH 5.5, the lag time before the onset of PCE dechlorination extended up to 10 days (Figure 3.3.1), whereas at pH 7.2, PCE dechlorination started within 2 days of inoculation. Importantly, PCE to *c*DCE reductive dechlorination was sustained at pH 5.5.

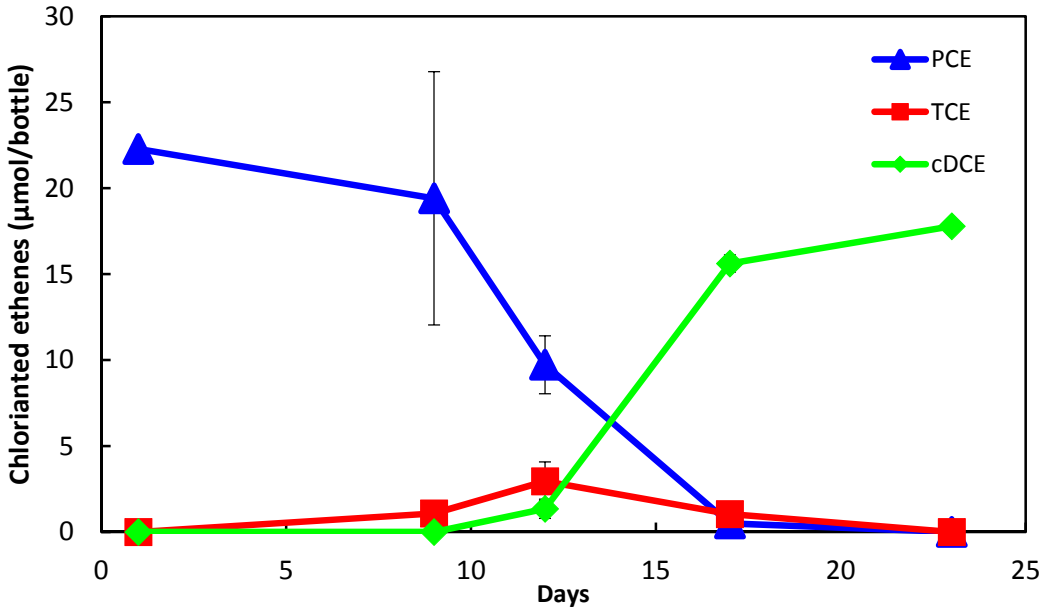

Figure 3.3.1. PCE degradation by *Sulfurospirillum multivorans* at pH 5.5 following repeated transfers in pH 5.5 medium. Error bars represent one standard deviation below or above the average of triplicate samples. PCE, blue triangles; TCE, red squares; *c*DCE, green diamonds.

3.3.2. pH effects on the PCE-to-ethene dechlorinating consortium BDI

3.3.2.a. *Dhc* growth at pH 5.5 and pH 7.2

The PCE-to-ethene dechlorinating consortium BDI contains multiple *Dhc* strains carrying different RDase genes, including *tceA*, *bvcA* and *vcrA*. Batch culture studies were performed to evaluate the responses of *Dhc* strains carrying the different RDase genes to incubation in pH 5.5 versus pH 7.2 medium. qPCR was applied to monitor the total *Dhc* abundance by measuring the *Dhc* 16S rRNA gene, and the enumeration of the *tceA*, *bvcA* and *vcrA* RDase genes informed about the abundances of different *Dhc* strains. In pH 5.5 medium inoculated with BDI, PCE was not degraded, and the *Dhc* cell numbers did not increase. By comparison, about 75% of the initial amount of PCE was dechlorinated to ethene in pH 7.2 incubations over a 2-week incubation period, and qPCR demonstrated *Dhc* growth (Figure 3.3.2). The *Dhc* 16S rRNA gene copies increased from $1.55 \pm 0.42 \times 10^8$ mL^{-1} (cells introduced with the inoculum) to $6.99 \pm 1.99 \times 10^8$ mL^{-1}. The *vcrA* and *tceA* genes increased from $1.57 \pm 0.09 \times 10^8$ and $1.29 \pm 0.11 \times 10^8$ mL^{-1} to $4.92 \pm 1.79 \times 10^8$ and $2.31 \pm 0.47 \times 10^8$ mL^{-1}, respectively. *Dhc* Strain BAV1 carrying the *bvcA* gene is part of consortium BDI but this strain is not competitive in cultures fed with PCE and was consequently not detected, which was also reported in a previous publication (Amos et al. 2008a).

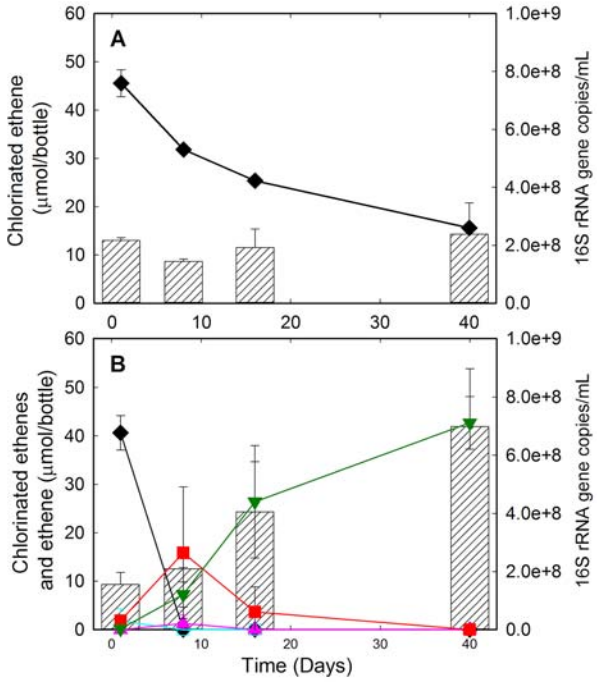

Figure 3.3.2. PCE dechlorination at pH 5.5 (panel A) and 7.2 (panel B) by the PCE-to-ethene-dechlorinating consortium BDI containing multiple *Dhc* strains over a 40-day incubation period. No dechlorination activity and no *Dhc* growth occurred at pH 5.5 (panel A). The apparent PCE decrease at pH 5.5 was due to abiotic loss (e.g., sorption to the rubber stoppers). At pH 7.2, PCE was degraded to ethene and *Dhc* growth was observed as determined by qPCR (panel B). (Solid black diamonds-PCE, open cyan squares-TCE, solid pink triangles-*c*DCE, solid red squares-VC, solid green inverted triangles-ethene, shaded bars-*Dhc* 16S rRNA gene copy numbers).

These results demonstrate that no *Dhc* growth occurred in pH 5.5 medium. Depending on the size of the inoculum (i.e., the number of cells transferred to fresh medium), some limited PCE dechlorination was observed at high inoculation density. However, *Dhc* growth was never observed in pH 5.5 medium and no PCE dechlorination activity occurred in pH 5.5 transfer cultures. The limited reductive dechlorination activity in some 1st generation pH 5.5 transfer cultures was attributed to dechlorinators that maintained residual activity but cell division and growth did not occur. This is a relevant observation and emphasizes that reports of reductive dechlorination following bioaugmentation at low pH sites must be carefully interpreted, because the activity may not be sustained, unless pH adjustment is implemented.

3.3.2.b. Tolerance and resilience of the PCE-to-ethene dechlorinating consortium BDI to pH changes

To explore the effects of low pH exposure on *Dhc* growth and reductive dechlorination performance, consortium BDI biomass generated in pH 7.2 medium was collected by centrifugation, suspended in pH 5.5 medium, and then exposed to pH 5.5 for 8, 16, and 40 days. A schematic overview of the experimental approach is depicted in Figure 3.3.3.

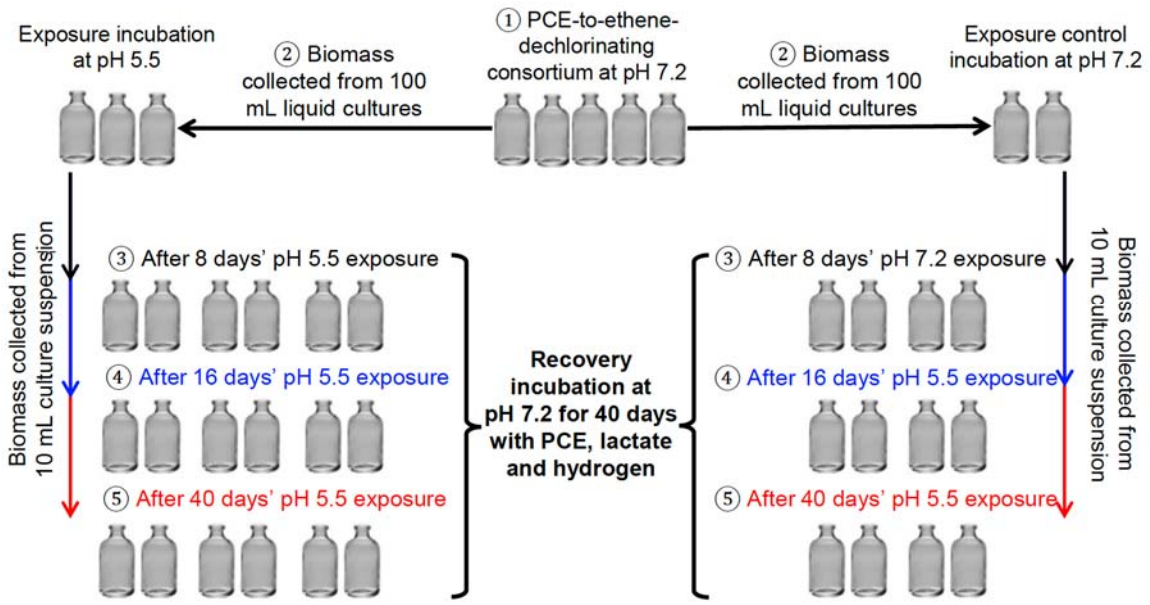

Figure 3.3.3. Experimental scheme to test the recovery of a PCE-to-ethene dechlorinating bacterial consortium BDI exposed to pH 5.5 stress, with the pH 7.2 incubation set serving as the control group.

Consortium BDI biomass exposed to pH 5.5 for 8 days recovered dechlorination activity following transfer to pH 7.2, and PCE was dechlorinated to VC and some ethene (about 10% of initial PCE amount) within the 40-day pH 7.2 recovery period (Figure 3.3.4 A,B). qPCR analysis demonstrated that the 16S rRNA, *tceA* and *vcrA* genes increased 39.2 ± 9.6-, 50.9 ± 8.9- and 14.2 ±7.4-fold, respectively, within this 40-day recovery period at pH 7.2 following the 8-day exposure to pH 5.5 (Figure 3.3.5). PCE-to-VC dechlorination was also observed in pH 7.2 recovery experiments with consortium BDI biomass that experienced a 16-day exposure to pH 5.5 (Figure 3.3.4 C), and the *Dhc* 16S rRNA, *tceA* and *vcrA* genes increased 11.5 ±3.9-, 41.3 ± 15.6- and 6.3 ± 2.5-fold, respectively, within the 40-day pH 7.2 recovery period (Figure 3.3.5). Following a 40-day exposure to pH 5.5, the consortium degraded PCE to *c*DCE and small amounts of VC (about 6.2% of initial PCE amount) within the 40-day pH 7.2 recovery period (Figure 3.3.4 E), and the *Dhc* 16S rRNA, *tceA* and *vcrA* genes increased 6.0 ± 3.8-, 11.6 ± 8.8- and 2.5 ± 1.1-fold (Figure 3.3.5).

Statistical analysis performed on average fold increases of 16S rRNA, *tceA* and *vcrA* genes indicated no differences in terms of *Dhc* growth upon transfer to pH 7.2 medium between the pH 5.5 and pH 7.2 (control group) after an 8-day exposure period (16S rRNA gene: p-value = 0.211; *tceA* gene: p-value = 0.567; *vcrA* gene: p-value: 0.242, Table 3.3.3). Similarly, no significant difference was seen between cultures maintained at pH 5.5 versus pH 7.2 during a 16-day exposure period and transferred to pH 7.2 medium (Table 3.3.3). These findings suggest that exposure to pH 5.5 for up to 16 days had minimal impact on *Dhc* survival and recovery of dechlorination activity to VC. Conversely, *Dhc* biomarker gene fold increases between the pH 5.5 group and pH 7.2 control group after 40 days of pH 5.5 exposure were statistically significant (16S rRNA gene: *p*-value =0.014; *tceA* gene: *p*-value = 0.034; *vcrA* gene: *p*-value: 0.000, Table 3.3.3).

Table 3.3.3. Average fold increase of *Dhc* biomarker genes in pH 5.5 and pH 7.2 batch reactor incubations. Asterisks (*) denote statically significant values.

Genes	Exposure Time (Days)	Average Fold Increase		*p*-Value of t-Test
		pH 5.5 (n=6)	pH 7.2 (n=4)	
Dhc 16S rRNA	8	39.2	76.2	0.211
	16	11.5	29.9	0.304
	40	6.0	38.0	0.014*
tceA	8	50.9	70.2	0.567
	16	41.3	32.8	0.743
	40	11.6	58.7	0.034*
vcrA	8	14.2	41.7	0.242
	16	6.3	33.1	0.174
	40	2.6	28.7	0.000*

These data indicate that the longer 40-day exposure period significantly affected the recovery of *Dhc* from low pH stress. The VC-to-ethene dechlorination step was most strongly inhibited, and only the cultures initiated with biomass exposed to pH 5.5 for 8 days produced some ethene (about 10% of the initial PCE amount) within the 40-day pH 7.2 recovery period (Figure 3.3.4 A). In contrast, the pH 7.2 control cultures produced ethene (67% of the initial PCE amount), demonstrating that the manipulation of the biomass (e.g., centrifugation and resuspension) was not the reason for the limited reductive dechlorination activity recovered from biomass following pH 5.5 exposure (Figure 3.3.4 B,D,F).

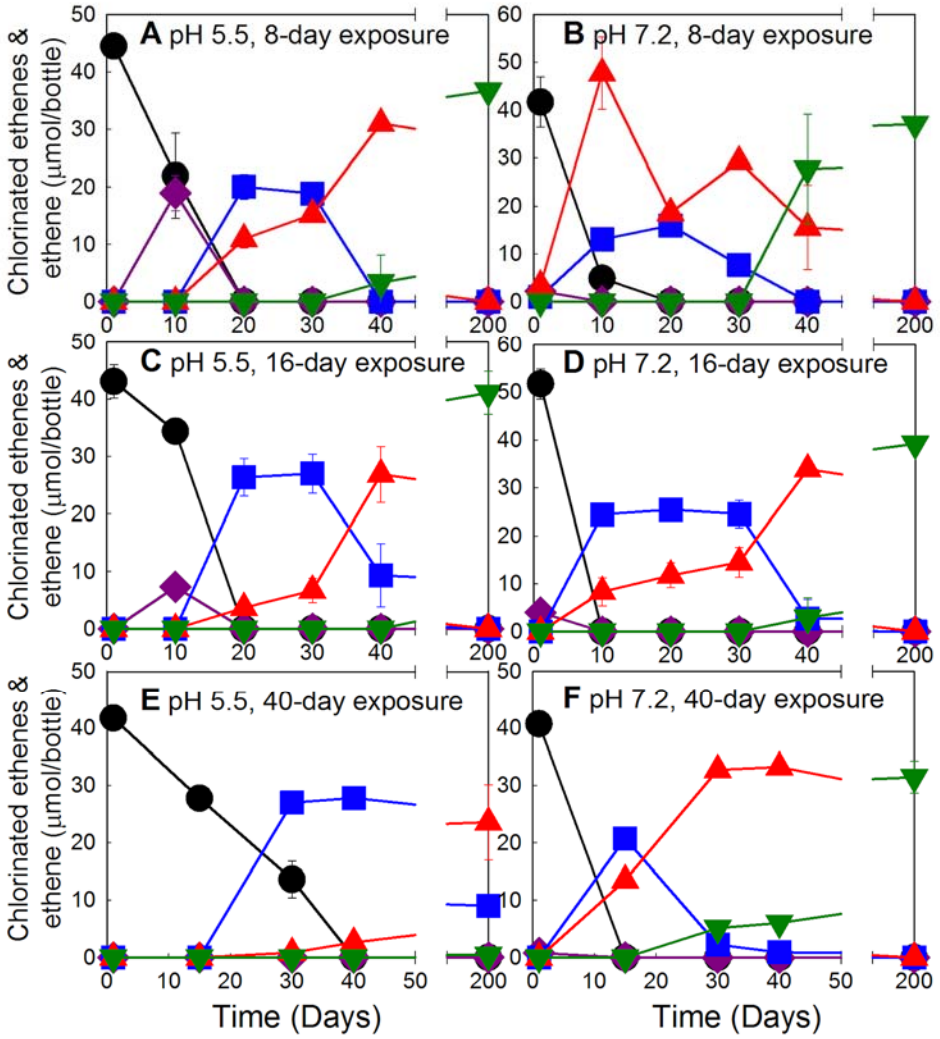

Figure 3.3.4. PCE degradation in BDI pH 7.2 transfer cultures following pH 5.5 (left column) or pH 7.2 (right column) exposure for up to 40 days. Figures 3A, 3C and 3E plot PCE degradation after 8, 16, and 40 days of pH 5.5 exposure, respectively. Figures 3B, 3D, and 3F depict the control groups after 8, 16, and 40 days pH 7.2 exposure, respectively. Final measurements were conducted on Day 200. The error bars indicate one standard deviation. Solid black circles – PCE; solid dark purple diamonds – TCE; solid blue square – *c*DCE; solid red triangle – VC; solid dark green inverted triangles – ethene.

After an extended 200-day recovery period, consortium BDI biomass from 8 and 16 days of pH 5.5 exposure regained the capability of complete degradation of all chlorinated ethenes to ethene (Figure 3.3.4 A,C); however, no ethene was produced in the cultures derived from biomass that experienced 40 days of pH 5.5 exposure (Figure 3.3.4 E). These findings indicate that the duration of exposure to low pH influences the ability of *Dhc* to recover from low pH induced stress. Further, these data reveal a *Dhc* strain-specific response, suggesting that *Dhc* strain GT carrying the VC RDase *vcrA* was more susceptible to pH stress than *Dhc* strain FL2 carrying the *tceA* gene.

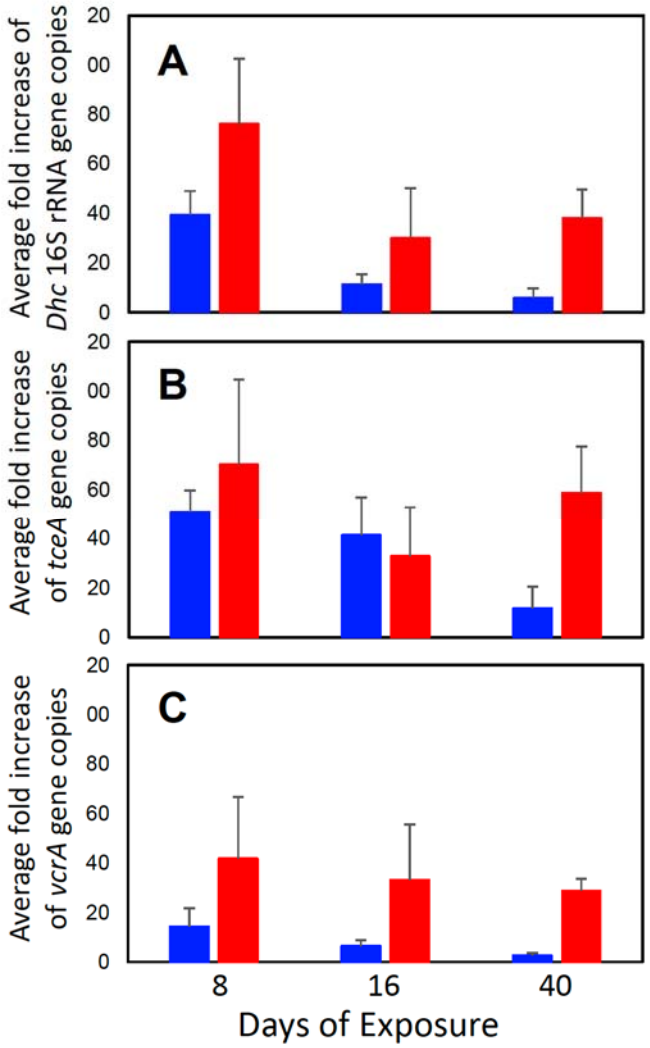

Figure 3.3.5. Average fold increase of 16S rRNA (A), *tceA* (B) and *vcrA* (C) genes measured after a 40-day incubation period in pH 7.2 transfer cultures that were prepared with biomass collected from cultures incubated for 8, 16, and 40 days at pH 5.5 (blue bars) or pH 7.2 (red bars). The error bars indicate plus one standard error (for pH 5.5 n=6; for pH 7.2 n=4).

These laboratory findings imply that the distribution and abundance of *Dhc* in aquifers with low pH groundwater should be limited, and *Dhc* would be expected to be more abundant in groundwater with circumneutral pH. To assess whether pH affects the distribution and abundance of *Dhc* at sites impacted with chlorinated ethenes, a total of 221 groundwater wells from 23 sites were investigated. These groundwater wells were chosen for the availability of both pH and microbiological data. In 50 groundwater samples, *Dhc* 16S rRNA genes were below 100 copies L^{-1}, and these data were omitted from subsequent analyses. The pH of the remaining 171 groundwater samples ranged from 4.5 to 8.3, with a median pH of 6.4. *Dhc* 16S rRNA gene copy numbers in these 171 groundwater samples ranged from 100 to 4.0×10^6 copies L^{-1}, with a median

of 6.96×10^5 copies L^{-1} (Figure 3.3.6). Since the optimal pH range for *Dhc*-containing bioaugmentation consortia is 6.0–8.3 (Löffler et al. 2013), pH values were categorized into two intervals: acidic (4.5–6.0) and circumneutral (6.0–8.3).

The survey of *Dhc* biomarker genes in wells with available groundwater pH information demonstrated that the average *Dhc* abundance in the pH range 6.0–8.3 was about 1.52-fold higher than that in the pH range 4.5–6.0, suggesting pH affected the abundance of *Dhc*. Comparison of the average *Dhc* abundance between the acidic and circumneutral pH ranges suggested a statistical difference between the average *Dhc* abundances (df [degree of freedom] = 67.4, p-value=0.009). The mean *Dhc* abundance for the acidic pH range (i.e., pH 4.5–6.0) was 7.49×10^5 gene copies L^{-1}. By comparison, the average *Dhc* abundance for the circumneutral pH range was 1.14×10^6 gene copies L^{-1}. The abundances of the RDase genes *tceA* and *vcrA* between acidic and circumneutral pH ranges followed similar patterns (i.e., higher average gene copy numbers for the circumneutral pH range), although the average *vcrA* gene copy numbers in pH 4.5–6.0 and pH 6.0–8.3 wells were 3.4- and 4.9-fold higher than the average *tceA* gene copy numbers in pH 4.5–6.0 and pH 6.0–8.3 wells, respectively (Figure 3.3.6). Statistical analysis of the average *tceA* and *vcrA* gene abundances at the two pH ranges indicated significant differences (*vcrA*: p-value=0.001; *tceA*: p-value=0.015, Table 3.3.4). The analysis of total bacterial 16S rRNA gene abundances indicated no significant differences between the 4.5–6.0 pH and the 6.0-8.3 pH categories (p-value=0.314, Table 3.3.4).

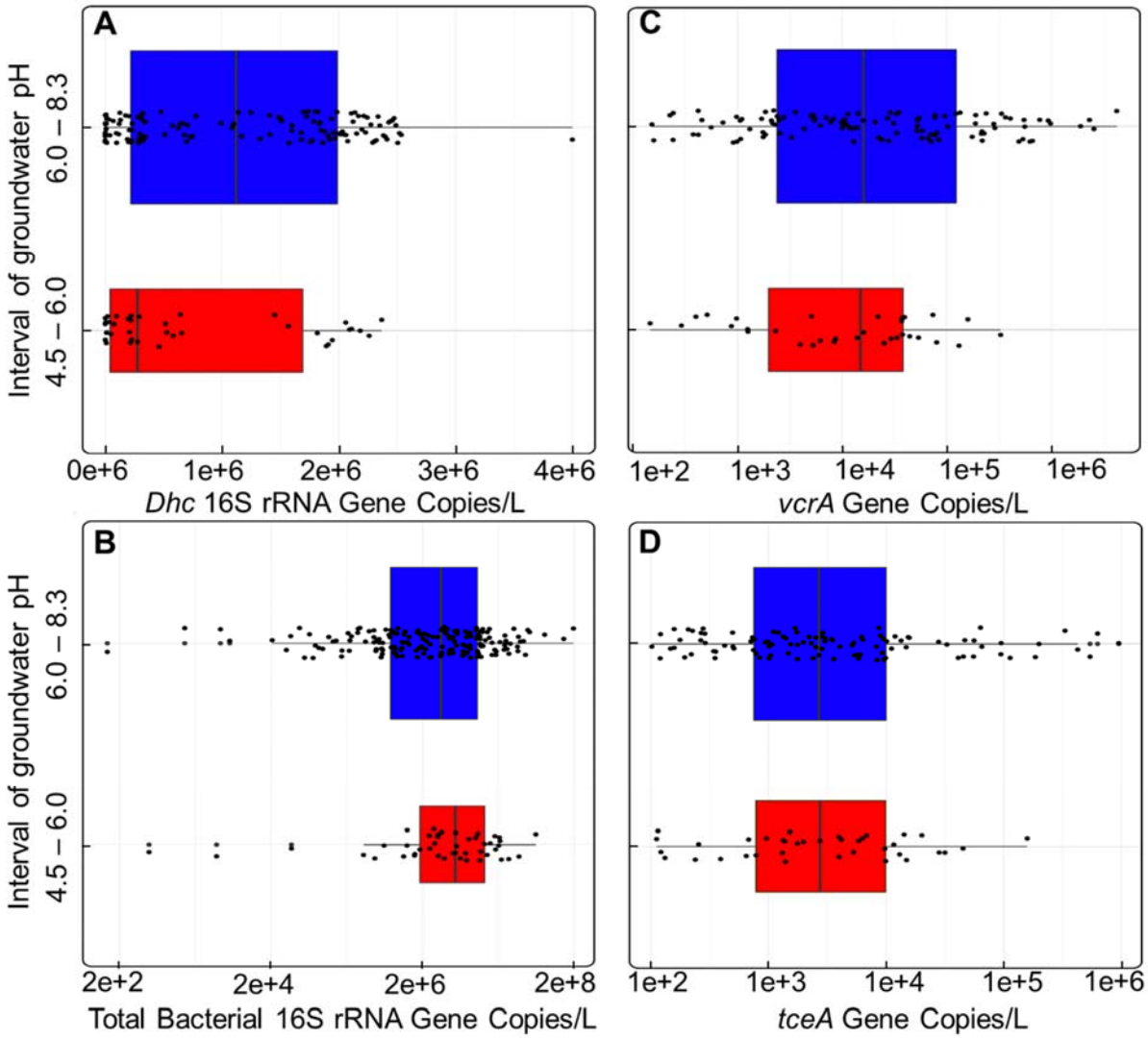

Figure 3.3.6. Distribution of *Dhc* 16S rRNA (A), total bacterial 16S rRNA (B), *vcrA* (C), and *tceA* (D) gene copy numbers from a survey of 171 groundwater wells contaminated with chlorinated ethenes. The pH 4.5–6.0 and pH 6.0–8.3 categories represent unfavorable and optimal pH ranges for the growth and activity of *Dhc*, respectively.

Table 3.3.4. One-way t-test of *Dhc* 16S rRNA, *tceA*, *vcrA* and total bacterial 16S rRNA gene abundances in groundwater collected from 171 sites with pH values ranging between 4.5 and 8.3. Samples were categorized into two pH intervals 4.5–6.0 and 6.0–8.3 based on the optimal pH range determined for *Dhc*-containing consortia (i.e., pH 6.0-8.3).

Gene	Average copies/L		t-value	df [a]	p-value
	pH 4.5–6.0	pH 6.0–8.3			
***Dhc* 16S rRNA**	7.49×10^5	1.14×10^6	-2.44	67.4	0.009**
tceA	1.11×10^4	4.15×10^4	-2.19	121.8	0.015*
vcrA	3.77×10^4	2.05×10^5	-3.04	117.2	0.001**
Total bacterial 16S rRNA	1.06×10^7	1.20×10^7	-0.49	126.1	0.314

[a] df: degree of freedom
Asterisks indicate significance levels: ** 0.01, * 0.05

3.3.3. Enrichment of Novel Dechlorinators under Low pH Conditions

3.3.3.a. Reductive dechlorination of PCE in microcosms at pH 5.5 and pH 7.2

Aquifer, sediment and soil samples were obtained from geographically distinct locations, including materials from sites impacted with chlorinated ethenes where PCE and TCE reductive dechlorination daughter products and low pH groundwater were reported (Table 3.3.5).

Table 3.3.5. List of soil, sediment, groundwater, and aquifer samples used for establishing microcosms.

#	Sample ID	Locations	Sample Type	Substrates		PCE Degradation End Product(s)	
				Electron Donor	Electron Acceptor	pH 5.5	pH 7.2
1	MW-BOS	Fort Pierce, FL, USA	Soil	Lactate + H_2	PCE	X	X
2	PNNL	Hanford, WA, USA	Soil	Lactate + H_2	PCE	X	X
3	DP	CA, USA	Soil	Lactate + H_2	PCE	X	X
4	-	Brazil	Soil	Lactate + H_2	PCE	X	X
5	Third Creek	Knoxville, TN, USA	Sediment	Lactate + H_2	PCE	Ethene	Ethene
6	Neckar River	Stuttgart, Germany	Sediment	Lactate + H_2	PCE	Ethene	Ethene
7	Trester	Rotenberg, Germany	Soil	Lactate + H_2	PCE	VC, Ethene	VC, Ethene
8	Creek	Rotenberg, Germany	Soil	Lactate + H_2	PCE	X	X
9	McGuire AFB	New Jersey, USA	Soil, GW	Lactate + H_2	PCE	X	X
10	-	USA	Soil, GW	Lactate + H_2	PCE	X	X
11	NAVFAC SE	Charleston, SC, USA	Soil, GW	Lactate + H_2	PCE	Ethene	Ethene
12	Shady Valley	TN, USA	Sediment	Lactate + H_2	PCE	*c*DCE	*c*DCE
13	Axton Cross	Holliston, MA, USA	Soil, GW	Lactate + H_2	PCE	VC	Ethene
14	-	San Diego, CA, USA	Soil	Lactate + H_2	PCE	X	X
15	Tidal Flat	Kangwha, South Korea	Tidal flat sediment	Lactate + H_2	PCE	X	TCE
16	Conrail Rail Yard	Elkhart, IN, USA	Soil, GW	Lactate + H_2	PCE	Ethene	Ethene

A minus (-) sign indicates that the contaminated site name and exact location was not disclosed.
The X indicates that no PCE dechlorination was observed. GW, groundwater

PCE to ethene reductive dechlorination was observed in microcosms established at pH 5.5 and pH 7.2 with samples collected from five sampling sites (#5, 6, 7, 11 and 16 in Table 3.3.5). Microcosms established with the soil sample from the ACS site (#13) degraded PCE to ethene at pH 7.2, but VC was the dechlorination end product at pH 5.5 (Figure 3.3.7). Microcosms established with acidic peat bog material from the Shady Valley location (#12) showed PCE to *c*DCE dechlorination at pH 5.5 and pH 7.2. The tidal flat sample (#15) degraded PCE to TCE at

pH 7.2, but not at pH 5.5. No PCE dechlorination activity was detected in the microcosms established with the other site materials tested.

Attempts to establish stable PCE-to-ethene-dechlorinating enrichment cultures in pH 5.5 medium were not successful for any of the ethene-producing microcosms. PCE dechlorination activity was lost following two consecutive transfers in pH 5.5 medium, except the ACS enrichment cultures, which maintained PCE-to-*c*DCE reductive dechlorination activity at pH 5.5 (Figure 3.3.7). By comparison, transfer cultures derived from the ethene-producing pH 7.2 ACS microcosms maintained PCE-to-ethene dechlorination activity following consecutive transfers to pH 7.2 medium (Figure 3.3.7). At pH 4.5, PCE dechlorination to *c*DCE was observed in microcosms established with materials from the ACS site, but PCE dechlorination activity could not be maintained at this pH in transfer cultures (i.e., in the absence of the solid phase).

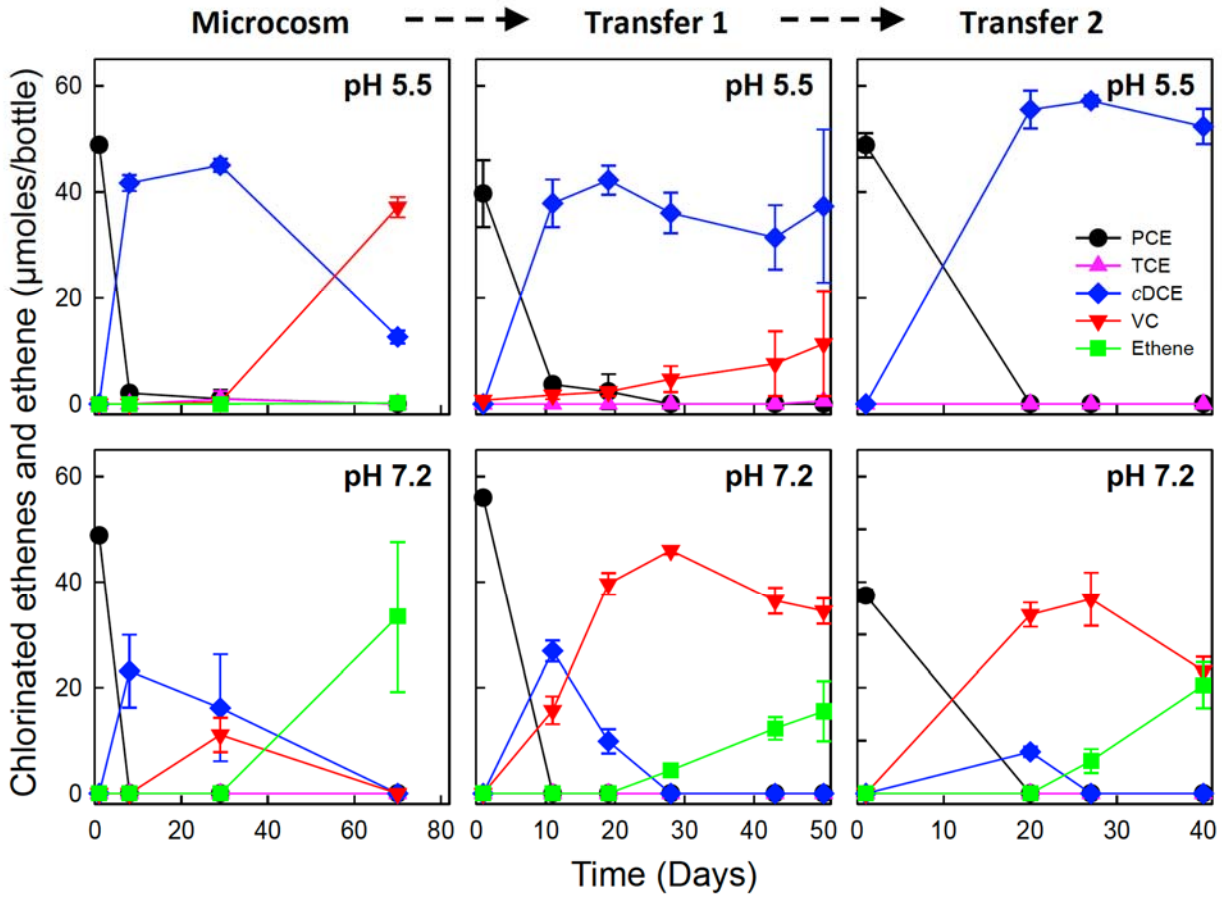

Figure 3.3.7. PCE dechlorination in ACS microcosms and 1st and 2nd generation transfer cultures at pH 5.5 (top panels) and pH 7.2 (bottom panels). The error bars represent one standard deviation below or above the average of triplicate batch cultures.

3.3.3.b Effects of pH on microbial community structure

Of all 16 samples tested, only the ACS cultures demonstrated PCE dechlorination at both pH 5.5 and pH 7.2 following repeated transfers at the respective pH values. To investigate the changes

in community structure in response to pH differences, and to identify the dechlorinator(s) responsible for the measured reductive dechlorination activity in enrichment cultures derived from the ACS microcosms that sustained PCE dechlorination at both pH 5.5 and pH 7.2, 16S rRNA gene amplicon sequencing was performed. After removing low quality reads, 69,030 sequences (17,441,054 total base pairs) and 103,503 sequences (26,171,881 total base pairs) were obtained from the ACS pH 5.5 and the pH 7.2 enrichments, respectively. A total of 172,409 sequences from the pH 5.5 and the pH 7.2 enrichment cultures were classified into 815 operational taxonomic units (OTUs) based on a 98% identity cutoff, and only 41 sequences could not be classified according to the SILVAngs empirical threshold ((sequence identity + alignment coverage) / 2 >= 93%) (Quast et al. 2013). Rarefaction analysis of sequences showed that the rarefaction curves did not plateau, suggesting that the sequencing effort did not capture the diversity of low abundance members in both the pH 7.2 and the pH 5.5 enrichment cultures (Figure 3.3.8).

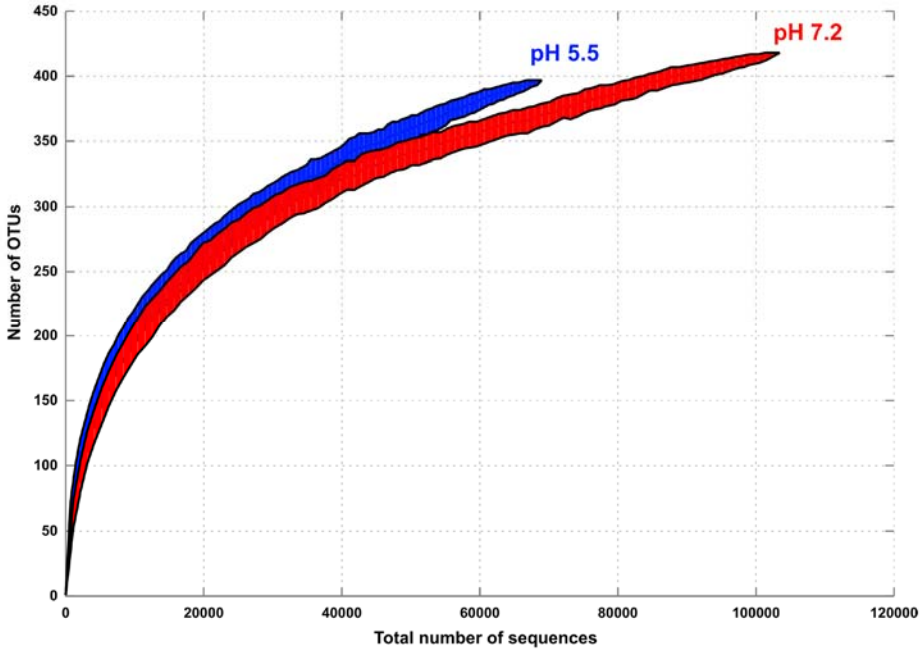

Figure 3.3.8. Rarefaction curves of pH 7.2 (red) and pH 5.5 (blue) enrichments. Acidic conditions reduced community richness. Each rarefaction curve is accompanied by a pair of lines representing the corresponding upper and lower 95% confidence intervals.

Sequences representing the phyla Proteobacteria and Firmicutes were most abundant in the pH 5.5 and pH 7.2 ACS enrichment cultures, respectively (Figure 3.3.9). The phyla Proteobacteria, Firmicutes, and Bacteroidetes were relatively enriched and contributed 57.9%, 31.8%, and 7.2%, respectively, to the classified sequences in the pH 5.5 enrichment, compared with 2.8%, 59.6%, and 3.0%, respectively, in the pH 7.2 enrichment. At pH 7.2, sequences of the phyla Caldiserica (4.0%), Chloroflexi (21.9%) and Spirochaetes (4.4%) were more abundant (Figure 3.3.9). Sequences representing the phyla Aigarchaeota, Thaumarchaeota, Chlorobi, Lentisphaerae, Nitrospirae and Synergistetes were present in the pH 7.2 PCE-to-ethene-dechlorinating enrichment, but were not observed in the pH 5.5 enrichment, indicating their preference for

circumneutral pH conditions. By comparison, sequences representing the phyla Euryarchaeota, Nanoarchaeota, Dictyoglomi, Fusobacteria and Thermotogae were detected in pH 5.5 PCE-to-*c*DCE-degrading ACS enrichment culture, but not in the pH 7.2 cultures. Furthermore, the most abundant genera in pH 5.5 ACS enrichment cultures differed from those dominating in the pH 7.2 enrichment cultures. At pH 7.2, the 16S rRNA gene sequences of the genera *Dhc* (phylum Chloroflexi) and *Acetobacterium* (phylum Firmicutes) dominated the enrichment and accounted for 22.6% and 57.6% of all sequences, respectively. In contrast, *Desulfovibrio* (phylum Proteobacteria) (33.0%), *Sulfurospirillum* (phylum Proteobacteria) (25.2%), and *Megasphaera* (phylum Chloroflexi) (19.9%) sequences dominated the pH 5.5 enrichment (Table 3.3.6).

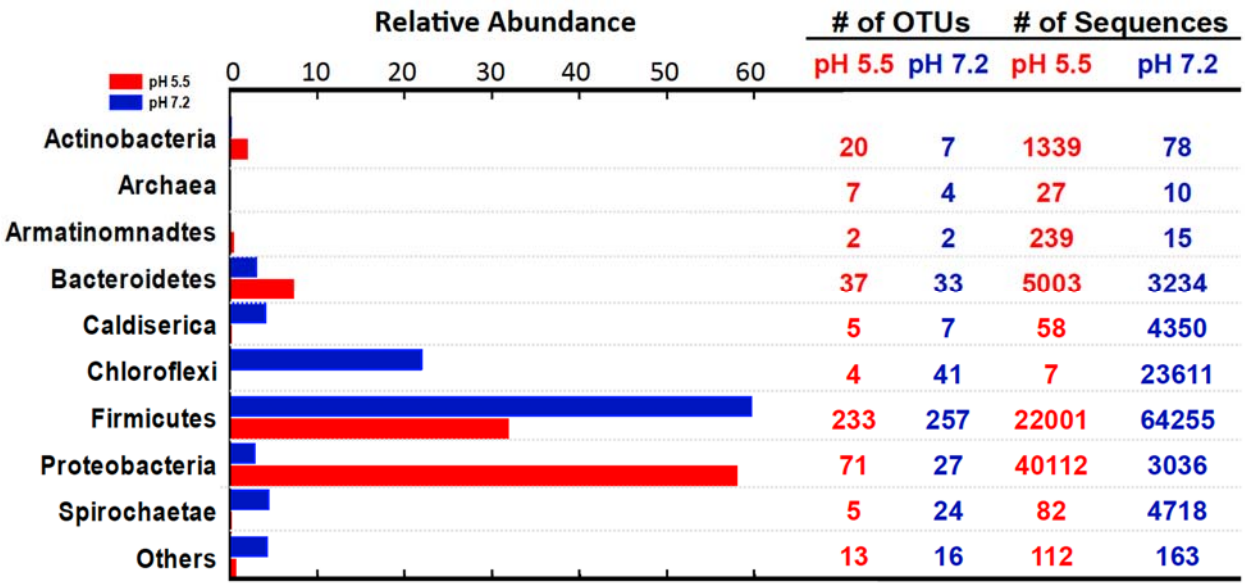

Figure 3.3.9. Relative abundance comparison of the phyla dominating the pH 5.5 and pH 7.2 PCE dechlorinating enrichments cultures. The numbers of Operational Taxonomic Units (OTUs) and total classified sequences within each phylum are shown on the right.

Table 3.3.6. Bacterial community structure in ACS pH 5.5 and pH 7.2 enrichment cultures. The percentage values indicate the abundances of representative OTUs as determined by 16S rRNA gene amplicon sequence analysis.

Genus	% of sequences	
	pH 7.2	**pH 5.5**
Dehalococcoides	22.6	0.0
Acetobacterium	57.6	0.0
Spirochaetaceae Uncultured	4.6	0.1
Caldisericum	4.2	0.1
Desulfuromonadales BVA18	2.6	0.0
vadinBC27	1.1	0.0
Desulfovibrio	0.1	33.0
Sulfurospirillum	0.2	25.2
Megasphaera	0.0	19.9
Propionibacterium	0.0	1.5
Pelosinus	0.0	1.00
Others	7.0	19.2
Total	100.0	100.0

3.3.3.c. Isolation of two *Sulfurospirillum* strains capable of low pH PCE reductive dechlorination

From the ACS enrichment, which was the only enrichment showing sustained PCE-to-*c*DCE reductive dechlorination at pH 5.5, two isolates were obtained. Isolate ACS_{TCE} dechlorinated PCE to TCE and isolate ACS_{DCE} dechlorinated PCE to *c*DCE (Figure 3.3.10). Both isolates grew with PCE in defined mineral salts medium at pH 5.5, and dechlorinated PCE at similar rates of 28.3±2.3 μmoles Cl^- released per liter and day. Isolate ACS_{TCE} generated TCE as the dechlorination end product, whereas isolate ACS_{DCE} dechlorinated PCE and TCE to *c*DCE. Approximately 30% higher dechlorination rates were measured for both isolates at pH 7.2 (Figure 3.3.10). Isolates ACS_{TCE} and ACS_{DCE} shared highly similar 16S rRNA genes (99.7% identity) and affiliated with the genus *Sulfurospirillum* within the ε-Proteobacteria class. Isolate ACS_{TCE} and isolate ACS_{DCE} shared 98.6% and 98.5% 16S rRNA gene sequence identity, respectively, with the characterized PCE-to-*c*DCE dechlorinator *Sulfurospirillum multivorans* (NR_121740.1). A phylogenetic analysis based on available *Sulfurospirillum* 16S rRNA gene sequences demonstrated that ACS_{TCE} and ACS_{DCE} isolates were most closely related to the PCE dechlorinator *Sulfurospirillum* sp. strain JPD-1 (AY189928.1) with 99.7% and 99.6 % sequence identity, respectively (Figure 3.3.11). The accession numbers of 16S rRNA gene sequences of selected bacteria used to construct the phylogenetic tree are listed in Table 3.3.7.

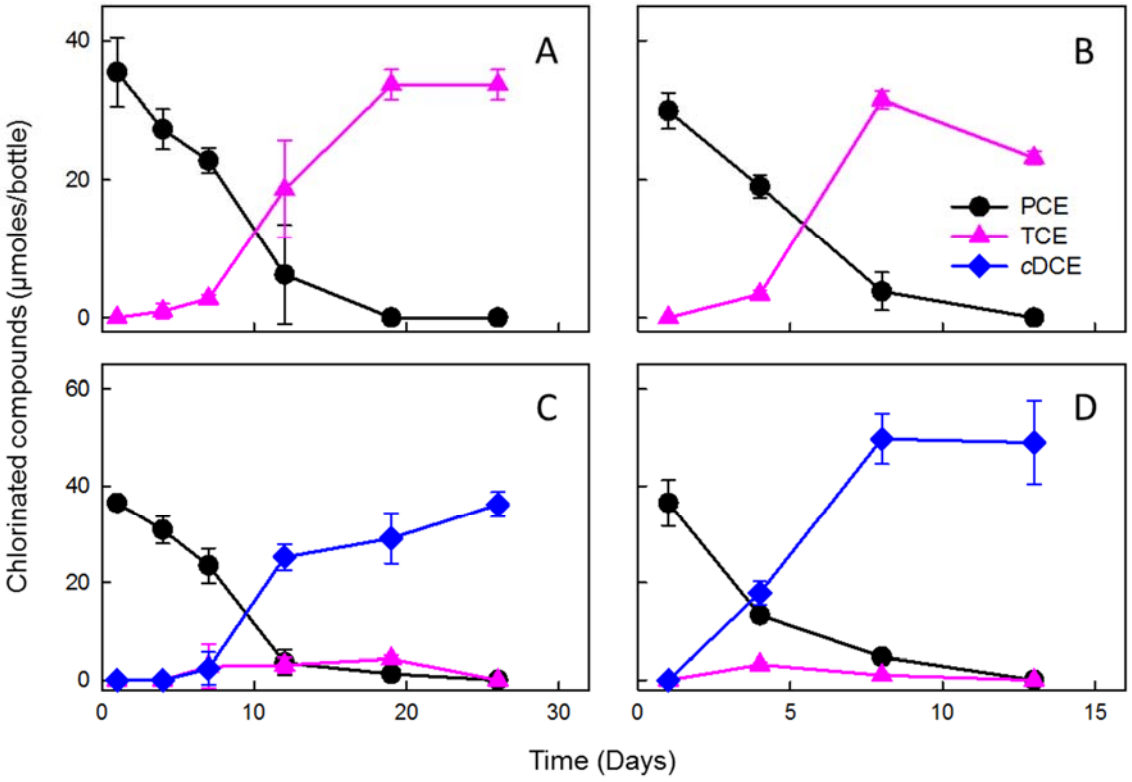

Figure 3.3.10. PCE reductive dechlorination by *Sulfurospirillum* isolates strain ACS_{TCE} and ACS_{DCE} at pH 5.5 and pH 7.2. PCE-to-TCE dechlorination by strain ACS_{TCE} at pH 5.5 (A) and pH 7.2 (B). PCE-to-*c*DCE dechlorination by strain ACS_{DCE} at pH 5.5 (C) and pH 7.2 (D). The isolates were grown with lactate as carbon source and electron donor. Error bars represent one standard deviation below or above the average of duplicate batch cultures.

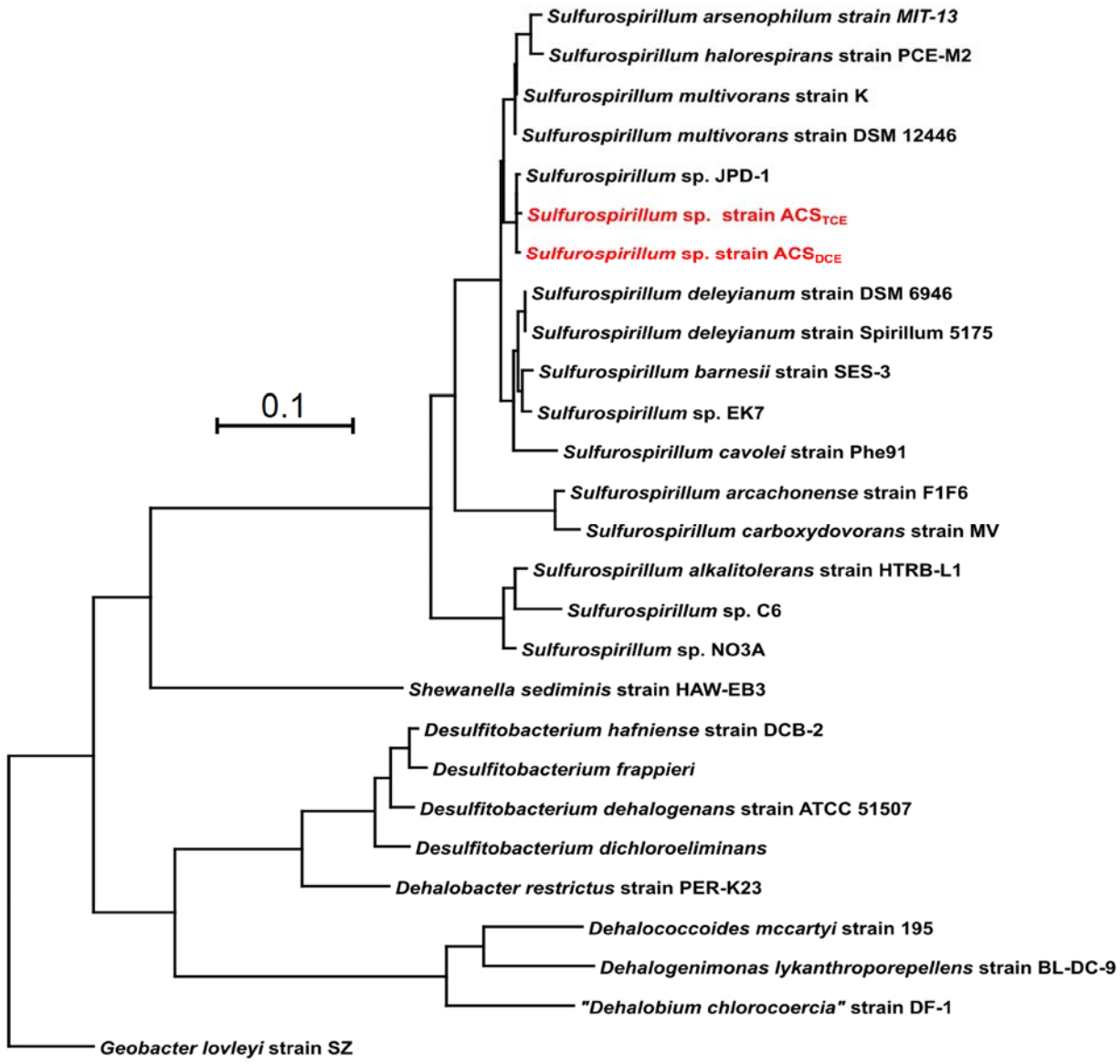

Figure 3.3.11. Phylogenetic affiliation of *Sulfurospirillum* sp. strain ACS$_{TCE}$ and ACS$_{DCE}$ based on 16S rRNA gene sequences. Strain ACS$_{TCE}$ and strain ACS$_{DCE}$ are most closely affiliated with *Sulfurospirillum* sp. strain JPD-1. Sequence accession numbers are listed in Table 3.3.7. The scale bar indicates nucleotide substitutions per site.

Table 3.3.7. Accession numbers of 16S rRNA gene sequences of selected bacteria used to build the *Sulfurospirillum* phylogenetic tree.

Name	Accession Number	Sequence Length (nt)
Dehalobacter restrictus strain PER-K23	NR_121722.1	1576
"*Dehalobium chlorocoercia*" strain DF-1	AF393781.1	1214
Dehalococcoides mccartyi strain 195	NR_074116.1	1435
Dehalogenimonas lykanthroporepellens strain BL-DC-9	NR_074337.1	1492
Desulfitobacterium dehalogenans strain ATCC 51507	NR_074128.1	1447
Desulfitobacterium dichloroeliminans	AJ565938.1	1467
Desulfitobacterium frappieri	U40078.1	1655
Desulfitobacterium hafniense strain DCB-2	NR_122068.1	1554
Geobacter lovleyi strain SZ	NR_074979.1	1551
Sulfurospirillum alkalitolerans strain HTRB-L1	GQ863490.1	1437
Sulfurospirillum arcachonense strain F1F6	NR_026408.1	1433
Sulfurospirillum arsenophilum strain MIT-13	NR_044806.1	1321
Sulfurospirillum barnesii SES-3	NR_102929.1	1497
Sulfurospirillum carboxydovorans strain MV	AY740528.1	1354
Sulfurospirillum cavolei strain Phe91	NR_041392.1	1336
Sulfurospirillum deleyianum strain DSM 6946	NR_074378.1	1497
Sulfurospirillum deleyianum strain Spirillum 5175	NR_026422.1	1431
Sulfurospirillum halorespirans strain PCE-M2	AF218076.1	1489
Sulfurospirillum multivorans strain DSM 12446	NR_121740.1	1498
Sulfurospirillum multivorans strain K	NR_044868.1	1464
Sulfurospirillum sp. C6	DQ228139.1	1201
Sulfurospirillum sp. EK7	AJ535704.1	1431
Sulfurospirillum sp. JPD-1	AY189928.1	1415
Sulfurospirillum sp. NO3A	AY135396.1	1300
Sulfurospirillum sp. strain ACS_{DCE}	KX101070	1375
Sulfurospirillum sp. strain ACS_{TCE}	KX101071	1015
Shewanella sediminis strain HAW-EB3	NR_074819.1	1535

Several *Sulfurospirillum* isolates (e.g., *Sulfurospirillum* sp. strain MV, *Sulfurospirillum multivorans*, *Sulfurospirillum halorespirans* and *Sulfurospirillum* sp. strain JPD-1) capable of PCE reductive dechlorination have been described, and activity has been reported between pH 6.0 and 8.0 (Jensen and Finster 2005, Kodama et al. 2007, Luijten et al. 2003, Scholz-Muramatsu et al. 1995). *Sulfurospirillum multivorans* has served as a model organism for exploring biochemical aspects of organohalide respiration and is physiologically well characterized, with a pH optimum for growth between 7.0 and 7.5 (Scholz-Muramatsu et al. 1995). Among the PCE-dechlorinating pure cultures tested in this study, *Sulfurospirillum multivorans* was the only organism capable of sustained dechlorination activity at pH 5.5, indicating that the pH range of

this organism extends to pH 5.5. Two distinct *Sulfurospirillum* isolates, ACS_{TCE} and ACS_{DCE}, that dechlorinated PCE at pH 5.5 were obtained from the ACS microcosms. Furthermore, a recent study exploring silicate minerals for pH control demonstrated that *Sulfurospirillum* was enriched in a PCE-to-*c*DCE-dechlorinating consortium at pH 5.5 (Lacroix et al. 2014, Rouzeau-Szynalski et al. 2011). Two different *Sulfurospirillum* populations were identified in consortium SL2 as part of this study (Rouzeau-Szynalski et al. 2011), and a functional genotyping approach identified two distinct reductive dehalogenase genes responsible for PCE-to-TCE and PCE-to-*c*DCE reductive dechlorination (Buttet et al. 2013).

The ability of *Sulfurospirillum* to grow with PCE as electron acceptor under low pH conditions distinguishes this group from other PCE dechlorinators, and has practical implications for bioremediation. The treatment of dense non-aqueous liquids (DNAPL) ganglia and pools remains a major remediation challenge, and prior work demonstrated that *Sulfurospirillum multivorans* was able to dechlorinate PCE to *c*DCE in the presence of free-phase PCE and contribute to enhanced PCE DNAPL dissolution (Amos et al. 2007a, Amos et al. 2008b). The large amount of hydrochloric acid released from microbial dechlorination activity at the DNAPL-groundwater interface decreases local groundwater pH, and a sustained process requires pH-tolerant dechlorinators. Batch culture experiments demonstrated that the *Sulfurospirillum multivorans* PCE reductive dechlorination rates can exceed PCE dissolution rates, thus effectively avoiding high aqueous phase PCE concentrations and associated toxicity (Amos et al. 2007a). High dechlorination rates and activity under low pH conditions suggest that PCE-respiring *Sulfurospirillum* spp. can be relevant contributors to PCE-DNAPL dissolution and PCE reductive dechlorination in low pH groundwater, and these unique properties suggest that bioaugmentation approaches for achieving enhanced PCE-DNAPL dissolution would benefit from consortia comprising pH-tolerant, PCE-dechlorinating *Sulfurospirillum* spp. Of course, this process would result in a *c*DCE plume, which is not a desirable remediation outcome, and additional efforts would be required to achieve detoxification. For example, the installation of downstream bioreactive barriers and pH adjustment, as appropriate, can be envisaged, to stimulate reductive dechlorination based on *Dhc* activity, or aerobic oxidation, either co-metabolic (e.g., methanotrophs) (Anderson and McCarty 1997) or metabolic (i.e., *Polaromonas* sp. strain JS666) (Coleman et al. 2002).

3.3.4. Influence of the Solid Phase on pH Effects on the Microbial Reductive Dechlorination Process

In a few microcosms established with aquifer material or sediment, PCE dechlorination to ethene was observed at pH 7.2 and pH 5.5 (Table 3.3.5). Solids-free transfer culture maintaining PCE-to-ethene dechlorination activity could be established in pH 7.2 medium, but all attempts to sustain ethene formation at pH 5.5 in transfer cultures were not successful. To further explore how physical and chemical properties of solids affect dechlorination activity at pH 5.5, a series of batch reactors experiments were conducted. Solid materials (i.e., Third Creek sediment, aquifer material from a chlorinated solvent site in California, and Federal Fine Ottawa sand) (ca. 20 g) were transferred to separate 160-mL glass serum bottles. Reduced mineral salts medium (pH 5.5) amended with 5 mM lactate was added to a total volume of 100 mL before the vessels were closed with butyl rubber stoppers and autoclaved. Following sterilization, the pH of replicate vessels was measured to verify that the sterilization process had not affected the aqueous phase pH. PCE was added and following a 1-day equilibration period, the vessels were inoculated with the PCE-to-ethene dechlorinating consortium BDI, and dechlorination was monitored. Microcosms

containing Third Creek sediment and DP aquifer material supported dechlorination of PCE to VC and ethene, whereas no dechlorination activity was observed with Federal Fine Ottawa sand microcosms (Figure 3.3.12). Apparently, the solid phase properties affected the ability of dechlorinators to degrade PCE to ethene in pH 5.5 medium. Of note, ethene formation in the same pH 5.5 medium in the absence of solids was not observed, demonstrating that the solid phase played a crucial role for reductive dechlorination to occur.

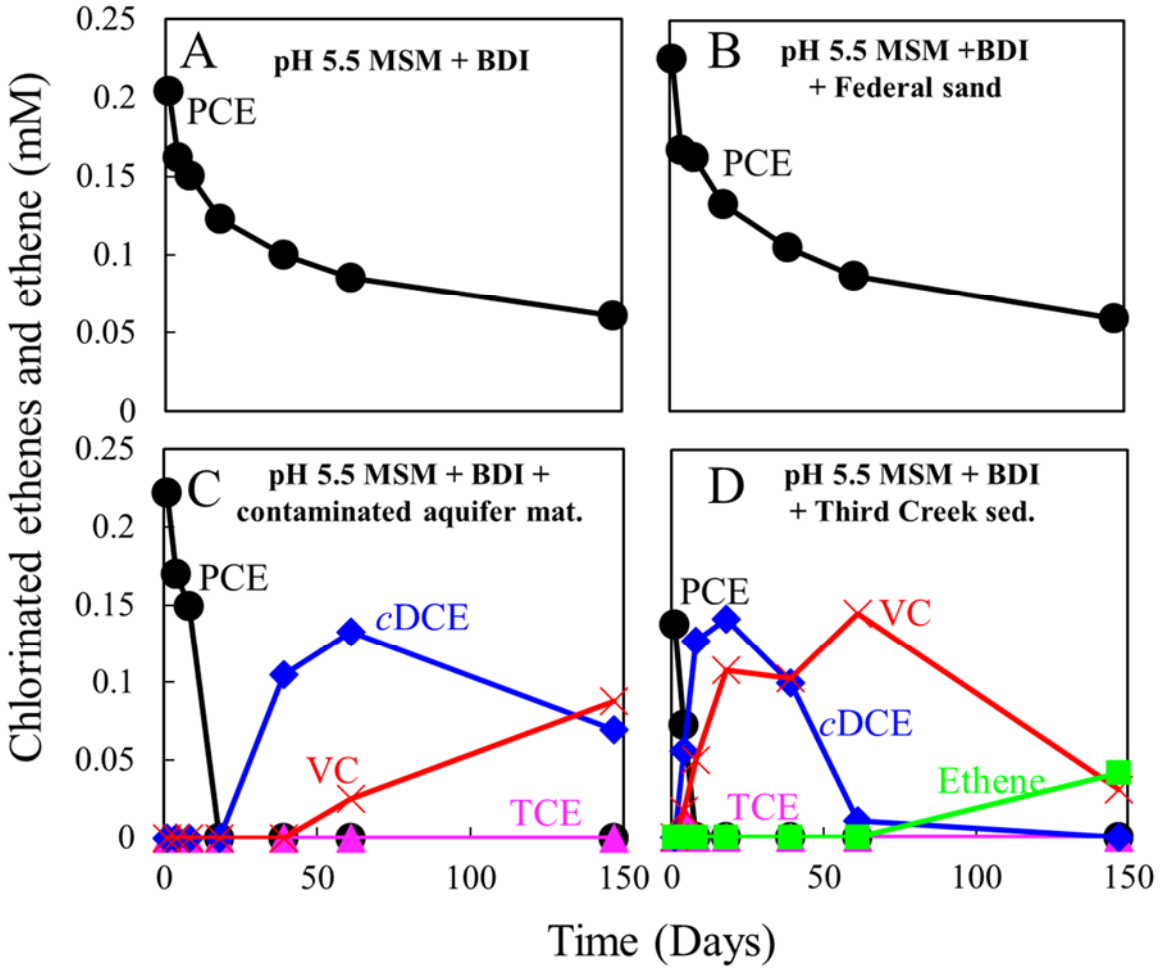

Figure 3.3.12. PCE dechlorination by BDI culture at pH 5.5 without solids (Panel A) or with different types of solid materials (Panel B: federal sand; Panel C: Dupont aquifer material; Panel D: Third Creek sediments).

To possibly explain these observations, the physical and chemical characteristics of the three solid phases were determined (Table 3.3.8).

Table 3.3.8. Physical and chemical properties of solid materials tested in microcosms experiments to support microbial reductive dechlorination activity at pH 5.5. These analyses were performed by the University of Georgia Agricultural & Environmental Services Laboratories (http://aesl.ces.uga.edu/)

Sample	LBC [1] (ppm $CaCO_3$ /pH)	pH $CaCl_2$ [2]	Equiv. water pH	Base Saturation (%)	CEC [3] (meq/ 100g)	Ca Mehlich 1 mg/kg (ppm)	Fe	K	Mg	Mn	Na	P
Third Creek sediment	450	7.26	7.86	100.0	26.13	4384	2.5	40.1	483.7	138.9	18.2	1.4
DP aquifer material	235	7.28	7.88	100.0	13.88	1033	37.0	59.9	787.8	54.8	458.1	84.4
Federal Fine sand	N.A. [4]	7.65	8.25	42.7	0.82	42	3.1	5.2	8.3	0.08	13.2	1.1

[1] Lime Buffer Capacity; [2] Soil pH and Salt Concentration; [3] Cation Exchange Capacity; [4] Not available

Major differences were observed in the solid materials' cation exchange capacity (CEC) and the lime buffer capacity (LBC). A preliminary conclusion of these experimental efforts is that the CEC and the LBC affect local pH conditions, and microorganisms, including dechlorinators, experience more favorable (i.e., higher) pH conditions near the solid-liquid interface. Thus, reductive dechlorination to VC and ethene was possible near solid-liquid interface, possible catalyzed by biofilms, where dechlorinators were protected from inhibitory pH in the medium.

The observation that *Dhc* activity and dechlorination to ethene can occur at pH 5.5 in the presence of certain solid phases (presumably related to CEC and LBC) has implications for bioremediation at sites with low pH groundwater. While all laboratory experiments performed in the absence of solids indicated that ethene formation does not occur at pH 5.5, the microcosm experiments hint that the solid phase materials can affect the local pH environment and support pH-sensitive microbial activity, including reductive dechlorination. The situation at low pH sites in more complicated and groundwater pH is not the only parameter that determines if the microbial reductive dechlorination process can be productive or not. While dechlorination activity of non-attached (planktonic) dechlorinators in low pH groundwater is unlikely, the microcosms experiments with Third Creek sediment and the DP aquifer material indicate that the properties of the solid phase materials play a crucial role in generating local pH environments that enable microbial activity in a saturated medium with a bulk phase aqueous pH too low to allow *Dhc* dechlorination activity and detoxification to ethene. Further research is warranted to correlate the solid phase properties that allow reductive dechlorination to ethene to occur in aquifers with low pH groundwater. A major goal should be to develop analytical procedures that generate predictive understanding of the capacity of the solid phase to support microbial reductive dechlorination to environmentally benign end products (i.e., ethene).

CHAPTER 4

CONCLUSIONS AND IMPLICATIONS

4.1. IMPACTS OF THERMAL TREATMENT ON GROUNDWATER GEOCHEMISTRY AND COMBINED REMEDIES (TASK 1)

1. Thermal treatment of soils resulted in volatile fatty acid (VFA) release, even in soils with relatively low organic carbon (OC) content (e.g., Federal Fine Ottawa sand with 0.01% OC). However, OC content did not consistently correlate with the rate or extent of VFA release. Inclusion of carboxyl and phenyl functional group content improved predictions of VFA release from natural soils and aquifer materials as a function of temperature.
2. Soil heating in a 1-D flow system causes the release of VFAs including formate, acetate, propionate and butyrate to the aqueous phase. Release of acetate is favored at lower temperatures, while increasing temperatures lead to release of other low molecular weight VFAs like VFAs such as propionate, potentially providing a sustained source of reducing equivalents and minimizing competition for electron donors.
3. 3. VFAs are released rapidly from the solid phase once a threshold temperature of approximately 50 °C was reached, suggesting that gradual subsurface heating may provide a more sustained source of reducing equivalents than a rapid or stepwise heating regime.
4. VFAs released during soil heating can theoretically provide sufficient reducing equivalents to drive microbial reductive dechlorination in the absence of an external electron donor source, even when low (1%) overall efficiency is assumed.
5. Thermally-released VFAs (e.g., acetate and formate) from soils containing greater than 0.8% OC were able to support the transformation of tetrachloroethene (PCE) to vinyl chloride (VC) and ethene by a dechlorinating consortium located immediately downgradient from the heated zone (90ºC) without addition of electron donor amendments.
6. In column experiments, low temperature heating (35 ºC) improved microbial reductive dechlorination performance, resulting in up to 3.5 times greater ethene production compared to a similar system operated at typical groundwater temperature (15 ºC). These observed improvements in microbial reductive dechlorination of PCE during low temperature heating of soil columns were greater than previously reported in batch enrichment culture and microcosm studies.

4.2. EFFECTS OF METAL SULFIDE FORMATION AND DISSOLUTION ON AQUIFER PERMEABILITY (TASK 2)

1. Substantial reductions in permeability were observed due to the formation of iron (II) sulfide (FeS) precipitates that restricted or blocked pore throats. Column studies demonstrated that FeS precipitation can cause permeability reductions of up to 80 %, and that this impact is most apparent in soils with high organic carbon content (e.g., 2.4 % w/w).

2. FeS precipitation at low flow rates led to decreases in permeability and porosity of up to 95.8% and 12.7%, respectively.
3. Oxidation of FeS at low flow rates led to a reversal of the porosity losses incurred during FeS precipitation.
4. In aquifer cell studies, FeS precipitation caused local reductions in permeability, which led to preferential flow. Following re-establishment of oxic conditions, iron oxide formation resulted in further reductions in permeability and changes in preferential flow paths.

4.3. IMPACTS OF REMEDIAL STRATEGIES ON pH AND MICROBIAL REDUCTIVE DECHLORINATION (TASK 3)

1. Among the PCE-dechlorinating pure cultures tested, only *Sulfurospirillum multivorans* demonstrated PCE-to-*c*DCE reductive dechlorination at pH 5.5. From microcosms and enrichment cultures showing PCE-to-*c*DCE dechlorination activity at pH 5.5, two distinct *Sulfurospirillum* isolates were obtained. These findings suggest that *Sulfurospirillum* play relevant roles for PCE reductive dechlorination in low pH environments.
2. Reductive dechlorination to ethene was not sustained in pH 5.5 medium, and no evidence was obtained that *Dehalococcoides mccartyi* strains grow at pH 5.5.
3. The duration of low pH exposure affects the recovery of *Dehalococcoides mccartyi* growth and reductive dechlorination activity. Strain-specific recovery was observed, and *Dehalococcoides mccartyi* strains implicated in vinyl chloride reductive dechlorination were most sensitive to low pH exposure.
4. pH affected reductive dechlorination activity and had a profound effect on microbial community structure.
5. A survey of samples collected from 171 groundwater wells indicated that *Dehalococcoides mccartyi* biomarker genes were generally more abundant at sites with groundwater in the circumneutral pH range (6~8.3) than in the acidic pH range (4.5~6.0).
6. Dechlorination of PCE to ethene occurred in some pH 5.5 microcosms, but this activity could not be sustained in solids-free enrichment cultures. Experiments with autoclaved solids and the PCE-to-ethene dechlorinating consortium BDI demonstrated that solid phase properties affect the cultures ability to dechlorinate PCE to ethene. Solid phase characteristics generate micro-environments within aggregates or near the solid-water interface where microbes experience favorable (i.e., circumneutral) pH conditions than in the bulk aqueous phase. Initial soil characterization efforts suggest that the cation exchange capacity (CEC) plays an important role in enabling reductive dechlorination in low pH groundwater.

4.4. RESEARCH IMPLICATIONS

Results obtained under SERDP Project ER-2129 provide site managers, regulatory officials, consultants, and researchers with new information about the impacts of thermal treatment and

biostimulation on groundwater quality, biogeochemistry and remediation performance. For thermal treatment, this work demonstrated that thermally-released electron donors and fermentable substrates, which are able to support microbial reductive dechlorination of PCE to ethene, should be considered as part of a treatment train with enhanced bioremediation, particularly in low-permeability zones where substrate delivery is challenging. Additionally, results of column studies showed that low temperature heating (35 ºC) improved microbial reductive dechlorination of PCE to ethene, and may reduce the accumulation of *c*DCE. Column studies demonstrated FeS precipitate formation, caused by the activity of ferric iron- and sulfate-reducing bacteria, could aquifer permeability. In field settings, local changes in soil permeability and preferential flow could contribute to slower contaminant mass transfer (e.g., dissolution and desorption), which could decrease mass flux and increase source zone longevity. Alternatively, such permeability reductions may increase local residence times, which could facilitate more complete reaction processes, including dechlorination of PCE to ethene. Fermentation reactions and enhanced dechlorination activity following biostimulation can lower groundwater pH and impact reductive dechlorination activity. The time of low pH exposure is a crucial parameter impacting the ability of *Dehalococcoides mccartyi* to recover dechlorination activity. Initial reductive dechlorination activity at low pH sites following bioaugmentation may be due to residual activity of the dechlorinating biomass, and careful monitoring of reductive dechlorination biomarkers is recommended to determine the sustainability of the process. Of note, samples from low pH sites with dechlorination daughter products were analyzed but no evidence was obtained for reductive dechlorination activity. Careful inspection suggested that the daughter products were transported with the groundwater from upgradient locations with favorable pH conditions. This example demonstrates that the interpretation of monitoring data from low pH sites must be carefully conducted. While *Dehalococcoides mccartyi* strains could not sustain reductive dechlorination activity in pH 5.5 medium, the addition of solid phase with high cation exchange capacity allowed ethene formation with a bulk aqueous phase pH of 5.5. Apparently, the solid phase properties affected microbial reductive dechlorination activity under low pH conditions, and future research efforts should explore if predictive understanding of the effects of the solids on microbial reductive dechlorination activity can be attained.

CHAPTER 5

LITERATURE CITED

AATDF (1997) Technology Practices Manual for Surfactants and Cosolvents. Program, A.A.T.D.F. (ed), Houston, TX.

Adamson, D.T., Lyon, D.Y. and Hughes, J.B. (2004) Flux and Product Distribution during Biological Treatment of Tetrachloroethene Dense Non-Aqueous-Phase Liquid. Environmental Science & Technology 38(7), 2021-2028.

AFCEE (2004) Principles and practices of enhanced anaerobic bioremediation of chlorinated solvents, p. 458, US DoD Air Force Center for Environmental Excellence and ESTCP.

Aguilar-Hinojosa, Y., Meza-Figueroa, D., Villalba-Atondo, A.I., Encinas-Romero, M.A., Valenzuela-García, J.L. and Gómez-Álvarez, A. (2016) Mobility and Bioavailability of Metals in Stream Sediments Impacted by Mining Activities: the Jaralito and the Mexicana in Sonora, Mexico. Water, Air, & Soil Pollution 227(9), 345.

Amos, B.K., Christ, J.A., Abriola, L.M., Pennell, K.D. and Löffler, F.E. (2007a) Experimental evaluation and mathematical modeling of microbially enhanced tetrachloroethene (PCE) dissolution. Environ Sci Technol 41(3), 963-970.

Amos, B.K., Daprato, R.C., Hughes, J.B., Pennell, K.D. and Löffler, F.E. (2007b) Effects of the nonionic surfactant Tween 80 on microbial reductive dechlorination of chlorinated ethenes. Environmental Science & Technology 41, 1710-1716.

Amos, B.K., Ritalahti, K.M., Cruz-Garcia, C., Padilla-Crespo, E. and Löffler, F.E. (2008a) Oxygen effect on *Dehalococcoides* viability and biomarker quantification. Environ Sci Technol 42(15), 5718-5726.

Amos, B.K., Suchomel, E.J., Pennell, K.D. and Loffler, F.E. (2009a) Spatial and temporal distributions of *Geobacter lovleyi* and *Dehalococcoides* spp. during bioenhanced PCE-NAPL dissolution. Environmental Science and Technology 43(6), 1977-1985.

Amos, B.K., Suchomel, E.J., Pennell, K.D. and Löffler, F.E. (2008b) Microbial activity and distribution during enhanced contaminant dissolution from a NAPL source zone. Water Res 42(12), 2963-2974.

Amos, B.K., Suchomel, E.J., Pennell, K.D. and Löffler, F.E. (2009b) Spatial and temporal distributions of *Geobacter lovleyi* and *Dehalococcoides* spp. during bioenhanced PCE-NAPL dissolution. Environmental Science & Technology 43(6), 1977-1985.

Amos, B.K., Sung, Y., Fletcher, K.E., Gentry, T.J., Wu, W.M., Criddle, C.S., Zhou, J. and Löffler, F.E. (2007c) Detection and quantification of *Geobacter lovleyi* strain SZ: Implications for bioremediation at tetrachloroethene- and uranium-impacted sites. Applied and environmental microbiology 73(21), 6898-6904.

Anderson, J.E. and McCarty, P.L. (1997) Transformation yields of chlorinated ethenes by a methanotrophic mixed culture expressing particulate methane monooxygenase. Appl Environ Microbiol 63(2), 687-693.

Aziz, C.E., Wymore, R.A. and Steffan, R.J. (2013) Bioaugmentation for Groundwater Remediation. Stroo, H.F., Leeson, A. and Ward, C.H. (eds), pp. 141-169, Springer New York, New York, NY.

Bakke, B., Stewart, P.A. and Waters, M.A. (2007) Uses of and exposure to trichloroethylene in us industry: a systematic literature review. J Occup Environ Hyg 4(5), 375-390.

Berggren, D.R., Marshall, I.P., Azizian, M.F., Spormann, A.M. and Semprini, L. (2013) Effects of sulfate reduction on the bacterial community and kinetic parameters of a dechlorinating culture under chemostat growth conditions. Environmental Science & Technology 47(4), 1879-1886.

Buttet, G.F., Holliger, C. and Maillard, J. (2013) Functional genotyping of *Sulfurospirillum* spp. in mixed cultures allowed the identification of a new tetrachloroethene reductive dehalogenase. Appl Environ Microbiol 79(22), 6941-6947.

Cápiro, N.L., Löffler, F.E. and Pennell, K.D. (2015) Spatial and temporal dynamics of organohalide-respiring bacteria in a heterogeneous PCE–DNAPL source zone. Journal of contaminant hydrology 182, 78-90.

Cápiro, N.L., M.L.B., D.S., Stafford, B.P., Rixey, W.G. and Alvarez, P.J.J. (2008) Microbial community response to a release of neat ethanol onto residual hydrocarbons in a pilot-scale aquifer tank. Environmental Microbiology 10(9), 2236–2244.

Cápiro, N.L., Wang, Y., Hatt, J.K., Lebrón, C.A., Pennell, K.D. and Löffler, F.E. (2014) Distribution of organohalide-respiring bacteria between solid and aqueous phases. Environ Sci Technol 48(18), 10878-10887.

Caporaso, J.G., Lauber, C.L., Walters, W.A., Berg-Lyons, D., Huntley, J., Fierer, N., Owens, S.M., Betley, J., Fraser, L., Bauer, M., Gormley, N., Gilbert, J.A., Smith, G. and Knight, R. (2012) Ultra-high-throughput microbial community analysis on the Illumina HiSeq and MiSeq platforms. ISME J 6(8), 1621-1624.

Christ, J.A., Ramsburg, C.A., Loeffler, F.E., Pennell, K.D. and Abriola, L.M. (2005a) Coupling aggressive mass removal with microbial reductive dechlorination for remediation of DNAPL source zones - A review and assessment. Environmental Health Perspectives 113(4), 465-477, doi: 410.1289/ehp.6932.

Christ, J.A., Ramsburg, C.A., Löffler, F.E., Pennell, K.D. and Abriola, L.M. (2005b) Coupling aggressive mass removal with microbial reductive dechlorination for remediation of DNAPL source zones - A review and assessment. Environmental Health Perspectives 113(4), 465-477, doi: 410.1289/ehp.6932.

Coleman, N.V., Mattes, T.E., Gossett, J.M. and Spain, J.C. (2002) Biodegradation of *cis*-dichloroethene as the sole carbon source by a β-Proteobacterium. Appl Environ Microbiol 68(6), 2726-2730.

Cope, N. and Hughes, J.B. (2001) Biologically-enhanced removal of PCE from NAPL source zones. Environmental Science & Technology 35(10), 2014-2021.

Costanza, J., Davis, E.L., Mulholland, J.A. and Pennell, K.D. (2005) Abiotic degradation of trichloroethylene under thermal remediation conditions. Environmental Science & Technology 39(17), 6825-6830.

Costanza, J., Flethcher, K.E., Löffler, F.E. and Pennell, K.D. (2009) Fate of TCE in Heated Fort Lewis Soil. Environmental Science and Technology 43(3), 909-914.

Costanza, J. and Pennell, K.D. (2007) Distribution and Abiotic Degradation of Chlorinated Solvents in Heated Field Samples. Environmental Science & Technology 41(5), 1729-1734.

Daniels, J.L. and Cherukuri, R. (2005) Influence of Biofilm on Barrier Material Performance. Practice Periodical of Hazardous, Toxic, and Radioactive Waste Management 9(4), 245-252.

Davis, E.L. (1997) How Heat Can Enhance In-situ Soil and Aquifer Remediation: Important Chemical Properties and Guidance on Choosing the Appropriate Technology. (EPA/540/S-97/502), U.S. EPA National Risk Management Research Laboratory, Ada, OK.

De Bruin, W.P., Kotterman, M., Posthumus, M.A., Schraa, G. and Zehnder, A. (1992) Complete biological reductive transformation of tetrachloroethene to ethane. Applied and environmental microbiology 58(6), 1996-2000.

Duhamel, M. and Edwards, E.A. (2006) Microbial composition of chlorinated ethene-degrading cultures dominated by *Dehalococcoides*. FEMS Microbiology Ecology 58, 538-549.

EPA (2016) Average temperature of shallow ground water. Agency, U.S.E.P. (ed).

Equeenuddin, S.M., Tripathy, S., Sahoo, P. and Panigrahi, M. (2013) Metal behavior in sediment associated with acid mine drainage stream: role of pH. Journal of Geochemical Exploration 124, 230-237.

ESTCP (2009) State-of-the-Practice Overview of the use of In Situ Thermal Technologies for NAPL Source Zone Cleanup, ESCTP Project ER-0314, Environmental Security Technology Certification Program, Washington, D.C.

Fennell, D.E., Gossett, J.M. and Zinder, S.H. (1997) Comparison of butyric acid, ethanol, lactic acid, and propionic acid as hydrogen donors for the reductive dechlorination of tetrachloroethene. Environ Sci Technol 31(3), 918-926.

Fletcher, K.E., Costanza, J., Cruz-Garcia, C., Ramaswamy, N.S., Pennell, K.D. and Löffler, F.E. (2010) Effects of elevated temperature on Dehalococcoides dechlorination performance and DNA and RNA biomarker abundance. Environmental Science & Technology 45(2), 712-718.

Fletcher, K.E., Costanza, J., Cruz-Garcia, C., Ramaswamy, N.S., Pennell, K.D. and Löffler, F.E. (2011a) Effects of elevated temperature on *Dehalococcoides* dechlorination performance and DNA and RNA biomarker abundance. Environmental Science & Technology 45(2), 712-718.

Fletcher, K.E., Costanza, J., Pennell, K.D. and Löffler, F.E. (2011b) Electron donor availability for microbial reductive processes following thermal treatment. Water Research 45(20), 6625-6636.

Fletcher, K.E., Ritalahti, K.M., Pennell, K.D., Takamizawa, K. and Löffler, F.E. (2008) Resolution of culture *Clostridium bifermentans* DPH-1 into two populations, a

Clostridium sp. and tetrachloroethene-dechlorinating *Desulfitobacterium hafniense* strain JH1. Appl Environ Microbiol 74(19), 6141-6143.

Ford, H.W., Calvert, D.V. and Beville, B.C. (1968) Hydraulic conductivity of soils and filter materials in Florida wetland citrus. Transactions of ASAE 11, 566-567.

Freeze, R.A. and Cherry, J.A. (1979) Groundwater, Prentice-Hall Inc., TIC, Englewood, New Jersey.

Friis, A.K., Albrechtsen, H.J., Cox, E. and Bjerg, P.L. (2006) The need for bioaugmentation after thermal treatment of a TCE-contaminated aquifer: Laboratory experiments. Journal of contaminant hydrology 88, 235-248.

Friis, A.K., Albrechtsen, H.J., Heron, G. and Bjerg, P.L. (2005) Redox processes and release of organic matter after thermal treatment of a TCE-contaminated aquifer. Environmental Science & Technology 39, 5787-5795.

Friis, A.K., Heimann, A.C., Jakobsen, R., Albrechtsen, H.J., Cox, E. and Bjerg, P.L. (2007) Temperature dependence of anaerobic TCE-dechlorination in a highly enriched *Dehalococcoides*-containing culture. Water Research 41, 335-364.

Gadd, G.M. and Griffiths, A.J. (1978) Microorganisms and Heavy-Metal Toxicity. Microbial Ecology 4(4), 303-317.

Gerritse, J., Renard, V., Gomes, T.P., Lawson, P.A., Collins, M.D. and Gottschal, J.C. (1996) *Desulfitobacterium* sp. strain PCE1, an anaerobic bacterium that can grow by reductive dechlorination of tetrachloroethene or ortho-chlorinated phenols. Archives of microbiology 165(2), 132-140.

Giller, K.E., Witter, E. and Mcgrath, S.P. (1998) Toxicity of heavy metals to microorganisms and microbial processes in agricultural soils: a review. Soil Biol Biochem 30(10), 1389-1414.

Good, N.E., Winget, G.D., Winter, W., Connolly, T.N., Izawa, S. and Singh, R.M. (1966) Hydrogen ion buffers for biological research. Biochemistry 5(2), 467-477.

Hale, G.P. and MacIver, B.N. (1970) Laboratory Soils Testing. Engineers, D.o.t.A.O.o.t.C.o. (ed), p. 8, U.S. Army Engineer Waterways Experiment Station (WES).

He, J., Ritalahti, K.M., Yang, K.-L., Koenigsberg, S.S. and Löffler, F.E. (2003) Detoxification of vinyl chloride to ethene coupled to growth of an anaerobic bacterium. Nature 424(6944), 62-65.

He, J., Sung, Y., Krajmalnik-Brown, R., Ritalahti, K.M. and Löffler, F.E. (2005) Isolation and characterization of *Dehalococcoides* sp. strain FL2, a trichloroethene (TCE)- and 1,2-dichloroethene-respiring anaerobe. Environmental Microbiology 7(9), 1442-1450.

Herczeg, A.L., Rattray, K.J., Dillon, P.J., Pavelic, P. and Barry, K.E. (2004) Geochemical Processes During Five Years of Aquifer Storage Recovery. Ground Water 42(3), 438-445.

Heron, G., Carroll, S. and Nielsen, S.G. (2005) Full-scale removal of DNAPL constituents using steam-enhanced extraction and electrical resistance heating. Ground Water Monitoring and Remediation 25(4), 92-107.

Heron, G., Parker, K., Galligan, J. and Holmes, T.C. (2009) Thermal Treatment of Eight CVOC Source Zones to Near Nondetect Concentrations. Ground Water Monitoring and Remediation 29(3), 56-65.

Holliger, C., Schraa, G., Stams, A. and Zehnder, A. (1993) A highly purified enrichment culture couples the reductive dechlorination of tetrachloroethene to growth. Applied and environmental microbiology 59(9), 2991-2997.

Jensen, A. and Finster, K. (2005) Isolation and characterization of *Sulfurospirillum carboxydovorans* sp. nov., a new microaerophilic carbon monoxide oxidizing epsilon Proteobacterium. Antonie Van Leeuwenhoek 87(4), 339-353.

Katoh, K., Misawa, K., Kuma, K. and Miyata, T. (2002) MAFFT: a novel method for rapid multiple sequence alignment based on fast Fourier transform. Nucleic Acids Res 30(14), 3059-3066.

Kavanaugh, M.C., Rao, P.S.C., Abriola, L., Cherry, J., Destouni, G., Falta, R., Major, D., Mercer, J., Newell, C., Sale, T., Shoemaker, S., Siegrist, R.L., Teutsch, G. and Udell, K. (2003) The DNAPL Cleanup Challenge: Source Removal or Long Term Management (EPA/600/R-03/143), Report of an Expert Panel to the U.S. EPA National Risk Management Laboratory and Technology Innovation Office, Washington, D.C.

Kodama, Y., Ha le, T. and Watanabe, K. (2007) *Sulfurospirillum cavolei* sp. nov., a facultatively anaerobic sulfur-reducing bacterium isolated from an underground crude oil storage cavity. Int J Syst Evol Microbiol 57(4), 827-831.

Kozich, J.J., Westcott, S.L., Baxter, N.T., Highlander, S.K. and Schloss, P.D. (2013) Development of a dual-index sequencing strategy and curation pipeline for analyzing amplicon sequence data on the MiSeq Illumina sequencing platform. Appl Environ Microbiol 79(17), 5112-5120.

Kristiansen, R. (1981) Sand-Filter Trenches for Purification of Septic Tank Effluent: I. The Clogging Mechanism and Soil Physical Environment. J Environ Qual 10(3), 353-357.

Kube, M., Beck, A., Zinder, S.H., Kuhl, H., Reinhardt, R. and Adrian, L. (2005) Genome sequence of the chlorinated compound respiring bacterium *Dehalococcoides* species strain CBDB1. Nature biotechnology 23(10), 1269-1273.

Laak, R. (1970) Influence of Domestic Wastewater Pretreatment on Soil Clogging. Journal (Water Pollution Control Federation) 42(8), 1495-1500.

Lacroix, E., Brovelli, A., Barry, D.A. and Holliger, C. (2014) Use of silicate minerals for pH control during reductive dechlorination of chloroethenes in batch cultures of different microbial consortia. Appl Environ Microbiol 80(13), 3858-3867.

Leeson, A., Beevar, E., Henry, B., Fortenberry, J. and Coyle, C. (2004) Principles and practices of enhanced anaerobic bioremediation of chlorinated solvents, DTIC Document.

Löffler, F.E., Sanford, R.A. and Ritalahti, K.M. (2005) Enrichment, cultivation, and detection of reductively dechlorinating bacteria. Methods in enzymology 397, 77-111.

Loffler, F.E., Sanford, R.A. and Tiedje, J.M. (1996) Initial Characterization of a Reductive Dehalogenase from Desulfitobacterium chlororespirans Co23. Applied and environmental microbiology 62(10), 3809-3813.

Löffler, F.E., Tiedje, J.M. and Sanford, R.A. (1999) Fraction of electrons consumed in electron acceptor reduction and hydrogen thresholds as indicators of halorespiratory physiology. Applied and environmental microbiology 65, 4049-4056.

Löffler, F.E., Yan, J., Ritalahti, K.M., Adrian, L., Edwards, E.A., Konstantinidis, K.T., Müller, J.A., Fullerton, H., Zinder, S.H. and Spormann, A.M. (2013) *Dehalococcoides mccartyi* gen. nov., sp. nov., obligately organohalide-respiring anaerobic bacteria relevant to halogen cycling and bioremediation, belong to a novel bacterial class, *Dehalococcoidia* classis nov., order *Dehalococcoidales* ord. nov. and family *Dehalococcoidaceae* fam. nov., within the phylum *Chloroflexi*. International Journal of Systematic and Evolutionary Microbiology 63(Pt 2), 625-635.

Luijten, M.L., de Weert, J., Smidt, H., Boschker, H.T., de Vos, W.M., Schraa, G. and Stams, A.J. (2003) Description of *Sulfurospirillum halorespirans* sp. nov., an anaerobic, tetrachloroethene-respiring bacterium, and transfer of *Dehalospirillum multivorans* to the genus *Sulfurospirillum* as *Sulfurospirillum multivorans* comb. nov. Int J Syst Evol Microbiol 53(3), 787-793.

Macbeth, T.W., Truex, M., Powell, T. and Michalsen, M. (2012) Final report: combining low-energy electrical resistance heating with biotic and abiotic reactions for treatment of chlorinated solvent dnapl source areas, Environmental Security Technology Certification Program.

McCarty, P.L., Chu, M.-Y. and Kitanidis, P.K. (2007) Electron donor and pH relationships for biologically enhanced dissolution of chlorinated solvent DNAPL in groundwater. European Journal of Soil Biology 43(5), 276-282.

McGuire, T.M., McDade, J.M. and Newell, C.J. (2006) Performance of DNAPL source depletion technologies at 59 chlorinated solvent-impacted sites. Groundwater Monitoring & Remediation 26(1), 73-84.

Mitchell, R. and Nevo, Z. (1964) Effect of Bacterial Polysaccharide Accumulation on Infiltration of Water Through Sand. Appl. Environ. Microbiol. 12(3), 219-223.

NRC (2004) Contaminants in the Subsurface: Source Zone Assessment and Remediation, National Academy Press, Washington, D.C.

NRC (2013) Alternatives for Managing the Nation's Complex Contaminated Groundwater Sites, The National Academies Press, Washington, DC.

Ogata, G. and Bower, C.A. (1965) Significance of Biological Sulfate Reduction in Soil Salinity. Soil Sci Soc Am J 29(1), 23-25.

Ohnishi, A., Hasegawa, Y., Abe, S., Bando, Y., Fujimoto, N. and Suzuki, M. (2012) Hydrogen fermentation using lactate as the sole carbon source: solution for ‘blind spots’ in biofuel production. RSC Advances 2(22), 8332-8340.

Olaniran, A.O., Balgobind, A. and Pillay, B. (2013) Bioavailability of heavy metals in soil: impact on microbial biodegradation of organic compounds and possible improvement strategies. International journal of molecular sciences 14(5), 10197-10228.

Quast, C., Pruesse, E., Yilmaz, P., Gerken, J., Schweer, T., Yarza, P., Peplies, J. and Glockner, F.O. (2013) The SILVA ribosomal RNA gene database project: improved data processing and web-based tools. Nucleic Acids Res 41(Database issue), D590-596.

Ramsburg, C.A., Abriola, L.M., Pennell, K.D., Loffler, F.E., Gamache, M., Amos, B.K. and Petrovskis, E.A. (2004) Stimulated microbial reductive dechlorination following surfactant treatment at the Bachman Road site Environmental Science & Technology 38(22), 5902-5914.

Ritalahti, K., Amos, B., Sung, Y., Wu, Q., Koenigsberg, S. and Löffler, F. (2006a) Quantitative PCR targeting 16S rRNA and reductive dehalogenase genes simultaneously monitors multiple *Dehalococcoides* strains. Applied and environmental microbiology 72(4), 2765-2774.

Ritalahti, K.M., Amos, B.K., Sung, Y., Wu, Q., Koenigsberg, S.S. and Löffler, F.E. (2006b) Quantitative PCR targeting 16S rRNA and reductive dehalogenase genes simultaneously monitors multiple Dehalococcoides strains. Applied and environmental microbiology 72(4), 2765-2774.

Robinson, C., Barry, D., McCarty, P.L., Gerhard, J.I. and Kouznetsova, I. (2009) pH control for enhanced reductive bioremediation of chlorinated solvent source zones. Science of the total environment 407(16), 4560-4573.

Rouzeau-Szynalski, K., Maillard, J. and Holliger, C. (2011) Frequent concomitant presence of *Desulfitobacterium* spp. and "*Dehalococcoides*" spp. in chloroethene-dechlorinating microbial communities. Appl Microbiol Biotechnol 90(1), 361-368.

Ruggiero, C.E., Boukhalfa, H., Forsythe, J.H., Lack, J.G., Hersman, L.E. and Neu, M.P. (2005) Actinide and metal toxicity to prospective bioremediation bacteria. Environmental Microbiology 7(1), 88-97.

Sanford, R.A., Cole, J.R. and Tiedje, J.M. (2002) Characterization and description of *Anaeromyxobacter dehalogenans* gen. nov., sp. nov., an aryl-halorespiring facultative anaerobic myxobacterium. Applied and environmental microbiology 68(2), 893-900.

Schaefer, C.E., Condee, C.W., Vainberg, S. and Steffan, R.J. (2009) Bioaugmentation for chlorinated ethenes using Dehalococcoides sp.: Comparison between batch and column experiments. Chemosphere 75(2), 141-148.

Scheutz, C., Durant, N.d., Dennis, P., Hansen, M.H., Jørgensen, T., Jakobsen, R., Cox, E.e. and Bjerg, P.L. (2008) Concurrent ethene generation and growth of Dehalococcoides containing vinyl chloride reductive dehalogenase genes during an enhanced reductive dechlorination field demonstration. Environmental Science & Technology 42(24), 9302-9309.

Schink, B. and Friedrich, M. (1994) Energetics of syntrophic fatty acid oxidation. FEMS microbiology reviews 15(2-3), 85-94.

Scholz-Muramatsu, H., Neumann, A., Meßmer, M., Moore, E. and Diekert, G. (1995) Isolation and characterization of *Dehalospirillum multivorans* gen. nov., sp. nov., a tetrachloroethene-utilizing, strictly anaerobic bacterium. Arch Microbiol 163(1), 48-56.

Seshadri, R., Adrian, L., Fouts, D.E., Eisen, J.A., Phillippy, A.M., Methe, B.A., Ward, N.L., Nelson, W.C., Deboy, R.T., Khouri, H.M., Kolonay, J.F., Dodson, R.J., Daugherty, S.C., Brinkac, L.M., Sullivan, S.A., Madupu, R., Nelson, K.T., Kang, K.H., Impraim, M., Tran, K., Robinson, J.M., Forberger, H.A., Fraser, C.M., Zinder, S.H. and Heidelberg, J.F. (2005) Genome sequence of the PCE-dechlorinating bacterium *Dehalococcoides ethenogenes*. Science 307(5706), 105-108.

Stroo, H.F., Leeson, A., Marqusee, J.A., Johnson, P.C., Ward, C.H., Kavanaugh, M.C., Sale, T.C., Newell, C.J., Pennell, K.D., Lebron, C.A. and Unger, M. (2012) Chlorinated ethene source remediation: lessons learned. Environ Sci Technol 46(12), 6438-6447.

Stroo, H.F., Unger, M., Ward, C.H., Kavanaugh, M.C., Vogel, T.M., Leeson, A., Marqusee, J.A. and Smith, B.P. (2003) Remediation chlorinated solvent source zones. Environmental Science & Technology 37, 224A-230A.

Sung, Y., Fletcher, K.E., Ritalahti, K.M., Apkarian, R.P., Ramos-Hernandez, N., Sanford, R.A., Mesbah, N.M. and Löffler, F.E. (2006) *Geobacter lovleyi* sp. nov. strain SZ, a novel metal-reducing and tetrachloroethene-dechlorinating bacterium. Appl Environ Microbiol 72(4), 2775-2782.

Sung, Y., Ritalahti, K.M., Sanford, R.A., Urbance, J.W., Flynn, S.J., Tiedje, J.M. and Löffler, F.E. (2003) Characterization of two tetrachloroethene-reducing, acetate-oxidizing anaerobic bacteria and their description as *Desulfuromonas michiganensis* sp. nov. Appl Environ Microbiol 69(5), 2964-2974.

Suyama, A., Iwakiri, R., Kai, K., Tokunaga, T., Sera, N. and Furukawa, K. (2001) Isolation and characterization of *Desulfitobacterium* sp. strain Y51 capable of efficient dehalogenation of tetrachloroethene and polychloroethanes. Biosci Biotechnol Biochem 65(7), 1474-1481.

Swift, R.S. (1996) Methods of soil analysis: chemical methods, part 3. Sparks, D.L., Page, A.L., Helmke, P.A. and Loeppert, R.H. (eds), Soil Science Society of America, American Society of Agronomy, Madison, WI.

Thomas, S.H., Sanford, R.A., Amos, B.K., Leigh, M.B., Cardenas, E. and Löffler, F.E. (2010) Unique ecophysiology among U (VI)-reducing bacteria as revealed by evaluation of oxygen metabolism in Anaeromyxobacter dehalogenans strain 2CP-C. Applied and environmental microbiology 76(1), 176-183.

Triplett Kingston, J.L., Dahlen, P.R. and Johnson, P.C. (2010) State-of-the-Practice Review of In Situ Thermal Technologies. Groundwater Monitoring & Remediation 30(4), 64-72.

Tront, J.M., Amos, B.K., Löffler, F.E. and Saunders, F.M. (2006) Activity of *Desulfitobacterium* sp. strain Viet1 demonstrates bioavailability of 2, 4-dichlorophenol previously sequestered by the aquatic plant Lemna minor. Environ Sci Technol 40(2), 529-535.

Truex, M., Powell, T. and Lynch, K. (2007) In situ dechlorination of TCE during aquifer heating. Ground Water Monitoring and Remediation 27(2), 96-105.

USEPA (2004) In Situ Thermal Treatment of Chlorinated Solvents Fundamentals and Field Applications (EPA 542-R-04-010), U.S. Environmental Protection Agency, Office of Solid Waste and Emergency Response Washington, D.C.

van Beek, C.G.E.M. (1984) Restoring Well Yield in the Netherlands. Journal American Water Works Association 76(10), 66-72.

van der Zaan, B., Hannes, F., Hoekstra, N., Rijnaarts, H., de Vos, W.M., Smidt, H. and Gerritse, J. (2010) Correlation of *Dehalococcoides* 16S rRNA and chloroethene-reductive dehalogenase genes with geochemical conditions in chloroethene-contaminated groundwater. Applied and environmental microbiology 76(3), 843-850.

van Genuchten, M. (1981) Non-equilibrium transport parameters from miscible displacement experiments, USDA Science and Educational Administration; U.S. Salinity Laboratory, Riverside, CA.

Wagner, D.D., Hug, L.A., Hatt, J.K., Spitzmiller, M.R., Padilla-Crespo, E., Ritalahti, K.M., Edwards, E.A., Konstantinidis, K.T. and Löffler, F.E. (2012) Genomic determinants of organohalide-respiration in Geobacter lovleyi, an unusual member of the Geobacteraceae. BMC genomics 13(1), 200.

Wang, J. and Wan, W. (2009) Factors influencing fermentative hydrogen production: a review. International journal of hydrogen energy 34(2), 799-811.

Wang, Y., Li, Y., Kim, H., Walker, S.L., Abriola, L.M. and Pennell, K.D. (2010) Transport and retention of fullerene nanoparticles in natural soils. Journal of Environmental Quality 39(6), 1925-1933.

Wolin, E., Wolin, M.J. and Wolfe, R. (1963) Formation of methane by bacterial extracts. Journal of Biological Chemistry 238(8), 2882-2886.

Wood, W.W. and Bassett, R.L. (1975) Water quality changes related to the development of anaerobic conditions during artificial recharge. Water Resources Research 11(4), 553-558.

Zheng, D., Carr, C.S. and Hughes, J.B. (2001) Influence of hydraulic retention time on extent of PCE dechlorination and preliminary characterization of the enrichment culture. Bioremediation Journal 5(2), 159-168.

CHAPTER 6

APPENDICES

6.1. LIST OF SCIENTIFIC AND TECHNICAL PUBLICATIONS

6.1.1. Articles in peer-reviewed journals

Y. Yang, N.L. Cápiro, J. Yan, T.F. Marcet, K.D. Pennell and F.E. Löffler. (2017) "Resilience and Recovery of Dehalococcoides mccartyi from following Low pH Exposure." *Federation of European Microbiological Societies (FEMS) Microbiology Ecology, Anaerobic Biological Dehalogenation thematic issue*.(*in revision*)

Costanza, J., T.F. Marcet, N.L. Cápiro and K.D. Pennell. (2017) "Tetrachloroethene Release and Degradation during Combined Electrical Resistance Heating (ERH) and Sodium Persulfate Oxidation." *Ground Water Monitoring and Remediation*. (s*ubmitted*)

Marcet, T.M., N.L. Cápiro, L.A. Morris, S.M. Hassan, Y. Yang. F.E. Löffler and K.D. Pennell. (2017) "Release of Fermentable Substrates and Electron Donors during Thermal Treatment of Soils." *Environmental Science and Technology*. (*in revision*)

Y. Yang, N.L. Cápiro, T.F. Marcet, J. Yan, K.D. Pennell and F.E. Löffler. (2017) "Organohalide Respiration if Chlorinated Ethenes under Low pH Conditions." *Environmental Science and Technology*. (*accepted, in press*) DOI: 10.1021/acs.est.7b01510

Cápiro, N.L., F.E. Löffler and K.D. Pennell. (2015). "Spatial and Temporal Dynamics of Organohalide-Respiring Bacteria in Heterogeneous PCE-DNAPL Source Zone.**"** *Journal of Contaminant Hydrology. 182:* 78-90

Cápiro, N.L., Y. Wang, J. K. Hatt, K.D. Pennell and F.E. Löffler. (2014). "Distribution of Organohalide-Respiring Bacteria between Solid and Aqueous Phases." *Environmental Science and Technology. 48* (18): 10878–10887

Fletcher, K.E., J. Costanza, K.D. Pennell, and F.E. Löffler. (2011) "Electron donor availability for microbial reductive processes following thermal treatment." *Water Research 45(20),* 15*: 6625-6636.*

6.1.2. Conference or symposium abstracts

Cápiro, N. L., T.F. Marcet, Y. Yang, S.P. Gaeth, F.E. Löffler and K.D. Pennell. "Examining the Secondary Impacts of Biostimulation on Water Quality and Sustained Bioremediation." American Geophysical Union (AGU) Fall meeting, December 14-18, 2015.

Marcet, T.F., S.P. Gaeth, N.L. Cápiro, Y. Yang, F.E. Löffler and K.D. Pennell. "Impacts of Iron (II) Sulfide Precipitation on the Permeability of Porous Media." Battelle Third International

Symposium on Bioremediation and Sustainable Environmental Technologies; Miami, FL, May 18-21, 2015.

Cápiro, N.L., T.F. Marcet, J. Costanza, Y. Yang, F.E. Löffler, K.D. Pennell. "Characterization of Byproducts Released during Thermal Treatment to Support Reductive Dechlorination." Remediation Technology Summit; Westminster, CO. March 2-4, 2015

Marcet, T.F., K.D. Pennell and N.L. Cápiro. "Implications of Iron (II) Sulfide Precipitation on Aquifer Permeability" at the UCOWR-NIWR-CAUHSI conference; Medford, MA. June 18-20, 2014.

Marcet, T. F., N. L. Cápiro, Y. Yang, J. Costanza, F. E. Löffler and K. D. Pennell. "Evaluating the Potential for Thermal Treatment of Soils to Supply Electron Donors to a PCE-to-Ethene Dechlorinating Consortium." Battelle Ninth International Conference on Remediation of Chlorinated and Recalcitrant Compounds; Monterey, CA. May 2014.

Cápiro, N. L., T.F. Marcet, Y. Yang, F.E. Löffler and K.D. Pennell. "Secondary Impacts of *In Situ* Thermal Treatment and Anaerobic Bioremediation on Groundwater Quality." Battelle Ninth International Conference on Remediation of Chlorinated and Recalcitrant Compounds; Monterey, CA. May 2014.

Marcet, T. F., Y. Yang, J. Costanza, F. E. Löffler, N. L. Cápiro, K. D. Pennell. "Quantification of Electron Donor Release during Thermal Treatment." Battelle Bioremediation and Sustainable Environmental Technologies Symposium; Jacksonville, FL, June 2013.

Cápiro, N.L., T.F. Marcet, Y. Yang, S.H. Warner, F.E. Löffler and K.D. Pennell. "Secondary Impacts of *In Situ* Remediation on Groundwater Quality: Metal Sulfide Formation and pH Reduction." Remediation Technology Summit; Westminster, CO. March 4-6 2013.

Cápiro, N.L., K.D. Pennell, F.E. Löffler, Y. Yang and T.F. Marcet. "Secondary Impacts of In Situ Remediation on Groundwater Quality and Post-Treatment Management Strategies." Gordon Research Conference; Environmental Sciences: Water; Holderness, NH, June 24-29, 2012.

Pennell, K.D., N.L. Cápiro, T.F. Marcet, F.E. Löffler and Y. Yang. "Secondary Impacts of In Situ Remediation on Groundwater Quality and Post-Treatment Management Strategies." Battelle Eighth International Conference on Remediation of Chlorinated and Recalcitrant Compounds; Monterey, CA. May 2012

Pennell, K.D., F.E. Löffler, N.L. Cápiro, Y. Yang, and T.F. Marcet. "Secondary Impacts of In Situ Remediation on Groundwater Quality and Post-Treatment Management Strategies." SERDP/ESTCP Partners in Environmental Technology Technical Symposium & Workshop, Washington, DC, November 29- December 1, 2011.

6.1.3. Text books or book chapters

Pennell, K. D., N. L. Cápiro, and D. I. Walker. (2014) "Chapter 11: Surfactant and Cosolvent Flushing" *Chlorinated Solvent Source Zone Remediation, Section IV. Remediation Technologies.* C. Herb Ward and Hans Stroo (Eds.) Strategic Environmental Research Development Program. Springer, New York, 2014. 353-394.

Pennell, K.D. and N.L. Cápiro. (2014) "Innovation Technologies for Chlorinated Solvent Remediation." International Seminars on Nuclear War and Planetary Emergencies 46th Session: pp. 231-251.